Regulation of Large Conductance Calcium- and Voltage-Activated Potassium (BK) Channel Splice Variants by Protein Kinase A

Lorraine Sheila Coghill

Presented for the Degree of Doctor of Philosophy

The University of Edinburgh

2003

Declaration

This work was carried out in the Membrane Biology Group, School of Biomedical and Clinical Laboratory Sciences, College of Medicine, University of Edinburgh. The composition of this thesis is my own, except where stated otherwise.

Lorraine Coghill

February, 2003

Acknowledgements & Thanks

So many people have been invaluable to me during the course of my studies and I am incredibly grateful to all for not only helping me technically and, on occasions, inspirationally, but for putting up with the strops and bouts of despair that seem to be integral to the PhD experience. Thank you all so much. I would like to thank all past and present members of the Membrane Biology Group (MBG) (School of Biomedical and Clinical Laboratory Science, University of Edinburgh) especially (in completely random order); Mark Kerrigan, Lijun Tian, Martin Hammond, Hannah Florance, Daniel Collins, Helene Widmer, Janet Philp, Rory Duncan, Mel Johnson, Pam Holland, Derek Robertson, Wipa Suginta, Steve MacDonald, Eliane Salvo-Chirnside, and of course, enormous, special thanks to my supervisor, Mike Shipston.

I would like to pass on my deepest thanks to the following people for technical advice and support: Roger Clegg of the Hannah Research Institute (Ayr, Scotland, U.K., KA6 5HL) for advice on PKA and the use of his wonderful α-PKAc antibody; Hans-Günther Knaus and Maria Trieb (Institute for Biochemical Pharmacology, University Innsbruck, Peter-Meyer Strasse 1, A-6020 Innsbruck, Austria) for use of their channel reactive antibodies; Irwin Levitan and Yi Zhou (Department Of Neuroscience, University of Pennsylvania School of Medicine, Philadelphia, Pennsylvania 19104) for expression vectors expressing PKAc and various channel fusion constructs; Linda Sharp (Genes & Development Group, School of Biomedical and Clinical Laboratory Science, University of Edinburgh) for confocal microscopy assistance; Nathan Harris (Moredun Research

Institute, Pentlands Science Park, Bush Loan, Penicuik, East Lothian) and Hannah Florance (Edinburgh Protein Interaction Centre, Institute of Cell & Molecular Biology, University of Edinburgh) for mass spectrometry; Mel Johnson and Rory Mitchell (MBG) for antibodies and immunoprecipitation advice; Jonathan Bard (Genes & Development Group, School of Biomedical and Clinical Laboratory Science, University of Edinburgh) for use of the TO-PRO-3 stain; and Rory Duncan and Janet Philp (MBG) for the STREX pGEX5x-1vector and for putting up with continual stupid questions.

My family and friends have been an amazing source of support continually, from the tantrums to just letting me spraff at them. I'm sure I'll have forgotten someone but I'd like to mention (again, completely random order!): Mum, Dad & John (finally over!), Mark & Martin (you should have known after Teviot!), Clare & David (what can I say?), the girls; Eve, Hannah, Lynne, Sarah, Stacey as well as the future scientists whose in-depth conversations over the last few months have helped to keep me sane; James, Michael & Lewis. Huge hugs and thanks to Hannah, Karen, Lijun, Andrew, Derek and finally, Daniel (your faith in me has been a fantastic support & much more than mine ever was).

Thank you all,

Lorraine

February, 2003

Abstract

Large conductance calcium- and voltage-activated potassium (BK) channels are important determinants of endocrine, vascular and neuronal cell excitability, displaying diverse regulation through several mechanisms including reversible protein phosphorylation. Although transcribed from only one gene (*KCNMA1*), native BK channels achieve functional and regulatory diversity through alternative splicing of pre-mRNA. This is exemplified by the different response of two major BK channel splice variants to protein kinase A (PKA). Channels expressing a unique, 58 residue, cysteine-rich insert (STREX) located within the intracellular C-terminal domain of the channel are inhibited by PKA, whereas channels lacking this insert (ZERO) are activated. This suggests that splicing of the BK channel gene is critical to the regulation of BK channels by reversible phosphorylation. However, whether the BK channel α-subunit is phosphorylated directly by PKA or if the kinase associates as part of a signalling complex with the mammalian channel protein is undetermined. Thus, this thesis aimed to investigate the molecular nature of the regulation and interaction of PKA with BK channel variants.

Two experimental strategies were pursued: i.) generation of recombinant fusion proteins of the BK channel α-subunit C-terminal domain to identify putative PKA consensus phosphorylation sites and domains critical to the assembly of a PKA-BK channel complex, and ii.) generation and expression of epitope-tagged full-length channels in a heterologous expression system to enable the investigation of channel phosphorylation and complex assembly *in vivo*.

In conjunction with site-directed mutagenesis, biochemical phosphorylation analyses and the development of phospho-specific antibodies revealed a conserved PKA phosphorylation site at serine residue, S869, that is also a potential target for CaMKII but not PKC. In addition, a STREX insert serine residue, STREX S4, was identified as a PKA-mediated phosphorylation target, possibly functioning as a PKC but not CaMKII phosphorylation target residue.

The catalytic subunit of PKA co-immunoprecipitated with both the STREX and ZERO BK channel splice variants *in vivo* and complex assembly was dependent upon a conserved leucine zipper motif, LZ1, within the C-terminal domain of the BK channel α-subunit. PKA interaction was mediated via a ~130 amino acid region encompassing LZ1 and required intermediary adapter protein(s).

These data suggest that the different response of the STREX and ZERO channels to PKA is likely to result from the differential phosphorylation of specific PKA consensus motifs within the splice variants and not as a result of differential association of the kinase.

Finally, co-immunoprecipitation assays suggested heteromultimerisation between the STREX and ZERO α-subunit variants *in vivo*. Such interactions may contribute further to the regulatory diversity of BK channels.

Abbreviations

AA	arachidonic acid
AC	adenylate cyclase
AKAP	A-kinase anchoring protein
Amp	ampicillin
AMPA	α-amino-3-hydroxy-5-methyl-4-isoxazole propionate
ATP	adenosine 5'-triphosphate
BAPTA	1,2-bis[2-aminophenoxy]ethane-N,N,N',N',tetraacetic acid
BK channel	large conductance calcium- and voltage-activated potassium channel
bp	base pair
bRIA	mammalian cell IP buffer
bRIA-T	bRIA + 1 % Triton X-100
BSA	bovine serum albumin
CaM	calmodulin
CaMK	calmodulin kinase
cAMP	adenosine-3',5'-cyclic monophosphate (cyclic AMP)
cfu	colony forming units
cGMP	guanosine-3',5'-cyclic monophosphate (cyclic GMP)
ChTX	charybdotoxin
8-CPT-cAMP	8-(4-chlorophenylthio)-cAMP
CTP	cytidine 5'-triphosphate
Da	Dalton
DEPC	diethyl pyrocarbonate
DHS-I	dehydrosoyasaponin-I
DMEM	Dulbecco's Modified Eagle Medium
DNA	deoxyribonucleic acid
dNTP	deoxynucleotides triphosphate namely dATP, dCTP, dGTP, dTTP
DTT	dithiothreitol
1-EBIO	1-ethyl-2-benzimidazolinone
ECL	enhanced chemiluminescence

EDRF	endothelium-derived relaxing factor
EDTA	ethylenediaminetetraacetic acid
EGFP	enhanced green fluorescent protein
EGTA	ethyleneglycol-bis(β-aminoethylether)-N,N,N',N'-tetraacetic acid
FCS	foetal calf serum
FITC	fluorescein isothiocyanate isomer
FSG	fish skin gelatin
GC	guanylate cyclase
GS4B	glutathione sepharose 4B
GST	glutathione-S-transferase
GTP	guanosine 5'-triphosphate
HA	hemagglutinin
HEK293	human embryonic kidney cell line 293
HEPES	N-[2-hydroxyethyl]piperazine-N'-[2-ethanesulphonic acid]
HPA stress axis	hypothalmic-pituitary-adreno-cortical stress axis
HP-thioredoxin	polyhistidine (H_6) -thioredoxin
HRP	horseradish peroxidase
IbTX	iberiotoxin
IF	immunofluorescence
IgG	immunoglobulins
IP	immunoprecipitation
IPTG	isopropyl β-D-thiogalactopyranoside
ITS	insulin-transferrin-sodium selenite
kDa	kilo Dalton
KLH	keyhole limpet hemocyanin
LB	Luria Berani – broth/agar
LDS-LB	lithium dodecyl sulphate - loading buffer
MALDI-TOF	matrix-assisted laser desorption/ionisation – time of flight mass spectroscopy
MBG	Membrane Biology Group
MCS	multiple cloning site

MOPS	3-[N-morpholino] propane sulphonic acid
MthK	*Methanobacterium thermoautotrophicum* potassium channel
NADH/$^+$	nicotinamide adenine dinucleotide
NEM	N-ethyl-maleimide
NiNTA	nickel-nitrilotriacetic acid
NMDA	N-methyl-D-aspartate
NO	nitric oxide
NOS	nitric oxide synthase
OA	okadaic acid
OD	optical density
P	phosphorylated
PBS	phosphate buffered saline
PBS-T	PBS + 0.05 % Tween 20
PCR	polymerase chain reaction
PGS	protein-G-sepharose; protein from group C streptococci that binds Fc portion of IgG bound to sepharose
PHAS-I	phosphorylated heat-and acid-stable protein regulated by insulin
PI	protease inhibitors
PK	protein kinase
PKA	protein kinase A. Also known as cAMP-dependent protein kinase (cAPK) & A-kinase
PKAc	PKA catalytic subunit
PKAr	PKA regulatory subunits
PKC	protein kinase C
PKG	protein kinase G
P_o	mean channel open probability
PP	protein phosphatase
PP1	protein phosphatase 1
PP2A	protein phosphatase 2A
Ptac	promoter – IPTG regulated
PTZ	pentylenetetrazole

PVDF	polyvinylidene fluoride
RNA	ribonucleic acid
SDM	site directed mutagenesis
SDS	sodium dodecylsulphate (sodium lauryl sulphate)
SDS-LB	SDS-loading buffer
SDS-PAGE	SDS-polyacrylamide gel electrophoresis
STET	sucrose, Tris, EDTA, Triton X-100 Buffer (See Section 2.1.2)
STREX	stress regulated, or stress axis related exon
STREX channel	BK channel splice variant that expresses the STREX insert
TBE	Tris, boric acid, EDTA buffer (See Section 2.1.1)
TEA^+	tetraethylammonium
TET	tetracycline
TFB	TransFormation buffer
T_m	melting temperature
2TM/P	2 transmembrane-pore domain (See Section 1.3.2.1)
TRITC	tetramethylrhodamine isothiocyanate
TTB	Towbin transfer buffer
TTP	thymidine 5'-triphosphate
V5-H_6	V5-polyhistidine
v/v	volume per volume
w/v	weight per volume
ZERO channel	BK channel splice variant lacking splice inserts

List of Figures

Chapter One: An Introduction to BK Channels

Chapter Two: Materials & Methods

Chapter Three: Characterisation of Fusion Proteins & Phospho-Specific Antibodies

Chapter Four: Characterisation of PKA-Mediated Phosphorylation of BK Channel Splice Variants

Chapter Five: The BK Channel Complex

Chapter Six: General Discussion & Future Work

Appendices

List of Tables & Schemes

Contents

Chapter One:

An Introduction to BK Channels

Chapter One:
An Introduction to BK Channels

1.1 Introduction: BK channels in the potassium channel super-family

The large super-family of the potassium channels encompasses a wide range of structurally and functionally diverse transmembrane ion channels responsible for conducting the physiologically critical cation, potassium (Figure 1.1; [1-3]). Within this family, the calcium-activated potassium (K_{Ca}) channels are distinct due to their activation by elevations in intracellular calcium with the subsequent potassium ion efflux contributing to cellular hyperpolarisation [3, 4]. These channels were sub-divided according to the relative potassium conductance into three sub-families (Scheme 1.1).

Scheme 1.1: Relative conductances of the three K_{Ca} channel families [1, 3, 4]

K_{Ca} channel sub-family	Abbreviation	Conductance range in symmetrical K^+ (pS)
Small conductance	**SK**	**4-14**
Intermediate conductance	**IK**	**20-80**
Large conductance	**BK**	**150-350**
Voltage-activated potassium channels		8-27

Figure 1.1
The potassium channel super-family

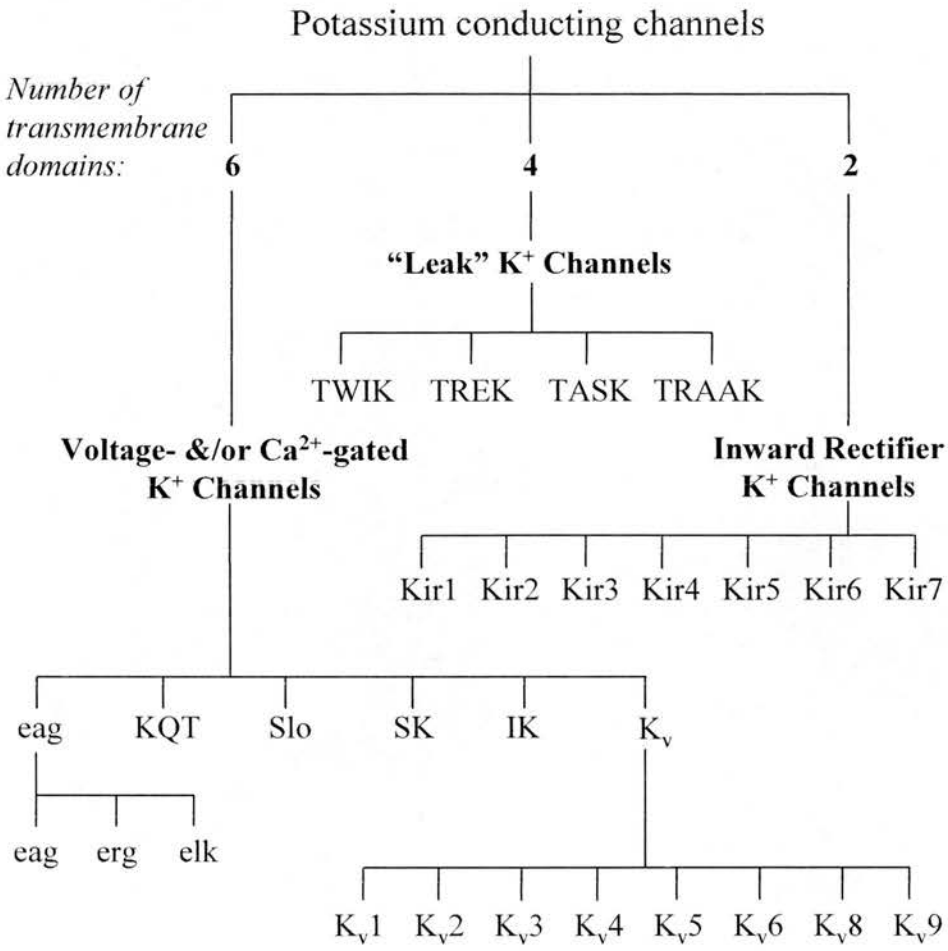

Figure 1.1: Schematic representation of the potassium channel super-family family tree. Potassium ion (K^+) conducting channels are divided into three groups according to the predicted membrane topology; the number of transmembrane domains. Each group is divided into families according to sequence homology (not gene families) and can be further divided into subfamilies (Based on Coetzee *et al*, 2001 [3]).

The large conductance calcium- and voltage-activated potassium channels (BK channels, also known as maxi-K or Slo channels) possess an unusually large potassium conductance approximately ten-fold greater than that of other potassium channels [4-6] (See Scheme 1.1). In addition, BK channels couple the calcium-responsiveness that is characteristic of the K_{Ca} channel family with a voltage-sensitivity that echoes the intrinsic property of voltage-gated potassium channels (Kv) [4-7]. This unique dual activation provides a critical and fundamental link between the electrical and metabolic state of a cell [8] and is just one of several distinct features that cause these intrinsic ion channels to be distinct among the potassium channel super-family.

Since their discovery in mammalian sarcoplasmic reticulum in 1980 [9], BK channels have been a focus of interest due to their proposed roles in several disease mechanisms and their numerous, unique structural, molecular and functional properties. The elucidation of many of these novel features has been investigated by several individual studies and has been facilitated greatly by the initial cloning of the BK channel gene of *Drosophila melanogaster*, the *Slowpoke* (*Slo I*) gene, by Atkinson and by Adelman [10, 11]. *Slowpoke* gene homologs from numerous species have been identified by sequence homology, leading to the elucidation of an ion channel with near ubiquitous expression and conservation throughout the cells and tissues of the majority of multicellular organisms [12-17] (Reviewed: [4-7]). This is indicative of an ion channel under great evolutionary pressure and thus, of great physiological importance [4-6].

Such physiological importance is illustrated by the ubiquity and requirement of BK channels in several physiological processes ranging from action potential frequency modulation to endocrine secretion and cochlea hair cell electrical tuning (Section 1.2). Remarkably, such functional diversity results from proteins encoded by just one gene with alternative pre-mRNA splicing producing distinct BK channel proteins (Section 1.3). Additionally, the channels respond to several, distinct, integrating signal transduction pathways (Section 1.4) with some of the effecting proteins suggested to complex directly with the core BK channel protein (Section 1.5). Thus, BK channels are of great interest physiologically, biochemically, and molecularly, with their unique features, ubiquity, variability, and functional importance, all contributing to the individuality and fascination of BK channels.

1.2 The physiological roles of BK channels

Similarly to the majority of Kv channels, the sensitivity of BK channels to membrane depolarisation enables their integral role in the shaping of action potential repolarisation [1, 2]. Consequently, BK channels influence neuronal plasticity, resting membrane potential, the control of neuronal firing frequency and spike inhibition during sustained depolarisation [18-23]. Additionally, BK channels are observed presynaptically in peripheral and central nervous tissues where they facilitate synaptic transmission and neurotransmitter release [19, 20, 24]. Such BK channels exhibit an electrophysiology, functionality and pharmacology distinct from their axonal and cell body counterparts that are involved in spike potentiation [19, 20, 23, 24]. This demonstrates ion channel

specialisation relative to sub-cellular location [20, 23, 24] and is conspicuous particularly in dedicated sensory cells such as cochlea hair cells where BK channels are integral to the precision electrical tuning of the basolateral membrane tonotopic axis (Section 1.3.1.2) [25-30].

Uniquely, as BK channel activity is enhanced by increasing intracellular calcium, the incumbent hyperpolarisation is crucial to the negative feedback of calcium signalling, terminating calcium entry by closing voltage-gated calcium channels [8]. Through such dual electrical/metabolic regulation, BK channels are critical to several cellular secretion processes ranging from sweating to neurotransmitter release. The BK channels of epithelial cells including glandular tissues [31, 32] are suggested to be integral to calcium-mediated transepithelial fluid secretion such as that of equine sweat glands [31]. In endocrine tissues such as glomus and chromaffin cells, BK channels are implicated in the control and feedback of catecholamine secretion [33, 34]. Thus, BK channels are implicated in numerous, wide-ranging physiological processes including pancreatic hormone secretion [35], kidney filtration [20, 36, 37], the fight or flight response (Reviewed: [38]) and even emotional reactions [39].

Although present in skeletal muscle, BK channels are prevalent in smooth muscle where they are implicated in the control and regulation of contractile tone and activity rate [40-42]. Thus, they influence multiple muscular functions including arterial relaxation and the maintenance of blood pressure [43-46], motility in the gastrointestinal tract [41],

urinary bladder voiding [47], bronchiole gas exchange [48, 49] and contribute to changes in uterine contractability during pregnancy [50-54].

BK channels are implicated in protective responses to several pathological conditions and physiological disorders including incontinence [55], stroke and ischaemia [7] and in conditions where neuronal spikes are prohibitively small or absent [56]. Additionally, BK channels are present within algal tonoplast membranes and are the only non-ATP-dependent potassium channels detected in the inner mitochondrial membrane suggestive of a putative calcium-buffering role in these organelles [57-59].

Thus, the ubiquity of these novel channels implicates them in several physiological and pathophysiological processes and they are demonstrated to be integral to several of these functions. BK channels achieve such diversity and specialisation, yet are encoded by only one gene.

1.3 The BK channel α-subunit

The BK channel α-subunit is encoded by one gene, *Slo1,* the mammalian orthologue recently renamed *KCNMA1*, and is responsible for forming the potassium-conducting pore of the functional BK channel tetramer [3].

1.3.1 *Slo1* / *KCNMA1* gene

The *Drosophila melanogaster* Slowpoke mutant has a distinct behavioural phenotype characterised by semi-flightlessness and "sticky feet"; an inappropriate immobilization of the insects on a surface following over-stimulation by bright light or a heat pulse [60, 61]. The basis of this phenotype was found to result from defective calcium-activated potassium currents in nerve and muscle tissue derived from mutation of the *Slowpoke* (*Slo1*) gene [61-63]. Subsequently, the gene was cloned [10, 11] and found to display sufficient homology to Shaker potassium channel genes to indicate that the translated protein was a member of the voltage-gated potassium channel super-family (Figure 1.1) [64, 65]. Following this crucial discovery, *Slo1* homologues have been identified and described in numerous species ranging from frogs (Kukuljan, M., Hofmann, A.D., Chouimard, H.A., Rojas, C. and Ribera, A.B., 2000 (unpublished): ncbi accession no. #AF274053) to mice ([12]: #NM_010610) and from chickens ([66]: #U23823) to cows ([67]: #U60105) with the human gene mapped to chromosome 10 at position 10q22.2-10q.23.1 and renamed *KCNMA1* ([68]: #NM_002247) [3, 6].

KCNMA1 is highly conserved with greater than 97 % identity observed at the amino acid level among mammalian homologues [5]. Such identity is astonishing, especially when the gene is encoded nearly ubiquitously throughout the cells and tissues of organisms [5, 6][1] where numerous distinct and divergent physiological processes rely upon its expression of the BK channel α-subunit protein (Section 1.2). Electrophysiological

[1] Cardiac myocytes do not express the KCNMA1 gene product and are the only mammalian cell type observed not to encode the gene (Review: [5]).

investigations of BK channels from different cellular sources have uncovered variation in the single channel characteristics with divergent kinetics, calcium sensitivities and responses to various modulators among the contrasting properties observed [5, 13, 69]. Although the unique metabolism and intracellular environment account for some of this variation (Section 1.4) [5], such diversity usually results from multi-gene ion channel families for example, the Shaker family (K_v channels: See Figure 1.1) [1, 2, 69]. However, as the BK channel α-subunit is encoded by only one gene, variation results from multiple promoters [61, 70] and extensive pre-mRNA splicing [5, 6, 12, 13].

Slo2 & Slo3

Two genes encoding channels displaying structural homology to *Slo1* have been described recently and adjoined to the *Slo* family by virtue of their dual activation by voltage sensitivity and intracellular signalling [6]. The SLO-2 paralogue, also called Slack ("sequence like a calcium-activated potassium channel") is expressed abundantly in *Caenorhabdiitis elegans* brain and skeletal muscle and is sensitive to voltage and, synergistically, to calcium and chloride [71] whilst the murine SLO-3 channel links the cellular membrane potential to intracellular pH in spermatotocytes [72]. However, they appear distinct from BK channels in amino acid sequence and physiological function [7].

1.3.1.1 Tissue-specific transcriptional promoters

Expression of the *Drosophila Slo1* gene is suggested to result from at least five distinct, tissue-specific transcriptional promoters transcribing BK channels with dissimilar N-

terminii that prime the channels for tissue-specific functions to confer the appropriate phenotypic behaviour [61, 70, 73-75].

1.3.1.2 Splicing of the BK channel α-subunit gene

Alternative pre-RNA splicing is a dynamic mechanism that enables the generation of multiple proteins with divergent functional and regulatory properties from a single gene by the processing of the nuclear pre-mRNA into several discrete isoforms with distinct exon combinations (Figure 1.2) [76-78]. Small variations in the mRNA sequence can induce profound functional influence to enhance the specialisation and functional diversity of a particular protein [76-78]. Thus, splicing is employed commonly and has been described for assorted proteins including transcription factors, hormone receptors and ion channels such as the N-type calcium channel and, crucial to this study, the BK channel [3, 77-79].

Alternative pre-mRNA splicing enables the generation of BK channel variants with distinct properties ranging from differences in calcium- and voltage-dependence, ion conductance and the kinetics of activation and inactivation, to regulatory differences such as the specific regulatory influence of individual signal transduction pathways [4, 5, 69, 77, 80-82]. Several splice sites have been identified within the mammalian BK channel α-subunit-encoding gene [13, 80] with additional sites suggested in avian homologues [27]. Two splice sites have been identified in the mammalian N-terminal and five in the cytoplasmic C-terminal domain-encoding region (Figures 1.2, 1.3 & 1.4,

Figure 1.2
Alternative RNA splicing

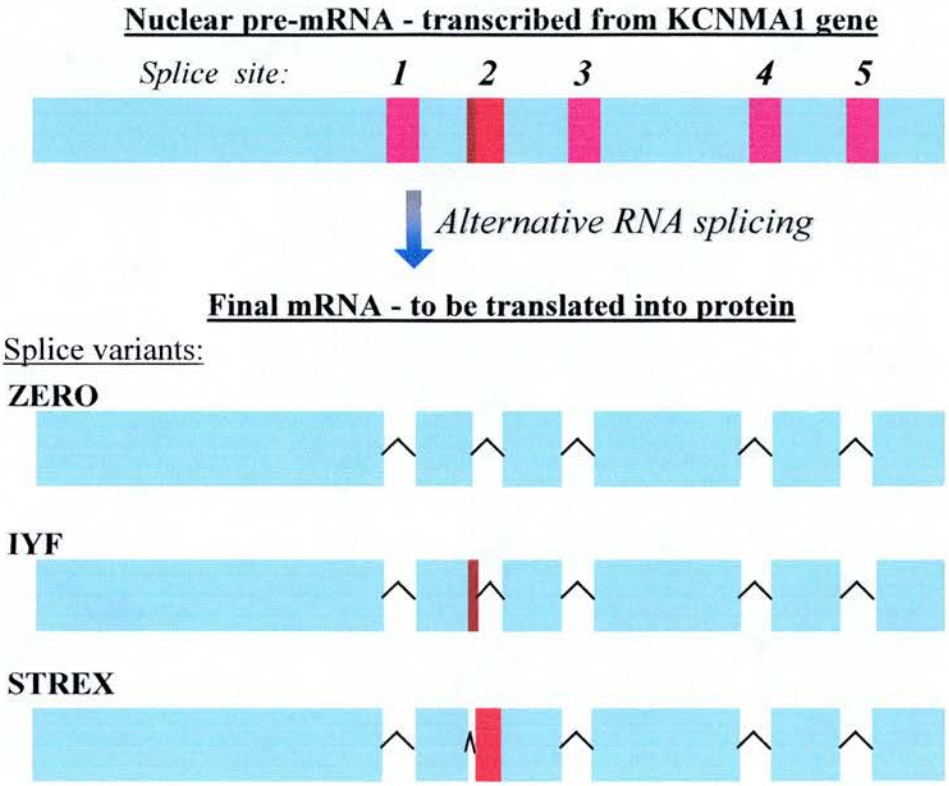

Figure 1.2: Simplified schematic diagram of the mechanism by which alternative RNA splicing generates distinct isoforms of proteins such as the BK channel α-subunit. Transcribed nuclear pre-mRNA contains introns, sequences removed prior to translation, and exons, retained sequences that are translated into protein. Alternative RNA splicing produces various exon combinations yielding multiple mRNA isoforms. In the example illustrated, a simplified and non-scaled representation of the BK channel α-subunit gene, KCNMA1, five major splice sites are shown (See Figure 1.3) and result in several distinct BK channel proteins. For example, splicing at site 2 may generate three individual BK channel isoforms; ZERO from mRNA encoding none of the splice sites, STREX with a 174 base exon, and IYF subunits resulting from an alternative 9 base pair exon.

Section 1.3.2.2.2) [3]. Several distinct exons are recognized at each site exemplified by the human gene for which in excess of twenty-nine distinct exons are suggested [4-6, 82, 83]. With the potential complexity of BK channel alternative pre-mRNA splicing, over 500 unique transcripts could result [77] potentially expressing the same number of distinct BK channel isoforms. However, nowhere near this number is described currently. Such variability has profound implications for physiological specialisation as it produces the capacity to express the specific BK channel splice variant or combination of variants to cater perfectly for the dynamic and unique spatial and temporal requirements of the cell or sub-cellular location [77, 82].

Reverse transcription polymerase chain reaction (RT-PCR) in combination with patch clamping has enabled investigation of the differential expression patterns of splice variants *in vivo* and has uncovered distinct splice variant expression implicating precise physiological specialisation of BK channels through RNA splicing [26, 27, 29, 69, 77, 84]. Perhaps the most elegant example of this is the tonotopic gradient of avian and reptilian cochleae [26, 27]. Hair cells along the cochlea are mapped tonotopically, each tuned precisely to a specific frequency partly instigated by the intrinsic electrical properties of the specific BK channel splice variants expressed by the individual cell [26-30]. The precise allocation of BK channel splice variants depends upon the resonant frequency of the individual cell and *vice versa*, illustrating perfectly organ manipulation of the differential properties of BK channel splice variants to engender precise and effective specialisation [26, 27, 29, 84, 85]. Such specialisation has been suggested on a neuronal level with different brain regions expressing specific ratios of BK channel

splice variants to enable precise tuning of neuronal electrical excitability [82]. Even on a subcellular level, nerve terminals and cell bodies may express distinct splice variants to cater perfectly to the physiological function of the location [19, 20, 24].

Far from remaining static, BK channel splice variant expression is influenced by dynamic factors such as during development [86, 87] and hormonal signalling [50, 84]. This enables cells and organs to alter electrical excitability, adapting to respond appropriately and effectively to a particular stimulation. Splicing of the STREX exon illustrates distinctly such regulation of splicing and the functional consequences of the dynamic process.

1.3.1.2.1 The STREX insert

Adrenal chromaffin cells express at least three discrete BK channel splice variants, two of which possess distinct functional properties when analysed in heterologous expression systems [69]. Channels encoding a cysteine-rich 58 amino acid insert (STREX) at splice site 2 have increased calcium sensitivity, slower deactivation and faster activation that occurs at more negative potentials than ZERO channels that do not express the insert [69, 84]. Thus, these channels open more easily and minimise the duration of the action potential [84]. Quantitative RT-PCR investigation of the ratio of ZERO channel to STREX insert-containing channel expression found that hypophysectomy (pituitary removal) in rats, a process that abolishes stress axis function, reduced the proportion of STREX insert-containing mRNA in the adrenal medulla

without altering total channel transcription [84]. Indeed, an altered whole cell excitability of adrenal chromaffin cells from hypophysectomised rats demonstrates a change in splice variant expression [88]. Subcutaneous injection of adrenocorticotropic hormone (ACTH) reactivated glucocorticoid release and restored the splice variant ratio [84]. Thus, stress hormones including glucocorticoids and adrenal androgens are suggested to induce complex alternative splicing of BK channel mRNA to fine-tune the chromaffin cell excitability and secretory response [84, 88, 89, 90] leading to the naming of the insert, STREX, for *stress-regulated*, or *stress axis-related-exon* [84]. Increasing the proportion of STREX channel expression enables increased repetitive firing to sustain rapid adrenaline secretion during the stress response [38, 88, 89]. Thus, a correlation between the state of the hypothalamic-pituitary-adrenal axis of an animal and the STREX:ZERO channel expression ratio is observed [38, 89].

Similarly, the STREX:ZERO channel expression ratio alters in the murine myometrium during gestation [50]. Although levels of STREX channel mRNA and the resultant protein remain constitutively expressed throughout pregnancy, expression of the ZERO channel is only detected midterm leading to an increase in total BK channel expression [50]. Due to the lower sensitivity of ZERO channels to calcium and voltage compared to that of STREX channels, the intrinsic excitability of the myometrium alters during gestation [50]. This may be beneficial in regulating pre-term uterine contraction and is suggested to result from the fluctuations in oestrogen and/or progesterone that occur during pregnancy altering splicing of the BK channel gene [50].

Conversely, depolarisation of GH_3 pituitary cells has been shown to inhibit alternative splicing of the STREX exon via the calmodulin kinase (CaMK) IV signalling pathway [91]. CaMKIV decreases the expression of STREX-encoding mRNA by interacting with a CaMKIV-responsive RNA element (CaRRE) to lower the expression of STREX channels and thus decrease the calcium sensitivity and opening probability of the GH_3 cell BK channels [91]. Consequently, long-term adaptation of the firing properties of pituitary cells is achieved [91].

1.3.2 Channel topology & structural features

1.3.2.1 Structural features conserved with other Kv channels

Members of the Kv channel multi-gene family respond to membrane depolarisation by enabling potassium ion permeation through a central pore formed by the association of four independent, associated subunits (See Figure 1.7) [1-3, 92]. These crucial ion channels share a common structural topology through the core, channel-forming subunit that exhibits a modular structure with distinct, intrinsic domains responsible for distinct, intrinsic properties, namely gating, voltage sensitivity and ion selectivity [3, 92, 93].

The BK channel α-subunit shares the conserved, core structural characteristics of Kv channels with the six transmembrane helices, S1-S6 (Figures 1.3 & 1.4) [93]. The potassium channel super-family "trademark", 2TM/P (2 transmembrane-pore) domain, is observed comprising helices S5 and S6 with the linking P-loop that is structurally analogous to the prokaryotic KcsA channel whose tertiary structure was resolved by X-

ray crystallography [94] (Reviewed by Sansom *et al*, 1998 [92]). The P-loops line the functional pore and constitute the ion conduction pathway surface including the conserved glycine-tyrosine-glycine (G-Y-G) motif that, in part, forms the selectivity filter via stereochemical oxygen atom checkpoints [1, 95-97]. The oxygens surrogate for the potassium ion hydration shell to maintain hydrogen bonding and lower the interaction energy whilst inhibiting, both physically and energetically, the entry of larger and smaller ions [97-101] (Reviewed: [92, 96]). This enables the conserved, selective, high cation permeation with the characteristic potassium-conducting channel selectivity sequence of $K^+ > Rb^+ > Cs^+ > Na^+ > Li^+$ [92, 96, 98, 102-104] Reviewed: [1, 93, 105]. The pore region shares sequence homology with other potassium channels and is inhibited by wide-spectrum potassium channel blockers such as tetraethylammonium (TEA^+) and charybdotoxin (ChTx), inhibitors that interact specifically with pore residues to occlude ion flux [12, 96, 106-111]. This demonstrates that BK channels share common, conserved residues with other Kv channel pores [12, 96, 106-111].

The membrane depolarisation-induced activation of Kv channels, including BK channels, occurs via the conserved voltage sensor comprised of positively charged residues within the S4 transmembrane helix (Figure 1.4) [112] (Reviewed in *Choe, 2002* [93]). Although the precise molecular mechanism of this response is not understood fully, point mutation studies and the use of spectroscopic probes affixed to the helix [112], have determined that conserved, charged residues are sensitive to changes in membrane potential [113, 114]. Depolarisation alters the membrane electric field inducing a conformational sliding movement of the S4 helix via the responsive

Figure 1.3
The murine BK channel protein sequence

Figure 1.3: The amino acid sequence of the murine BK channel STREX splice variant illustrating important features. The murine STREX channel sequence (NCBI accession number: AAD49225) differs from the ZERO channel (NCBI accession number: NP_034740) by the insertion of the 58 residue STREX insert (red text) at splice site 2 (pink arrow, number 2) which contains a putative PKA phosphorylation consensus motif (red box in STREX sequence). Standard one letter amino acid code used. Features that are shared between the two splice variants include the following:

- transmembrane helices, S0-S6 (light blue text)
- putative cytoplasmic helices, S7-S10 (dark blue text)
- the pore domain (light blue box; GYG motif underlined)
- conserved voltage sensor arginines (+)
- an N-terminal EF hand motif (green box)
- the major RCK domain - responsible for tetramerisation (purple text)
- the calcium bowl (yellow box)
- two putative leucine zipper (LZ) motifs (Neon blue box; integral residues underlined)
- several putative phosphorylation target residues (red boxes; individual protein kinases are indicated above serine or tyrosine residues)
- serine protease-like domain (orange arrow ►)

Also indicated are:

- five sites of splice variation (pink arrows ▼)
- the start and end points of the fusion proteins used in this study (gray arrows ►; See Chapter 3; Table 3.1)

Figure 1.3
The murine BK channel protein sequence

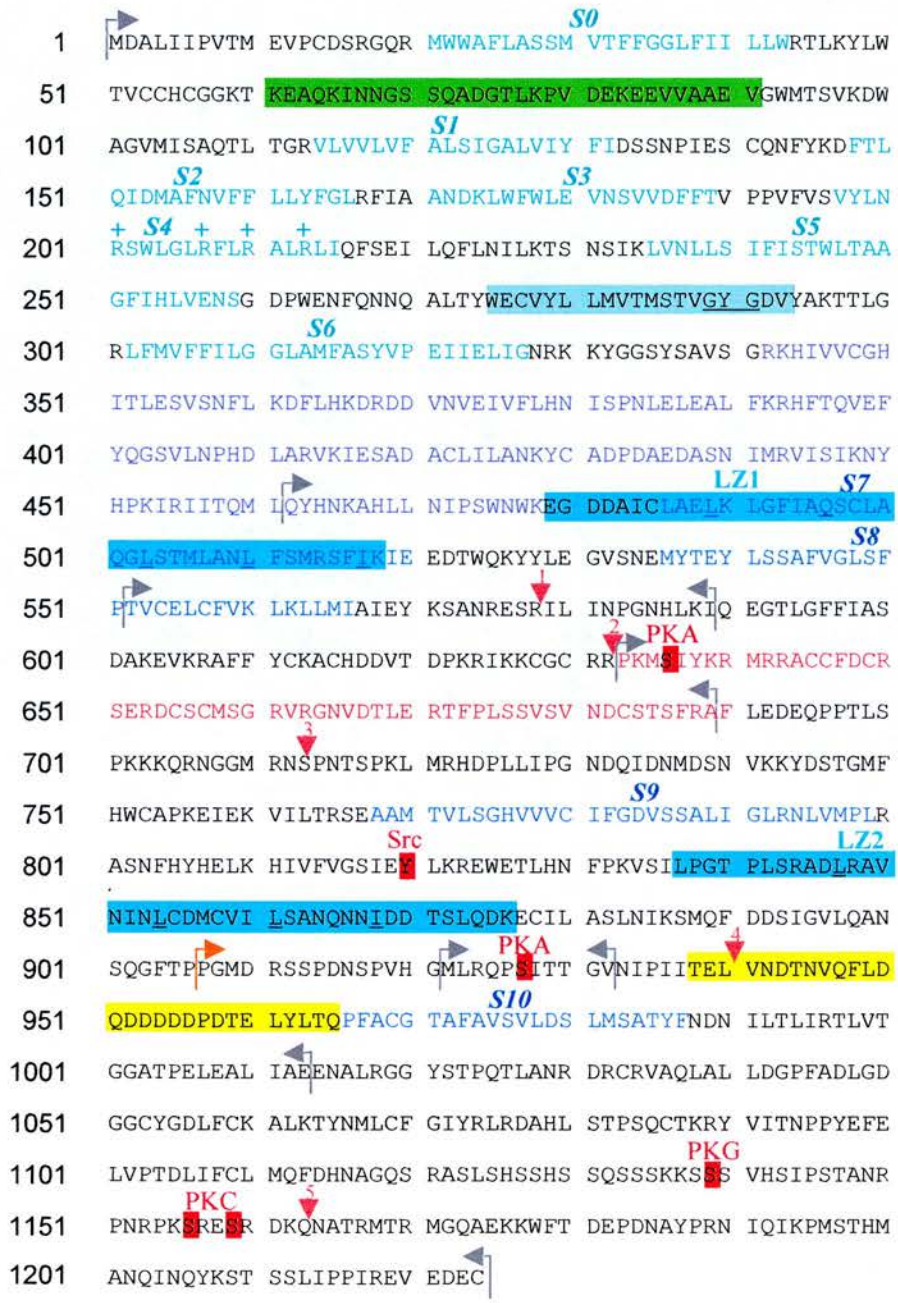

Figure 1.4
BK channel topology

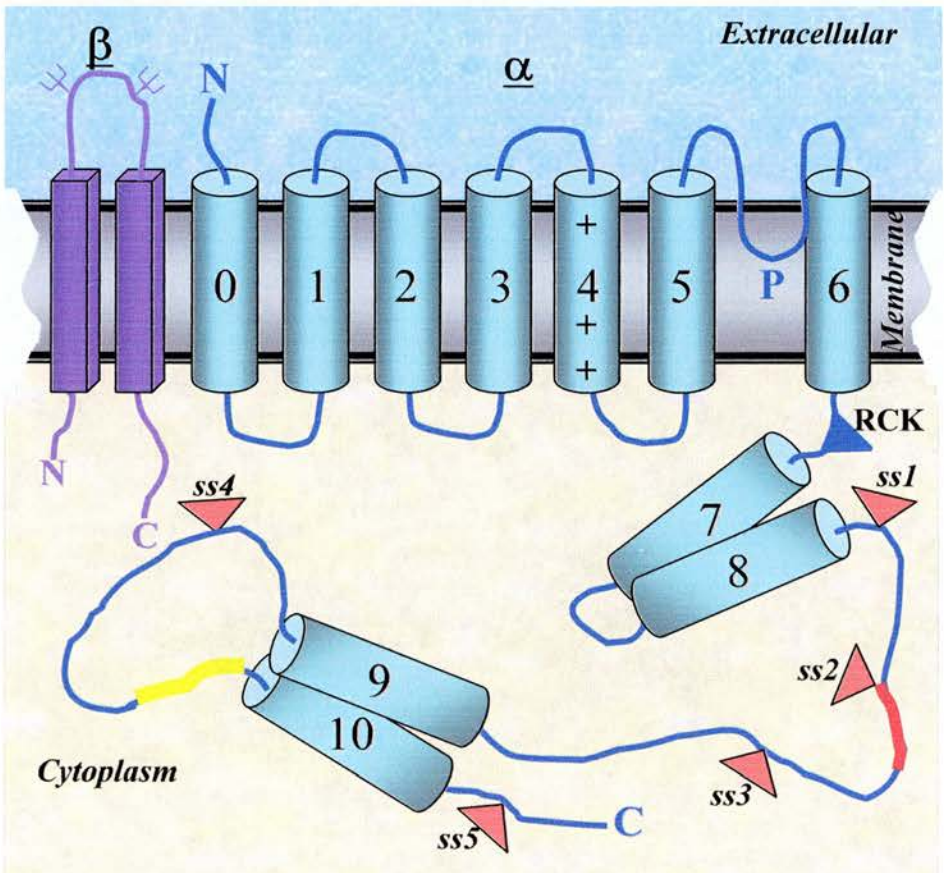

Figure 1.4: Schematic representation of the BK channel α-subunit predicted membrane topology. The BK channel α-subunit is proposed to resemble Kv channel topology through transmembrane (TM) helices, S1-S6, with the charged S4 voltage sensor, P-loop and K^+-selective filter. It differs by an additional N-terminal, TM-helix, S0, integral to β-subunit interaction, and an extended, cytoplasmic C-terminal domain responsible for many modulatory interactions. This domain comprises four putative α-helices, S7-S10, the putative tetramerisation domain, RCK, the calcium bowl (yellow), and five established sites of splice variation (*ss1-5*) including *ss2* where STREX inserts (red). The β-subunit (purple) comprises two TM-helices, intracellular termini and extracellular glycosylation. Not to scale.

charged residues [114] (Reviewed: *Choe, 2002* [93]). The movement propagates through transducing elements to open the potassium ion conduction pathway, providing the structural basis of Kv and BK channel voltage sensitivity [112, 114, 115] (specific to BK channels: [113] Reviewed: *Choe, 2002* [93]).

1.3.2.2 Structural features distinct to BK channels

Although the "core" region of the BK channel α-subunit protein shares certain structural and topological characteristics with other potassium-conducting channels, the ion channel protein maintains its individuality through several, unique properties.

1.3.2.2.1 BK channel pore

Even within the "core" region there are notable differences, the most distinct due to the high ion flux (See Scheme 1.1) [3, 103]. The BK channel pore is suggested to exhibit distinct electrostatic and conformational pore properties resulting from unique aromatic and associated residues that provide proximal cation binding sites to maximise the ionic repulsion between fluxing potassium ions and unique negative vestibule charges to increase local potassium ion concentrations for faster reactivity [103]. Indeed, the distinct peptidyl toxin-pharmacology of BK channels compared to Kv channels, suggests distinct outer vestibule structures. Each peptidyl toxin possesses a distinct structure that enables or precludes its interaction with a potassium channel pore. Thus, α-KTx 2.x and α-KTx 3.x toxin subfamilies block Kv channels yet have no influence on BK channels

[106]. Concomitantly, the asymmetric charge of the scorpion venom, Iberiotoxin (IbTX or α-KTx 1.3), makes it a high-affinity, BK channel-specific blocker [12, 106, 116-120].

1.3.2.2.2 Carboxyl-Terminal Domain

The carboxyl-terminal domain of the BK channel α-subunit protein is unique among the potassium channel super-family [10]. Comprising ~80 kDa, it constitutes ~70 % of the total protein mass (~126 kDa), producing a protein of more than 1100 residues in length compared to around 550 amino acids for the average Kv channel [4, 5].

Although the precise topology of this domain is undetermined currently, the region is suggested to be soluble, cytoplasmic, and include four putative α-helices, S7-S10 (Figure 1.4) [113, 121, 122]. *In vitro* expression of a truncated S9-S10 peptide in *Xenopus* oocytes indicated such solubility and demonstrated that removal of the C-terminal tail inhibits native channel activity which can be reconstituted by co-expression of the S9-S10 peptide or longer, truncated regions of the C-terminal tail, thus highlighting the integrity of the region to BK channel function [123]. Indeed, several accessory proteins and other modulatory factors directly or indirectly associate with, or exert influence through, this domain (Sections 1.4 & 1.5) and the hyper-conservation of certain C-terminal regions is demonstrative of crucial influence [124]. One such region is the "calcium bowl".

The Calcium Bowl

Located in the hyper-conserved region between helices S9 and S10 (Figures 1.3 & 1.4), the "calcium bowl" is involved in the modulation of the BK channel by the ubiquitous second messenger, calcium [8, 123, 124]. The 28-residue, negatively charged, aspartate-rich motif was identified by mutagenesis [123-125] and exhibits homology with calcium-binding proteases [67] and plasma membrane calcium pumps [124]. Unlike the calcium-sensitive regions of SK and IK channels, the calcium bowl is suggested to bind the cation directly and not via intermediary proteins such as calmodulin [4, 102]. Other additional regions such as the RCK (regulator of potassium conductance) domain (Figures 1.3 & 1.4) are implicated in calcium sensing by their analogy to homologous regions in other calcium-gated channels [8, 109, 124, 126] (Crystal structure of *Methanobacterium thermoautotrophicum* potassium channel (MthK) RCK domain: [127]). It should be noted that a recent study has suggested that the BK channel can be regulated by calcium in the absence of the calcium bowl and RCK domain suggesting that another domain of the channel protein may be involved in calcium-regulation of BK channels [128]. BK channels can function as purely voltage-gated in the absence of calcium, but this requires high-voltage depolarisation of ~100 mV [121, 129-133]. In the presence of physiological calcium levels, the ion shifts the voltage range of activation to more negative potentials with calcium concentrations above 100 nM acting synergistically with depolarisation to induce channel activation and increase the open probability (P_o) [18, 121, 126, 134]. Such synergistic activation is unique; Kv channels are sensitive to voltage but not calcium [135] and the other K_{Ca} channels, IK and SK

channels, are activated by calcium and not depolarisation (Reviewed Vergara *et al*, 1998 [4]).

As each α-subunit of the BK channel tetramer has a calcium bowl [102] and, as multiple binding sites per subunit are possible, the calcium-binding permutations and the subsequent influence upon the channel kinetics is complex [8, 134]. In addition to the influence of voltage, additional factors such as phosphorylation state, associated, auxiliary proteins, and the particular BK channel splice variant are likely to affect calcium-mediated gating. Thus, gating is not just novel, rapid and allosteric [102], but convoluted and thus too complex to describe within the limits of this thesis. Studies investigating the phenomenon are described in the following references: [130-140] and reviewed in Magleby, 2001 [141].

However, the synergistic regulation of BK channels by calcium and voltage provide a crucial, unique, molecular link between the cellular metabolism and the electrical state of the cellular membrane [134, 142].

Splicing

In contrast to the hyper-conservation of the calcium bowl, the C-terminal tail region of the BK channel α-subunit is also the region of the greatest diversity among BK channel isoforms due to the presence of several sites of alternative splicing throughout the domain (Figures 1.2 & 1.3; See Section 1.3.1.2) [10, 13]. As the C-terminal tail is the target of many accessory regulatory factors (Sections 1.4 & 1.5) including calcium, the

modulatory and functional differences observed between individual splice variants may be attributable to splicing in this region [50, 82, 125] (See above & Section 1.3.1.2),

1.3.2.2.3 Tetramerisation domain

The crystal structure of the *Shaker* potassium channel tetramerisation domain was determined as a β-strand structure at the cytoplasmic N-terminal domain of the channel subunit protein [143]. This T1 domain induces specific *Shaker-Shaker* subunit assembly and homologous regions in other potassium channels are suggested to function similarly [143, 144]. However, BK channels do not include T1 due to the additional N-terminal S0 transmembrane helix and the extracellular N-terminal (See Figure 1.4). However, gating studies determined at least four calcium ion-binding sites per BK channel suggestive of BK channel α-subunit tetramerisation [102]. Thus, BK channels exhibit a distinct tetramerisation domain, BK-T1 or RCK, characterised as a Rossman fold and present as hydrophobic patches at the S6 transmembrane helix S6 - C-terminal domain interface (Figures 1.3 & 1.4) [145, 146]. The RCK domain is analogous to the *Methanococcus jannaschii* Ktr potassium import system KTN domain, a region responsible for NADH/NAD^+(nicotinamide adenine dinucleotide)-binding and tetramerisation and, although it does not bind NADH, it displays sufficient analogy to enable tetramerisation [145, 147]. Analysis of the MthK channel RCK domain crystal structure, suggested to be integral to calcium binding (See Section 1.3.2.2.2), reveals the formation of a "gating ring" structure at the intracellular pore vestibule formed from the

association of eight RCK domains [145]. Analogous associations of BK channel α-subunit RCK domains may indeed, prove to be integral to channel tetramerisation.

Homomultimerisation v. Heteromultimerisation

The stoichiometry of individual splice variants in a BK channel tetramer is yet to be determined but, as regions of splice variation are distinct from the RCK domain, theoretically, phenotypically distinct BK channel α-subunit splice variants could associate to form functional channels. Channels could result from one, two, three, or four different splice variants with perhaps subtle differences and a range of intermediary gating, regulatory, pharmacological and functional differences contributing to the wide physiological variation and tissue-specific specialisation of BK channels. Although homotetrameric assembly is uncovered commonly [3, 148, 149], such heteromultimeric assembly is observed in several Kv channel families ([150-154] Reviewed: [2,3,155]). The presence of different BK channel splice variants in single hair cells from the chick cochlea [26] and in rat adrenal chromaffin cells [156] suggests that this may apply to BK channels too [26, 34, 149, 156]. Indeed, heterologous expression of the BK channel α-subunit with subunits from the low conductance potassium channel Slack (SLO-2) is suggested to form functional, intermediate-conductance channels by co-association, providing indirect yet evocative evidence of the ability of different BK channel splice variants to form heteromultimers [157].

1.3.2.2.4 Amino-Terminal Domain

As noted above, BK channels possess a conserved, additional transmembrane helix, S0, absent from other potassium-conducting channels (Figure 1.4) [4, 5]. The region is conserved and vital to effective ion channel function and has been implicated in influencing several key channel features including channel open time, ion conductance and voltage-dependence [158]. The generation of chimeras suggests that the region is crucial to α-subunit interaction with modulatory β-subunits [159].

The β-subunits

Many ion channels associate with accessory β-subunits that modulate their activation and BK channels are no exception [160-162]. Bi-functional cross linking [163], biochemical purification [164] and co-immunoprecipitation [165] of the BK channel complex have identified four individual β-subunits that confer distinct regulatory influences upon BK channel activity. The β-subunits do not form ion channels when expressed in the absence of α-subunits, but alter intrinsic properties of the BK channel, namely calcium sensitivity, gating kinetics, toxin sensitivity and response to modulators such as protein kinases [29, 160, 161, 164, 166-171]. This expands the physiological range and specialisation of BK channels, "exaggerating" kinetic variation between BK channels comprised of different α-subunit splice variants [29, 170]. For example, investigation of the kinetics of four individual BK channel splice variants noted eight functionally distinct channels following heterologous co-expression with and without a β-subunit [170]. Indeed, the distinct influences of the different β-subunits upon BK

channel activity suggests that co-expression of the individual β-subunits with the channels could result in several functionally distinct channels in native cells.

All four β-subunits share a common topology of two transmembrane helices with intracellular termini, N-linked glycosylation and molecular weights between 25-31 kDa (Figure 1.4) [6, 163, 172]. The first thirty-one residues of the N-terminal region of the pore-forming, α-subunit are suggested to associate with β-subunits via non-covalent interactions in a 1:1 stoichiometry [159, 164, 165] enabling four, individual β-subunits to encircle a functional BK channel pore tetramer. However, RT-PCR [69, 170, 173], in situ hybridisation [29, 161], immunohistochemistry [161] and electrophysiology [69, 161, 163] have demonstrated that α-subunits may not be saturated by β-subunit in all native tissues [29]. Indeed, β is not obligatory and, in contrast to the ubiquitous α-subunit, is absent from certain tissues [69, 169] including rat skeletal tissue [169], murine corticotropes [80] and certain mammalian brain neurons [161, 163]. Conversely, high expression of particular β-subunits is observed in hippocampal and cochlea cells [173], and in various smooth muscle tissues [163, 164, 174] including tracheal and aortic [158, 161, 171].

Despite the common topology, sequence identity between different human β-subunits is low with between 43 to 21 % identity observed with hβ1 and hβ2, and hβ1 and hβ4 respectively [175]. Even within a β-subunit sub-group less conservation is observed

than with the α-subunit with 82-85% identity observed between different mammalian β1 species compared to greater than 95% for the pore forming subunit [161].

β1

The β1 subunit (KCNMB1) was the first to be characterised [165, 176] and is the best described of the four distinct proteins. It is enriched in peripheral tissues especially smooth, but not skeletal, muscle and exhibits limited expression in the brain [69, 160, 166-168, 175, 177, 178], implicating β1 in the facilitation of the role of BK channels in setting arterial muscle tone and fine-tuning low frequency cochlea hair cells [29].

The subunit increases BK channel calcium sensitivity whilst slowing activation in a calcium-dependent manner without altering channel expression, single channel conductance or ionic selectivity [136, 160, 166-168, 175, 177, 178]. The mechanism of this modulation is uncharacterised, however, the β1 protein is suggested to regulate the rates of transition between open and closed states to increase the duration of activity bursts thus increasing the P_o [169]. The subunit is suggested to modulate the protein kinase regulation and pharmacological properties of BK channels too [166, 167], decreasing sensitivity to ChTX [171] and rendering the channel sensitive to dehydrosoyasaponin-I (DHS-I) activation [160]. Intriguingly, two-hybrid assays and electrophysiological investigation upon heterologous co-expression of β1 and the chloride-conducting channel, CLCA1, indicated a physical association and modulation of the chloride current amplitude suggesting that the BK channel β-subunits may interact with other ion channels *in vivo* [179].

β2

The β2 subunit (KCNMB2, referred to as β3 by Xia *et al*, 1999 [180]) induces rapid inactivation and thus, rapid single channel openings upon BK channels [6, 172, 181] in several tissues including adrenal chromaffin cells, various neurons [6, 172, 182, 183] and pancreatic β-cells where they are observed to modulate neurosecretion patterns [180, 184]. The distinct, cytosolic N-terminal protein has been characterised by nuclear magnetic resonance (NMR) and found to exhibit a "ball and chain" inactivation structure similar to that of Kv channels [181] (Review of Kv channel inactivation: [93]). Removal of this region produces a protein with high sequence and functional similarity to the β1 subunit [175].

β3 & β4

The β3 subunit (KCNMB3) is enriched in testes and has slight influence only, increasing BK channel activation [185]. In contrast, the novel β4 subunit (KCNMB4) exhibits low expression outwith the nervous system and is enriched in brain tissue where it slows BK channel gating kinetics, reduces channel sensitivity to IbTX and ChTX, and modulates calcium sensitivity in a calcium dependent manner; inhibiting openings at low calcium concentrations whilst increasing openings in high calcium conditions [172, 185, 186].

1.4 BK Channel Modulation

As described in Section 1.2, BK channels perform a wide range of physiological functions that exhibit and require specialisation by channels manifesting a wide kinetic, regulatory and sensitivity range. Much of this specialisation is attributable to splice

variation and the β-subunit, but some results from the intrinsic and dynamic intracellular properties of the cell or subcellular location. Many cellular factors influence BK channel activity including the lipid, pH and redox environment, and accessory factors such as protein kinases, protein phosphatases and hormones illustrating the responsiveness of the channels to several, distinct signal transduction mechanisms. This enables BK channels to react to and facilitate many physiological processes, acting as a linchpin to multi-sourced modulation allowing diverse, rapid and extensive ion channel responses. Some of these regulatory mechanisms are described below.

1.4.1 Phosphorylation

The effectiveness, efficiency and plasticity of reversible protein phosphorylation make it one of the most common mechanisms of protein modulation. Numerous signal transduction pathways mediate their appropriate physiological responses through manipulation of specific protein kinases and protein phosphatases controlling the reversible phosphorylation and subsequent functional regulation of particular target proteins ranging from transcription factors to ion channels [187-188]. Activated protein kinases induce the hydrolysis and transfer of the terminal phosphate of adenosine 5'-triphosphate (ATP) onto the hydroxyl group of serine, threonine or tyrosine residues of specific, targeted consensus sequences whereas catalytically active protein phosphatases act in opposition, mediating the dephosphorylation of such residues. The application of ATP with no exogenous protein kinase to reconstituted, cloned, and native BK channels from several, distinct sources alters channel activity and calcium sensitivity [190-198].

Some studies have reported a direct ATP-mediated influence upon BK channel activity in the absence of protein kinase activation through a mechanism that is undetermined currently [142, 189]. However, generally, the use of non-hydrolysable ATP analogues such as AMP-PNP have no influence upon channel activity [190-192]. This suggests ATP hydrolysis, implicating BK channels or closely associated proteins as targets of *in vivo* phosphorylation by native, proximal protein kinases [190]. The reversibility of this modulation implicates the activity of protein phosphatases and thus demonstrates the dynamic, critical use of reversible protein phosphorylation in the regulation of BK channels [190-198]. Although the role of protein phosphatases has not been investigated as fully as that of protein kinases and thus, is not discussed as much in this text, their role in reversing phosphorylation to maintain the dynamic plasticity of this mode of regulation should not be overlooked (Review of protein phosphatase influences on ion channels: [199]).

1.4.1.1 Signal transduction pathways

Several, distinct protein kinases are implicated as regulators of BK channel activity including serine-threonine phosphorylating kinases such as protein kinase A (PKA) [166, 190, 191, 194, 200-206], protein kinase C (PKC) [193, 201, 207, 208] and protein kinase G (PKG) [37, 196, 209-212] and tyrosine-phosphorylating protein kinases such as Src tyrosine kinase [204, 213]. Equally, protein phosphatases (PP) such as PPI and PP2A are implicated as BK channel modulators [190, 191, 194-196]. Individual protein kinases and phosphatases are activated by distinct signal transduction pathways demonstrating convergent, multi-origin regulation of these ubiquitous ion channels [5,

214]. For example, the ubiquitous serine-threonine protein kinase, PKA, is regulated by changes in the intracellular cyclic adenosine monophosphate (cAMP) concentration influenced by indirect hormonal modulation of membranous adenylate cyclase by several physiological processes and responses [215-217]. The inactive protein kinase exists as a tetrameric holoenzyme composed of two regulatory (PKAr) and two catalytic subunits (PKAc) (See Appendix A) [214, 217, 218]. Elevation of intracellular cAMP activates the holoenzyme inducing release of catalytically active PKAc subunits able to phosphorylate target proteins [214, 218] (Representative PKA-phosphorylation targets illustrated: [219-223]). In contrast, the equally ubiquitous PKC is stimulated by phospholipids and calcium generated and released through inositol phospholipid hydrolysis via activation of phospholipase C (PLC) [206] (Review: [214, 218, 224]). Other protein kinases that are suggested as BK channel regulators include protein kinase G (PKG), stimulated by elevation of intracellular cyclic guanylate monophosphate (cGMP) following activation of guanylate cyclase (GC) isoforms by nitric oxide (NO) (See Section 1.4.2.2) or by peptides including atrial naturetic peptide (ANP) [196, 209-211]; and certain calcium and calmodulin-activated protein kinases including calmodulin-activated protein kinases II and IV (CaMKII & CaMKIV) [138, 225] and Src tyrosine kinase [213]. Responsiveness to such diverse signal transduction pathways illustrates the convergent use of these integral ion channels through the common mechanism of reversible phosphorylation providing an important demonstration to the ability of the channels to remain critical to so many diverse physiological processes.

1.4.1.2 Protein kinase consensus motifs & phosphorylation targets

Although the physical mechanism of phosphorylation is maintained consistently by all protein kinases, the targeting of phosphorylation is distinct to each type of protein kinase with specific consensus motifs required (Table 1.1) [226-228]. Thus, different protein kinases are likely to phosphorylate at different target residues, implicating distinct modes of channel regulation, either directly via phosphorylation of the BK channel α-subunit, or indirectly through intermediary protein modulation.

Direct phosphorylation of BK channel protein

The ^{32}P from γ-^{32}P-labelled ATP, incorporated into a 125 kDa protein corresponding to the human BK channel following addition of exogenous PKG, or the constitutively active analogue, PKG-Iα [211]. The effect was not observed with inactivated kinase, implying that a direct, catalytic phosphorylation is responsible [211]. Indeed, sequence analysis in combination with site directed mutagenesis has identified several putative phosphorylation target sequences within the α-subunit, particularly in the C-terminal domain (Figure 1.5) [5, 211].

Serine-942 of the *Drosophila* BK channel was identified as a putative site of direct phosphorylation by PKA following the inhibition of the PKA-mediated response [190, 205]. Mutation of the residue to non-phosphorylatable alanine also precluded channel activation by PKA in detached patches, further implicating direct phosphorylation [190, 205]. Although the mammalian equivalent of this motif is less specific for PKA than the

Table 1.1:
Protein kinase consensus motifs

Protein kinase	Optimal consensus motif	Other suitable consensus motifs
PKA	R-R/K-X_{1-2}-S/T	R-X_{1-2}-S/T K-M-S/T K-R-X-X-S/T
PKC	S/T-X-K/R	R/K-X_{0-2}-S/T-X_{0-2}-R/K R/K-X_{1-2}-S/T
PKG	R/K_{1-2}-X_{1-2}-S/T	S/T-X-K/R
CaMKII	X-R-X-X-S/T	X-R-X-X-S/T-V
Src	R/K-X_{2-3}-D/E-X_{2-3}-Y	

Table 1.1: Optimal protein kinase consensus motifs. The accepted optimal consensus motifs of protein kinases A (PKA), C (PKC), G (PKG), calmodulin kinase II (CaMKII) and Src tyrosine kinase are illustrated together with other suitable, common consensus motifs [226-228]. Other motifs that are not shown may function as consensus motifs for these protein kinases also. Phosphorylatable residues are highlighted in red. Standard one letter amino acid code used.

Figure 1.5
Putative phosphorylation target sites in the BK channel C-terminal domain

Figure 1.5: BK channel residues identified as protein kinase phosphorylation targets. Site directed mutagenesis studies have identified several residues in the cytoplasmic C-terminal domain of BK channel α-subunit protein as possible targets of protein kinase-directed phosphorylation. In the murine channel sequence, these sites include the conserved PKA target, S869, and the STREX splice variant-specific putative PKA phosphorylation target, STREX S4. Also, the possible PKC targets, S1098 and S1101, the PKG S1081 phosphorylation site and the tyrosine-kinase Src phosphorylation target, Y762. Many other sites may exist including targets for other kinases and indeed, splice variation (splice sites 1-5 indicated by pink triangles) may introduce or preclude phosphorylation sites. Standard one letter amino acid code used.

Drosophila sequence, comprising R-Q-P-S869 in comparison to the insect R-R-G-S942 (See Table 1.1), mutation of the serine also inhibits PKA-mediated regulation of the mammalian BK channel [205, 229]. Similarly, mutagenesis of the canine smooth muscle BK channel serine-1072 to alanine inhibited PKG-mediated activation of the channel suggestive of direct PKG-phosphorylation at the site [209].

In other situations regulation of BK channel activity by various protein kinases can be influenced by integrating signal transduction pathways via direct phosphorylation of the α-subunit protein [195]. Priming of the S1151-S1154 tandem PKC consensus motif of certain bovine aortic smooth muscle BK channel splice variants makes channels responsive to PKG, but not PKA [195]. Inhibition of PKC-phosphorylation, or assay of splice variants lacking the S1151-S1154 motif, switches channel responsiveness from PKG to PKA thus implicating a complex, integrative regulation of the ion channels via direct protein phosphorylation [195]. The responsiveness of a particular BK channel to a specific protein kinase in a particular system or cell type is, therefore, likely to be influenced by several factors including the associated proteins, the sequence of signal transduction pathway stimulation and the BK channel splice variant expression [195, 210]. For example, rat small arterial BK channels are suggested to respond to PKA, but not PKG [230], rat hippocampal neuronal and rabbit distal colon epithelial BK channels are responsive to PKA, and not PKC [191, 200] and dopamine-induced vascular relaxation of porcine coronary arteries results from PKG and not PKA [210]. Additionally, in rat anterior pituitary tumour cells conditional phosphorylation between

PKA and PKC is suggested at distinct sites that can be reversed by distinct protein phosphatases [192]. Although the molecular mechanisms of these effects are uncharacterised, they may explain, at least in part, why BK channels exhibit a range of responses to protein kinases and phosphatases in different locations and under different physiological conditions [195, 210] and even why some BK channels are reported as being unresponsive to protein kinase activity [142].

Indirect phosphorylation influencing BK channel activity

Alternatively, certain protein kinases may exert their influence on BK channel activity indirectly through phosphorylation and subsequent activation/inactivation of auxiliary or intermediary proteins [161]. Conserved protein kinase consensus motifs in the β4-subunit implicate this as a possible pathway of regulation, influencing the functional coupling of the auxiliary protein to the channel [161, 186]. Similarly, PKG in bovine tracheal smooth muscle cells is suggested to influence the activity of BK channels by stimulating protein phosphatase action on the phosphorylated BK channel protein [231]. Additionally, association of the novel protein, Slob, with *Drosophila* BK channels is dependent on its phosphorylation by CaMKII (See Section 1.5.2).

1.4.1.3 Splicing influences BK channel regulation by reversible phosphorylation

As suggested by the integrative PKA-PKG-regulation observed with bovine aortic smooth muscle BK channels (See above, [195]), the effect of a particular protein kinase on channel activity can be influenced by splicing of the channel α-subunit mRNA,

providing another facet of the specialisation and functional diversity exhibited by BK channels (See Section 1.3.1.2). The STREX insert provides a perfect illustration of this. Channels expressing the cysteine-rich insert not only possess distinct kinetics and calcium/voltage-sensitivities in comparison to their insert-less, ZERO, counterparts (See Section 1.3.1.2.1), but also display variation in the PKA-mediated response [69, 80, 229]. Activation of endogenous PKA induces heterologously expressed ZERO channel activation, whereas STREX channels are inhibited [80, 229]. Such distinctive divergence may be critical to the role of the splice variants in various physiological processes including the hypothalmic-pituitary-adreno-cortical (HPA) stress axis where the STREX:ZERO channel ratio is crucial to the dynamic effectiveness and responsiveness of the stress response (Section 1.3.1.2.1) [80, 84, 89, 229]. The molecular mechanism that underlies this distinct variation in PKA-mediated response is uncharacterised currently. However, several putative phosphorylation target sites are identified within the 58 residue STREX insert sequence including one motif of notable homology to the optimal PKA consensus motif (Serine 4, Figure 1.6) [229]. Such sites may co-phosphorylate or compete with and override other phosphorylatable residues in the channel sequence inducing the inhibition of channel activity. Equally, the presence of the insert in the regulatory-critical C-terminal domain (Section 1.3.2.2.2) may alter the domain structure conformationally, particularly probable due to the presence of the multiple STREX cysteine residues, amino acids that are often critical in forming protein secondary structures [69]. This may create or obstruct phosphorylation target sites or influence the association of regulatory proteins that are crucial to the PKA-mediated response, perhaps even the kinase itself. Intriguingly, the presence of the STREX insert

Figure 1.6
STREX insert protein sequence

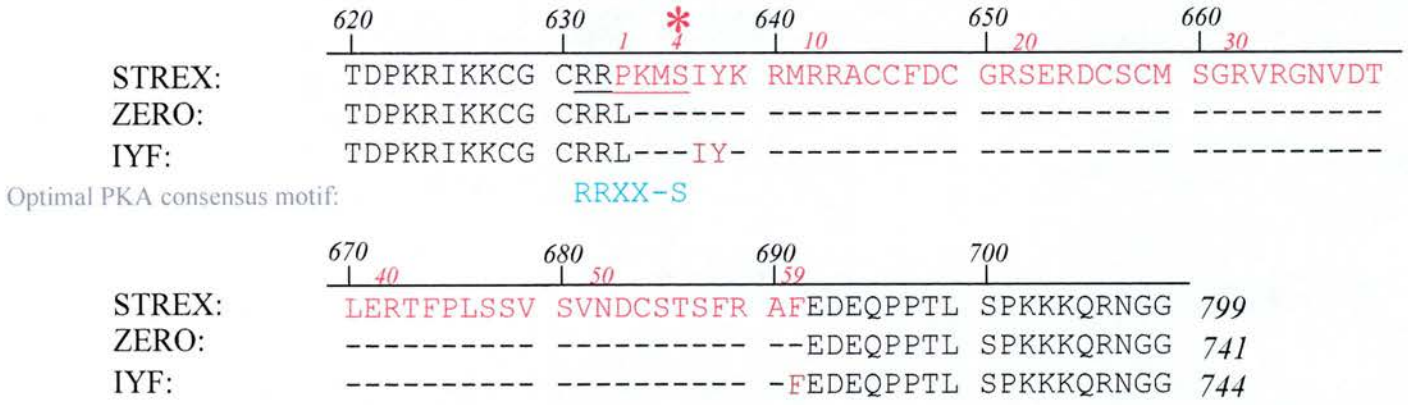

Figure 1.6: Sequence alignment of three BK channel splice variants at splice site 2. The STREX insert (red text) comprises a 58 residue long sequence (red numbering) present at splice site 2 in the STREX channel sequence. The sequence adds several putative phosphorylation target residues to the channel sequence, in particular, $RRPKMS_4$ at the start of the insert (underlined, target serine marked) is analogous to the optimal PKA phosphorylation consensus motif (blue text). The STREX insert is absent from ZERO channels, and another splice variant, IYF, expresses the residue trio at splice site 2. Other BK channel splice variants exist and some are described for splice site 2. Standard one letter amino acid code used.

in the channel sequence is required for BK channel sensitivity to glucocorticoids [229, 232]. Glucocorticoids, including synthetic dexamethasone, are suggested to induce the synthesis of proteins that stimulate protein phosphatases or a phosphatase-like protein to influence the effects of PKA upon splice variant activity [194, 233].

1.4.2 Other modes of regulation

In addition to reversible phosphorylation, many other factors influence BK channel activity, providing further evidence for the intrinsic nature of these vital channels to many, diverse physiological processes. The wide variation and number of these putative regulatory factors is outlined within the following section (Figure 1.7). This overview is not definitive but serves to illustrate how diverse regulatory pathways may converge to regulate BK channel function and activity.

1.4.2.1 Hormones

Oestradiol

Steroid hormones such as oestrogen and progesterone initiate physiological effects via nuclear receptors, stimulating genomic effects namely the transcription and translation of proteins [214, 218]. However, recent evidence suggests that oestrogens may instigate rapid cellular responses by non-genomic action upon the BK channel complex [234-236]. Oestradiol and analogues such as the chemotherapeutic xenoestrogen, tamoxifen ([*Z*]-1-[*p*-dimethylaminoethoxyphenyl]-1,2-di-phenyl-1-butene), are suggested, at physiological/therapeutic concentrations, to interact with the BK channel β1, and

possibly β3 and β4, subunits via an extracellular binding site or auxiliary protein [185, 234-236]. This activates BK channels influencing the kinetics and activation potentials affecting physiological functions such as vascular smooth muscle tone [234-236]. The effect is not observed in β1 subunit knock out mice and the rapidity, reversibility and observance of the effect in cell-free patches highlights the non-genomic nature of the response [235]. Addition of non-membrane-permeable tags such as bovine serum albumin (BSA) or ethylbromide to oestradiol compounds does not inhibit the effect of the hormone, indicating that the influence occurs at an extracellular binding site [234, 236]. Thus, other hormones and signalling agents could interact extracellularly with the BK channel complex in addition to intracellular signalling. Steroidal bile acids have been implicated [237].

1.4.2.2 Nitrocompounds

Activation of cellular nitric oxide synthase (NOS) generates production of endothelium-derived relaxing factor (EDRF), nitric oxide (NO) [196, 238]. This diffusible gas activates soluble guanylate cyclase (GC) inducing cGMP production and subsequent activation of PKG, which, as noted above (Section 1.4.1), regulates BK channels by phosphorylation [196, 239]. However, GC inhibition or removal of ATP or GTP in combination with NOS stimulation or exogenous NO application still results in BK channel stimulation is some systems indicating a PKG-independent pathway [36, 239, 240]. NO has been reported to remove the calcium requirement for BK channel activation enabling activation at nanomolar calcium concentrations, well below those

required under basal conditions [36]. Conversely, inhibition of NOS reduces the BK channel Po in rat smooth muscle cells [241]. Thus, NO and various, related nitrocompounds or their by-products are suggested to modulate BK channels via direct chemical modification of the channel protein or associated proteins [36, 239]. This indicates that drugs that stimulate NO synthesis, such as the barbiturate, thiopentone [242], and 1-ethyl-2-benzimidazolinone (1-EBIO) [44], may induce their effects, at least in part, through this mechanism [44, 242]. Such nitrocompound stimulation of BK -stimulation and the subsequent decrease in membrane excitability that underlines reduced posterior pituitary hormone secretion [36], the pathophysiology of cirrhosis [243], and the influence of the peptide vasodilator, bradykinin [244].

1.4.2.3 Redox Reagents / pH

The redox potential of the sub-cellular, cytoplasmic environment surrounding the BK channel influences channel activity [245]. Chemical reducing agents such as dithiothreitol activate cloned human BK channels, whereas oxidising agents such as hydrogen peroxide inhibit [245]. This implies that native, intracellular redox reagents, including NADH and glutathione, may modulate the channels *in vivo*, perhaps regulating the oxidative stress response [246-250]. However, the *Drosophila* BK channel is not responsive to redox reagents suggesting that the effect is not universal and may not be an important method of modulation [245]. The effect may result from reagents altering the ionisation state of integral BK channel residues that affect the response to other regulatory factors such as the β1 subunit [245, 246]. In heterologously expressed rat BK

channels, the presence of the cysteine-rich STREX insert makes the channels ten-fold more sensitive to inhibition by oxidation than ZERO channels that do not express the insert demonstrating that sequence differences due to splice variation can be influential to such regulation [251]. Indeed, alteration of the ionisation state of residues may be the basis of the pH response of BK channels, where activation follows a decrease in the test solution proton concentration (pH 7.0 – 7.8) and inhibition follows an increase [252, 253].

1.4.2.4 Lipids

Recognition of bacterial lipid endotoxins during mammalian cell infection induces NOS expression that stimulates BK channels through PKG and NO (See Sections 1.4.1 & 1.4.2.2) contributing to the pathophysiology of septic shock and bacterial meningitis [254, 255]. Following exogenous application of the *E.coli* endotoxin, lipopolysaccharide, to murine arterial smooth muscle, BK channels are activated rapidly and reversibly, an effect observed with NOS inhibitor, N^{ω}-nitro-L-arginine, treatment and in NOS-knock-out mice cells [256]. This suggests that the lipid induces PKG- and NO-independent channel activation either directly, or by intermediate proteins [256].

Even in non-stress situations, lipids may influence BK channel activity. The common fatty acid, arachidonic acid (AA), is synthesised and travels in the circulation for uptake by the central nervous system and metabolism into ion channel-influencing active factors [257, 258]. Intact, non-metabolised AA is suggested to activate certain rat GH3 cell BK channel splice variants, increasing calcium-sensitivity through a putative,

cytosolic AA-binding site or via interacting proteins [212, 259]. AA is proposed not to influence the membrane properties to affect its influence [259] although the membrane lipid content is influential to BK channel activity [260, 261]. The conductance of bovine smooth muscle BK channels reconstituted into charged lipid bilayers is higher than in neutral membranes [260], and the differential properties of cell body and presynaptic channels (See Section 1.3.1.2) is partially attributed to the distinct proteolipid environments of the subcellular locations [20]. Indeed, ethanol, which induces analgesia and parethesia, is suggested to disturb membrane lipids non-specifically, increasing BK channel Po [262-264]. Thus, the plasma membrane lipids could be influential to BK channel specialisation.

1.4.2.5 Pharmacological activators & inhibitors

As mentioned in the introduction to this section (Section 1.4), several factors may influence the activity of BK channels, far too many to explain in detail in this thesis. Therefore, only a few of these are described below.

Activators

The benzimidazolones, compounds including NS004, NS1608, NS1619, niflumic acid and 1-EBIO, are suggested to activate BK channels directly [43, 44, 119, 136, 138, 265-270]. Other putative BK channel activators include cromakalim [271], the alkylating agent, N-ethyl-maleimide (NEM) [36], the indicator azo dye, Evans Blue [43, 272, 273], and the anilide carbinol, ZD6169 at high concentrations, 50 μM, although lower

concentrations activate ATP-activated potassium channels [274]. Additionally, the saponin, DHS-I, is observed to activate BK channels in the presence of β-subunits, but not in the absence of the auxiliary protein (See Section 1.3.2.2.4; [160])

Inhibitors

Indole diterpene alkaloids including verruculogen, penetrem A, aflatrem and the fungal mycotoxin, paxilline, are among the most potent BK channel blockers, acting at a site distinct from the ChTX binding site (See Section 1.3.2.1) [119, 184, 275] (Reviewed Kaczorowski *et al*, 1996 & 1999 [65, 276]). A serine-proteinase-like domain (See Figure 1.3) is proposed in the BK channel α-subunit C-terminus that enables the interaction of inhibitory serine protease inhibitors, namely bovine pancreatic trypsin inhibitor and chicken ovoinhibitor [67]. Other putative inhibitors include gadolinium [47], verapamil [277], tetrandrine, an alkaloid that may act via cAMP signalling [43, 273], and the convulsant, pentylenetetrazole (PTZ) [241].

1.4.3 Overview of BK Channel Modulation

Thus, the modulation of BK channels is influenced by several, distinct signal transduction pathways, through multiple mechanisms including reversible phosphorylation of the channel and auxiliary proteins, hormone regulation, and changes in pH and the redox state surrounding the channel. The intrinsic cellular and subcellular environments are influential to channel activity through characteristic features including the lipid environment. Pathological conditions such as bacterial infection and ischemia

affect BK channel regulation and various drugs are determined as influential to channel activity also. All of these factors are in addition to the intrinsic voltage and calcium regulation that are characteristic of BK channels. Some of the influences are illustrated in Figure 1.7 and it is probable that several other factors will be uncovered with the elucidation of the molecular mechanisms underlying the overall, complex modulation of the BK channel. Thus, BK channels integrate many cellular and extracellular, homeostatic and pathological signalling pathways enabling the diverse, rapid and extensive responses that facilitate the significance of BK channel to numerous, varied physiological processes (Section 1.2).

1.5 The BK Channel Complex

As illustrated in Sections 1.3 and 1.4, BK channel activity is influenced by several, diverse, independent signalling pathways (Figure 1.7), some of which exert their influence directly upon the BK channel α-subunit protein through signalling proteins including the β-subunits, protein kinases and protein phosphatases. Indeed, co-immunoprecipitation and yeast two-hybrid strategies have identified novel as well as well-documented proteins that may assemble with BK channels, in addition to the accessory β-subunits (discussed in Section 1.3.2.2.4). The ability of BK channels to respond rapidly to many protein signals led to the suggestion of the channel tetramer functioning as a scaffold, forming a channel complex that encompasses several signalling proteins bound either directly or indirectly through intermediary, scaffolding proteins [6, 125, 204]. Such proteins are proposed to associate intimately with the

channel protein in sufficient proximity to facilitate rapid and thus effective ion channel responses, removing the need for the prohibitive, time-limiting translocation of signalling molecules to the channel tetramer [125, 278]. Such complexes are described for other ion channels [125], including Kv channels [279, 280], calcium channels [281] and N-methyl-D-aspartate (NMDA)-receptors [282, 283]. The body of evidence supporting such a model for BK channels is increasing.

1.5.1 Protein kinases & protein phosphatases

In the absence of exogenous protein kinase or phosphatase, reconstituted BK channels and those investigated in excised membrane patches, still exhibit the regulatory effects of reversible phosphorylation [190, 196, 200, 202, 204]. This implicates close associations between the channel tetramer and endogenous protein kinases and/or phosphatases and suggests that that the channel may be part of a multi-protein regulatory complex [204, 284]. For example, rat brain BK channels have been suggested to associate with a PKC-like protein kinase [284], a PP1-like protein phosphatase [284] and PKA [200]. The *Drosophila* BK channel from native and heterologous expression sources co-immunoprecipitates simultaneously with the independently regulated Src kinase and the catalytic subunit of PKA (PKAc) [204]. Co-immunoprecipitation suggests a physical interaction and this was shown to be independent of the phosphorylation state of the channel with the C-terminal domain characterised as the location of PKAc association [204]. However, although PKAc is suggested to bind directly to the BK channel protein, Src may associate indirectly through an auxiliary, bridging protein(s) [204]. In mammalian systems, even the occurrence and the nature of

a PKAc-BK channel interaction is undetermined although other mammalian channels are noted to bind protein kinases directly [285-287]. Mammalian cells often express AKAPs (A-kinase anchoring proteins), accessory proteins that bind to the regulatory subunits of PKA with nanomolar affinity via hydrophobic interactions, anchoring the protein kinase to directly bind to the channel, proximal to target proteins to facilitate efficient phosphorylation (Figure 1.7) [202, 278, 288]. AKAPs have been found to mediate the targeting of PKA to several, distinct ion channels including calcium channels [278, 289] and AMPA (α-amino-3-hydroxy-5-methyl-4-isoxazole propionate)/kainite receptors [288]. Thus, mammalian BK channels may interact with protein kinases via AKAPs or similar anchoring proteins. The AKAP inhibitor, Ht31, is reported to block ATP-dependent regulation of BK channels in equine smooth muscle cells [290]. Further investigations of the interactions may uncover the molecular mechanism that may underlie such associations.

Other protein kinases and phosphatases may associate functionally with the BK channel [194, 231]. However, it should be noted that a protein kinase or phosphatase may be associated functionally and thus be able to promote phosphorylation/dephosphorylation, but may not interact physically as to co-immunoprecipitate with the channel. For example, CaMKII phosphorylates human and *Drosophila* BK channels *in vivo* and *in vitro*, but co-immunoprecipitates with the human form only [204]. Equally, protein-protein interactions may be influenced by BK channel splice variation and by the metabolic state of the signal transduction pathways of the cell.

Figure 1.7
The BK channel: structure, complex & modulation

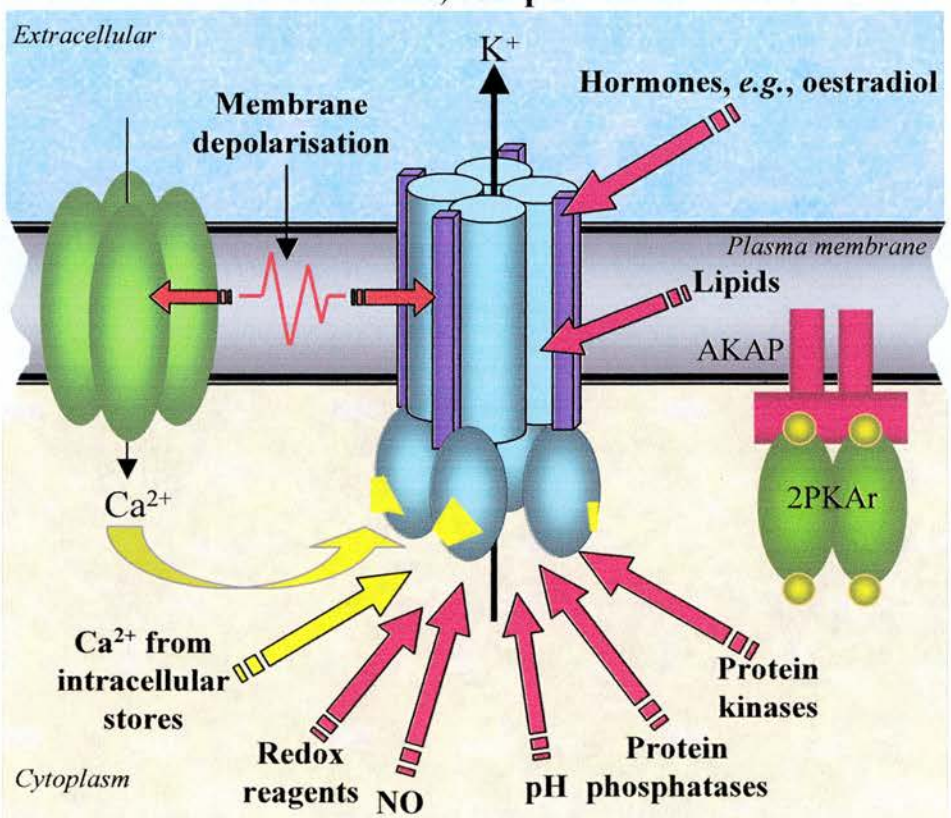

Figure 1.7: Modulation of the BK channel. BK channels (blue) are modulated by several, distinct signal transduction pathways. Intrinsic modulation by membrane depolarisation (red), and by intracellular calcium through the calcium bowl (yellow) occurs. Intracellular calcium concentrations are influenced by release from intracellular stores and activation of Ca_v channels (light green). Other modulatory factors include β-subunits (purple), hormones, nitrocompounds such as nitric oxide (NO), redox reagents, pH, lipids and various pharmacological agents. Reversible phosphorylation of the BK channel protein and/or accessory proteins by various protein kinases and protein phosphatases is also implicated. Some factors may associate as part of a channel complex, perhaps via bridging proteins like AKAPs, and divergent influences are observed depending upon factors including channel splicing and cellular protein expression.

1.5.2 Accessory proteins

In addition to the β-subunits (Section 1.3.2.2.4) and protein kinases and phosphatases (Section 1.5.1), other proteins have been identified as associating with the BK channel complex. Yeast two-hybrid screens with a *Drosophila* BK channel identified a novel protein that associated with the ion channel, the Slowpoke-binding protein (Slob) [291, 292]. The CaMKII-phosphorylated Slob protein bound the 14-3-3 adapter protein ζ isoform in native *Drosophila* tissues and in heterologous systems, bridging 14-3-3ζ and the BK channel [292]. As 14-3-3 proteins are suggested to act as scaffolds for regulatory proteins including protein kinases, this association may be crucial to the formation and maintenance of the BK channel complex, and may be influential to BK channel regulation, perhaps especially in processes such as cell cycle control and apoptosis in which 14-3-3 proteins are implicated [292].

1.5.3 Overview of the BK channel complex

Increasing evidence is accumulating suggesting that the BK channel exists as a complex of several auxiliary and regulatory proteins bound around the central pore. Described in the above section are some putative associating proteins that may directly or indirectly associate with the BK channel tetramer. However, these proteins may not associate in all species, cell type, sub-cellular location and with particular splice variants and may be dependent dynamically upon the metabolic state of the cell. The possible protein associations are numerous and are likely to vary depending upon such factors. The complex may be large, composed of several additive factors. Not all regulatory proteins

may be associated at all times, if at all. Indeed, PKG is not observed to associate with the channel, although it is implicated in direct phosphorylation of the BK channel α-subunit [195]. However, the benefits in forming a channel complex both in efficiency and effectiveness support the idea that BK channels exist as a dynamic complex.

1.6 Overview & aims of this thesis

In conclusion, BK channels represent a unique yet integral subset of potassium channels that manifest many distinct properties that allow them to participate in, and be critical to, a wide range of important physiological functions through multi-sourced regulation, responsive to several signal transduction pathways, both homeostatic and pathological. Therefore, these channels are of great interest physiologically, in their functional roles; biochemically, in their complex modulation; and biophysically, in their complex kinetics and activation. All this resulting from only one gene, with variation in the intrinsic channel characteristics resulting at least in part from pre-mRNA splicing.

This study aims to investigate the molecular basis of mammalian BK channel regulation by PKA. In Chapter 3, the various fusion proteins and antibodies used in this study are described. Chapter 4 investigates whether the α-subunit protein is a direct target of PKA-mediated phosphorylation and addresses the influence of the STREX insert on channel phosphorylation. In Chapter 5, the assembly of the BK channel complex is investigated, determining if PKA can associate with the α-subunit.

Chapter Two:

Materials & Methods

Chapter Two: Materials & Methods

2.1 General materials & reagents

General molecular biology reagents used throughout this study were of analytical grade and obtained from Sigma Chemical Company, except where stated otherwise. Unless indicated, solutions were autoclaved (100 kPa, 20 mins, B&T autoclave 225EH).

2.1.1 Molecular biology reagents

DEPC-Treated Distilled Water

0.05 % diethyl pyrocarbonate (v/v; DEPC) in distilled water (dH_2O).

TBE Buffer

50x TBE Buffer: 2.2 M Tris, 2.45 M boric acid, 80 mM ethylenediaminetetraacetic acid (EDTA) in dH_2O. Diluted as required.

DNA Loading Buffer

6x stock prepared with 720 µl 50x TBE Buffer, 330 µl glycerol, and bromophenol blue, diluted to 1x with dH_2O and DNA for use.

DNA Markers

1 kb markers (Gibco), diluted 1/10 for use.

2.1.2 Biochemistry reagents

Luria Berani (LB) Broth and Agar

10 g tryptone (BD), 5 g yeast extract (BD), and 5 g NaCl were dissolved in 1 L dH_2O and the pH raised to pH 7.4 with NaOH. For LB-agar, 3.75 g of Bacto-Agar (BD) was added to 250 ml LB broth and all solutions were autoclaved prior to use.

Isopropyl β-D-thiogalactopyranoside (IPTG, Calbiochem)

IPTG was stored at –20 ^{0}C as a 1 M solution, prepared by dissolving 2.383 g in 10 ml of dH_2O. This sugar induces recombinant protein synthesis from plasmids containing the *lac* operon, such as the pGEX plasmids used in this study.

STET Buffer

8 % sucrose (w/v); 10 mM Tris HCl, pH8.0; 0.5 M EDTA; 0.5 % Triton X-100 (v/v).

Phosphate buffered saline (PBS)

137 mM NaCl, 2.7 mM KCl, 4.3 mM Na_2HPO_4, 1.47 mM KH_2PO_4, adjusted to pH 7.1.

Phosphate buffered saline + Tween-20 (PBS-T)

0.05 % (v/v) Tween-20 added to PBS.

2.1.2.1 Antibiotic Solutions

Ampicillin (Amp)

A stock solution of 100 mg/ml in dH_2O was diluted to 100 μg/ml in LB broth and agar for selection of bacteria expressing pcDNA3, pGEX and pBAD/Thio-TOPO vectors.

Tetracycline (TET)

Stock solutions of 5 mg/ml in ethanol were diluted to 50 μg/ml in LB broth and agar for selection of the *E.coli* XL1-Blue strain.

Geneticin (G418, Calbiochem)

Stock solution of 0.8 g/ml in dH_2O stored at –20 ^{0}C, used at 0.8 mg/ml final concentration for selection of pcDNA3 plasmids in HEK293 cells.

2.1.2.2 Protein Analysis Solutions

Laemmli Buffer – SDS-PAGE Running Buffer

10x Stock: 35 mM sodium dodecylsulphate (SDS), 0.25 M Tris and 2 M glycine in dH_2O. Dilute to 1x for use as running buffer for non-radioactive protein electrophoresis.

SDS-Polyacrylamide Gel Electrophoresis Loading Buffer (SDS-LB)

2x stock of 125 mM Tris, pH 6.8, 20 % glycerol (v/v), 4.1 % SDS (w/v), in dH_2O with sufficient bromophenol blue to turn the solution blue. This stock was stored at –20 ^{0}C and used as 1x for diluting protein samples.

Protein Markers

Kaleidoscope pre-stained standards (BioRad) with a range of 200 – 6.5 kDa.

Towbin Transfer Buffer (TTB)

10x TTB (Stock Solution): 0.25 M Tris, 35 mM SDS, and 2 M glycine in dH_2O. Diluted to 1x for use in 10 % ethanol (v/v).

Lithium dodecyl sulphate - Loading Buffer (LDS-LB)

A 2x stock solution was prepared by mixture of 320 µl dH_2O, 250 µl LDS Sample Buffer (Invitrogen), and 100 µl 0.5 M 2-mercaptoethanol for use as the NOVEX gel (Invitrogen) loading buffer.

MOPS SDS Running Buffer

Prepared as 20x Buffer: 1 M MOPS (3-[N-morpholino] propane sulphonic acid), 1 M Tris base, 69.3 mM SDS, 20.5 mM EDTA, pH 7.7. Used as 1x for running NOVEX gels (Invitrogen).

2.2 General Molecular Biology Protocols

General molecular protocols were based upon those of Sambrook et al (1989) [293] *unless stated otherwise.*

2.2.1 Transformation of plasmid DNA into bacterial cells

50 – 100 µl of competent bacteria cells were incubated with ~10 ng plasmid DNA (4 ^{0}C, 30 mins). Heat shock to induce plasmid uptake (42 ^{0}C, 45 sec) was followed by recovery (4 ^{0}C, 2 mins) and dilution with 400 µl LB broth. Cultures were incubated with agitation (37 ^{0}C, 45 mins), then 50-200 µl plated onto a LB agar plate with antibiotic appropriate for plasmid selection. Plates were incubated at 37 ^{0}C for ~16 hours.

2.2.1.1 Bacterial strains

The XL1-Blue (Stratagene) and JM109 (Stratagene) strains of *Escherichia coli (E.coli)* were employed in this study when amplification of DNA was required.

The BL21-RIL *E.coli* strain (Stratagene) was used for recombinant protein expression. The strain does not express the Lon and OmpT proteases, reducing recombinant protein proteolysis compared to that of other bacterial strains. In addition, the strain expresses greater quantities of arginine (R), isoleucine (I), and leucine (L) tRNAs than other BL21 varieties (314). The efficiency of recombinant protein expression is proposed to be influenced by the contrasting levels of certain tRNAs in a bacterial system and that of the organism from which the protein has been isolated [294]. Comparison of the codon usage of native *E.coli* and the species that the fusion partners and BK channel protein was isolated from is illustrated in Table 2.1. As *E.coli* employ R, I and L codons less than the other species, use of the BL21-RIL strain should decrease this difference, encouraging effective and efficient recombinant protein production. This may contribute particularly to the successful expression of the leucine zipper fusion protein that encompasses a high proportion of isoleucine and leucine residues (Section 3.2.1.2).

2.2.2 Determination of bacterial exponential growth

Determination of exponential growth of *E.coli* cells was achieved by measurement of the optical density of a culture at 600 nm (OD_{600}) using a Cecil CE2040 spectrophotometer. Values indicative of the phase are between 0.4 and 0.8.

Table 2.1
Comparative codon usage of species

CODON	EXPRESSES		ORGANISMS	
		Escherichia coli	*Mus musculus*	*Schistosoma japanicum*
		Expression system & source of thioredoxin fusion tag	Source of cloned BK channel	Source of GST fusion tag
AGA	Arginine	3.6	11.3	13.9
AGG	Arginine	2.1	11.6	3.5
AUA	Isoleucine	6.8	7.0	18.2
CUA	Leucine	4.2	7.8	8.8

Numbers refer to triplet frequency use per thousand codons (www.kazusa.or.jp/codon/) [295].

The native recombinant expression system, *E.coli*, uses less of the above arginine, isoleucine and leucine codons than mouse (*Mus musculus*), or the helminth (*Schistosoma japanicum*).

2.2.3 Rubidium chloride preparation of competent cells

Competent cells were prepared as described by Hanahan (1985) [296].

A single colony of *E.coli* competent cells from a LB-agar plate* was inoculated into 5 ml LB broth* and incubated with constant shaking (37 ^{0}C, ~16 hours), then inoculated into 250 ml LB broth* and grown at 37 ^{0}C with constant agitation until the cells reached the exponential growth phase. Cells were centrifuged (4500 g, 4 ^{0}C, 5 mins) and the pellet resuspended on ice in 100 ml of TFB1 (TransFormation Buffer I; 30 mM potassium acetate, 10 mM $CaCl_2$, 50 mM $MnCl_2$, 100 mM RbCl, 15 % glycerol (v/v) adjusted to pH 5.8 with 1 M acetic acid and sterilised through 0.2 μm filter). Resuspension in 10 ml of ice-cold TFB2 (TransFormation Buffer II: 10 mM MOPS, 75 mM $CaCl_2$, 10 mM RbCl, adjusted to pH 6.5 with 1 M KOH and sterilised through 0.2 μm filter) followed a second centrifugation (5 mins, 4500 g, 4 ^{0}C). Cells were incubated (1 hr, 4 ^{0}C), aliquoted, and snap-frozen by dry ice / isopropanol treatment prior to storage at –70 ^{0}C.

*no antibiotic added except during XL1-Blue competent cells preparation using 50 μg/ml TET.

2.2.3.1 Test of the transformation efficiency of competent cells

Competent cells were transformed with 1 μg, 0.1 μg and 0.01 μg of control plasmid DNA, 100 μl plated on LB-agar plates with appropriate antibiotic and incubated (16 hrs, 37 ^{0}C). To assess background, negative control reactions were performed in the absence

of plasmid DNA. The numbers of colonies (colony forming units, cfu) on each test plate were used to calculate a value for the transformation efficiency of the competent cells, employing the following algorithm [297]:

Transformation efficiency =

$$\left[\frac{\text{cfu}}{\text{ng vector plated}}\right] \cdot \left[\frac{10^3 \text{ ng}}{1\ \mu\text{g}}\right] \cdot \left[\text{Dilution plated}\right]$$

Typical transformation efficiencies of 10^7 - 10^8 cfu / μg were obtained for prepared competent cells. Cells displaying significantly lower efficiencies were discarded.

2.2.4 Bacterial glycerol stocks

~0.85 ml of bacteria culture incubated with agitation (37 ^{0}C, ~16 hrs) was diluted with ~0.15 ml sterile glycerol, suspended by vortexing and snap-frozen in an isopropanol / dry ice bath prior to long-term storage at –70 ^{0}C. Cultures were recovered by inoculation into LB broth with appropriate selecting antibiotic.

2.2.5 Determination of Protein Concentration (Bradford Assay)

Analysis of protein concentration was determined following the procedure of Bradford [298].

20 μl dilutions of the protein of interest were combined with 50 μl 1 M NaOH and 1 ml Bradford's Reagent (0.01 % Serva Blue G (w/v) dissolved in 85 % phosphoric acid

(v/v), 95 % ethanol (v/v), and dH_2O, at a ratio of 10:5:85 by vol.). Solutions were mixed by vortexing, incubated at room temperature for 10 mins, and the absorbance at 590 nm measured. Protein concentration was determined by comparison to a standard curve, prepared by Bradford analysis of standard concentrations of bovine serum albumin (BSA).

2.3 General DNA Analysis Protocols

2.3.1 Agarose gel electrophoresis

Gels composed of 1x TBE buffer, 1 % agarose (w/v; Promega, U.K.) and ethidium bromide (0.5 μg/ml) to allow visualisation of DNA under ultraviolet light. Gels were run on the Pharmacia Gel Electrophoresis Apparatus GNA-100 in 1x TBE Buffer.

2.3.2 Purification of DNA from agarose gels

DNA bands cut from agarose gels were purified using the QIAGEN QIAEX II purification kit following the QIAGEN protocol as follows; bands were dissolved in Buffer QX1 (1:3 weight:volume, 50 ^{0}C) and incubated (10 mins, 50 ^{0}C) with 10 μl QIAEX II slurry permitting DNA-slurry association. Washing with Buffer QX1 and Buffer PE preceded air-drying of the pellet (10-15 mins, ~16 ^{0}C) and incubation in 20 μl DEPC dH_2O (5 mins, ~16 ^{0}C) to release the DNA into solution. The slurry was removed by centrifugation (30 sec, 10 000 g; Eppendorf Centrifuge 5415C).

2.3.3 Restriction digestion of DNA

Endonuclease digestion of DNA at particular motifs allowed the production of complimentary ends of plasmid and insert allowing ligation and subsequent construct formation, and to assess DNA fragments following construct formation.

~1 µg of DNA was combined with endonuclease(s) (Promega/New England BioLabs) in appropriate buffer (Promega/New England BioLabs) and incubated at a temperature and for a period appropriate for optimal endonuclease activity as recommended by the enzyme manufacturers. Samples were analysed by agarose gel electrophoresis (Section 2.3.1).

2.3.4 Alkaline Lysis: Plasmid DNA purification

Purification of plasmid DNA was performed as described by Birnboim & Doly (1979) [299].

2.3.4.1 Mini-preparation

The cellular pellet from ~1.5 ml of bacteria culture (incubated 37 ^{0}C, ~16 hrs; centrifuged 30 sec, 10 000 g) was resuspended in 250 µl Resuspension Solution (10 mM Tris HCl, pH 8.0; 1 mM EDTA, pH 8.0; 8 % RNase A (v/v)) and incubated for 5 mins at room temperature to promote suspension and RNA degradation. Addition and gentle mixing of 250 µl Lysis Solution (0.2 M NaOH; 1 % SDS (w/v)) promoted plasma membrane and hydrophobic protein solubilisation to lyse the bacterial cells whilst denaturing plasmid and chromosomal DNA. Within 5 mins, 350 µl of Neutralisation

Solution (3 M K^+, 5 M acetate: 60 ml 5 M potassium acetate, 11.5 ml glacial acetic acid, 28.5 ml dH_2O) was added gently and incubated (–20 ^{0}C, 5 mins). This aided the precipitation of the insoluble dodecylsulphate potassium salt with insoluble aggregates of chromosomal DNA and aggregated proteins that were removed by centrifugation (5 mins, 10 000 g). Interstrand rehybridisation maintained plasmid DNA in solution, and 850 µl phenol:chloroform:isoamyl alcohol (25:24:1) was added and mixed to enable separation of the aqueous plasmid DNA from any phenol-soluble proteins and non-plasmid DNA. 850 µl isopropanol was added to the separated aqueous phase precipitating the double stranded plasmid DNA. Following centrifugation (30 mins, 10 000 g), the supernatant was aspirated and 70 % ethanol (v/v) added to remove residual salt and replace the less volatile isopropanol. Plasmid DNA was resuspended in 50 µl Resuspension Solution after centrifugation (30 sec, 10 000 g) and ethanol removal.

2.3.4.2 Midi- and maxi- preparations

Alkaline lysis purification of plasmid DNA on midi- (<200 µg) or maxi- (>200 µg) scales were performed using the QIAGEN HiSpeed™ Midi Plasmid Preparation and QIAGEN QIAfilter™ Plasmid Maxi Preparation Kits respectively, following the manufacturer's instructions.

2.3.5 Ethanol extraction

To concentrate nucleic acid solutions, 3 M sodium acetate, pH 5.5, was mixed with DNA solution (1:10 by volume). Addition of ice-cold, 100 % ethanol and glycogen

(2.5:0.01:1 DNA solution by volume) aids DNA precipitation and isolation. The DNA pellet was washed with 70 % ethanol (v/v) following centrifugation (10 000 g, 30 mins) and resuspended in an appropriate volume of Resuspension Solution (See Section 2.3.4).

2.3.6 DNA quantification & determination of contamination

Measurement of the optical density of a DNA solution at 260 nm, OD_{260}, determined the nucleic acid concentration. The ratio of OD_{260}:OD_{280} was used as a measure of protein and phenol contamination, with values less than 1.8 indicative of high contamination.

2.4 Molecular cloning & manipulation

2.4.1 Polymerase chain reaction amplification of DNA sequences

The Polymerase Chain Reaction (PCR) was used to amplify regions of mouse BK channel splice variant cDNA allowing sub-cloning of the DNA fragments into bacterial plasmids and also, to confirm the success of directional sub-cloning.

Primers, designed to anneal specifically to the regions of interest (Figure 2.1), were generated by MWG Biotech Co. and are listed in Table 2.2. Primers amplifying the STREX exon introduced restriction sites into the PCR product to facilitate cloning into the pGEX5x-1 plasmid. Primers used to produce TA-vector inserts were designed to account for the 3' adenine overhangs of the PCR products.

Figure 2.1
Primers used in murine BK channel sequence

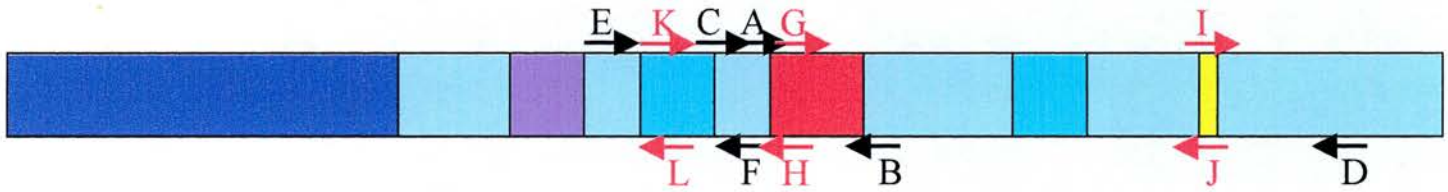

KEY: Colours represent sequences that translate to form following regions of protein:

- N-terminal domain – Transmembrane domains
- C-terminal domain – Cytoplasmic domain
- RCK, tetramerisation domain
- Leucine zipper regions
- STREX insert
- Serine-869

Figure 2.1: Schematic diagram illustrating the target locations of primers aligned to the murine BK channel gene. The cloning primers are represented by black arrows and the mutagenic primer by red arrows, and are labeled as detailed in Table 2.2. The cloning primers were used to produce insert sequences, as described in Table 3.1, that were used to create the constructs employed in this study. Not to scale.

Table 2.2
Cloning & mutagenic primers

Primer	Name	Restriction Site Introduced	Target vector / mutagenic	T_m (^{0}C)	Sequence (5' – 3')
A	Exon Forward	Bam HI	pGEX5x-1	72.9	GGT CGT GGG ATC CCC AAG ATG TCC ATC TAC AAG AGA
B	Exon Reverse	Sal I	pGEX5x-1	74.0	ATC CCC GAA TTC GGC ACG GAA ACT GGT GGA GCA ATC
C	ΔN-ΔC Forward	-	pBAD/Thio-TOPO	60.0	GTT TGT GAG CTG TGT TTT GTG
D	ΔN-ΔC Reverse	-	pBAD/Thio-TOPO	64.0	CTC AGC TAT TAG AGC CTC AGA
E	LZ1 Forward	-	pBAD/Thio-TOPO	53.7	CAG TAT CAC AAC AAG GCC
F	LZ1 Reverse	-	pBAD/Thio-TOPO	53.7	GAT CTT AAG GTG GTT CCC
	Trx Forward	-	Within pBAD/Thio-TOPO	45.4	TTC CTC GAC GCT AAC CTG
	pBAD Reverse	-	Within pBAD/Thio-TOPO	36.0	GAT TTA ATC TGT ATC AGG
G	S4A Forward	-	Mutagenic	80.4	AGG CGG CCC AAG ATG GCC ATC TAC AAG AGA ATG
H	S4A Reverse	-	Mutagenic	80.4	CAT TCT CTT GTA GAT GGC CAT CTT GGG CCG CCT
I	S869A Forward	-	Mutagenic	74.5	ATG TTA CGC CAG CCG GCC ATC ACA ACT GGG GTC
J	S869A Reverse	-	Mutagenic	74.5	GAC CCC AGT TGT GAT GGC CGG CTG GCG TAA CAT
K	LZ1mut Forward	-	Mutagenic	80.5	GCT CAA GGC GCC TCC ACA ATG CTT GCC AAT GCC TTC TCT ATG AGG
L	LZ1mut Reverse	-	Mutagenic	80.5	CCT CAT AGA GAA GGC ATT GGC AAG CAT TGT GGA GGC GCC TTG AGC

Primers used to amplify regions of the murine BK channel sequence (illustrated schematically in Figure 2.1) to enable construct generation (See Table 3.1) or mutagenesis (red text). Lettering refers to Figure 2.1.

Typically, cloning reactions were performed with the following components: 1-10 ng DNA, 10 pmol of forward primer and 10 pmol of reverse, 10 nmol each of dATP, dCTP, dGTP, and dTTP (Pharmacia Biotech), 75 pmol (=2.5 mM) Mg^{2+} within 1x Expand™ High Fidelity Buffer (Boehringer Mannheim), and 2.6 U Expand™ Taq/Pwo Enzymes (Boehringer Mannheim), all in DEPC dH_2O to a final reaction volume of 50 µl. The enzyme was added "hot start"; following heating of the reaction mixture to 95 ^{0}C, to inhibit non-specific primer associations. Negative controls were performed with non-specific DNA or DEPC dH_2O replacing the DNA. PCR reactions used for rapid screening were performed as above, but used *Taq* polymerase and appropriate buffers (Promega). All reactions were performed in a Perkin-Elmer GeneAmp PCR System 2400 with cycling parameters (Table 2.3) specific to the primer pair used, relative to the respective melting temperatures (T_m; Table 2.2). Samples were analysed by agarose gel electrophoresis (Section 2.3.1).

2.4.2 Ligation of insert DNA into plasmids

2.4.2.1 Ligation of restricted fragments

Insert and vector digested by the appropriate restriction endonucleases (Section 2.3.3), separated by agarose gel electrophoresis (Section 2.3.1) and purified from the agarose (Section 2.3.2) were analysed by electrophoresis to confirm purification and enable approximation of the relative DNA concentrations.

Table 2.3
Cycling parameters of cloning PCR reactions

Insert amplified	Forward Primer *	Reverse Primer *	Cycling parameters		
			Step 1	Step 2	Step 3
STREX exon	A	B	1x *95 ^0C – 30 sec*	30x *95 ^0C – 30 sec* *60 ^0C – 30 sec* *72 ^0C – 1 min*	1x *72 ^0C – 30 sec* *4 ^0C – ∞*
ΔN-ΔC constructs	C	D	1x *95 ^0C – 30 sec*	30x *95 ^0C – 30 sec* *55 ^0C – 30 sec* *72 ^0C – 1 min*	1x *72 ^0C – 30 sec* *4 ^0C – ∞*
LZ1 constructs	E	F	1x *95 ^0C – 30 sec*	30x *95 ^0C – 30 sec* *49 ^0C – 30 sec* *72 ^0C – 1 min*	1x *72 ^0C – 30 sec* *4 ^0C – ∞*

* Primer labels refer to Table 2.2 & Figure 2.1

In general, three experimental 10 µl reactions of varying insert concentration were performed in the presence of vector, 1 U T4 ligase (Promega) and 30 mM Tris HCl, pH 7.8, 10 mM $MgCl_2$, 10 mM dithiothreitol (DTT), 1 mM adenosine triphosphate (ATP), (Promega) as recommended by the enzyme manufacturer [300]. Reactions omitting the insert and enzyme were performed in parallel as controls of vector re-annealing and contamination. Reactions were incubated (16 ^{0}C, ~16 hours) prior to transformation into competent XL1-Blue or JM109 *E.coli* cells.

2.4.2.2 Ligation into TOPO vector

Fresh PCR product was incubated with TOPO vector (~20 ^{0}C, 5 mins) and transformed into TOP10 *E.coli* cells (Invitrogen) as recommended by the vector manufacturer [301].

2.4.2.3 Assessment of ligation transformants

Assessment of ligation efficiency was determined by the presence or absence of colonies on the control plates; the presence of colonies indicated bacteria that do not contain the insert within their plasmid and thus, experimental plates were discounted. If the experiment demonstrated no or low background, individual colonies from experimental plates were inoculated into 5 ml LB/amp cultures for DNA analysis via alkaline lysis (Section 2.3.4.1) and test restriction digests (Section 2.3.3) or insert orientation-specific PCR reactions (Section 2.4.1).

2.4.3 Site directed mutagenesis (SDM)

Site directed mutagenesis was performed using the Stratagene Quikchange™ Site-Directed Mutagenesis Kit following the manufacturer's instructions [302]. 5-50 ng DNA were polymerised by 2.5 U *Pfu* DNA polymerase (Promega) with 125 ng of each mutagenic primer (MWG Biotech Co.; See Figure 3.4) and 2.5 mM of dATP, dCTP, dGTP and dTTP in 1x reaction buffer (10 mM KCl, 6 mM $(NH_4)_2SO_2$, 20 mM Tris-HCl, pH8.0, 2 mM $MgCl_2$, 0.1 % Triton X-100 (v/v), 10 μg/ml BSA), diluted to final volume of 50 μl with DEPC dH_2O. PCR was performed in a Perkin-Elmer GeneAmp PCR System 2400 for 16 cycles (95 ^{0}C, 30 sec; 55 ^{0}C, 1 min; 68 ^{0}C, 2 min/kb plasmid length), and 10 U *Dpn1* (Promega) incubated with each reaction (37 ^{0}C, 1 hr) to digest parental, non-mutated, DNA prior to transformation into XL1-Blue *E.coli* cells. DNA was then isolated (as Section 2.3.4) to allow confirmation of mutagenesis by sequencing (MWG Biotech Co.).

2.5 Recombinant protein expression & purification from bacterial expression systems

2.5.1 Recombinant protein expression

250 ml LB/amp media inoculated from a BL21-RIL *E.coli* colony expressing the plasmid of interest (See Section 2.2.1) was incubated with agitation (37 ^{0}C) until reaching exponential growth (See Section 2.2.2). Test cultures were exposed to a range of induction temperatures, durations and inducer concentrations to determine the most effective conditions for soluble recombinant protein production. For pGEX5x-1 plasmid

recombinant protein translation, 0.5 mM IPTG for ~16 hrs at 16 ^{0}C was most successful, and for the pBAD/Thio-TOPO vector, 0.02 % L-arabinose (w/v) under the same conditions.

2.5.1.1 Solubility test

A bacterial cell pellet from an induced 1 ml test culture was resuspended in 100 µl ice-cold STET buffer, lysed with 10 µl of 50 mg/ml lysozyme, vortexed and incubated on ice (20 mins). The insoluble fraction, pelleted by centrifugation (~30 sec, 10 000 g) and resuspended in SDS-LB, was compared to the soluble fraction (diluted 1:1 in 2x SDS-LB) by SDS-PAGE analysis (Section 2.7.1).

2.5.2 Purification of GST-tagged proteins

Purification of GST-fusion proteins was performed using an optimised protocol based on that recommended by the slurry manufacturer [303].

Cell pellets (6 000 g, 15 min) from 250 ml LB/amp GST (Glutathione-S-transferase)-tagged protein inductions were washed in 5 ml ice cold PBS, re-pelleted (6 000 rpm, 15 min), resuspended in 4 ml ice cold STET + protease inhibitors (Boehringer Mannheim) and lysed by lysozyme (500 µl of 50 mg/ml; stirred 30 mins, 4^{0}C) and sonication (8 x 10 sec, 6 microns, Soniprep 150, Sanyo). Following centrifugation (10 000 g, 30 mins), the supernatant was diluted with 27 ml 0.1x PBS, pH 8.5 and incubated with stirring (1 hr, 4 ^{0}C) with 5 ml 50 % GS4B (w/v; glutathione sepharose 4B; Amersham Pharmacia) pre-equilibrated with PBS. The GS4B was washed repeatedly with PBS then exposed to an

affinity pull-down assay (Section 2.9.2) or incubated in 2.5 ml Elution Buffer (50 mM Tris base, 10 mM glutathione; 30 mins, 4 ^{0}C) to elute the GST-fusion proteins competitively.

Note: GS4B was prepared, stored and regenerated following manufacturer's instructions (Amersham Pharmacia).

2.5.3 Ni^+NTA purification of His-tagged proteins

Purification of 6x Histidine (His_6)-tagged proteins was performed using nickel-nitrilotriacetic acid (Ni^+NTA) metal-affinity chromatography matrices following the manufacturer's recommended protocol for batch purification under native conditions [304]. Cell pellets (6 000 g, 15 min) from 250 ml LB/amp His_6-tagged protein inductions were resuspended in 2 ml Lysis Buffer (50 mM NaH_2PO_4, 300 mM NaCl, 10 mM imidazole, pH 8.0) + EDTA-free protease inhibitors (Roche) per g cell pellet and lysed by lysozyme-treatment (1 mg/ml; stirred 30 mins, 4^{0}C) and sonication (8 x 10 sec, 6 microns). Following centrifugation (10 000 g, 30 mins, 4 ^{0}C), the supernatant was incubated with stirring (1 hr, 4 ^{0}C) with 50 % Ni^+NTA (w/v) pre-equilibrated with Lysis Buffer (1 ml Ni^+NTA per 4 ml lysate). The Ni^+NTA was washed repeatedly with Washing Buffer (50 mM NaH_2PO_4, 300 mM NaCl, 20 mM imidazole, pH 8.0) then exposed to an affinity pull-down assay (Section 2.9.2) or the His_6-tagged protein was eluted by 4x 0.5 ml Elution Buffer (50 mM NaH_2PO_4, 300 mM NaCl, 250 mM imidazole, pH 8.0).

2.5.4 Immunoprecipitation

Bacterial cell pellets (induced where appropriate as in Section 2.5.1; centrifuged 6 000 g, 10 min, 4 ^{0}C) were resuspended in 2 ml Lysis Buffer (150 mM NaCl, 50 mM Tris, pH 8.0, 1 % Triton-X-100 (v/v)) + protease inhibitors (Roche) per g wet pellet weight as recommended by Invitrogen [305]. Cells were lysed by lysozyme treatment (1 mg/ml; stirred 30 mins, 4^{0}C) and sonication (8 x 10 sec, 6 microns) and spun (10 000 g, 20 mins, 4 ^{0}C). The supernatant was pre-cleared with 50 µl of 50 % protein-G-sepharose (PGS; w/v) in Lysis Buffer per 1 ml supernatant (agitated - 1 hour, 4 ^{0}C), then spun (10 000 g, <1 min, 4 ^{0}C) and the pre-cleared supernatant incubated with agitation (16 hrs, 4 ^{0}C) with 50 µl 50 % PGS (w/v) and the appropriate antibody (Table 2.4). The slurry pellet (10 000 g, <1 min, 4 ^{0}C) was washed (3x 200 µl Lysis Buffer, 1x 200 µl dH_2O) and suspended in 25 µl 2x SDS-LB for direct protein analysis, or exposed to *in vitro* phosphorylation (Section 2.8) or affinity pull-down (Section 2.9.3).

2.6 Recombinant protein expression & purification from mammalian expression systems

2.6.1 Mammalian cell culture

Human embryonic kidney 293 (HEK293) cells were maintained in Dulbecco's Modified Eagle Medium (DMEM; Gibco) + 10 % foetal calf serum (v/v; FCS; Harlan) at 37 ^{0}C, 5 % CO_2 in a CO_2-incubator (Wolf Laboratories), and passaged following standard tissue culture procedures [306] using Trypsin-EDTA (Gibco) to release confluent cells.

2.6.2 Transfection & creation of stable cell lines

HEK293 cells at ~50 % confluency were transfected with cDNA using LIPOFECTAMINE™ Reagent (Gibco) following the manufacturer's instructions. 0.5-1 μg cDNA / ml final reaction volume were used routinely with a 1:1 cDNA ratio applied in co-transfections. Cells transfected transiently were harvested for immunofluorescence or immunoprecipitation 24-72 hours after transfection. Stable cell lines were created by adding a selection media with an antibiotic appropriate to the resistance of the transfected plasmid 24 hours after transfection. The selection media was replaced every 48 hours to remove dead cells for ~2 weeks until no further cell death was observed. Cells were then passaged and following recovery, maintained in selection media as a stable cell line.

2.6.3 Immunoprecipitation

Immunoprecipitation of proteins from mammalian cell lines was performed using a method based upon those of Rotman et al *(1995) and Fanger* et al *(1999)* [222, 307].

Stable cell lines were grown in 75 cm^2 tissue culture flasks until reaching confluency whilst transient transfections were harvested 24-72 hrs following transfection. Flasks were washed twice with 1 ml bRIA (50 mM Tris-HCl, pH 7.5, 0.5 mM $MgCl_2$, 0.2 M NaCl, 10 mM EDTA, 20 mM sodium pyrophosphate, 100 mM sodium fluoride, 1 mg/ml BSA), then suspended in 300 μl bRIA + 1 % Triton X-100 (v/v; bRIA-T) + protease inhibitors prior to sonication (4 x 10 sec, 8 mA). Insoluble material was removed by centrifugation (10 000 g, 15 min, 4 ^{0}C) and the lysate pre-cleared by incubation with 20

µl of 50 % PGS in bRIA-T (w/v; agitation, 1 hr, 4 ^{0}C). The immunoprecipitating antibody at the appropriate dilution (Table 2.4) with 40 µl 50 % PGS in bRIA-T (w/v) was added to the pre-cleared lysate and incubated (4 hrs, 4 ^{0}C). The pellet was washed (3x bRIA-T, 1x dH_2O) and diluted with 20 µl 2x SDS-LB for direct analysis, or exposed to *in vitro* phosphorylation (Section 2.8) or affinity pull-down (Section 2.9.3).

2.6.4 Analysis on BK channel expression *in vivo* in HEK293 cells

2.6.4.1 -EGFP visualisation

Transiently transfected or stable cell lines were grown on coverslips until ~40-50 % confluency was observed (typically 24-72 hrs following passage/transfection). Cells were washed gently three times with PBS + 2 mM Ca^{2+} + 1 mM Mg^{2+} removing debris, then fixed (4 % paraformaldehyde in PBS (v/v), pH 7.1, 20 mins, ~16 ^{0}C). Fixing was quenched (50 mM NH_4Cl, 10 mins, ~16 ^{0}C) following washing (3x PBS), then washed (3x PBS). Nuclear material was stained with TO-PRO-3™ (Molecular Probes) (10 mins, ~16 ^{0}C), then coverslips re-washed (3x PBS), mounted with Mowiol (Calbiochem) and stored at 4 ^{0}C prior to confocal microscopy.

2.6.4.2 Confocal microscopy

Labelled proteins fixed on coverslips prepared as described in Section 2.6.4.1 were visualised using confocal microscopy on a Zeiss 510 LSM in conjunction with Linda Sharp. EGFP was excited at 478 nm to produce a fluorescent emission peak with a

maximum at 507 nm (green). TO-PRO3™ (Molecular Probes) was excited at 642 nm, with emission at 661 nm (blue).

2.6.5 Electrophysiology

Patch clamp electrophysiology was performed in conjunction with Dr Lijun Tian. Isolated inside-out patches from HEK293 cells were depolarised to +20, +40, and +60 mV in physiological K^+ gradient in the presence of 0.2 μM free Ca^{2+}. Data acquisition was controlled by an Axopatch 200B amplifier and pCLAMP6 software (Axon Instruments Inc.). All recordings were filtered at 2 kHz and sampled at 10 kHz. Bath solution: 140 mM KCl, 1 mM BAPTA (1,2-bis[2-aminophenoxy]ethane-N,N,N',N',tetraacetic acid), 10 mM HEPES (N-[2-hydroxyethyl]piperazine-N'-[2-ethanesulphonic acid), 30 mM glucose, pH 7.4 in 2 mM MgATP, with free Ca^{2+} buffered to 0.2 μM. Pipette solution: 140 mM NaCl, 5 mM KCl, 0.1 mM $CaCl_2$, 5 mM $MgCl_2$, 10 mM HEPES, 20 mM glucose, pH 7.4. Patch pipettes manufactured from Garner #7052 glass with resistance of 1.5 – 3 MΩ in physiological saline. Steady state mean open probability was determined over at least 20 sec of recording.

2.7 Protein analysis

2.7.1 Polyacrylamide gel electrophoresis

Non-radioactive protein samples in SDS-LB were heated (42 ^{0}C, ~5 mins for full-length channel immunoprecipitations. 100 ^{0}C, ~5 mins for all other samples) and analysed by standard SDS-polyacrylamide gel electrophoresis (SDS-PAGE) protocols using the Mini

Protean® 3 Cell gel electrophoresis system (BioRad) run in Laemelli Buffer (Section 2.1.2.2). Proteins with large molecular weights (>50 kDa) were analysed on gels of 7.5 % acrylamide (w/v) whilst smaller proteins (<50 kDa) were analysed on 10 % acrylamide gels, all with 3 % acrylamide stacking gels [As 308]. Gels were analysed by Western blotting (Section 2.7.2), or stained by Coomassie (15 mins in stain: 500 ml methanol, 100 ml acetic acid, 400 ml dH_2O, 1 g Coomassie R-250. Destain: 50 % methanol, 10 % acetic acid (v/v) in dH_2O), Colloidal Coomassie (1 hr; GelCode® Blue Stain Reagent, Pierce. Destain: dH_2O) or Silver stain (Section 2.7.1.1) to enable protein visualisation.

2.7.1.1 Silver stain

Silver staining of acrylamide gels was performed by the method of Wray et al (1981) [309].

Gels were fixed in 50 % methanol, 10 % acetic acid solution (v/v, 20 mins), then soaked in 50 % methanol (v/v, 20 mins). Following washing (dH_2O, 5 mins), gels were re-soaked in methanol and washed twice more, prior to staining (0.4 g silver nitrate, 21 ml of 0.36 % NaOH (v/v), 1.4 ml of 14.8 M NH_4OH made up to 100 ml with dH_2O; 20 mins, ~16 ^{0}C). The gel was transferred to developer (2.5 ml of 1 % citric acid (w/v), 0.25 ml of 38 % formaldehyde (v/v) in 500 ml dH_2O) after washing (5 mins, dH_2O). When sufficient protein visualisation was observed (typically 5-15 mins), further development was inhibited using a 50 % methanol, 10 % acetic acid (v/v) solution. Gels were rinsed and stored in dH_2O prior to drying.

2.7.2 Western blot analysis

Western blot analysis was performed using standard protocols for wet transfer of proteins in acrylamide gels (Section 2.7.1) onto polyvinylidene fluoride (PVDF, Amersham) membranes [310]. Membranes, activated by methanol, and gels were soaked in 1x Towbin Transfer Buffer (TTB) and transfer was performed in 1x TTB using a Hoefer TE22 Series Transphor Electrophoresis Unit (1 hr, 400 mA). Transferred membranes were blocked in PBS-T + 5 % Marvel (w/v; Premier Brands) for between 1 hr (at ~16 ^{0}C) and 16 hrs (at 4 ^{0}C), washed, and incubated in the appropriate primary antibody solution (Table 2.4). Secondary antibodies conjugated to horseradish peroxidase (HRP) were applied following washing (Table 2.4), and detection was performed by enhanced chemiluminescence (ECL) using Amersham reagents as described in the manufacturer's protocols. ECL reactions were detected by Konica MG-Super Rapid Medical Film developed in a Kodak SRX-101A X-ray developer. Unless stated otherwise, illustrated Western blots are typical of three independent experiments.

Antibodies were diluted appropriately (Table 2.4) in PBS-T + 1 % Marvel (w/v), except for the Diagnostic Scotland α-phospho- and α-non-phospho- antibodies that were diluted in PBS-T + 1 % Marvel (w/v) + competing peptides as illustrated in Table 2.4. Primary antibody incubations were performed at ~16 ^{0}C for 2-4 hrs, or 4 ^{0}C for ~16 hrs. Secondary antibodies were incubated with the membranes for 1-2 hrs at ~16 ^{0}C. Non-specific reactivity was assessed by test membranes and dot blot analysis (Section 2.7.2.1), exposing membranes to secondary antibodies without primary antibody

Table 2.4

Characteristics & use of antibodies: **A. Primary antibodies** **B. Secondary antibodies**

A.

Antibody	Species	Supplier	Epitope sequence (if known)	Dilution for use	
				WB	IP
α-V5	Mouse	Invitrogen	GKPIPNPLLGLDST	1/5000	1/1000
α-HA (12ca5)	Mouse	Roche	YPYDVPDYA	1/1000	1/250
α-PKAc	Sheep	R Clegg [311]	PGDTSNFDDYE	1/1000	1/250
α-11	Rabbit	HG Knaus [158]	V_{941}NDTNVQFLDQDDD	1/1000	-
α-HA (Y11)	Rabbit	Santa Cruz	YPYDVPDYA	1/333	-
α-STREX-1	Rabbit	HG Knaus	$M_{659(:27)}$SGRVRGNVDTLERT FP	1/2000	-
α-GST	Goat	Pharmacia	polyclonal	1/2000	-
α-GFP	Mouse	Clontech	-	1/1000	-
α-phospho-S869	Sheep	D-S	V_{919}HGMLRRQPS(p)ITTGV	1/1000 +[1]	-
α-S869	Sheep	D-S	V_{919}HGMLRRQPS ITTGV	1/1000 +[2]	-
α-phospho-STREX	Sheep	D-S	$C_{628(-5)}$GCRRPKMS(p)IYKRM	1/1000 +[2]	-
α-STREX	Sheep	D-S	$C_{628(-5)}$GCRRPKMS IYKRM	1/1000 +[1]	-

B.

Antibody	Species	Supplier	WB dilution
α-mouse-HRP	Sheep	Diagnostics Scotland	1/1000
α-goat/sheep-HRP	Donkey	Diagnostics Scotland	1/15000
α-rabbit-HRP	Donkey	Diagnostics Scotland	1/5000

Epitope sequence numbering as murine STREX BK channel (See Figure 1.3). Numbering within STREX insert (in brackets) as Figure 1.6. WB - Western blot, IP - immunoprecipitation, D-S - Diagnostics Scotland. Standard one letter amino acid code used.

[1] 10 μg/ml each of phospho-STREX & S869 peptides (Scheme 2.1)
[2] 10 μg/ml each of phospho-S869 & STREX peptides (Scheme 2.1)

incubation, pre-incubation of antibodies with target peptides and/or exposure of antibodies to positive and negative control proteins.

2.7.2.1 Generation of phospho-specific antibodies & dot blot analysis

Phospho-specific antibodies were generated commercially in sheep by Diagnostic Scotland against KLH (Keyhole Limpet Hemocyanin)-conjugated peptides of the S869 and STREX S4 regions of the BK channel (Scheme 2.1). Peptides were phosphorylated chemically to ensure phosphorylation was permanent. In the case of the S869 peptides, an additional cysteine residue was included at the N-terminal to enable conjugation to KLH. This was not necessary with the STREX peptides as cysteine is present in the native sequence.

Scheme 2.1: *Booster peptides for immunisation in sheep*
Sequence numbering of epitopes is as murine STREX BK channel (See Figure 1.3). Numbering within STREX insert is as in Figure 1.6 and shown in brackets. Standard one letter amino acid code used.

Peptide	Sequence
STREX	$-C_{628\,(STREX:-5)}$GCRRPKMSIYKRM
Phospho-STREX	$-C_{628\,(STREX:-5)}$GCRRPKMS(p) IYKRM
S869	$-C-V_{919}$HGMLRRQPSITTGV
Phospho-S869	$-C-V_{919}$HGMLRRQPS(p) ITTGV

Preliminary investigation of the specificity and cross-reactivity of these antibodies was performed by dot blot analysis with 10 μg of peptide (Scheme 2.1) / protein dotted onto methanol-activated PVDF membrane, and the membrane analysed by Western blot analysis (antibody-exposure and ECL-detection as Section 2.7.2).

2.7.2.2 Western blot membrane stripping

To enable re-probing of Western blot membranes, antibodies were removed by acid-stripping, incubating the membranes (15 mins, ~16 ^{0}C) in Stripping Buffer (0.2 M glycine, 0.5 % concentrated HCl (v/v), 0.005 % Tween-20 (v/v) in dH_2O). The membranes were washed in PBS-T then blocked prior to re-probing as described previously (Section 2.7.2).

2.7.3 Preparation of samples for mass spectrometry

Protein bands detected by colloidal stain can be analysed by mass spectrometry following in-gel digestion. The protein band of interest was excised, divided into ~1 mm^3 cubes, washed with milliQ water (300 μl, 15 mins) to remove the stain, then washed with CH_3CN (300 μl, 15 mins) to remove hydrophobic compounds. The supernatant was removed, and replaced with 100 mM NH_4HCO_3 (300 μl, 15 mins), then replaced repeatedly with 1:1 (v/v) 100 mM NH_4HCO_3 / CH_3CN (300 μl, 15 mins) until the stain was released fully from the gel pellets. The clear pellets were suspended in CH_3CN (100 μl, 5 mins) for dehydration then dried (5-30 mins) in a speedvac (Savant SPD111V).

Dehydrated bands were reduced and alkylated by addition of DTT and iodoacetamide: each band was suspended in 50 µl 10 mM DTT in 100 mM NH_4HCO_3 (56 ^{0}C, 1 hr), then the pellet resuspended in 50 µl 50 mM iodoacetamide in 100 mM NH_4HCO_3 (~16 ^{0}C, 30 mins, in dark). The pellet was washed with 100 mM NH_4HCO_3 (300 µl, 15 mins), 1:1 v/v 20 mM NH_4HCO_3 / CH_3CN (300 µl, 15 mins), and resuspended in 100 µl CH_3CN (5 mins) prior to speedvac dehydration (5 mins).

Bands were rehydrated and digested using 20 µl of 12.5 µg/ml modified trypsin in 20 mM NH_4HCO_3 (~16 ^{0}C, 24 hrs) before mass spectrometry analysis using an Applied Biosystems Voyager DE-PRO MALDI-TOF (delayed extraction protein matrix-assisted laser desorption/ionisation – time of flight mass spectroscopy) in conjunction with Nathan Harris, Moredun Institute, and Hannah Florance, Edinburgh University, following manufacturer's instructions. Acquired data was analysed using MS-Fit (UCSF) to identify the protein of interest.

2.8 Phosphorylation & dephosphorylation

Phosphorylation and dephosphorylation reactions were performed in conditions suitable for maximal catalytic activity of the protein kinase / protein phosphatase as recommended by the enzyme manufacturers [297, 312]. For safety and consistency, reactions employing [γ-^{32}P]-ATP were diluted in LDS-LB (Section 2.1.2.2), heated (70 ^{0}C, 10 mins) and 15 µl samples run on 12 % and 4-12 % Bis-Tris gels (Invitrogen) in MOPS SDS-Running Buffer (Section 2.1.2.2) using the NOVEX X-Cell Sure Lock™

electrophoresis system (Invitrogen). Gels were dried fully (Hoefer Slab Gel Dryer GD2000), then exposed to ^{32}P-sensitive film (BioMax MR-1 & MS film, Sigma) in an intensifying screen cassette (Kodak) for periods ranging from 1 hr to 36 hrs, and at temperatures of –70 ^{0}C or ~16 ^{0}C. Non-radioactive reactions were analysed by Western blotting (Section 2.7.2).

2.8.1 *In vitro* phosphorylation of soluble & immunoprecipitated proteins

2.8.1.1 *In vitro* PKA phosphorylation reactions with exogenous PKA

5 µg of purified protein or ~20 µg immunoprecipitation slurry (IP) of purified protein were incubated with 1 mM cold rATP, 10 µCi [γ-^{32}P]-ATP (1 µl, Amersham) and 40 U of pure PKA catalytic subunit (PKAc; bovine PKAc, 40 kDa, Promega) in 2 mM $MgCl_2$, 4 mM Tris HCl, pH 7.4 made up to 30 µl with dH_2O. Additionally, 100 nM of protein phosphatase inhibitor, okadaic acid (OA), were added to immunoprecipitation reactions. The peptide, kemptide, contains a strong PKA consensus motif [227] and therefore, was used in positive control reactions composed of: 0.1 mM cold rATP, 10 µCi [γ-^{32}P]-ATP and 40 U PKAc in 2 mM $MgCl_2$, 4 mM Tris HCl, pH 7.4 made up to 30 µl with dH_2O. Negative control reactions were performed by replacing PKAc with dH_2O. Reactions were incubated (30 ^{0}C, 10 mins), then quenched by placing on ice and the addition of an equal volume of 2x LDS-LB to analysis by autoradiography.

Time course assays were performed by the removal of 7.5 µl aliquots of 60 µl phosphorylation reactions at 0, 1, 3, 5, 10, 20, 30 mins following addition of the kinase

to the reaction mixture with continual incubation at 30 ^{0}C. The aliquots were diluted in 7.5 µl of LDS-LB prior to autoradiographic analysis.

2.8.1.2 *In vitro* PKA phosphorylation reactions with endogenous PKA

Following co-immunoprecipitation of PKAc with the –HA-tagged BK channels (See Chapter 5), *in vitro* phosphorylation reactions were performed on the immunoprecipitates without exogenous PKAc addition to determine if the endogenous, pulled down PKAc could phosphorylate the channels.

2.8.1.3 *In vitro* PKC phosphorylation reactions

In vitro PKC phosphorylation reactions were performed with 5 µg or a ~20 µg IP of purified protein incubated with 1 mM cold rATP, 10 µCi [γ-^{32}P]-ATP (1 µl, Amersham) and 45 U of pure PKC (rat, 82 kDa, Stratagene) in 400 mM MES (2-[N-morpholino] ethane sulphonic acid), pH 6.0, 100 mM $MgCl_2$, 10 mM $CaCl_2$, 10 mM ethylene glycol-bis(β-aminoethylether)-N,N,N',N'-tetraacetic acid (EGTA) buffer made up to 30 µl with dH_2O. 100 nM of protein phosphatase inhibitor, okadaic acid (OA), were added to immunoprecipitation reactions. 7.5 µg of the 21-25 kDa phosphorylated heat-and acid-stable protein regulated by insulin (PHAS-I, Stratagene) was used as a positive control of PKC phosphorylation [313], with negative control reactions performed in the absence of the kinase with dH_2O replacing PKC. Reactions were incubated (30 ^{0}C, 10 mins), then quenched by placing on ice and the dilution of the 30 µl reactions in 30 µl LDS-LB prior to autoradiographic analysis.

2.8.1.4 *In vitro* CaMKII phosphorylation reactions

5 µg of pure protein or ~20 µg IP slurry were pre-incubated (30 ^{0}C, 3 mins) with 0.08 mM cold rATP, 50 mM Tris HCl, pH 7.5, 10 mM $MgCl_2$, 0.5 mM dithiothreitol (DTT), 1 mM $CaCl_2$, 1 µM calmodulin (Calbiochem), 0.1 mg/ml BSA, or in negative control reactions, 0.08 mM cold rATP, 50 mM Tris HCl, pH 7.5, 10 mM $MgCl_2$, 0.5 mM DTT and inhibitory 1 mM EGTA, pH 7.2, both to final volume of 25 µl with dH_2O. 10 µCi [γ-^{32}P]-ATP and 20 U CaMKII (Calbiochem) in 50 mM Tris HCl, pH 7.5, 10 mM $MgCl_2$, 0.5 mM DTT, 0.1 mg/ml BSA to 5 µl volume with dH_2O were added and incubated (30 ^{0}C, 5 mins). Reactions were quenched by placing on ice and dilution in 2x LDS-LB before autoradiographic analysis.

2.8.1.5 Dephosphorylation assays

Dephosphorylation reactions were performed, based on the method of Murphy et al (1993) [314].

2.8.1.5.1 Dephosphorylation of GST-fusion proteins

Phosphorylation of GST-fusion proteins (as Section 2.8.1.1) was quenched on ice and excess GS4B added (30 µl 50 % slurry (w/v) / 100 µl assay volume) to bind the GST-fusion proteins. The slurry was washed (4x 100 µl Wash Buffer: 50 mM Tris HCl, pH 7.5, 1 mM DTT, 1 mM $MnCl_2$) to replace the phosphorylation assay components, then resuspended in 100 µl Wash Buffer and divided equally into five aliquots. Aliquots were treated either with 2 U protein phosphatase (PP2A or PP1, Promega) in the presence or absence of 100 nM of the phosphatase inhibitor, okadaic acid (OA, Alexis),

or with 100 nM OA alone in a final volume of 15 µl with Wash Buffer. A control aliquot was treated with 15 µl Wash Buffer only. Reactions were incubated with frequent agitation (37 ^{0}C, 30 mins) then quenched on ice. OA was added to a control reaction that had been incubated with protein phosphatase and all assays were diluted in 2x LDS-LB prior to analysis by autoradiography (See Section 2.8).

2.8.1.5.2 Dephosphorylation of peptides

Phosphorylation of peptides (as Section 2.8.1.1) was quenched on ice and the PKA-inhibitor, H-89, added (to 1 µM final concentration) to inhibit further phosphorylation. 30 µl phosphorylation reactions were divided equally into six 5 µl aliquots and treated with 2 U protein phosphatase (PP2A or PP1, Promega) in the presence or absence of 100 nM of the phosphatase inhibitor, okadaic acid (OA, Alexis) or with 100 nM OA alone or no additional reactants. All reactions were made up to a final volume of 20 µl with Wash Buffer (See above) then incubated (37 ^{0}C, 30 mins), quenched on ice and diluted in 20 µl LDS-LB prior to analysis by autoradiography (See Section 2.8).

2.8.2 *In vivo* stimulation of endogenous PKA

*In the context of these experiments the term "*in vivo*" is used to refer to heterologous BK channel expression in intact HEK293 cells and was performed by a method based on that of Mammen* et al *(1999)* [315].

75 cm^2 flasks expressing a stable cell line of –HA-tagged channels were grown to near confluency (~48 hrs following passage, as Section 2.6.2). ~16 hrs prior to assay, the

DMEM + FCS media were replaced by DMEM + 1 % ITS (v/v; insulin-transferrin-sodium selenite) liquid media supplement to remove glucocorticoids present in the FCS that can influence PKA regulation of BK channel activity [194, 233, 316]. For assay, flasks were washed twice (DMEM) then treated with a PKA stimulator, either 30 μM forskolin (Sigma) or 1 mM 8-(4-chlorophenylthio)-cAMP (8-CPT-cAMP; BIOLOG), and/or 100 nM of the protein phosphatase inhibitor, okadaic acid (OA; Alexis) in 5 ml DMEM. Control reactions were performed by incubation of a flask with 100 nM OA in 5 ml DMEM, or incubation in DMEM only. Following incubation (20 mins, 37 ^{0}C) cells were lysed and immunoprecipitated as Section 2.6.3 in the presence of forskolin / 8-CPT-cAMP / OA as appropriate.

2.9 Protein affinity assays

2.9.1 Lysate preparation

2.9.1.1 HEK cell lysate

A 75 cm^2 flask of HEK293 cells or a stable cell line were grown to ~100 % confluency and rinsed with ~5 ml PBS. Cells were scraped loose in 0.3 ml Lysate Buffer (20 mM Tris, 2 mM EDTA, 150 mM NaCl, 0.5 % Triton X-100 (v/v), pH 7.4) + protease inhibitors, sheared with a 26 G needle (Terumo) and spun to pellet the non-solubilised cellular components. Samples were stored at –70 ^{0}C until required.

2.9.1.2 Rat brain lysate

Rat brains were homogenised in ~3 ml Homogenisation Buffer (150 mM KCl, 2 mM $MgCl_2$, 5 mM EGTA, pH 7.4 + protease inhibitors (Boehringer Mannheim) per brain. Homogenate was centrifuged (800 g, 5 mins, 4 ^{0}C), and the pellet re-homogenised in 2-4 ml of Homogenisation Buffer prior to re-centrifugation (800 g, 5 mins, 4 ^{0}C). The pooled supernatant was separated by centrifugation (40 000 g, 45 mins, 4 ^{0}C) into the soluble cytosolic fraction and the insoluble membrane fraction. Samples were stored at –70 ^{0}C until required.

2.9.2 Affinity chromatography columns

Columns of GS4B slurry bound by GST-fusion proteins were prepared as described in Section 2.5.2 and washed in >10 column volumes Binding Buffer (50 mM Tris, 50 mM NaCl, 1 mM EDTA, 1 mM EGTA, 5 % glycerol (v/v), pH 7.4). Columns were arranged as illustrated in Figure 2.2 and loaded with rat brain lysate, HEK293 cell lysate (diluted 1:20 in Binding Buffer), or pure PKAc (Promega; diluted 80 U (1 µl): 0.5 ml Binding Buffer). Washing (5 x 10 ml Binding Buffer) was followed by high salt elution of associating proteins (3 x 2.5 ml Elution Buffer: 50 mM Tris, 1 M NaCl, 1 mM EDTA, 1 mM EGTA, 5 % glycerol (v/v), pH 7.4). Eluates were concentrated to 0.5 ml volume using a 10 kDa cut-off Centricon (Millipore) and frozen at –20 ^{0}C prior to analysis by SDS-PAGE. Controls were performed in parallel to experimental proteins.

Affinity chromatography upon His_6-tagged proteins bound to Ni^+NTA (prepared as described in Section 2.5.3) was performed as described above but in the absence of the divalent cation chelators, EDTA and EGTA.

Figure 2.2
Affinity pull-down assays

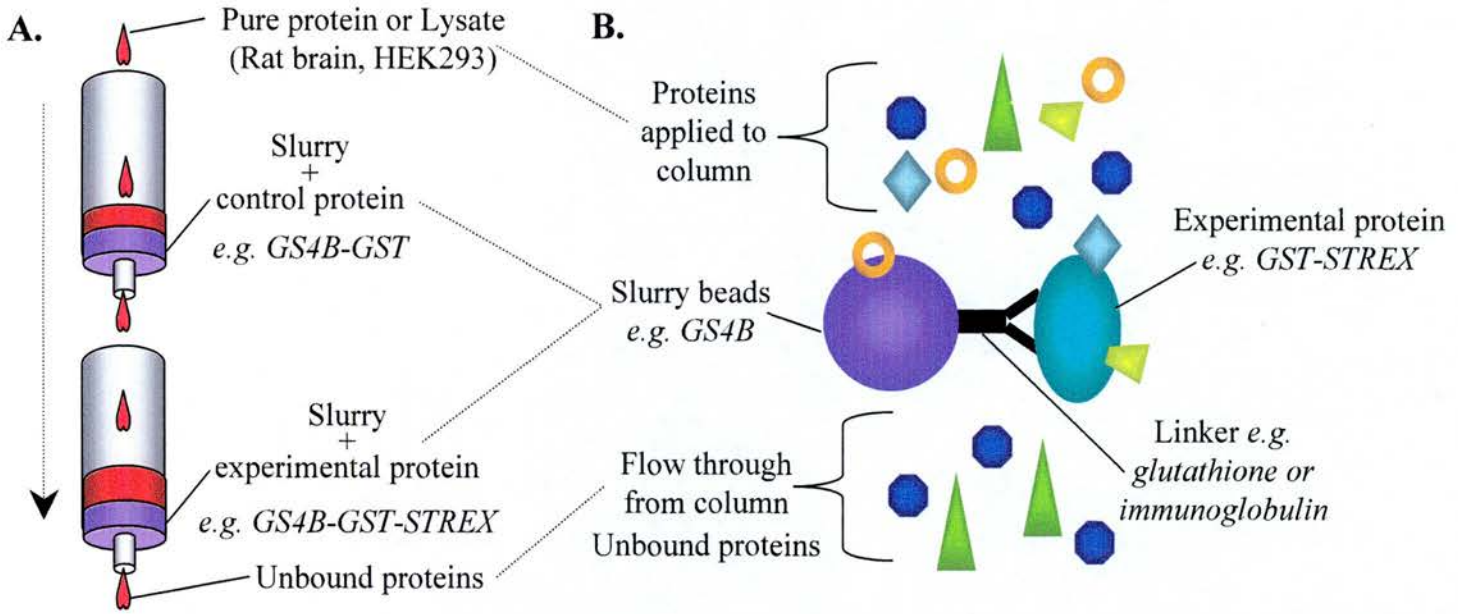

Figure 2.2: Schematic diagram illustrating affinity pull-down assay protocol & mechanism. **A**. For affinity pull-down assays cell lysate/purified proteins were poured sequentially through columns with the immobilised fusion tag alone followed by the immobilised fusion protein. **B**. Immobilisation of the fusion protein allows specific interactions to be assessed.

2.9.3 Co-immunoprecipitation

Immunoprecipitates (Sections 2.5.4 & 2.6.3) were incubated with 100 µl rat brain lysate, 100 µl HEK293 cell lysate, or 1 µl (80 U) pure PKAc (Promega; diluted in 100 µl appropriate Immunoprecipitation Buffer) for 2-4 hrs at 4 ^{0}C in the presence of protease inhibitors. The slurry was washed thoroughly (3x 100 µl appropriate Immunoprecipitation Buffer, 1x 100 µl dH_2O), and diluted in 30 µl 2x SDS-LB prior to analysis by Western blotting (Section 2.7.2). Controls were performed with tagged control proteins and by incubation of unbound slurry with the lysates/pure PKAc to exclude non-specific binding.

2.9.3.1 Competing peptides

The competing peptides to the leucine zipper 1 motif of the channel (Table 2.5) were added to the cellular lysate of immunoprecipitation assays prior to pre-clearing to a final concentration of 100 µM.

2.10 Miscellaneous

2.10.1 Primer design & DNA/protein sequence analysis

Primer design and analysis of the sequences of DNA and proteins were performed using the DNAStar package (Lasergene). DNA sequences that have been published previously were downloaded from www.ncbi.gov.uk [317]; Murine BK channel ZERO splice variant accession number: NP_034740. STREX splice variant NCBI accession number: AAD49225.

Table 2.5:
Comparison of the LZ1 peptide sequences to the channel leucine zipper 1 motif

Residue no:	494	495	496	497	498	499	500	501	502	503	504	505	506	507	508	509	510	511	512	513	514	515	516	517
Channel	I	A	Q	S	C	L	A	Q	G	L	S	T	M	L	A	N	L	F	S	M	R	S	F	I
Peptides:																								
LZ1	I	A	Q	S	C	L	A	Q	G	L	S	T	M	L	A	N	L	F	S	M	R	S	F	I
mLZ1	I	A	Q	S	C	L	A	Q	G	A	S	T	M	L	A	N	A	F	S	M	R	S	F	I

Table 2.5: LZ1 sequence alignment. The LZ1 peptide aligns to residues 494-517 of the murine, STREX BK channel sequence that encompass part of the Leucine Zipper 1 motif (Figure 1.3). Residues that are suggested to form the heptad repeat of the motif are highlighted in blue. Residues mutated in the mutant peptide, mLZ1, are shown in red with the relevant leucine to alanine mutations. Standard one letter amino acid code used. Appendix B illustrates an alignment of the murine BK channel LZ1 sequence with the equivalent domain in other species.

2.10.2 DNA sequencing

DNA sequencing was performed on all constructs to ensure correct insert insertion, sequence alignment and/or mutagenesis by MWG Biotech Co.

2.10.3 Densitometric analysis

Densitometric analysis of autoradiographic assays was performed by scanning the images (Hewlett Packard Deskscan & Arctools Photostudio) into Aida (Isatopenmeβgaräte) or ImageJ (NIH) densitometric packages.

2.10.4 Statistics

Data are expressed as mean ± S.E.M (standard error about the mean), n = number of independent experiments. Statistical analysis for each group was performed by standard student T-test analysis (Microsoft Excel) as described in the respective figure legend, with averaged data at $P < 0.05$.

2.11 Supplier Details

Alexis Biochemicals, Qbiogene Inc., 2251 Rutherford Road, Carlsbad, CA 92008, U.S.A.

Amersham Pharmacia Biotech, Amersham International plc, Amersham Place, Little Chalfont, Bucks., England, HP7 9NA

Arctools, http:/www.arctools.com

(BD) Becton Dickinson, 1 Becton Drive, Franklin Lakes, NJ 07417-1886, U.S.A.

BIOLOG Life Science Institute, Research Laboratory & Biochemicals, P.O.B. 108125, D-28071 Bremen, Germany

BioRad Laboratories, 2000 Alfred Nobel Drive, Hercules, CA 94547, U.S.A.

Boehringer Mannheim, See Roche

Calbiochem, CN Biosciences, Inc., La Jolle, CA 92039-2087, U.S.A.

Chemicon International Ltd., 28835 Single Oak Drive, Temecula, CA 92590, U.S.A.

Clontech U.K., Unit 2, Intec 2, Wade Road, Basingstoke, Hampshire, RG24 8NE

Diagnostics Scotland, Law Hospital, Carluke, Lanarkshire, Scotland, ML8 5QZ

Eppendorf – Helena Biosciences, Colima Avenue, Sunderland Enterprise Park, Sunderland, Tyne & Wear, SR5 3XB

Genemed Synthesis, Inc., 213 East Grand Avenue, Sth San Fransisco, CA 94080, U.S.A.

Gibco, See Invitrogen

Harlan Sera Lab Ltd., Dodgeford Lane, Belton, Loughborough, Leicestershire, LE12 9TE

Hewlett Packard, 2 Cadogan Square, 15 Blythswood Street, Glasgow, Scotland, G2 7AJ

Hoefer Scientific Instruments, 654 Minnesota Street, San Fransisco, CA 94107, U.S.A. & Unit 12 Croft Road Workshops, Hempstalls Lane, Newcastle-Under-Lyme, Staffs, ST5 0TW

Invitrogen Ltd. (Europe), PO Box 2312 9704 CH Groningen, The Netherlands & 3 Fountain Drive, Inchinnan Business Park, Paisley, PA4 9RF, U.K.

Konica Europe GmbH, Friedrich-Bergius-Str., Gewerbegebiet, 85662 Hohenbrunn, Germany

Millipore (U.K.) Ltd., The Boulevard, Blackmoor Lane, Watford, Hertfordshire, WD1 8YW

Molecular Probes, Inc., 4849 Pitchford Avenue, Eugene, OR 97402-8300, U.S.A.

MWG Biotech Company, Anzinger Strasse 7a, 85560 Ebersberg, Germany

New England BioLabs (U.K.) Ltd., 73 Knowl Piece, Wilbury Way, Hitchin, Hertfordshire, SG4 0TY, England

NIH (National Institute for Health, U.S.A), http://rsb.info.nih.gov/ij/

Pharmacia, See Amersham

Pierce / Perbio, PO Box 117, Rockford, IL 61105, U.S.A.

Premier Brands UK, Ltd., Bridge Road, Long Sutton, Spalding, Lincs., PE12 9EQ

Promega, 2800 Woods Hollow Road, Madison, WI 53711-5399, U.S.A.

QIAGEN Ltd, Boundary Court, Gatwick Road, Crawley, West Sussex, RH10 2AX

Raytest Isatopenmeßgaräte, GmbH, Benzstr. 4, D-75334, Straubenhardt, Germany

Roche Diagnostics GmbH, Roche Molecular Biochemicals, D-68298 Mannheim, Germany

Santa Cruz, Distribution: Autogen Bioclear U.K. Ltd, Holly Ditch Farm, Mile Elm, Calne, Wiltshire, SN11 0PY

Sigma Chemical Company, The Old Brickyard, New Road, Gillingham, Dorset, SP8 4XT

Stratagene, 11011 North Torrey Pines Road, La Jolla, CA 92037, U.S.A.

Terumo Europe Sucursal en España, Avda de Burgos 16D, 28036 Madrid, Spain

UCSF (University California, San Fransisco), www.prospector.ucsf.edu/ucsfbin3.4/msfit.cgi

Upstate Biotechnology, 10 Old Barn Road, Lake Placid, NY 12946, U.S.A.

Wolf Labs. Ltd., Commerce House, Market Street, Pocklington, York, YO42 2AB

Chapter Three:

Characterisation of Fusion Proteins & Phospho-Specific Antibodies

Chapter Three: Characterisation of Fusion Proteins & Phospho-Specific Antibodies

3.1 Introduction

The aim of this chapter is to serve as an introduction to the individual fusion proteins and phospho-specific antibodies developed for use during this study. The intention is to justify the application of the fusion proteins that were eventually employed, and to illustrate their conception, design, generation and ultimate purification. In addition, the specificity of phospho-specific antibodies will be demonstrated to validate their use in this study.

3.1.1 The fusion proteins

As described in the introduction to this study (Sections 1.3.1.2.1 & 1.4.1), the inclusion of the 58-residue long STREX insert at splice site two within the BK channel C-terminal tail domain confers the differential responses of two major BK channel splice variants to PKA [80, 229]. Application of the PKA activator, cAMP, to STREX insert-containing channels that are expressed heterologously initiates inhibition of channel activity [80, 229]. Parallel treatment of the ZERO isoform, which does not express the insert, effects the opposite response with such channel stimulation demonstrating that the presence of the insert is decisive to the PKA-mediated response of BK channels [80, 229]. The molecular basis of this influence may result from the STREX sequence affecting PKA-mediated phosphorylation of the channel protein, or from the insert impacting upon

protein-protein interactions underlying the PKA-response. To investigate these hypotheses, several fusion proteins encompassing equivalent regions from the proteins of the two channel splice variants were generated (Figure 3.1 & Table 3.1).

The STREX insert

Among the 58 residues of the STREX insert sequence is a putative PKA consensus motif engaging the STREX serine-4 residue as the potential target of PKA-mediated phosphorylation (See Section 1.4.1; Figure 1.6). The existence of this motif, and the presence of other phosphorylatable residues within the insert sequence, prompts the proposition that the STREX region provides additional or alternative PKA-phosphorylation sites that are absent from the ZERO channel sequence. The presence of the STREX insert in itself may obstruct phosphorylation of other conserved sites in the BK channel protein. Thus, alterations to the phosphorylation of the BK channel protein may underlie the contrasting responses of the two splice variants. Alternatively, the region may obstruct or produce binding sites for proteins associated with the channel PKA response and consequently alter the influence of the kinase. Therefore, to investigate these hypotheses, the 58 residues were isolated from the STREX channel sequence (Table 3.1 & Figures 3.1 and 3.2) and generated as a recombinant protein with a heterologous fusion partner (Section 3.2.1.1). This enabled the purification of a soluble fusion protein by the use of an *E.coli* expression system, thus permitting preliminary analysis of the region in the absence of the other segments of the BK channel protein and thereby simplifying assessment of possible functional roles.

Figure 3.1

Domains of the BK channel α-subunit protein

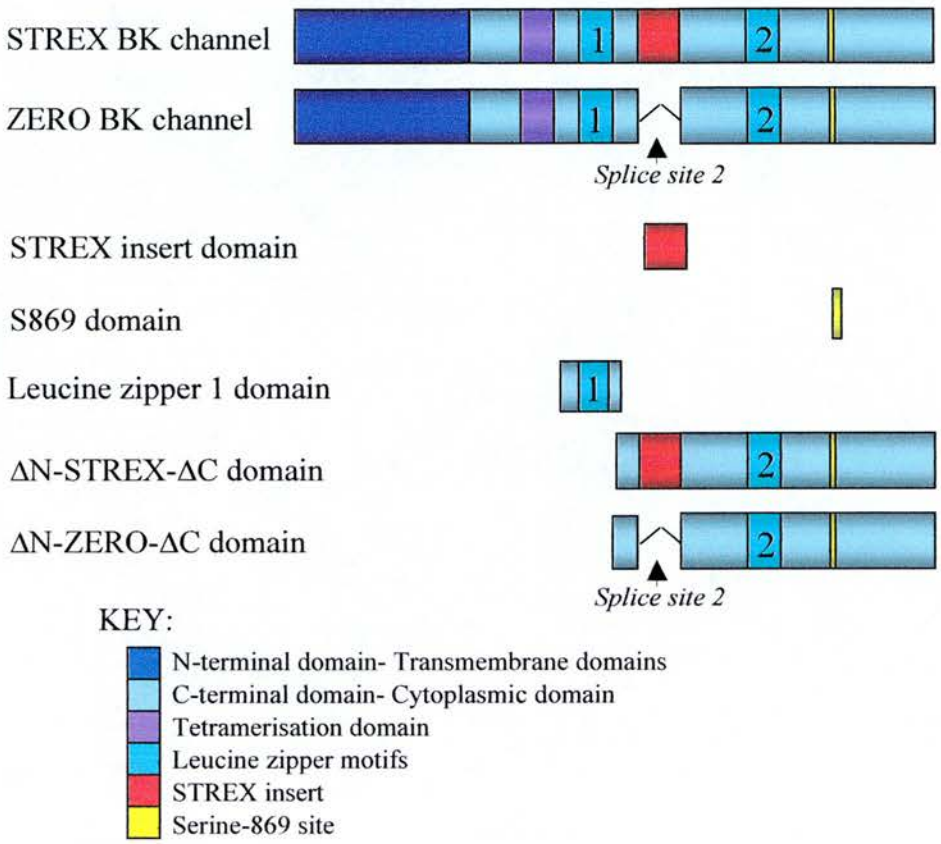

Figure 3.1: Schematic illustrating the regions of the BK channel α-subunit sequence encompassed by fusion proteins used in this study. Full length channel protein from the STREX BK channel splice variant is identical to the ZERO variant protein except for the inclusion of the 58 residue STREX insert at splice site 2 (The inverted V indicating the absence of the insert from the ZERO variant). To enable assessment of putative roles for individual segments of the C-terminal tail, particular regions were studied in isolation. These were the STREX insert and serine-869 sequences, the leucine zipper 1 motif, and a region of the C-terminal tail that encompassed splice site 2, serine-869, and the leucine zipper 2 motif (ΔN-ΔC). The diagram is not to scale. Segments are detailed in Table 3.1.

Table 3.1

Domains of the BK channel protein sequence encompassed by fusion proteins used in this study

Fusion	Start point		End point		Length		Mr	Characteristics					
	DNA * (bp)	Protein First* 4 residues	DNA * (bp)	Protein Last* 4 residues	DNA * (bp)	Number of residues	(kDa)	Splice site 2	S869	LZ1	LZ2	RCK domain	Ca^{2+} bowl
STREX channel	1	M_1DAL	3672	$EDEC_{1224}$	3672	1224	132	STREX	Yes	Yes	Yes	Yes	Yes
ZERO channel	1	M_1DAL	3672**	$EDEC_{1224}$	3498**	1166	125	ZERO	Yes	Yes	Yes	Yes	Yes
STREX insert	1897	P_{633}KMS	2071	$SFRA_{690}$	174	58	7	STREX	-	-	-	-	-
S869 site	2764	M_{922}LRQ	2797	$TTGV_{932}$	33	11	1	-	Yes	-	-	-	-
ΔN-STREX-ΔC	1654	T_{552}VCE	3039	$LIAE_{1013}$	1385	462	52	STREX	Yes	-	Yes	-	Yes
ΔN-ZERO-ΔC	1654	T_{552}VCE	3039**	$LIAE_{1013}$	1211**	404	45	ZERO	Yes	-	Yes	-	Yes
Thio-LZ1	1384	Q_{462}YHN	1767	$HLKI_{589}$	383	128	15	-	-	Yes	-	-	-

Mr - approximate molecular weight of fusion protein region calculated by DNAStar Biometrics package

\- - domains of the BK channel C-terminal tail section not included in the fusion protein sequence

* - numbering refers to murine STREX BK channel protein sequence. *NB* S869 is ZERO channel numbering retained to maintain consistency with the literature (equivalent to S927 of STREX channel sequence).

** - as numbering of ZERO channel nucleotides is altered for equivalence to STREX the actual length is 174 bp less than apparent length due to the absence of the STREX exon.

The fusion protein domains are illustrated diagrammatically in Figure 3.1. The BK STREX channel sequence is reproduced in Figure 1.3. Standard one letter amino acid code used.

The serine-869 residue

The serine-869 residue terminates a putative PKA consensus motif that is common to all BK channel splice variants and has been implicated as a factor in the response of the ZERO channel to PKA (Figure 3.1 & Table 3.1; See Section 1.4.1) [205, 229]. Therefore, to determine whether the region could be a functional target of the kinase, the sequence was analysed in isolation to prevent confusion arising from the presence of other potential phosphorylatable residues (Section 4.2.1).

The C-terminal tail

The C-terminal cytoplasmic tail region of the BK channel protein is integral to the regulation of the functional channel (See Section 1.3.2.2.2). The region encompasses several putative protein kinase consensus motifs that are conserved throughout all splice variants, as well as providing docking domains for particular accessory proteins (See Section 1.5). A section of the C-terminal domain that spanned the splice site two region, the location of STREX insertion, and the putative PKA-target motif incorporating serine-869 was isolated and generated as the ΔN-ΔC recombinant fusion proteins (Figure 3.1 & Table 3.1; Section 3.2.1.2). The tetramerisation domain and the very C-terminal region from these fusion proteins were excluded to prevent the polymerisation effects of these segments, and thus facilitated fusion protein purification. Comparison of the STREX and ZERO ΔN-ΔC fusion proteins enabled *in vitro* assessment of the influence of the STREX insert upon the C-terminal region of the channel protein, in particular, the relationship between the serine-4 and serine-869 sites.

The leucine zippers

Recent research has uncovered a fundamental role of leucine zipper motifs in the establishment of protein-protein interactions (See Chapter 5) [318]. Analysis of the BK channel sequence uncovers two putative leucine zippers that may be influential to the association of accessory proteins involved in protein kinase-mediated channel responses (Figure 3.1 & Table 3.1). Leucine zipper 2 is located between the STREX and S869 regions and thus, is encompassed by the ΔN-ΔC fusion proteins. Leucine zipper 1 is sequentially proximal to the STREX insert and was subsequently isolated as a distinct fusion protein for bacterial expression as a recombinant fusion protein (Section 3.2.1.2). Therefore, these fusion proteins enabled *in vitro* analysis of the motifs as potential accessory protein binding sites.

Protein regions for analysis

The fusion proteins described above express particular segments of the BK channel protein. By studying these specific regions in isolation from the native context, preliminary *in vitro* investigation of the possible functional roles of the regions can be assessed. This regimen simplified analysis by removing complicating factors present in natively expressed channels, such as accessory protein influences and the effect of other regions of the channel protein. Therefore, preliminary designation of a particular function to a specific region could be determined with minimal caveats to the analytical regime. However, to determine whether the designation is valid for the *in vivo* channel, full-length protein was investigated. Subsequent assessment of the functional roles of

the particular BK channel regions was achieved via examination of full-length, epitope-tagged BK channel proteins expressed in a mammalian expression system (Section 3.2.2).

3.1.2 Expression systems & fusion partners

Bacterial expression

Bacterial expression of recombinant protein is a valuable and effective experimental tool as high levels of protein expression can be achieved; up to 30 % of the total bacterial cellular protein [218]. This enables the implementation of biochemical techniques requiring large quantities of protein that for practical application, are unattainable from the native mammalian system. The fusion tags employed in this study facilitated such high level expression to enable the effective analysis of the fusion proteins (See Chapters 4 & 5) and each is described in detail within the appropriate section of this chapter (Section 3.2.1). All are commonly engaged biochemical devices that encourage high yields of soluble recombinant protein and thus aid high-level, inducible bacterial expression of the fusion proteins. They facilitate the solubility of the fusion protein within physiological conditions, eliminating the requirement of harsh pH and detergent treatments that can be detrimental to the protein and to further analytical techniques. Additionally, the fusion tags possess high affinity for a specific element that, when immobilised to a stable matrix, can enable the effective and elementary purification of the recombinant protein from the bacterial lysate to achieve fusion proteins of sufficient homogeneity and yield for further biochemical analysis.

The tags used throughout this study were not removed from the BK channel protein fragment prior to biochemical investigation. This facilitated analysis by maintaining protein solubility, authenticating characterisation where the tag encompasses an epitope, enabling immobilisation of the fusion protein to an inert matrix for affinity pull-down assays, prohibiting the requirement of complex electrophoresis conditions when the BK channel protein was small, and providing a means of further purification of the fusion protein. The fusion partners are not expected to influence the structure and function of associated proteins [303, 304]. However, analytical difficulties can arise from retaining the tag, such as the tag possessing or altering the properties of the experimental protein. The benefits of keeping the tags were considered to outweigh the disadvantages and therefore, corresponding controls were enforced throughout this study to exclude the fusion partner as the source of an experimental artefact (Discussed Chapters 4 & 5).

Mammalian expression & epitope tags

Basic differences between bacterial and mammalian protein translation render *E.coli* expression systems inappropriate for full-length channel expression [218] and therefore, epitope-tagged full-length BK channel proteins were expressed in a mammalian system. The mammalian system that was selected was the established cell line, human embryonic kidney 293 (HEK293). These cells are employed commonly for the expression of eukaryotic proteins due to the ease of maintenance, rapid multiplication, and the ability to express functional protein that has been translated and undergone appropriate post-translational modification [306]. HEK293 cells lack native BK channel

expression and thus facilitate the study of the epitope-tagged channels in the absence of a contaminating native population [80, 189], whilst providing a cell system with the required mammalian signalling pathways to enable investigation of the BK channel PKA response in a cellular environment analogous to the native tissue [306].

Use of an established cell line allows the creation of stable cell lines facilitating continuous and consistent recombinant protein expression [306]. Stable lines of the BK channel fusion proteins conveyed such fusion protein expression enabling consistent protein recovery to support the functional investigations of the channel proteins. Indeed, the epitope-tagged BK channel proteins expressed in HEK293 cells formed functional channels and thus permitted assessment of the specific roles and influences of particular protein domains, in particular that of the STREX insert, and whether phosphorylation of specific residues and association of individual accessory proteins may occur *in vivo*.

The epitope tags that were employed in this study are discussed in detail within the appropriate section of this chapter (Section 3.2.2). Previous investigations have described N-terminally tagged BK channel with disrupted voltage and calcium sensitivities [319], yet electrophysiological analysis of C-terminally tagged channels suggests limited or no influence [Tian, unpublished data]. Therefore, all tags were expressed at the C-terminal of the channel protein enabling purification of the fusion proteins by immunoprecipitation. Immunoprecipitation is a specific and effective tool in the isolation of proteins that may be difficult to segregate by other purification

techniques. The use of epitope-tags facilitated the immunoprecipitation of the channel subunits by providing an epitope common to all channel protein isoforms that was not influenced by the phosphorylation state of the complex. This allowed both *in vitro* and *in vivo* studies of channel phosphorylation (Chapter 4), as well as investigation of interacting proteins (Chapter 5). In addition, the use of different epitopes enabled examination of the heteromultimerisation of the splice variants (Chapter 5).

3.1.3 The phospho-specific antibodies

The study of the phosphorylation state of the BK channel fusion proteins was enriched by the generation of antibodies raised specifically against the phosphorylation state of the STREX insert serine-4 site, and the common, serine-869 residue. These antibodies facilitated the characterisation of BK channel phosphorylation in both fusion proteins and full-length channel protein (Chapter 4).

3.2 Results

3.2.1 Generation & characterisation of BK channel C-terminal fusion proteins for expression in *E.coli*

As described in the introduction to this chapter, regions of the BK C-terminal tail were isolated and expressed as fusion proteins in an *E.coli* recombinant expression system to facilitate preliminary investigation of the putative roles of specific sections of the channel protein.

3.2.1.1 GST-fusion proteins

The presence or absence of the 58-residue STREX insert in the BK channel sequence is influential to the contrasting regulation of the channels by PKA [80, 229]. To assess a possible functional role of the insert in underlying this differentiation, a glutathione-S-transferase (GST)-fusion protein was employed (Figure 3.2).

GST is used commonly as a fusion partner for recombinant protein expression in bacterial cultures. In addition to aiding the solubility of its fusion partners, the placement of the tag at the N-terminal of the STREX sequence is suggested to inhibit the bacterial protease recognition of the eukaryotic protein as a foreign entity, and thus facilitate the attainment of full-length recombinant protein [303]. The enzyme possesses a high affinity for glutathione, a property that is exploited to enable efficient and effective purification of GST-tagged proteins.

The 174 base pair (bp) sequence of the murine STREX exon was sub-cloned into pGEX vector, pGEX5x-1, by Rory Duncan and Janet Philp (Figure 3.2). Successful ligation was confirmed by digestion with endonucleases and by the polymerase chain reaction (Results not shown). Subsequent sequence analysis (MWG Biotech) established that insertion was in frame with the GST fusion partner gene.

Optimised induction and purification of the GST-STREX fusion protein was performed as described in Sections 2.5.1 & 2.5.2. During the protocol, samples were removed

Figure 3.2
The pGEX5x-1 plasmid

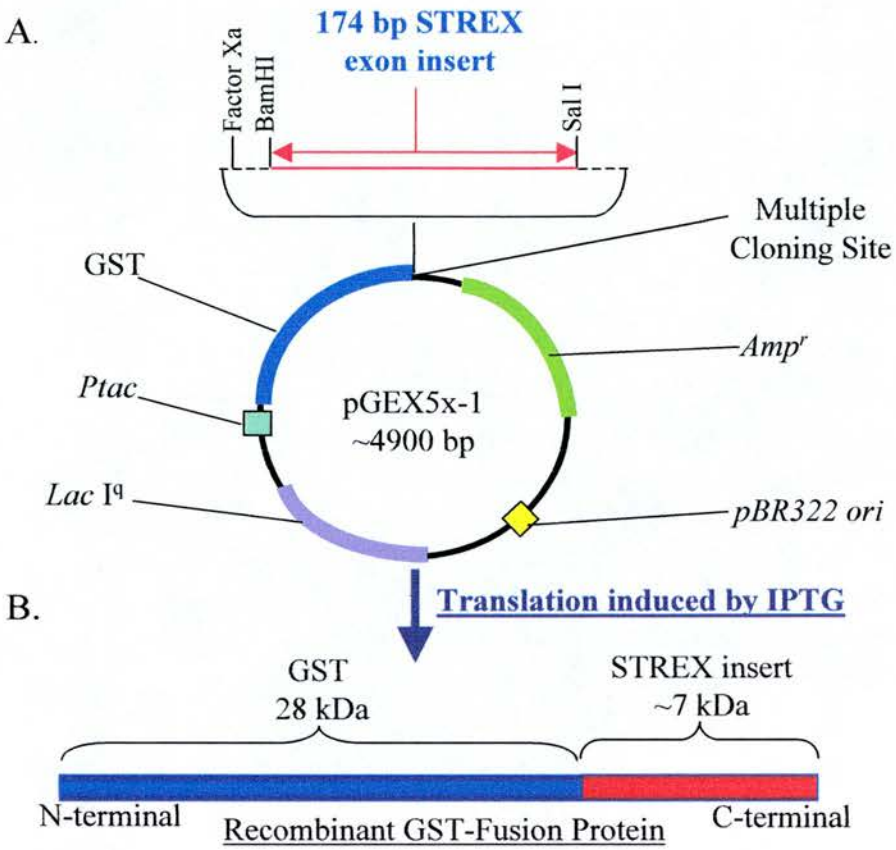

Figure 3.2: Diagram of the pGEX5x-1 vector & the location of the STREX exon insert. **A**. The 174 bp STREX exon sequence was amplified by PCR with flanking BamHI and SalI restriction sites. Ligation of the insert into the pGEX5x-1 plasmid multiple cloning site was sequentially in frame with the upstream GST-tag. **B.** The *tac* promoter (*Ptac*) confers IPTG-regulation of recombinant protein synthesis. Expression of the STREX-pGEX5x-1 plasmid in *E.coli* BL21-RIL cells resulted in the IPTG-induced generation of the ~35 kDa GST-STREX fusion protein. The *lac* I^q gene allows plasmid expression in any *E.coli* strain. *pBR322 ori* is the origin of replication of the plasmid, and *Amp*^{r} confers ampicillin resistance.

periodically and separated by SDS-PAGE to allow visualisation of the proteins by Coomassie stain (Sections 2.7.1). A representative analysis is illustrated in Figure 3.3.

Under optimised induction conditions, *E.coli* BL21-RIL cells expressing the STREX-pGEX5x-1 plasmid expressed the ~35 kDa GST-STREX fusion protein, consistent with the theoretical molecular weight of the fusion protein (Figure 3.2). Cultures incubated in the absence of the inducing sugar did not express the fusion protein demonstrating specific promoter control of recombinant protein expression. Such promoter integrity was confirmed by Western blot analysis employing the α-GST antibody (Results not shown).

Induced bacterial lysate was lysed by lysozyme and sonication to release the ~35 kDa protein into the soluble fraction. Incubation of the lysate with glutathione sepharose enabled binding of the GST-STREX fusion protein to the matrix by exploitation of the affinity of the GST fusion partner for glutathione. The native bacterial proteins were washed from the matrix together with a proportion of the recombinant protein indicative of incomplete association of the recombinant protein with the sepharose. Competitive elution of matrix-associated proteins released the pure ~35 kDa fusion protein together with a ~29 kDa protein later identified as a proteolytic degradation product (Section 3.2.1.1.3). Yields of 5-6 mg of recombinant protein / L of bacterial culture were achieved routinely. Confirmation of the identification of the ~35 kDa protein as GST-STREX was attained by Western blot analysis (Section 3.2.1.1.3).

Figure 3.3

Induction & purification of the GST-STREX fusion protein

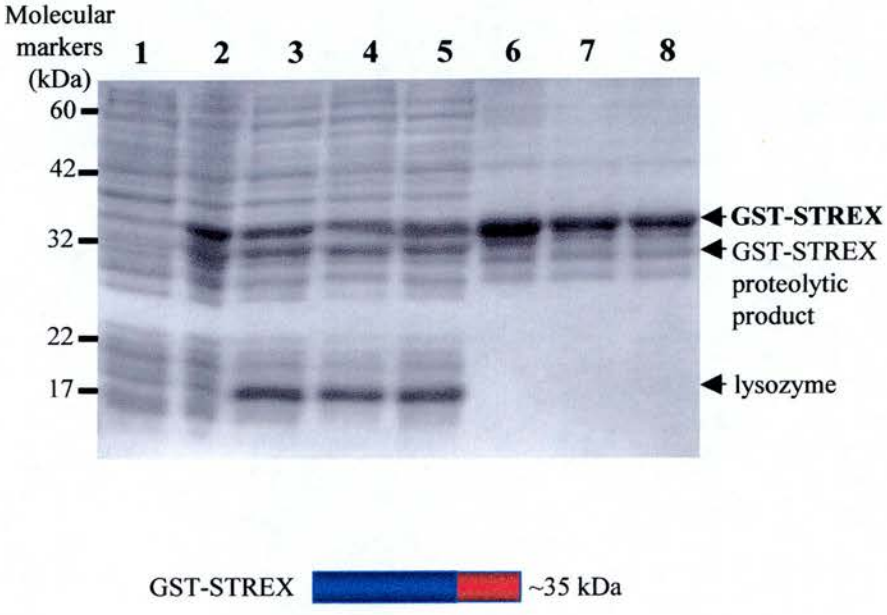

Figure 3.3: Representative Coomassie stained gel of GST-STREX induction and purification. Bacterial cultures expressing the STREX exon-pGEX5x-1 construct were induced with 0.5 mM IPTG for ~16 hours, stimulating synthesis of the 35 kDa GST-STREX fusion protein (lane 2; induced bacterial cell pellet), illustrated diagrammatically below the gel (See Figure 3.2). Induction is specific as the protein is not observed in non-induced cultures (lane 1; uninduced bacterial pellet). The recombinant protein was soluble following lysis by lysozyme (lane 3), and sonication (lane 4). Native bacterial proteins and the 17 kDa lysozyme enzyme were not bound by the glutathione sepharose (lane 5; wash from matrix incubated with bacterial lysate). Although a proportion of the fusion protein did not bind with the matrix (lane 5), most did (lane 6; matrix following lysate incubation and washing), and was eluted via competition by the glutathione buffer (lanes 7 & 8; elutions).

3.2.1.1.2 Generation of the GST-S4A fusion protein

The serine-4 residue of the STREX insert sequence is postulated to be a target of PKA-mediated phosphorylation [229]. To investigate whether mutation of the site can prevent phosphorylation, site directed mutagenesis was performed upon the STREX-pGEX5x-1 vector as described in Section 2.4.3. Mutagenic oligonucleotides were designed to mutate the serine-4-encoding codon to a triplet encoding the non-phosphorylatable alanine residue (Table 2.2, Figure 3.4). Subsequent sequence analysis (MWG Biotech) demonstrated successful mutation of the serine-4 residue, and IPTG-induction of the fusion protein in BL21-RIL *E.coli* cells resulted in expression of the ~35 kDa protein (Figure 3.4). Induction and purification of the fusion protein were performed as described for the GST-STREX fusion protein. The identification of the ~35 kDa GST-S4A fusion protein was confirmed by Western blot analysis (Section 3.2.1.1.3).

3.2.1.1.3 Characterisation & comparison of GST-fusion proteins

Western blot analysis employing antibodies raised against the GST fusion partner and the STREX insert was performed to characterise the GST-fusion proteins described above (Sections 3.2.1.1.1 & 3.2.1.1.2). Eluates from glutathione-sepharose affinity-purified GST-STREX, GST-S4A, and GST protein induced from the pGEX5x-1 vector, were assessed by Bradford analysis to determine the protein concentration (Section 2.2.5). Equal quantities of each were separated by SDS-PAGE for analysis by Coomassie or Western blotting (Figure 3.5).

Figure 3.4

Generation of the GST-S4A mutant fusion protein

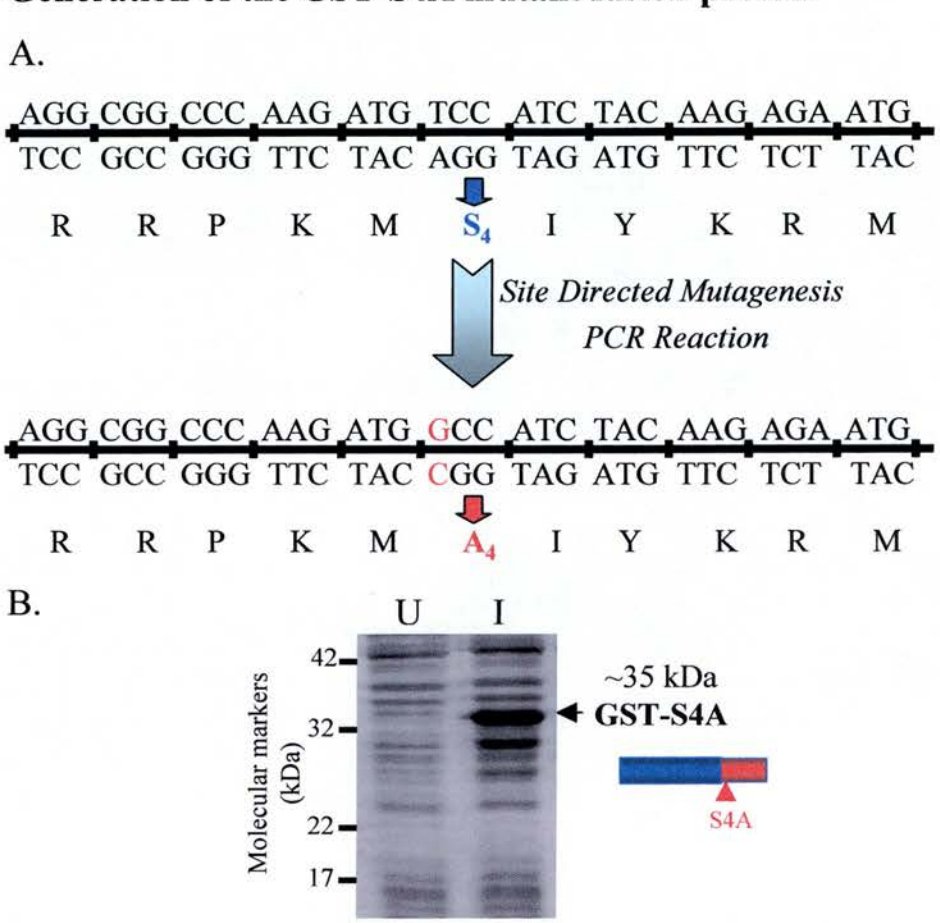

Figure 3.4: Site directed mutagenesis of the STREX insert S4 residue and induction of the ~35 kDa recombinant protein. A. The TCC codon of the wild type protein translates to the STREX insert serine-4 (S4) residue. Following site directed mutagenesis, the codon is altered to GCC, translating to non-phosphorylatable alanine. **B**. Comparison of IPTG-induced (I), and un-induced (U) S4A-pGEX5x-1-expressing bacterial pellets separated by SDS-PAGE and stained by Coomassie illustrates the specific and successful induction of the ~35 kDa GST-S4A recombinant protein, represented diagrammatically beside the gel (See Figure 3.2). Standard one letter amino acid code used.

Figure 3.5
Characterisation of the GST-fusion proteins

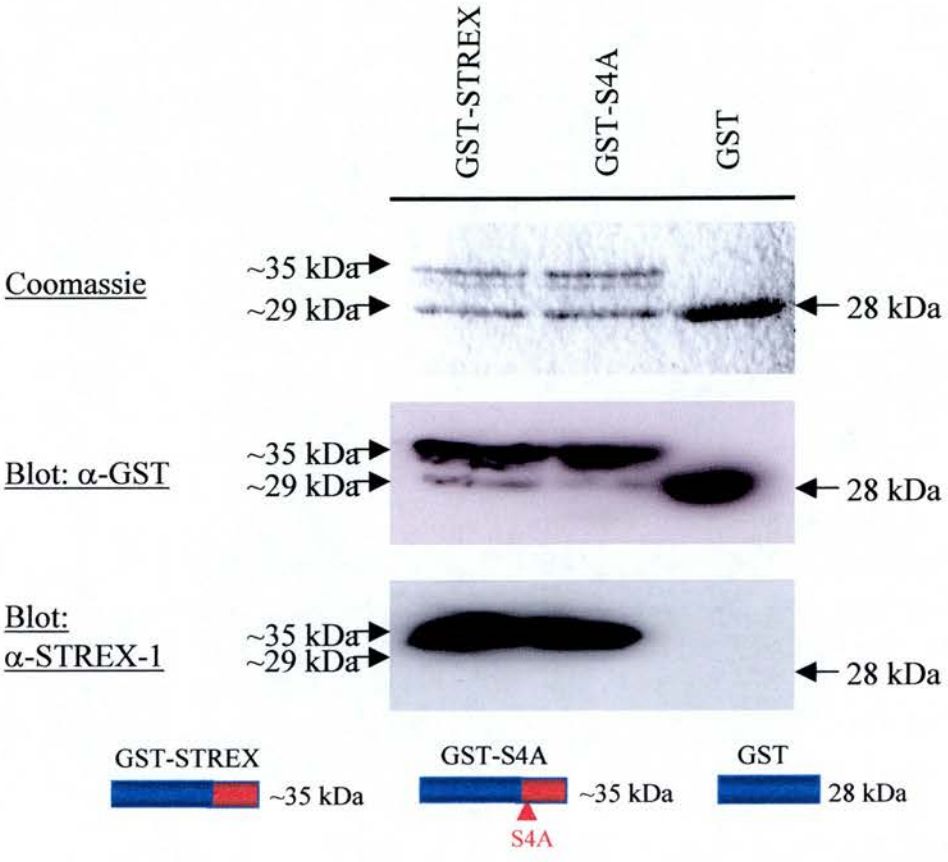

Figure 3.5: Representative SDS-PAGE analysis of the GST-STREX and GST-S4A proteins. Equal amounts (10 μg) of affinity purified GST protein and the GST-STREX and GST-S4A fusion proteins were separated by SDS-PAGE for analysis by Coomassie or Western blotting. The ~35 kDa GST-fusion proteins are visible by Coomassie stain and immunoreactive to α-GST and α-STREX-1 antibodies. The ~29 kDa proteolytic degradation products of the GST-fusion proteins are detected by Coomassie stain and the α-GST antibody, but not by α-STREX-1. GST is observed at 28 kDa under Coomassie stain and immunoreactive to α-GST, but not α-STREX-1. Fusion proteins are illustrated diagrammatically below the blots (See Figure 3.2). Western blot analysis: goat α-GST 1/2000; rabbit α-STREX-1 1/2000; α-goat/sheep-HRP 1/15000, α-rabbit-HRP 1/5000; detection by ECL.

Under the electrophoresis conditions employed, the GST-STREX and GST-S4A fusion proteins are observed at ~35 kDa by Coomassie staining, consistent with the predicted molecular weight (Figure 3.2). The proteins are immunoreactive to antibodies directed against both the GST-fusion partner and the STREX insert sequence. Immunoreactivity was not observed in the absence of the primary antibodies, nor did the primary antibodies show cross-reactivity against proteins to which they were not specifically raised (Data not shown) confirming the specificity of the antibodies.

Coomassie stain detected additional protein bands of ~29 kDa with both GST-fusion proteins. These proteins were not recognised by the α–STREX-1 antibody directed against the STREX insert, yet were identified by α–GST. This demonstrates that the 29 kDa proteins are GST-tagged polypeptides not expressing the full-length STREX epitope. GST was identified at 28 kDa, suggesting that the proteins are not GST contamination, but the products of proteolytic degradation of the fusion proteins. This assumption was confirmed by *in vitro* phosphorylation assays (See Section 4.2.2.1).

3.2.1.2 Thioredoxin-fusion proteins

Previous studies have described the generation of GST-fusion proteins of regions of the C-terminal tail of BK channels [202]. Purification of segments from the *Drosophila* BK channel produced very low yields requiring the application of detergents to enable solubilisation [202]. Such difficulties were found with the C-terminal tail region of the murine BK channel following the generation of insoluble GST-tagged fusion proteins

that encompassed the S869 region and the full-length of the C-terminal domain (Results not shown). Denaturation to enable solubilisation of the fusion proteins was not considered viable as the process influences the structure and biological activity of proteins. Subsequent refolding protocols could be applied, but previous investigations have suggested that the resultant protein recovery is low and may not resolve the native protein activity [304]. Therefore, the use of GST-fusion proteins of the C-terminal tail region was abandoned and, where appropriate, replaced by a thioredoxin-V5 epitope-polyhistidine-tagged (Thio-V5-H_6) fusion partner system (Figure 3.6). The exception to this was a small fusion protein encompassing the serine-869 region (See 3.1.1). The complete insolubility of fusion proteins of this region instigated the investigation of peptides of the site as discussed in Section 4.2.1.

Several studies have reported the successful application of thioredoxin as a fusion-partner for high yield expression of soluble recombinant protein in *E.coli* [304]. Fusion of the tag to regions of the murine BK channel C-terminal achieved successful solubilisation of the fusion proteins under native conditions. This enabled effective purification by exploitation of the affinity of the polyhistidine tag for nickel ions, and by the efficiency of the V5 region as an epitope, therefore, allowing subsequent application of the fusion proteins to *in vitro* assays investigating the possible physiological roles of the regions.

Figure 3.6

The pBAD/Thio-TOPO vector

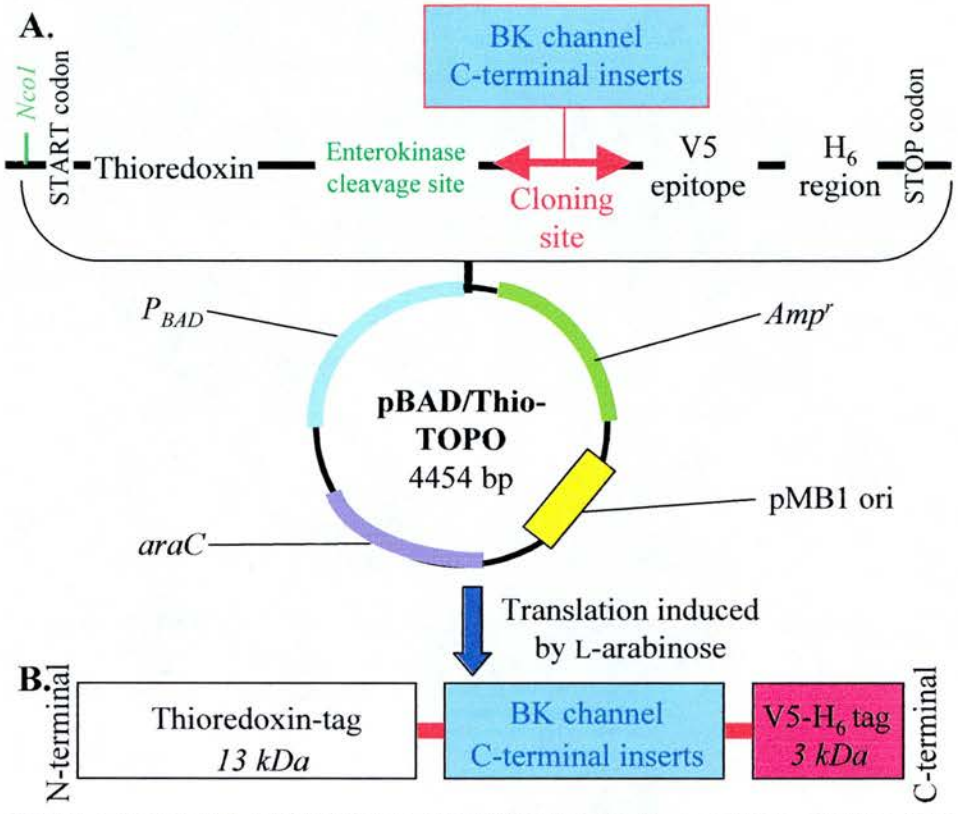

Figure 3.6: The pBAD/Thio-TOPO vector & location of the BK channel C-terminal constructs. A. TOPO cloning permitted the insertion of PCR-amplified regions of the BK channel C-terminal domain into the pBAD/Thio-TOPO cloning site. The primers employed positioned the inserts sequentially in frame with the thioredoxin gene proceeding the cloning site, and the polyhistidine region that follows. **B**. The *ara*BAD (P_{BAD}) promoter confers arabinose-regulation of recombinant protein synthesis. Expression of pBAD/Thio-TOPO constructs in *E.coli* resulted in the arabinose-induced expression of proteins tagged with 13 kDa Thioredoxin, and 3 kDa V5 epitope-polyhistidine (-V5-H_6) fusion partners. Fusion proteins are illustrated in Figure 3.7. *araC* is crucial to P_{BAD} transcriptional regulation, *pMB1 ori* is the origin of replication, Amp^r confers ampicillin resistance. The *Nco1* restriction site is highlighted in green.

Table 3.2
Composition of the Thio-V5-H_6-fusion proteins

FUSION PROTEIN	INSERT START * (bp)	INSERT END * (bp)	INSERT LENGTH (bp)	Mr OF TRANSLATED INSERT (kDa) {+ Thio-V5-H_6}	STREX	S869	LZ1	LZ2
ΔN-STREX-ΔC	1657	3039	1382	52 {68}	Intact	Intact	-	Intact
ΔN-ZERO-ΔC	1657	3039**	1208**	45 {61}	-	Intact	-	Intact
ΔN-S4A,S869A-ΔC	1657	3039	1382	52 {68}	S4A	S869A	-	Intact
ΔN-STREX,S869A-ΔC	1657	3039	1382	52 {68}	Intact	S869A	-	Intact
Thio-LZ1	1384	1767	383	15 {31}	-	-	Intact	-
Thio-mLZ1	1384	1767	383	15 {31}	-	-	Mutant	-

* - numbering refers to murine STREX BK channel sequence.

Mr - approximate molecular weight calculated by DNAStar Biometrics package

** - numbering of nucleotides in ZERO channel sequence is altered for equivalence to STREX. Therefore, actual length is 174 bp less than apparent due to the absence of the STREX exon.

\- - regions of the BK channel C-terminal tail section absent from the construct

{} - molecular weight of fusion protein including fusion tag, Thio-V5-H_6.

Table 3.2: Thio-V5-H_6 proteins' composition. The regions of the C-terminal tail of the murine BK channel gene that were inserted into the pBAD/Thio-TOPO vector are listed above highlighting the particular characteristics of interest to this study. The resultant recombinant proteins are illustrated diagrammatically in Figure 3.7.

Figure 3.7
The thioredoxin-V5-polyhistidine tagged fusion proteins

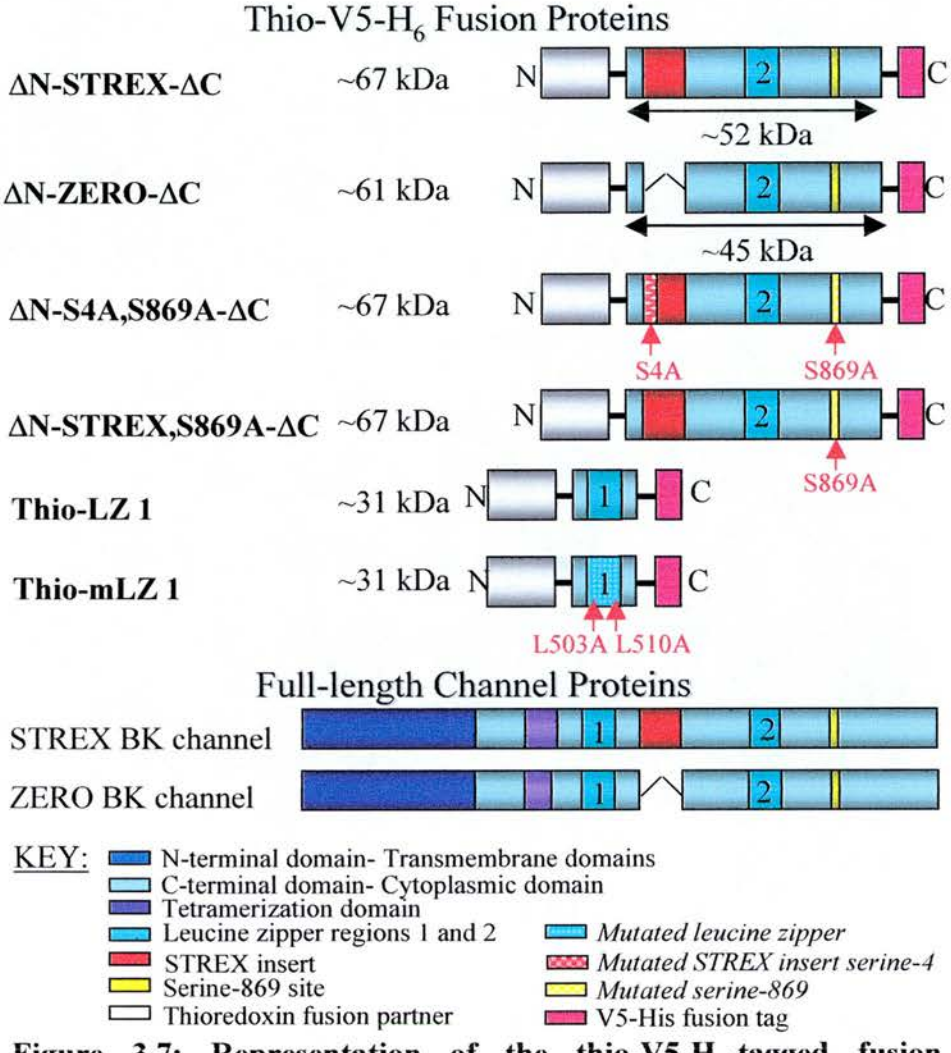

Figure 3.7: Representation of the thio-V5-H_6-tagged fusion proteins. The fusion constructs in pBAD/Thio-TOPO encompass the regions of the BK channel C-terminal tail as aligned to the full-length channel protein representations (not to scale). Mutations are indicated by red arrows. Thioredoxin at the N-terminal (N) and the V5-H_6 epitopes at the C-terminal (C) add 13 and 3 kDa respectively to the molecular weight of the fusion proteins (white and pink boxes). Table 3.2 describes the corresponding DNA sequences.

3.2.1.2.1 Generation of the thioredoxin-fusion proteins

Specific regions of the C-terminal tail from STREX, ZERO, and various mutant isoforms of the murine BK channel were amplified by PCR as described in Section 2.4, and as illustrated Table 3.2. The oligonucleotides employed (Table 2.2 & Figure 2.1) were designed to ensure that direct insertion of the PCR amplification products into the pBAD/Thio-TOPO vector was sequentially in frame with the respective fusion partners: thioredoxin, polyhistidine, and the V5 epitope (Figure 3.6). Plasmid DNA isolated from *E.coli* JM109 cells that were transformed successfully with the ligated vectors was analysed by PCR and restriction digestion to confirm successful insertion and correct orientation (Results not shown). Subsequent sequence analysis (MWG Biotech) verified that each of the insertions had ligated in the correct orientation, in-frame with the fusion partners.

3.2.1.2.2 Induction of the thioredoxin-fusion proteins

Successful insertion of the BK channel C-terminal tail regions into the pBAD/Thio-TOPO vector allowed induced expression of recombinant proteins tagged with the thioredoxin, V5 epitope, and polyhistidine fusion partners (Thio-V5-H_6) as described in Section 2.5.1. The resultant fusion proteins are illustrated diagrammatically in Figure 3.7. *E.coli* BL21-RIL strain was employed as the recombinant expression system, and specific induction of the fusion proteins was observed in cultures treated with the pBAD vector inducer, L-arabinose. A representative induction of the ΔN-STREX-ΔC fusion

protein is illustrated in Figure 3.8, where cell pellets from cultures exposed to L-arabinose were compared to those not induced with the sugar by SDS-PAGE separation. Differentiation of the impure recombinant protein among native bacterial proteins was not possible by Coomassie or Silver staining techniques and therefore immunoblotting was performed. The α-V5 antibody detected an ~70 kDa protein in the presence of L-arabinose only, consistent with the predicted molecular weight of the 67 kDa V5-tagged ΔN-STREX-ΔC fusion protein (Figure 3.7). Detection of lower molecular weight proteins suggests proteolytic degradation. Parallel results were obtained with the other fusion proteins indicating specific arabinose-induced synthesis of all the Thio-V5-H_6-tagged fusion proteins (Results not shown).

3.2.1.2.3 Purification & characterisation of the thioredoxin-fusion proteins

Nickel affinity chromatography

The Thio-V5-H_6-tagged fusion proteins were purified by affinity chromatography exploiting the strong affinity of the polyhistidine-tag for nickel ions following optimised induction and purification as described in Section 2.5.3. During the protocol, samples were removed periodically and suspended or diluted in SDS-LB to allow separation by SDS-PAGE and visualisation by immunodetection. Figure 3.9 illustrates such an analysis using the ΔN-STREX-ΔC fusion protein.

BL21-RIL *E.coli* cells expressing the BK channel C-terminal fusion protein–pBAD/Thio-TOPO plasmids were cultured at 37 ^{0}C until bacterial growth was

Figure 3.8

Induction of the ΔN-STREX-ΔC fusion protein

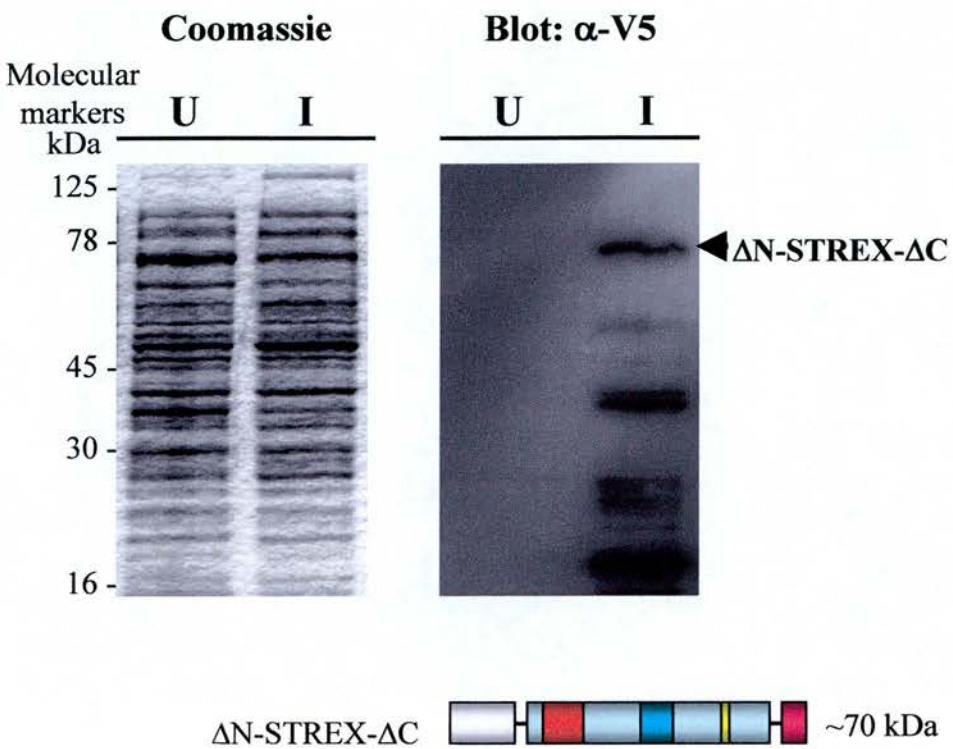

Figure 3.8: Representative Coomassie & Western blot analyses of the induction of the ΔN-STREX-ΔC fusion protein. Differentiation of the recombinant protein among the native bacterial proteins was not possible by Coomassie staining of SDS-PAGE separated uninduced (U) and arabinose-induced (I) cell pellets from *E.coli* expressing the ΔN-STREX-ΔC plasmid (0.2 % L-arabinose, 16 ^{0}C, ~16 hours). Western blot analysis of the samples employing the α-V5 antibody detects specific induction of the ~70 kDa V5-tagged ΔN-STREX-ΔC recombinant protein, indicated by an arrow and illustrated diagrammatically below the blots (See Figure 3.7). Western blot analysis:mouse α-V5 1/5000;α-mouse-HRP 1/2000; detection by ECL.

Figure 3.9

Purification of the Thio-V5-H_6 fusion proteins by Ni^+-column affinity chromatography

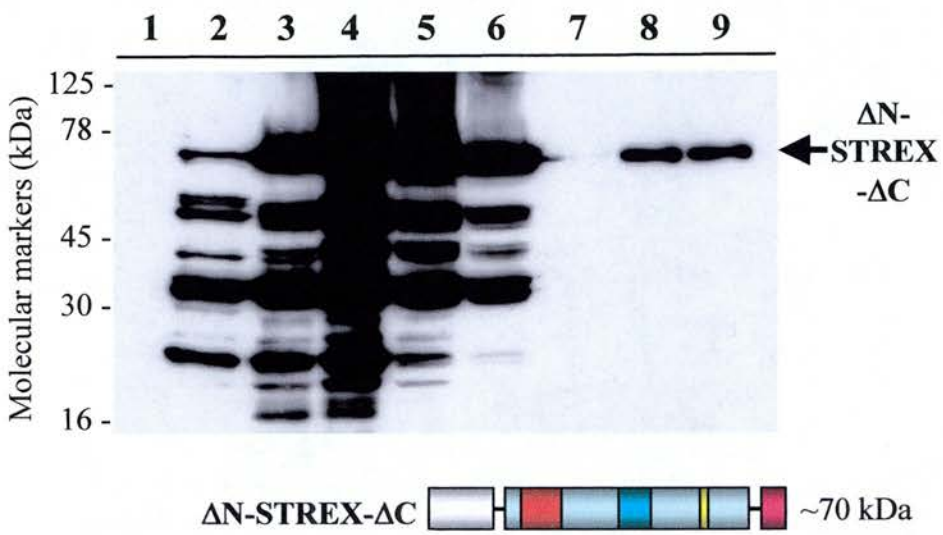

Figure 3.9: Representative Western blot illustrating the purification of the ΔN-STREX-ΔC fusion protein by Ni^+ affinity chromatography. 1- uninduced bacterial cell pellet; 2- induced bacterial cell pellet (0.2 % arabinose, 16 ^{0}C ~6 hours); 3- induced bacterial cell pellet (~16 hours); 4- cell pellet lysed by lysozyme and sonication; 5- cellular lysate; 6- Ni^+-sepharose following cellular lysate incubation; 7-column wash (after extensive washing); 8- first elution; 9- second elution. Bacterial cultures expressing the ΔN-STREX-ΔC construct were induced with 0.2% L-arabinose, stimulating synthesis of the ~70 kDa ΔN-STREX-ΔC fusion protein (lanes 2&3). Induction is specific as the protein is not observed in non-induced cultures (lane 1). Some recombinant protein was retained in the insoluble cell pellet (lane 4), but the majority remained soluble (lane 5) following cellular lysis. The fusion protein binds Ni^+-sepharose (lane 6) and is not washed from the matrix (lane 7), but is eluted by 250 mM imidazole (lanes 8&9) .The fusion protein is illustrated diagrammatically below the blot (See Figure 3.7). Western blot: mouse α-V5 1/5000, α-mouse-HRP 1/2000, Detection by ECL.

determined to have reached the exponential, protein-producing, phase. Induction with 0.2% L-arabinose was followed by incubation at 16 ^{0}C for ~16 hours and induced synthesis of the ~70 kDa ΔN-STREX-ΔC protein as detected by its immunoreactivity with the α-V5 antibody. The recombinant protein is visible in the insoluble and soluble fractions following lysozyme and sonication-induced lysis of the bacterial cells. It binds nickel-sepharose, and is eluted by a competitive elution buffer. Other immunoreactive proteins of lower molecular weights are detected throughout the lysis stage of the purification. However, in the final eluates, only the ~70 kDa protein is observed, suggesting specific purification. Equivalent results were obtained with the other ΔN-ΔC fusion proteins (Results not shown).

The eluates from the nickel-column purified ΔN-ΔC fusion proteins were analysed by Coomassie staining of SDS-PAGE separated samples to determine the homogeneity of the solutions. Figure 3.10 illustrates such an analysis upon the ΔN-STREX-ΔC and ΔN-ZERO-ΔC fusion proteins. The ~70 kDa ΔN-STREX-ΔC protein and the ~65 kDa ΔN-ZERO-ΔC fusion protein are detected, in addition to a ~75 kDa contaminant. The ~75 kDa protein is present in all eluates including purification performed upon non-induced bacterial lysate. This is indicative of the association of a native bacterial protein with the nickel-sepharose matrix.

Figure 3.10

The ΔN-ZERO-ΔC and ΔN-STREX-ΔC fusion proteins purified by Ni^{2+}-sepharose chromatography

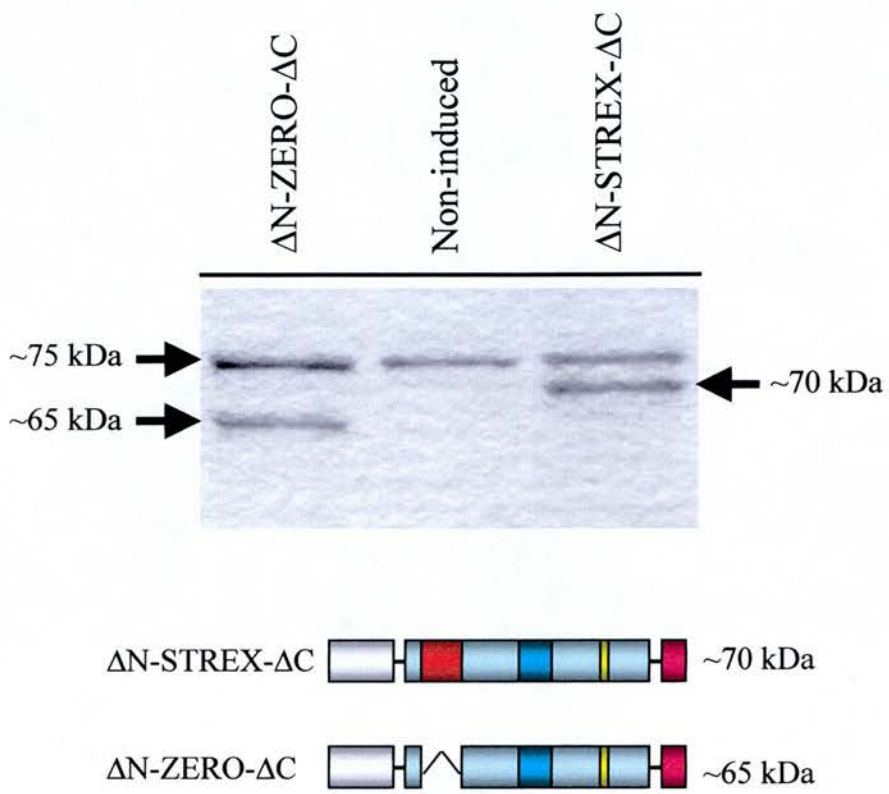

Figure 3.10: Representative Coomassie stain of Ni^{2+}-sepharose purified elutions. Eluates from nickel sepharose purifications of the ΔN-ZERO-ΔC and ΔN-STREX-ΔC, together with an eluate from non-induced bacterial lysate passed through the Ni^{2+} column, were separated by SDS-PAGE and visualised by Coomassie stain. The ~65 kDa ΔN-ZERO-ΔC, and the ~70 kDa ΔN-STREX-ΔC fusion protein, as illustrated diagrammatically below the gel (See Figure 3.7), are purified successfully with an additional ~75 kDa contaminating protein detected. The contaminant is also observed with non-induced bacterial lysate passed through the column.

Immunoprecipitation

Immunoprecipitation (IP) of the Thio-V5-H_6-fusion proteins from arabinose-induced bacterial cultures was performed as described in Section 2.5.4 by incubation of pre-cleared lysates with protein-G-sepharose (PGS) and the α–V5 antibody that was raised against the V5 fusion tag. The final IP pellets were separated by SDS-PAGE prior to analysis by immunoblotting and Coomassie staining. Figure 3.11 illustrates such analysis upon the ΔN-STREX-ΔC and ΔN-ZERO-ΔC fusion proteins.

The ~70 kDa ΔN-STREX-ΔC and ~65 kDa ΔN-ZERO-ΔC fusion proteins were immunoprecipitated successfully by the α–V5 antibody at concentrations sufficient to allow detection by Coomassie stain (> 300 ng) [308]. The ~75 kDa contaminating protein is not detected by this method, suggestive of non-co-purification. Additionally, the stain only distinguishes the fusion protein and IgG bands indicating the absence of detectable contaminating proteins. Parallel results were obtained from the immunoprecipitation of the other Thio-V5-H_6-fusion proteins (Results not shown).

Further characterisation of the Thio-V5-H_6 fusion proteins was achieved by Western blot analysis employing fusion protein-specific antibodies. These data are described in following chapters.

Figure 3.11

Immunoprecipitation of the ΔN-STREX-ΔC and ΔN-ZERO-ΔC fusion proteins

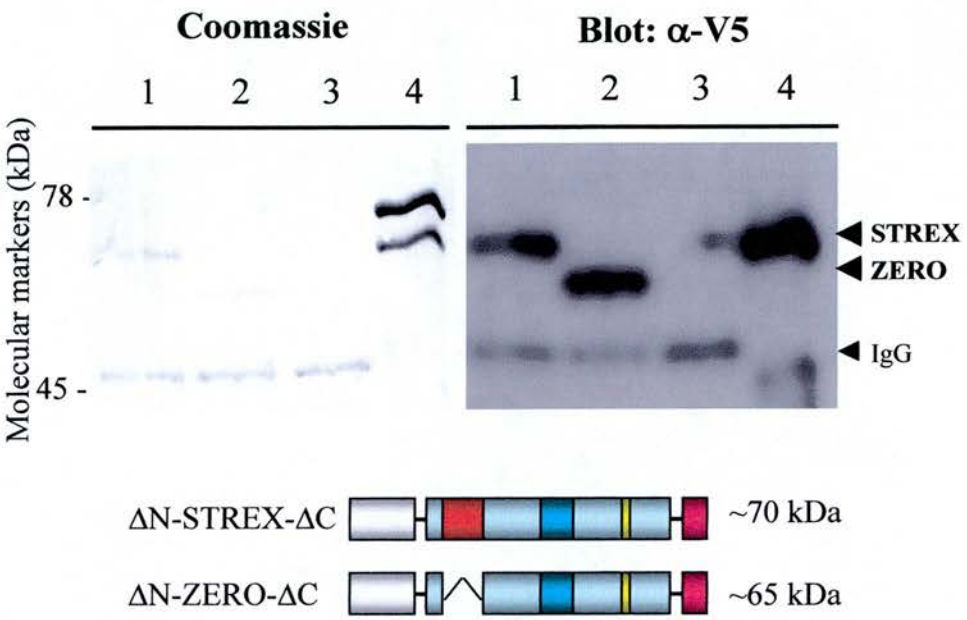

Figure 3.11: Representative Coomassie and Western blot analysis of ΔN-STREX-ΔC and ΔN-ZERO-ΔC immunoprecipitates, with comparison to Ni^{2+} sepharose purification. 1- ΔN-STREX-ΔC immunoprecipitation (IP) using α-V5 antibody; 2- ΔN-ZERO-ΔC IP; 3- non-induced bacterial lysate IP; 4- ΔN-STREX-ΔC eluate from Ni^{2+} affinity chromatography. IP of the ~70 kDa ΔN-STREX-ΔC and ~65 kDa ΔN-ZERO-ΔC fusion proteins pulls down sufficient protein to enable detection by Coomassie as well as Western blot analysis. The IP immunoglobulin (IgG) is observed at ~50 kDa, and is immunoreactive to α-mouse. No additional contaminating proteins are observed in the IPs. Purification of ΔN-STREX-ΔC by affinity chromatography isolates the fusion protein, but an additional ~75 kDa contaminating protein that is not immunoreactive to α-V5 is detected by Coomassie stain (See Figure 3.10). Fusion proteins are illustrated below the gels (See Figure 3.7). Western blot analysis: mouse-α-V5 1/5000, α-mouse-HRP 1/2000, detection by ECL.

3.2.2 Generation & characterisation of full-length BK channel fusion proteins for expression in a mammalian cell line

Investigation of the full-length BK channel protein was employed to validate the roles of specific C-terminal regions that were proposed from the *in vitro* studies using bacterially expressed fusion proteins. Expression of the functional channels in a mammalian system enabled *in vivo* assessment of the PKA response of BK channel splice variants and mutant channels (Chapters 4 & 5).

The channel proteins were expressed with epitope-tagged fusion partners at the C-termini. Three epitope tags were employed: hemagglutinin (-HA), V5-polyhistidine (-V5-H_6) and enhanced green fluorescent protein (-EGFP). The use of the tags was to facilitate efficient isolation of the channels by immunoprecipitation or immunodetection, without the requirement of channel-specific antibodies that may be influenced by the splice variant or phosphorylation state of the channel protein (See Section 3.1.2). HA and V5-H_6 are employed for this purpose commonly as they are relatively short protein sequences that induce minimal disruption to protein synthesis, structure or activity [320-322; Tian, unpublished results]. EGFP is a much larger fusion partner (27 kDa), but studies have indicated that it causes minimal disruption to the functionality of the BK channel when expressed at the C-terminal compared to N-terminal expression (See Section 3.1.2) [319; Tian, unpublished results]. The tag displays green fluorescence when excited at 478 nm enabling analysis of the location of the epitope tagged channels without the requirement of immunodetection techniques.

Therefore, the application of the epitope-fusion partners facilitated the study of the BK channel splice variants and their differential responses to PKA, by enabling *in vitro* and *in vivo* investigation of phosphorylation (Chapter 4) and channel-accessory protein associations (Chapter 5) upon channels that are expressed functionally and can be isolated in any phosphorylation state. Additionally, by employing different tags, the heteromultimerisation of the splice variants could be examined (Chapter 5).

3.2.2.1 Generation of the BK channel fusion proteins

The murine ZERO BK channel gene was inserted into the pcDNA3 mammalian-expression vector with an epitope fusion partner gene 3' and in-frame to the channel sequence as to generate channel protein with the carboxyl-terminal tag, –HA, -V5-H_6 or –EGFP. A restriction endonuclease and ligation regime, as described in Section 2.4, was enforced to generate the STREX and mutant isoforms of these fusion proteins. The regimen is illustrated by Figure 3.12, demonstrating the restriction of a region of the C-terminal tail of the BK channel that encompasses splice site two, the location of STREX exon, and the serine-869 expressing codon. Therefore, the ZERO channel sequence could be replaced with the equivalent segment from STREX and mutant channel variants, allowing the generation of the epitope-tagged isoforms of the BK channel that were employed in this study (Table 3.3 & Figure 3.13).

Figure 3.12

Restriction endonuclease regime to generate epitope-tagged BK channel isoforms

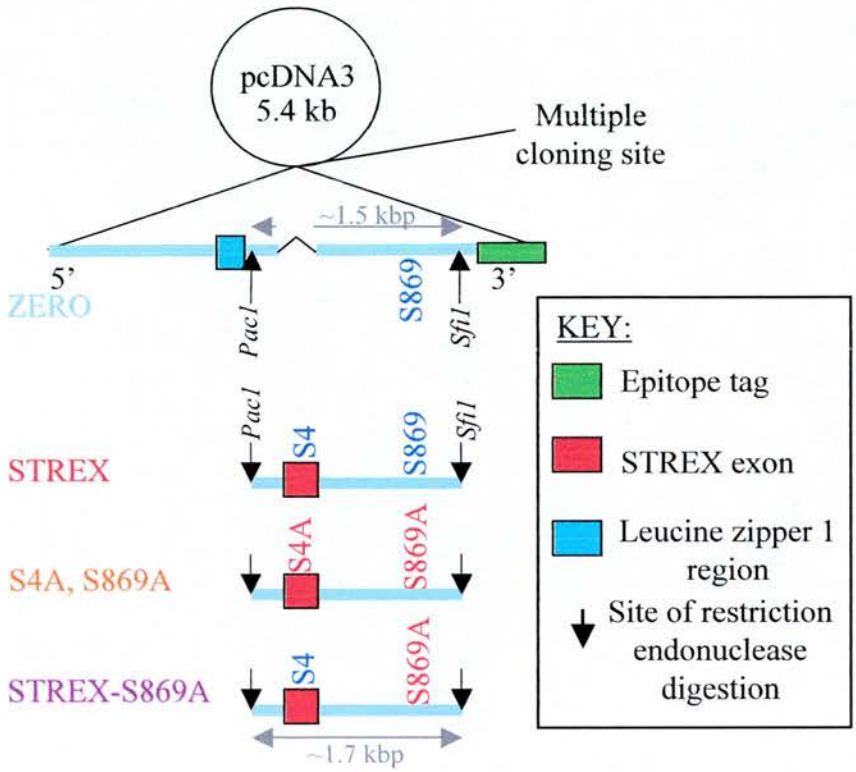

Figure 3.12: Epitope-tagged BK channel variants created by restriction digestion and ligation regime. The *PacI* endonuclease cut at base number 1743 within the murine BK channel sequence, downstream from the leucine zipper 1 region. *SfiI* digested at site 3282 in the ZERO isoform, equivalent to site 3456 within the STREX channel sequence, downstream from the serine-869 codon. The respective ZERO and STREX DNA fragments of ~1.5 and ~1.7 kbp were ligated into the appropriate pcDNA3 vector containing the corresponding N-terminal and C-terminal BK channel regions with the C-terminal epitope tag. This allowed the generation of the epitope-tagged isoforms of the murine BK channel that were used in this study.

Table 3.3

The epitope-tagged splice variants and mutants of the BK channel generated in this study

CHANNEL ISOFORM	EPITOPE TAG			Mr of untagged channel	CHARACTERISTICS			
	HA	**V5-H_6**	**EGFP**	**(kDa)**	**Splice site2**	**S869**	**LZ1**	**LZ2**
STREX	Y	Y	Y	132	STREX	Intact	Intact	Intact
ZERO	Y	Y	Y	125	No insert	Intact	Intact	Intact
S4A,S869A	Y	-	-	132	STREX-S4A	S869A	Intact	Intact
STREX,S869A	-	-	-	132	STREX	S869A	Intact	Intact
mLZ (STREX)	Y	-	-	132	STREX	Intact	Mutant	Intact
Mr of TAG (kDa)	<1	<1	27					

Y - epitope tagged channel used in this study

\- - epitope tagged channel not used in this study

Mr - predicted molecular weight (DNAStar Biometrics package)

Table 3.3: The epitope-tagged splice variants and mutant isoforms of the murine BK channel that were employed in this study. The BK channel splice variants and mutant channel genes were inserted into the pcDNA3 vector with an epitope tag 3' to the channel sequence to produce channel protein with a C-terminal epitope fusion partner (See Figures 3.12 & 3.13). The epitopes were the hemaggltinin (-HA), -V5-polyhistidine (-V5-H_6) and enhanced green fluorescent protein (-EGFP).

Figure 3.13
The epitope-tagged full length BK channel proteins

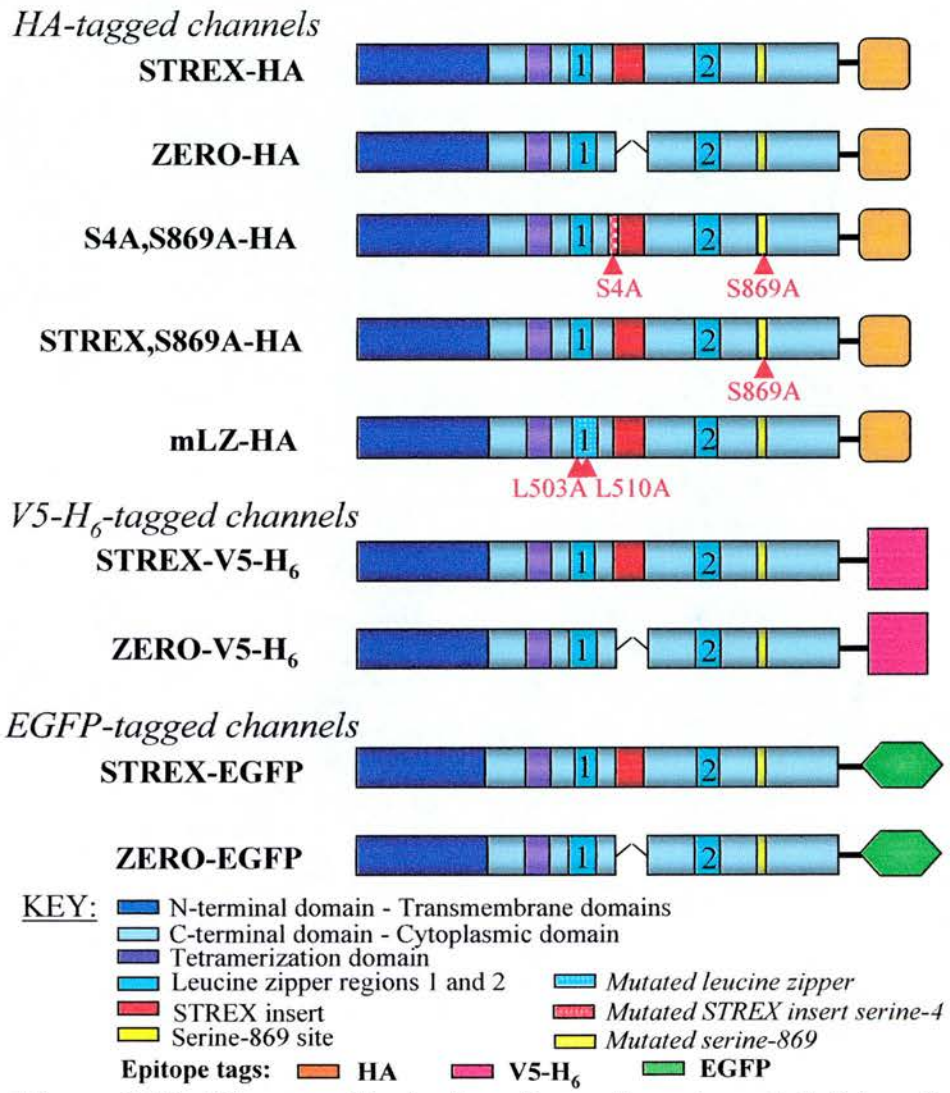

Figure 3.13: Diagram illustrating the epitope-tagged full-length channel fusion proteins. Channel proteins were tagged at the C-terminal by the -HA, -V5-H_6, or -EGFP epitopes. The splice variants are represented as described in Figure 3.1, with sites of mutation highlighted by arrows (Not to scale). Table 3.3 summarises this figure providing the molecular weights of the proteins. Corresponding DNA sequences are illustrated in Figure 1.3.

3.2.2.2 Functional expression of the BK channel fusion proteins

The BK channel-pcDNA3 vectors were transfected into the human embryonic kidney 293 cell line (HEK293) mammalian expression system and stable cell lines were generated using standard tissue culture protocols as described in Section 2.6.2. The pcDNA3 vector confers geneticin-resistance to cells that express it and therefore, HEK293 cells transfected with BK channel-pcDNA3 were selected and maintained by application of the antibiotic. The system facilitates successful translation and post-translational modification of tagged mammalian proteins and allows functional investigation of the channels in a mammalian cellular environment that lacks native BK channel expression [80, 189].

3.2.2.2.1 Immunoprecipitation

Antibodies directed against the -HA, -V5 and -EGFP tags were employed to assess expression of the channel fusion proteins in HEK293 cells. As described in Section 2.6, cell lines expressing the fusion proteins were grown in 5 % CO_2 at 37 ^{0}C until cultures were sufficiently confluent for harvesting. Cells were lysed by sonication and detergent treatment, prior to the addition of PGS and the appropriate antibody to the pre-cleared lysate. The final IP pellets were diluted with SDS-LB and separated by SDS-PAGE for Western blot analysis. Figure 3.14 illustrates the detection of some of the immunoprecipitated channel fusion proteins.

Figure 3.14
Expression of epitope-tagged BK channels in HEK293 cells

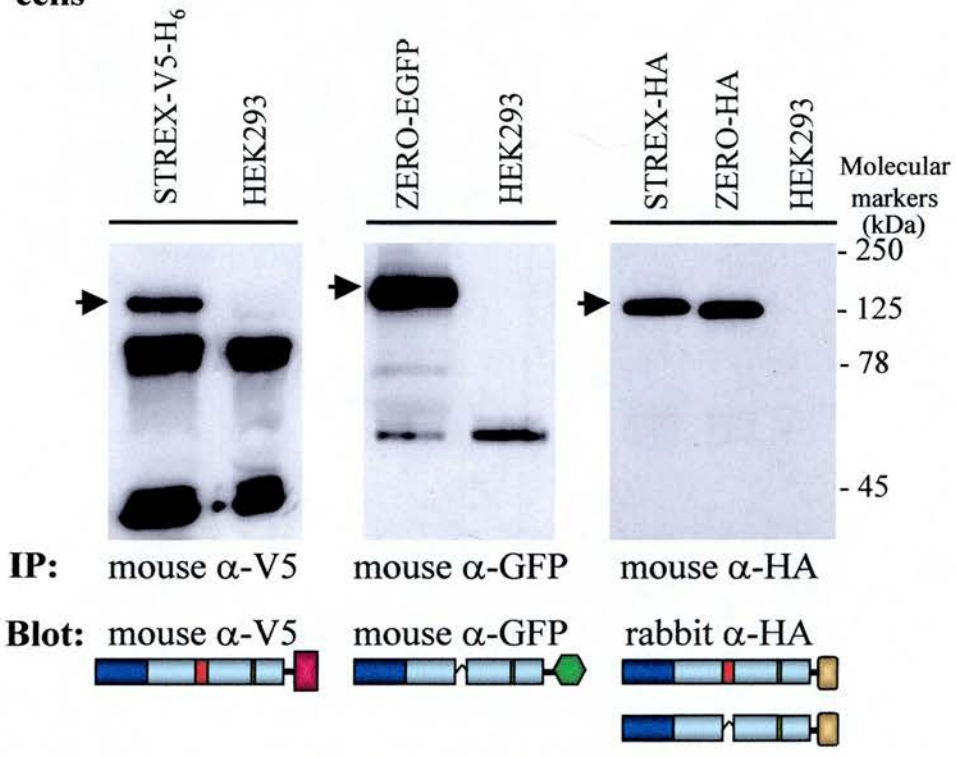

Figure 3.14: Representative Western blots illustrating expression of epitope-tagged BK channels in HEK293 cells. Epitope-tagged STREX and ZERO BK channel splice variants expressed in HEK293 cells were immunoprecipitated (IP) by antibodies directed against the respective tags (-V5, -EGFP, -HA epitopes). The channels, indicated by arrows and illustrated diagrammatically below the blots (For simplicity within the C-terminal domain only splice site 2 and the S869 site are illustrated, see Figure 3.13), are detected at ~125 kDa. The channels are not detected in IPs from untransfected HEK293 cells. Lower molecular weight bands observed in both transfected and untransfected cells in the left hand and middle panels are non-specific products including immunoglobulins (IgGs) detected by the α-mouse antibody. Western blot analysis: mouse α-V5 1/5000, mouse α-EGFP 1/1000, rabbit α-HA 1/333, α-mouse-HRP 1/2000, α-rabbit-HRP 1/5000, detection by ECL.

Immunoreactive proteins of ~125 kDa are observed in all BK channel-expressing systems, consistent with the predicted molecular weight of the channel fusion proteins (See Table 3.3). The proteins are not detected from native HEK293 cells nor cells transfected with pcDNA3 vector alone (As Figure 5.1). Comparison of the STREX and ZERO-HA-tagged channels demonstrates a slight difference in molecular weight indicative of the respective presence or absence of the STREX insert. These data demonstrate successful expression of the tagged channels by HEK293 cells at a level sufficient for detection by the appropriate immunoblotting antibody.

3.2.2.2.2 Fluorescence & Immunofluorescence

To assess the cellular location of the BK channel protein, HEK293 cells expressing the EGFP-tagged channels were fixed on glass coverslips, stained with the DNA-binding dye TO-PRO-3, and analysed by fluorescence microscopy as described in Section 2.6.4. Figure 3.15A illustrates a representative confocal microscopy image of ZERO-EGFP channels.

Excitation of the –EGFP tag and TO-PRO-3 dye induces green and blue fluorescence respectively. The blue TO-PRO-3 excitation demonstrates the location of the nuclear compartment. Although small pockets of green fluorescence are visible within the cytoplasmic region, indicative of channel protein trapped within cellular organelles, the majority of the EGFP signal is observed peripherally. This suggests that the majority of the EGFP-tagged channel protein is present at the cell membrane, demonstrating

Figure 3.15
Functional expression of epitope-tagged BK channels in HEK293 cells

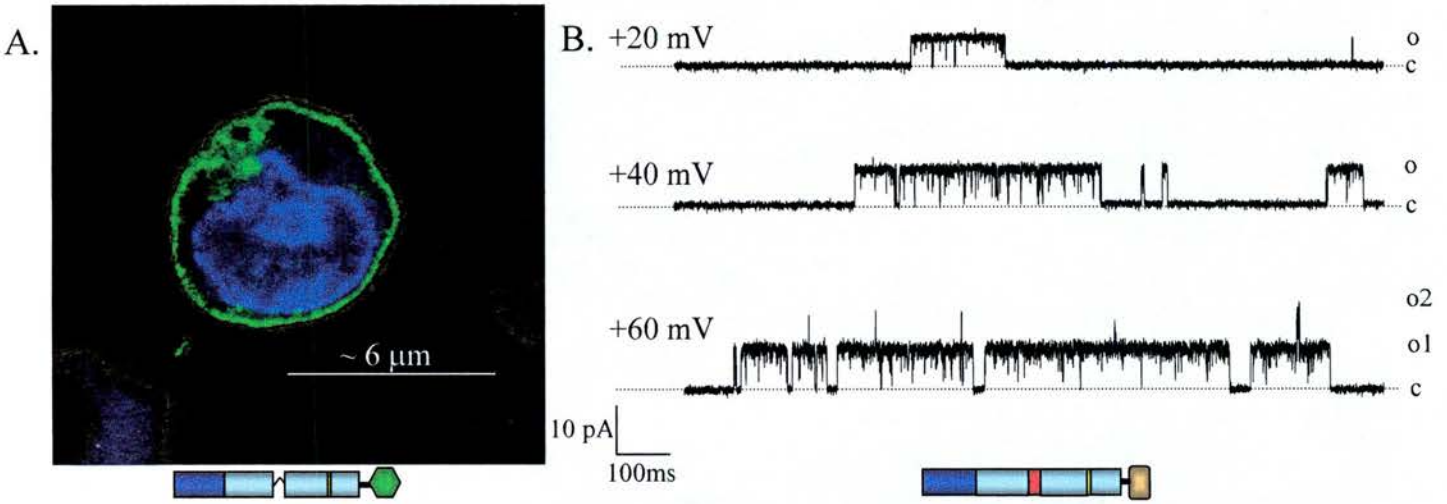

Figure 3.15: Representative confocal microscopy image and electrophysiological analysis of epitope-tagged BK channels expressed in HEK293 cells. A Confocal image of HEK293 cell expressing the ZERO-EGFP BK channel. Cells were stained with blue nuclear dye, TO-PRO-3. The EGFP tag fluoresces green, and indicates that the majority of the fusion protein was targeted to the plasma membrane. **B** Electrophysiological analysis of the STREX-HA channel. Inside-out patches were depolarised to +20, +40, and +60 mV in physiological K^+ gradient in the presence of 0.2 µM free Ca^{2+}. ***c*** indicates closed channels; ***o*** indicates channel opening. The single channel conductance is ~120 pS, characteristic of the large conductance of BK channels. Increasing the voltage across the membrane, increases the open probability.

successful targeting of the EGFP-tagged channel protein by the HEK293 cellular machinery. Equivalent analysis, performed by Lijun Tian, demonstrated a cellular membrane location for the EGFP-tagged BK channel isoforms in PC12 cells, indicating that other mammalian cell types can target the channels successfully (Results not shown).

3.2.2.2.3 Electrophysiology

To investigate the functionality of the BK channel fusion proteins expressed in HEK293 cells, electrophysiological analysis was employed. Cells expressing the epitope-tagged channels were cultured on coverslips and analysed by an inside-out configuration as described in Section 2.6.5. Figure 3.15B illustrates such an analysis upon the STREX-HA fusion protein. Stepping the voltage to +20, +40 and +60 mV, resulted in increased opening of channels with ~125 pS conductance, consistent with that of BK channels, and not of channels native to HEK293 cells [3]. This indicates that the STREX-HA channels are functionally expressed at the HEK293 cell membrane.

Electrophysiological analysis of the other BK channel fusion proteins that were used in this study was performed by Lijun Tian (Results not shown), and demonstrated that all the isoforms produced functional and correctly regulated channels.

3.2.3 Preliminary characterisation of phospho-specific antibodies

The phospho-specific antibodies employed in this study were directed against the phosphorylated and non-phosphorylated murine BK channel serine-869, and the STREX insert serine-4 sites. The antibodies were raised against phosphorylated and non-phosphorylated peptides encompassing these regions by Diagnostics Scotland (See Scheme 2.1). Preliminary assessment of the specificity of the antibodies was performed by dot-blot analysis upon these peptides as described in Section 2.7.2.1. A representative blot is illustrated in Figure 3.16.

Each of the antibodies recognised the peptide to which it was directed specifically: α-S869 recognised the S869 peptide but not the phosphorylated form, nor the STREX sequences; α-STREX[1] recognised the STREX peptide but not the phosphorylated form, nor the S869 peptides. Equally, the phospho-directed antibodies exhibited specific recognition of the specific phosphorylated sequences. This demonstrates that the antibodies successfully recognised the phosphorylation state of the sites within the peptides.

[1] This antibody differs from the α-STREX-1 antibody that was employed previously, as it is targeted to a different epitope of the STREX insert sequence. Illustrated diagrammatically - Figure 4.23.

Figure 3.16

Specificity of antibodies raised against phosphorylation states of BK channel serine residues

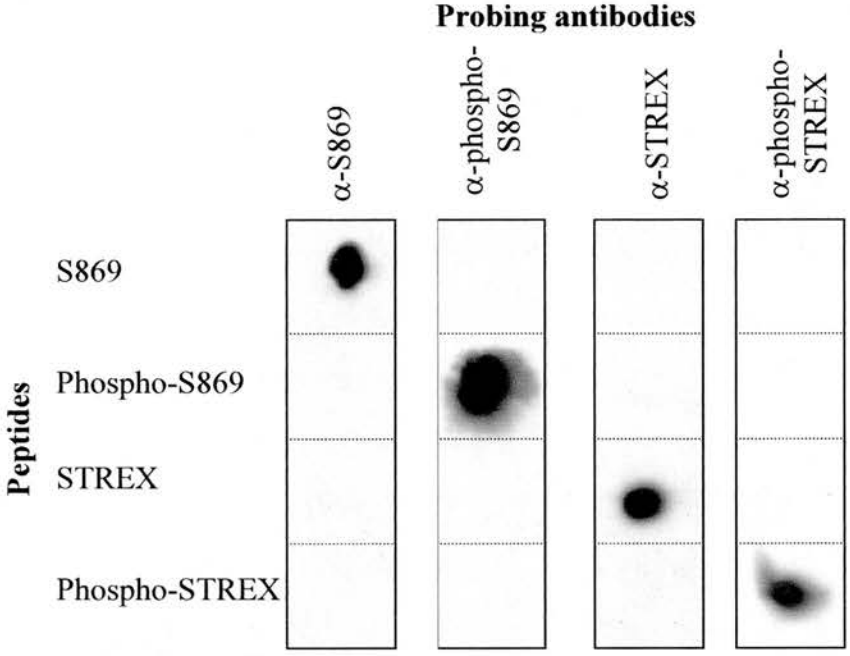

Figure 3.16: Preliminary dot blot analysis of the specificity of the the phospho- and non-phospho- directed antibodies. Antibodies raised against peptides of the phosphorylated and non-phosphorylated states of the serine-869 and STREX insert serine-4 site were used to probe the peptides to which the antibodies were raised. Peptides (4 μg) were dotted onto PVDF membrane and probed by the respective antibodies. Each antibody specifically recognised the peptide to which it was raised, with the phospho-directed antibodies immunoreactive only to the specific phosphorylated peptide to which they were raised, and the non-phospho antibodies recognising the specific non-phosphorylated peptide. Western blot analysis: primary antibodies 1/1000 with 1 μg/ml competing peptides (See Materials & Methods)*; α-sheep-HRP 1/15000; detection by ECL.

*Competing peptides added to maximise the specificity of the antibodies. Antibodies were still specific to target peptides in the absence of competing peptides.

3.3 Discussion

3.3.1 The GST-fusion proteins

As illustrated by Section 3.2.1.1, the GST-fusion proteins were purified successfully by glutathione column affinity chromatography. The induction and purification protocols were optimised following trials altering the induction, cell lysis and the protein purification procedures. The range of conditions examined included varying the temperature, IPTG concentration and period of induction, changing the method and buffer for lysis, and altering the matrix-lysate incubation period, wash conditions, and the temperature and elution protocols of purification. By studying the influence of changing these conditions, the procedure was optimised to produce eluates of maximal yield and purity as illustrated by Figure 3.3.

Following all purification procedures with the GST-STREX and GST-S4A fusion proteins, the ~29 kDa protein was always observed. The consistency of its appearance, and the subsequent identification as a proteolytic degradation fragment (Sections 3.2.1.1.3 & 4.2.2.1), suggest that there is proteolytic cleavage site within the STREX insert sequence. Further evidence of this assumption is provided in Chapter 4 (Discussed Section 4.3.2). However, the presence of this degradation fragment does influence analysis of the fusion proteins. Determination of the protein concentration of a solution by techniques such as Bradford assay measures the total protein content and therefore, the ratio of full-length ~35 kDa fusion protein to the fragment may be influential to analysis of a particular property, for example, when the density of mutant

and wild-type proteins is compared. This influence has been taken into account throughout this study.

The ~35 kDa purified protein was identified as GST-STREX by molecular weight, successful purification by glutathione affinity, indicative of a GST-tag, and the immunoreactivity to antibodies directed against the GST and STREX insert elements. The mutant protein, GST-S4A, was consistent with the wild type, verifying its application as a comparison to GST-STREX. These identifications justify the subsequent use of these proteins as tagged-models of the STREX insert for *in vitro* investigations of the STREX insert as a target for regulation by phosphorylation.

3.3.2 The Thio-V5-H_6-fusion proteins

Generation of the Thio-V5-H_6-fusion proteins was undertaken following the insolubility of GST-fusion proteins of these regions of the C-terminal tail of the BK channel protein (Section 3.2.1.2). As discussed in Section 3.2.1.2, the solubilisation of insoluble proteins can be unreliable, ineffective and damaging to the protein structure and biological activity. Therefore, in order to simplify the purification protocol and maintain consistency between different purifications, the use of GST-fusion partner system was abandoned, and the Thio-V5-H_6-tags employed.

As illustrated in Section 3.2.1.2, use of the Thio-V5-H_6-fusion partner system allowed the soluble expression and ultimate purification of fusion proteins of the BK channel C-

terminal tail region. Following the regimen, optimised similarly to that described for the GST-fusion proteins, produced less recombinant protein than with the GST-STREX fusions, with ~1 mg of purified recombinant protein / L of bacteria culture obtained compared to 5-6 mg / L with the GST fusion proteins. This lower level production was apparent following Coomassie stain of induced bacterial cell pellets, as illustrated in Figure 3.8, where recombinant protein expression cannot be differentiated from the native bacterial proteins, but requires analysis by Western blotting (*c.f.* GST-STREX induction, Figure 3.3). The ΔN-ΔC fusion proteins are significantly larger than the GST-fusions, ~70 kDa compared to ~35 kDa, and protein length can be an inhibitory influence in eukaryote protein expression by a prokaryote system. The longer length can encumber the translation machinery, and provides a greater availability of recognisable non-native protein for degradative bacterial proteases. However, even with the relatively short Thio-LZ1 fusion proteins (31 kDa), comparatively less purified protein was attained than with the GST fusions. Therefore, the amino acid content of the proteins may be a factor. Although the *E.coli* strain was employed due to its increased tRNA expression (See Section 2.2.1.1), the proteins may encode codons common to mammalian system that are relatively rare in prokaryotes. The consistency of this level of protein production may be due to the effectiveness of the pBAD vector promoter, P_{ara} (See Figure 3.6), or simply the efficiency of thioredoxin production by the bacteria. Whatever the cause, the expression, in combination with the solubilising asset of the thioredoxin protein, may be influential to the solubility of the resultant recombinant

protein, and results in sufficient soluble fusion protein for further biochemical investigations.

As illustrated by Figures 3.8 and 3.9, the ΔN-STREX-ΔC fusion protein is degraded by proteases to produce low molecular weight fragments that express the V5 epitope. However, unlike the GST-STREX proteins, there are no detectable proteolytic degradation products detected following purification by either nickel column affinity chromatography or immunoprecipitation observed under Coomassie staining or Western blot analysis (Figures 3.9, 3.10 and 3.11). This suggests that the fragments are either of too low a concentration to be detected, especially probable with the lower sensitivity of Coomassie stain in comparison with immunodetection, or that fragments do not possess the appropriate V5 and polyhistidine tags to enable their purification, and that those that do are too small to be detected by the electrophoresis conditions.

Purification of the Thio-V5-H_6-fusion proteins by nickel affinity chromatography, yielded a ~75 kDa bacterial contaminant (Figure 3.10). Although the contaminant is not immunoreactive to the α-V5 antibody, the presence of such a protein could hamper further investigations with the Thio-V5-H_6-tagged fusion proteins. It could interfere with investigation of Thio-V5-H_6-fusion protein associations and the comparable molecular weight of the protein to the ΔN-ΔC fusion proteins may confuse the assessment of phosphorylation. This is possible as mass spectrometry characterisation of the protein gave the likely identification as an *E.coli* tyrosine-protein kinase, ETK

(NCBI accession no.: P38134). Purification of the Thio-V5-H_6-fusion proteins by immunoprecipitation, did not yield the ~ 75 kDa bacterial contaminant (Figure 3.11). Therefore, this purification technique was determined to be preferable for such studies upon the Thio-V5-H_6-fusion proteins.

All the Thio-V5-H_6-fusion proteins were purified successfully by immunoprecipitation of the V5 epitope, as illustrated for ΔN-STREX-ΔC and ΔN-ZERO-ΔC in Figure 3.11, and as demonstrated for the others in the following chapters. This enabled their application as models for the investigation of the comparative functional role of the STREX and ZERO C-terminal tail regions.

3.3.3 Full-length BK-channel fusion proteins

The full-length epitope-tagged BK channel fusion proteins were purified successfully by immunoprecipitation of the epitope tags (Figure 3.14), demonstrating effective expression of all the tagged channel proteins in HEK293 cells. The Western blotting of the immunoprecipitated -V5-His and -EGFP channels employed the same detection antibody as was used for the immunoprecipitation, necessitating the application of a HEK cell lysate control to illustrate the immunoglobulin (IgG) bands and thus differentiate the channel proteins. Similar controls were employed in the following functional studies in addition to controls for non-specific epitope and immunoprecipitation associations.

The immunoprecipitation assays pull down tagged protein present in the total cellular lysate. The preparation of the lysate involves the application of detergents that solubilise membrane and hydrophobic cellular fractions and should therefore include the transmembrane channel protein. However, as the lysate results from the whole-cell milieu, effective membrane targeting of the channels cannot be assumed. Therefore, the fluorescence of the EGFP tag was crucial to the determination of channel location.

The fluorescence studies confirmed successful targeting of the majority of the recombinant protein to the membrane. As with any fusion protein system, the tag can be removed by the action of cellular proteases and therefore, result in an apparent false localisation of the protein of interest. This is unlikely under these experimental conditions due to the precise membrane targeting that is observed. EGFP is a soluble protein that is not membrane-associated [323, 324], and thus would not illustrate such precise membrane targeting if completely disassociated.

The -EGFP image (Figure 3.15A) demonstrates that the majority of the tagged protein is present at what is assumed to be the cellular membrane. This is suggested, due to the pattern and the diameter of the green fluorescent oval, and its relationship with the nuclear envelope. Some EGFP signal is observed within the cytoplasmic region of the cell within what is assumed to be intracellular compartments: endoplasmic reticulum, Golgi and vesicular organelles. This suggests that the signal represents BK channel protein that is being processed and targeted to the membrane, but has not reached its

destination. This protein fraction will also be isolated by the immunoprecipitation purification technique, and is unlikely to be associated with the same proteins as the functional, membrane-associated, tetrameric channel proteins. This may be influential to the associative studies of Chapter 5. However, the image does suggest that this fraction is the minority and therefore, should have minimal influence among the majority of functional channel protein.

The electrophysiological data (Figure 3.15B) demonstrates that the epitope channels are expressed, reiterating the immunoprecipitation results, and are targeted to the membrane, supporting the fluorescence data. Importantly, the electrophysiology demonstrates that the BK channels are expressed functionally. The large conductance and the increasing open probability with increasing voltage are characteristic of BK channels. HEK293 cells do not possess a native BK channel population [80, 189] and therefore, the large conductance is not native to the expressing cells but the result of recombinant protein expression. The successful characterisation demonstrates that the epitopes are not inhibitory to channel expression and function. Further studies by Lijun Tian illustrated that the channels were also regulated consistently to untagged channels with respect to the PKA-response (Results not shown).

Therefore, these data demonstrate that the epitope-tagged channels are expressed functionally at the cellular membrane of HEK293 cells, and can be isolated successfully by immunoprecipitation. This information is vital as it verifies the use of these channels

as models for native BK channel phosphorylation and protein-protein interactions as described in Chapters 4 and 5.

3.3.4 Phospho-specific antibodies

The phospho-specific antibodies identified the appropriate peptides specifically, with the α-phospho antibodies recognising the appropriate phosphorylated serine-869 or STREX serine-4, and the antibodies to the non-phosphorylated peptides immunoreactive to the appropriate unphosphorylated peptides. This specificity validates the antibodies as identifiers of the phosphorylation state of the serine-869 and STREX serine-4 residues and therefore, proposes the application of the antibodies for phosphorylation studies of the fusion proteins and full-length BK channel proteins. The antibodies may not associate correspondingly with the proteins and regions of the fusion proteins may be sufficiently similar to the epitopes to cause non-specific associations. However, these preliminary data do suggest that the antibodies may be used validly to indicate the phosphorylation state of the STREX serine-4 and serine-869 sites.

3.4 Chapter Summary

This chapter has introduced and characterised the individual fusion proteins and phospho-specific antibodies that were developed for use during this study to demonstrate the identification and validity of the use of these proteins in the investigation of the influence of PKA on BK channel splice variants.

Chapter Four:

Characterisation of PKA-Mediated Phosphorylation of BK Channel Splice Variants

Chapter Four:
Characterisation of PKA-mediated phosphorylation of BK channel splice variants

4.1 Introduction

Direct protein kinase-mediated phosphorylation of proteins is an effective, efficient, accommodating and therefore, common, mechanism of protein modulation [187]. Ion channels including sodium, calcium and potassium-conducting channels [187, 188, 222, 223, 325] are regulated by phosphorylation and a large body of evidence adds BK channels to this phosphorylation-regulated protein sub-set. Several protein kinases have been implicated as regulators of BK channel function including protein kinase C (PKC), protein kinase G (PKG), calmodulin-regulated protein kinase II (CaMKII) and, of particular interest to this study, protein kinase A (PKA) (See Section 1.4.1). The mechanisms underlying PKA-dependent regulation are undetermined, however, mutagenesis of putative PKA consensus motifs can occlude the PKA-mediated regulation of the mutant channels implicating the sites as targets of direct kinase-induced phosphorylation [198, 205, 229]. Further to this, mutagenesis of specific PKA consensus motifs of different splice variants can confer contrasting responses upon the PKA-regulation of the variants as is observed between STREX and ZERO channels [38, 69, 80, 229] (Discussed Section 4.1.1). This is suggestive of differential PKA-mediated phosphorylation between splice variants. Therefore, this chapter aims to investigate whether the BK channel α-subunit protein is a direct target for PKA phosphorylation, identifying PKA consensus motifs that may allow the differential responses of the STREX and ZERO splice variants.

4.1.1 Differential BK channel splice variant regulation by PKA

The serine-869 residue as a putative PKA-phosphorylation target

Analysis of the amino acid sequence of the BK channel α-subunit unveils several putative PKA consensus motifs. One such sequence, R-Q-P-S_{869}[1], is conserved in all mammalian BK channel splice variants and has been proposed through mutagenesis studies as a possible PKA phosphorylation target in mammalian and insect channels [190, 205, 229]. Although not an optimal PKA consensus sequence (Table 1.1), mutation of the murine ZERO BK channel serine-869 to an unphosphorylatable alanine residue abolishes the cAMP-induced activation of the channels demonstrating that an intact serine-869 site is required for the PKA response and implicating it as a possible target of direct PKA-targeted phosphorylation [190, 205, 229].

To determine whether the serine-869 residue is a target for PKA-mediated phosphorylation, peptides encompassing the S869 region were employed in a series of *in vitro* phosphorylation assays (Section 4.2.1). These peptides are described in detail in the appropriate section and enabled preliminary determination of whether the site could function as a PKA consensus motif.

The STREX insert as a putative PKA-phosphorylation target

As described in the introduction to this study (Section 1.3.1.2.1), heterologously expressed ZERO channels are stimulated by the activation of PKA whereas STREX isoforms are inhibited [80, 229]. Therefore, if phosphorylation of the channel protein underlies the PKA-mediated responses, the STREX insert is likely to influence the

[1] Murine R-Q-P-S_{869} equivalent to R-R-G-S_{942} of *Drosophila* BK channel [10].

functional effect of the kinase upon the channel proteins. The STREX insert may produce additional PKA-consensus motifs among its sequence. Such STREX phosphorylation consensus sites could compete with and override the phosphorylation of residues conserved in the ZERO and STREX channels, or could co-phosphorylate with sites common to both isoforms. Equally, the STREX insert may obstruct residues that are targeted in the ZERO variant, or conformationally produce alternative or additional consensus motifs that are structurally inaccessible in the ZERO form of the channel.

Investigation of the sequence of the STREX insert uncovers several putative protein kinase target residues including serine-4, a residue within a putative PKA consensus motif at the beginning of the STREX insert region (Figure 1.6). As described in Chapter One, PKA requires a motif analogous to the optimal consensus sequence for targeted phosphorylation (Table 1.1) and the STREX sequence, R-R-P_1-K_2-M_3-S_4, displays sufficient analogy to be considered as a putative target (Figure 1.6). Although not archetypal due to the structurally constraining proline residue and three, not two, intermediate residues, the observed plasticity of the kinase with respect to its consensus sequence implicates the STREX serine-4 as a possible target of PKA-directed phosphorylation (Table 1.1).

To investigate whether the STREX insert, in particular the serine-4 residue, can be a target of PKA-mediated phosphorylation in conditions favourable to kinase activity, the GST-STREX and mutant GST-S4A fusion proteins (Section 3.2.1.1) were employed in a series of *in vitro* phosphorylation assays (Section 4.2.2).

The influence of the STREX insert upon BK channel phosphorylation

As described above, serine-869 was implicated as a putative PKA-phosphorylation target following the observation of the critical effect its mutation incurred upon murine ZERO channels [80, 229]. However, mutagenesis of S869 site in the murine STREX splice variant does not abolish the inhibitory effect of the kinase, indicating that serine-869 is not essential for PKA-regulation of STREX channels [80, 229]. This supports the hypothesis that the STREX insert occludes consensus motifs or produces alternative PKA-consensus sites that override the phosphorylation of sites conserved in the ZERO and STREX channel proteins. Furthermore, this is indicative of differential PKA-mediated phosphorylation underlying the contrasting PKA-mediated regulation of the splice variants.

To investigate the implied differential phosphorylation of the serine-869 site induced by the presence of the STREX insert, the ΔN-ΔC recombinant fusion proteins were employed (Section 3.2.1.2). These fusion proteins comprise the C-terminal tail region of the BK channel spanning splice site two, the location of STREX insertion, and the serine-869-containing PKA-target motif (See Figure 3.1). Comparison of the *in vitro* phosphorylation of fusion proteins cloned from the ZERO and STREX channel isoforms enabled the study of the phosphorylation of the C-terminal tail region of BK channels, in particular the relationship between the phosphorylation states of the serine-869 and STREX serine-4 sites (Section 4.2.3).

Further analysis of the relationship between the putative phosphorylation targets, serine-869 and STREX serine-4, was achieved by implementation of BK channel protein *in extenso*, expressed as the HA-tagged fusion proteins (Section 3.2.2, Figure 3.13). These tagged proteins formed functional channel complexes that could be immunoprecipitated by exploitation of the HA-epitope (Section 3.2.2) enabling the assessment of the phosphorylation of full-length, functional channel protein expressed in a mammalian expression system analogous to native tissue. Thus, *in vitro* post-immunoprecipitation phosphorylation assays employing excess, exogenous, constitutively active PKA, and *in vivo* stimulation of native PKA within the HEK293 cell expression system were conducted (Section 4.2.4).

4.1.2 Phosphorylation assays

Characterisation of phosphorylation

Phosphorylation as a regulatory mechanism is more than the kinase targeting and the physical phosphorylation event. The characteristics of the process are integral to regulatory effectiveness and must be efficient, possess a degree of specificity and, vitally, must be reversible. Characterisation of the phosphorylation of some of the bacterially-expressed fusion proteins (Section 3.2.1) was performed to indicate whether particular sites and regions could be functional targets of phosphorylation in the *in vivo*, full-length functional channels, and to assess the efficiency of the *in vitro* experimental protocols. Simple time course experiments were performed to determine the rate and thus facilitate assay of the relative efficiency of PKA-mediated phosphorylation under the experimental conditions that were employed (Section 4.2.2). The specificity of the

proteins as PKA-targets was studied by examination of two common protein kinases, protein kinase C (PKC) and calmodulin kinase II (CaMKII), kinases that are implicated as regulators of BK channel function (See Section 1.4.1). The consensus motifs that they target differ slightly to PKA, but all phosphorylate at serine or threonine residues enabling the assessment of the degree of specificity of the proteins as protein kinase phosphorylation targets.

Protein kinases are stimulated via various signal transduction systems and induce the transfer of the terminal phosphate of ATP onto specific amino acids of particular target proteins. Concomitantly, protein phosphatases catalyse the removal of phosphate from target residues. Therefore, the two protein classes act in opposition to each other providing a regulatory feedback mechanism that is critical to the modulation of many cellular proteins (See Section 1.4.1). Electrophysiological investigation of BK channel modulation by PKA has suggested that protein phosphatases, in particular protein phosphatase 2A (PP2A) and protein phosphatase 1 (PP1), associate with the channel and reverse the effects of the kinase (See Section 1.4.1). Therefore, if the STREX insert and the S869 site are targets of reversible PKA-directed phosphorylation *in vivo*, they are likely to be dephosphorylated by PP2A and/or PP1. Consequently, the *in vitro* PKA-directed phosphorylation of the GST-STREX fusion protein and the S869 peptide should be reversible phenomena if the regions are phosphorylated functionally by PKA *in vivo*.

Mutagenesis

Throughout this study, serine to alanine mutations were used to replace the phosphorylatable hydroxyl side chain of serine with the phosphorylation-inert carboxyl of alanine whilst maintaining a similar mass and spatial arrangement that should impart minimal conformational disruption. Although, as with any mutation, the substitution could impart structural differences between the native and mutant fusion proteins as to inhibit phosphorylation of a distinct site or sites, or indeed, create additional phosphorylation consensus motifs, the similar conformation of the substitution makes this unlikely. Consequently, the inability of a protein kinase to phosphorylate a particular alanine mutant fusion protein *in vitro* when the non-mutant (serine) form is phosphorylated, suggests that serine-alanine substitution is sufficient to preclude phosphorylation of the residue and thus, implicates the residue as the protein kinase phosphorylation consensus site and, additionally, suggests that other residues within the protein are not phosphorylated.

Assays of phosphorylation

In vitro phosphorylation assays were performed upon all fusion proteins in order to assess phosphorylation under optimal conditions. Factors including buffering conditions, assay temperature, inclusion of excess hydrolysable ATP, and the use of constitutively active protein kinase facilitated such optimisation (See Section 2.8). Although such optimisation of catalytic activity was not possible, nor desired, during *in vivo* stimulation of PKA in HEK293 cells expressing the HA-tagged channels, the assay

conditions and incubation temperature were conducive to catalytic stimulation (See Section 2.8).

The method of analysis was integral to the assessment of fusion protein phosphorylation. Two protocols were performed, the use of radiolabelled ATP ([γ-^{32}P]-ATP) as the hydrolysable phosphate source and subsequent autoradiography, and the application of the phospho-specific antibodies that are immunoreactive to the phosphorylation state of the serine-869 and STREX serine-4 sites by Western blot analysis of the kinase-exposed fusion proteins (See Section 3.2.3). Autoradiography enables the detection of radiolabelled phosphate incorporation into proteins. This method does not identify the residues that are phosphorylated, whereas Western blotting was used to identify the phosphorylation state of the serine-869 and STREX serine-4 PKA-consensus sites. Therefore, in combination, the methods enabled the detection and characterisation of the phosphorylation state of the fusion proteins.

To determine the catalytic competence of the protein kinases during autoradiographic analysis, positive control peptides/proteins were employed. Kemptide possesses the motif, R-R-A-S (See Scheme 4.1), corresponding to the optimal PKA consensus sequence, R-R-X-S, and that of CaMKII, X-R-X-X-S (Table 1.1). Similarly, expression of an optimal PKC phosphorylation consensus motif in PHAS-I (phosphorylated heat- and acid-stable protein regulated by insulin) allows its use as a positive control of PKC catalytic activity. Conversely, negative controls were used to assess non-specific phosphate incorporation. Use of the fusion partners of the recombinant fusion proteins,

GST and Thioredoxin-V5-H_6, enabled the assessment of the tags as putative targets of phosphorylation and, as will be seen within the results of this chapter, were not phosphorylated under experimental conditions implicating phosphorylation of the cloned BK channel portion of the fusion protein.

Thus, this chapter aims to investigate whether the molecular basis of the differential PKA regulation of the STREX and ZERO BK channel splice variants is distinct PKA-mediated phosphorylation of the isoforms, with particular reference to the relationship between two putative phosphorylation target residues, the conserved serine-869 and the STREX insert serine-4.

4.2 Results

4.2.1 Reversible phosphorylation of the S869 site

As mentioned in Section 3.2.1.2, the analysis of PKA phosphorylation of the serine-869 site was performed using peptides due to the insolubility of fusion proteins spanning the S869 region of the BK channel sequence. The peptides, as illustrated below, encompass a sequence of eleven residues that surround the putative PKA consensus motif, R-Q-P-S_{869} (Figure 1.5). The mutant peptide, S869A, has an alanine residue replacing the phosphorylatable serine-869 to facilitate investigation of the phosphorylation of serine-869.

Scheme 4.1: The S869 peptide sequences
Standard one letter amino acid code used.

S869 peptide	**M**	**L**	**R**	**Q**	**P**	S_{869}	**I**	**T**	**T**	**G**	**V**
S869A peptide	**M**	**L**	**R**	**Q**	**P**	A_{869}	**I**	**T**	**T**	**G**	**V**
Kemptide – control peptide		L	R	R	A	S	L	G			

4.2.1.1 PKA phosphorylation of the S869 peptides

In vitro phosphorylation assays were performed using the S869 peptides as described in Section 2.8.1. The peptides were incubated in a magnesium-containing buffer in the presence of radiolabelled ATP ([γ-^{32}P]-ATP) and the constitutively active catalytic subunit of PKA (PKAc) at 30 ^{0}C. Reactions were separated by electrophoresis on Tris-Glycine gels, and radiolabelled phosphate incorporation analysed by autoradiography. Figure 4.1 illustrates the results of such an experiment.

In the presence of PKAc, robust radiolabelled phosphate incorporation was detected with the kemptide positive control peptide and with the S869 peptide as substrate. Phosphate incorporation is not detected in the absence of the kinase, nor with the mutant S869A peptide. No other signals are observed at this length of exposure of the ^{32}P-sensitive film to the experimental gel (between one to thirty minutes).

Thus, the S869 site of the S869 peptide is phosphorylated by PKA *in vitro*, with alanine substitution of the residue inhibiting peptide phosphorylation and thus suggesting that

Figure 4.1
PKAc phosphorylation of S869 peptide

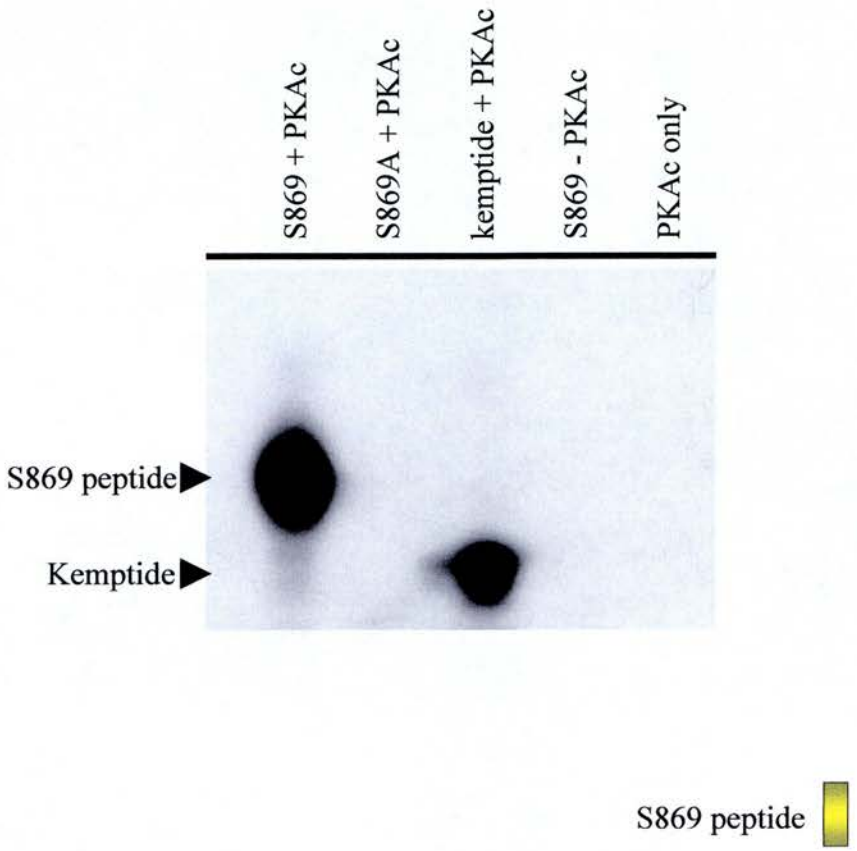

Figure 4.1: Representative autoradiograph of PKAc phosphorylation of S869 peptide. *In vitro* PKAc phosphorylation assays were performed in the presence of 10 μCi [γ-^{32}P]-ATP (10 mins, 30 ^{0}C). Samples were separated by electrophoresis and exposed to ^{32}P-sensitive film. Radiolabelled phosphate incorporation was observed with the S869 peptide and with the positive control peptide, kemptide, only in the presence of PKAc. The mutant S869A peptide was not phosphorylated.

phosphate incorporation is specific, and does not occur at other sites within the peptide sequence. Preliminary assays investigating the time course of PKA-phosphorylation of the S869 peptide determined that phosphorylation was maximal within 1 minute of kinase addition to the reaction (Results not shown). This indicates that the 10 minute incubation period used for the analysis illustrated in Figure 4.1 represents maximal phosphorylation of the S869 peptide by PKAc under the conditions of the experiment.

4.2.1.2 Phosphorylation of the S869 peptide by other protein kinases

To investigate the specificity of the S869 peptide as a PKA phosphorylation target, *in vitro* phosphorylation assays were performed using two serine/threonine protein kinases that are reported to influence BK channel activity; protein kinase C (PKC), and calmodulin kinase II (CaMKII).

4.2.1.2.1 PKC phosphorylation of the S869 peptide

Phosphorylation reactions employing radiolabelled ATP were performed as described in Section 2.8.1.3. Reactions were separated by electrophoresis on a Tris-Glycine gel and radiolabelled phosphate incorporation was detected by autoradiography. Figure 4.2 illustrates the results of such an experiment.

PKC phosphorylated the positive control, PHAS-I, indicating that the kinase is catalytically active *in vitro*. However, no phosphorylation was observed with S869 peptide or mutant, S869A peptide, even upon extended autoradiographic exposures, demonstrating that the S869 peptide is not a PKC-phosphorylation target *in vitro*.

Figure 4.2

PKC phosphorylation of S869 peptide

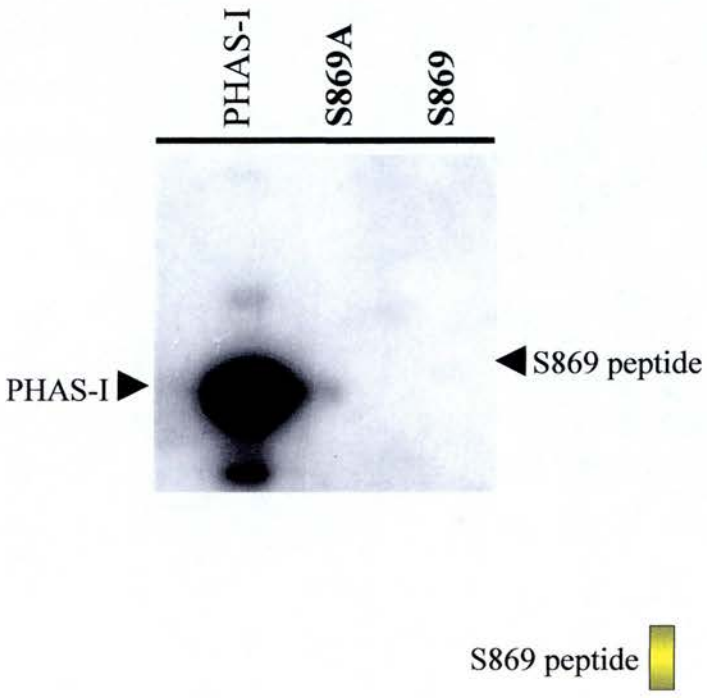

Figure 4.2: Representative autoradiograph of *in vitro* PKC phosphorylation of the S869 peptides. Reactions employing radiolabelled ATP were incubated at 37 ^{0}C for 10 mins prior to separation on 4-12 % Tris-Glycine gels and exposure to ^{32}P sensitive film. Under the experimental conditions employed, the radiolabel incorporated with the positive control, PHAS-I only. No other phosphorylation signals were observed.

Figure 4.3

CaMKII phosphorylation of S869 peptide

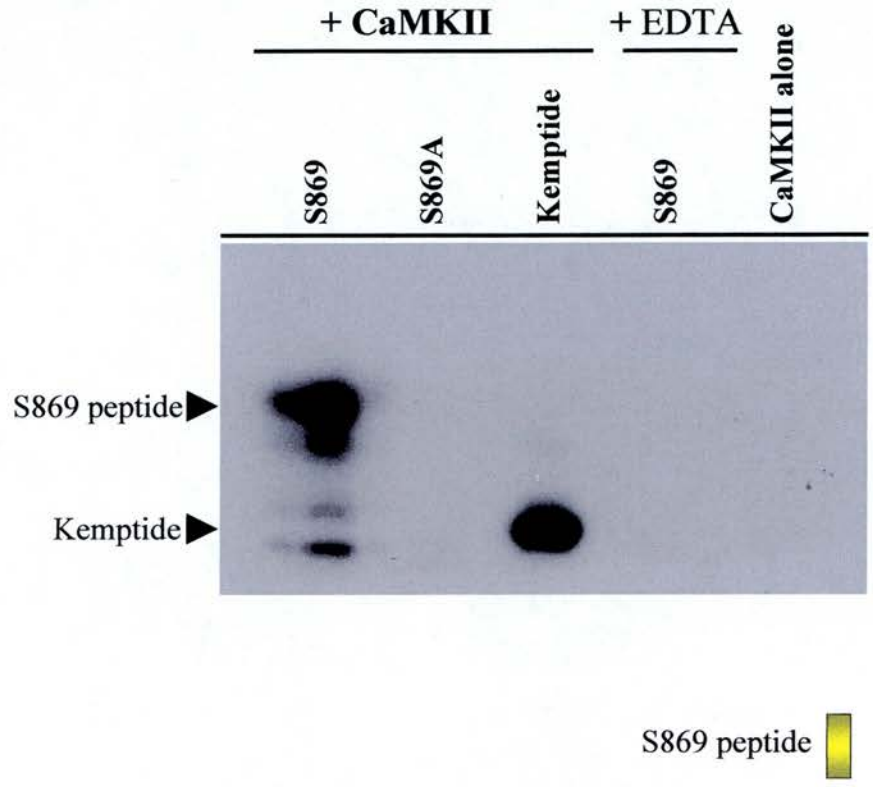

Figure 4.3: Representative autoradiograph of *in vitro* CaMKII-phosphorylation of S869 peptide. CaMKII assays using 10 μCi γ-^{32}P-ATP were incubated at 37 ^{0}C for 10 mins prior to separation on 4-12 % Tris-Glycine gels and exposure to ^{32}P sensitive film. Control reactions with the calcium chelator, EDTA, to inhibit the kinase were performed in parallel. Phosphorylation was observed with the positive control peptide, kemptide and with the S869 peptide. The lower molecular weight phosphorylation bands observed with the S869 peptide in this assay are suggested to be degradation fragments.

4.2.1.2.2 CaMKII phosphorylation of the S869 peptide

In vitro phosphorylation reactions employing radiolabelled ATP were performed using CaMKII activation buffer (Section 2.8.1.4). Control reactions exploited the divalent cation chelator, EDTA, to buffer calcium ions and subsequently inhibit kinase activity. Reactions were separated by electrophoresis on Tris-Glycine gels and radiolabelled phosphate incorporation was detected by autoradiography as illustrated in Figure 4.3.

Incorporation of the radiolabelled phosphate is apparent with the S869 peptide, as well as with the positive control peptide, kemptide (Figure 4.3). Phosphorylation is not observed when the kinase is inhibited by EDTA, nor is phosphorylation of the S869A mutant peptide observed. This indicates that the S869 peptide is phosphorylated by CaMKII *in vitro*, possibly at the S869 site, and thus implicates the S869 site as a putative CaMKII phosphorylation site *in vivo*.

4.2.1.3 Dephosphorylation of the S869 peptide

Dephosphorylation of the S869 peptide was investigated using the serine/threonine protein phosphatases, PP2A and PP1. The S869 peptide was phosphorylated by PKAc as described above (Section 4.2.1.1), then mixed with the PKA inhibitor, H-89 (1 μM), and divided equally among various dephosphorylation reaction conditions (Section 2.8.1.5.2). Reactions were incubated with the respective protein phosphatase in the presence or absence of the phosphatase inhibitor, okadaic acid (100 nM), with control reactions incorporating okadaic acid alone, or no supplementary phosphatase/phosphatase-inhibitor. Figure 4.4 illustrates an autoradiograph of such an

Figure 4.4
Dephosphorylation of S869 peptide: Autoradiography

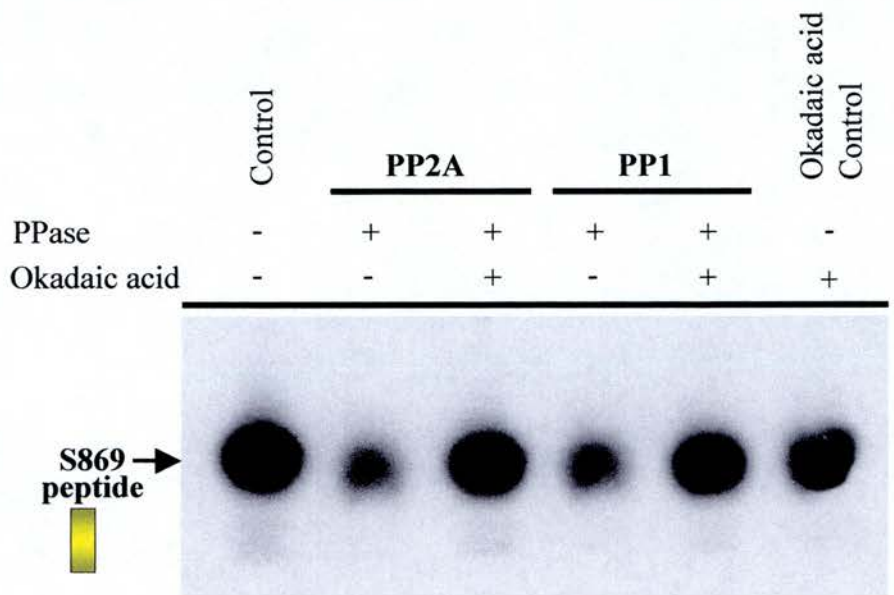

Figure 4.4: Representative autoradiograph of *in vitro* dephosphorylation of PKAc-phosphorylated S869 peptide. S869 peptide, phosphorylated by PKAc as previously, was incubated (30 mins, 37 ^{0}C) in the presence or absence of protein phosphatase, either PP2A or PP1, with or without okadaic acid (OA) as described above. PP2A and PP1 dephosphorylate the S869 peptide and the effect was inhibited by OA. OA alone had no effect upon phosphorylation. Densitometric analysis of the signals was performed to quantitate the autoradiograph results (Figure 4.5).

Figure 4.5
Dephosphorylation of S869 peptide: Densitometric analysis

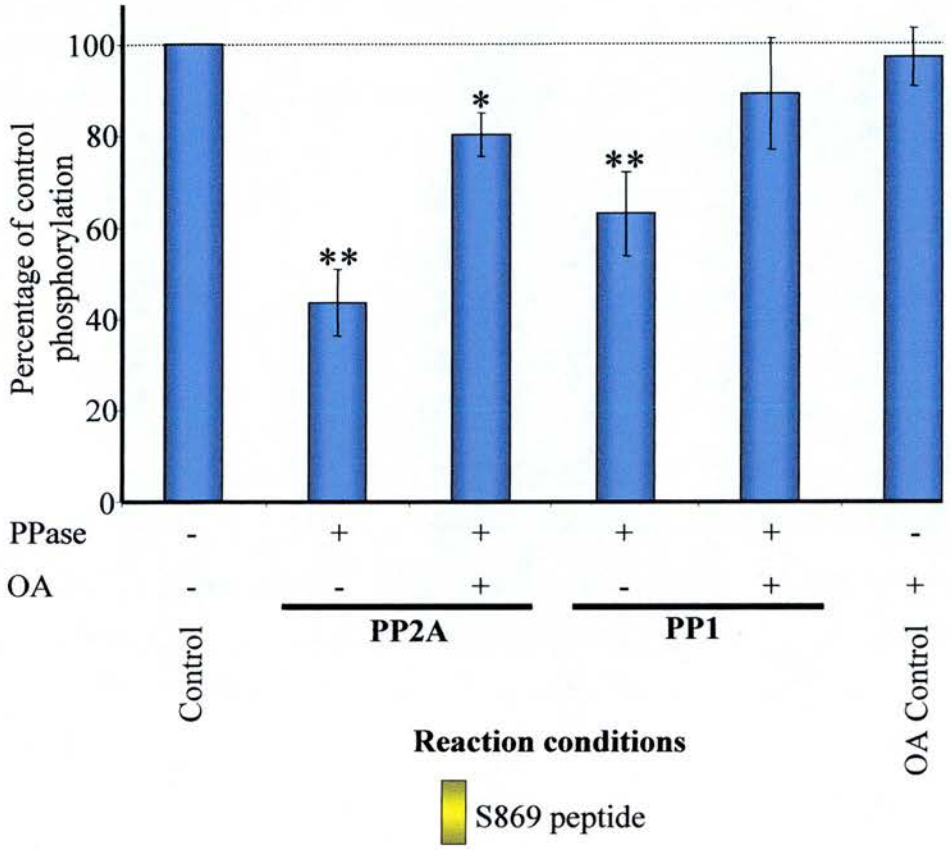

Figure 4.5: Summary of PP2A and PP1-mediated dephosphorylation of PKAc-phosphorylated S869 peptide. Summary of densitometric analysis from six independent assays of S869 peptide dephosphorylation performed as Figure 4.4. All data were normalised to the control PKAc-phosphorylated sample (100 %, Mean $\pm$ SEM, n=6, Statistical analysis by T-test comparison to control phosphorylation: * $P<0.05$, ** $P<0.01$). PP2A and PP1 dephosphorylated the peptides. This is inhibited by okadaic acid (OA) which does not influence phosphorylation when applied alone (OA control).

assay, with Figure 4.5 demonstrating the results of densitometric analysis (Section 2.10.3) from six independent experiments.

The PKAc-phosphorylated S869 peptide control was assigned as the maximal phosphorylation and all experimentally determined values were normalised to the density of this signal. PP2A significantly decreased the level of phosphorylation to 43 (± 7.1) %[2] of control phosphorylation ($P<0.001$). Equivalent treatment with PP1 also resulted in significant dephosphorylation to 63 (± 9.0) %[2] of control ($P<0.001$). Okadaic acid (100 nM) inhibited PP2A and PP1-mediated dephosphorylation, with phosphorylation in the presence of okadaic acid 80 (± 4.4) and 89 (± 4.2) %[2] of control phosphorylation respectively ($P\sim1$). Application of okadaic acid alone had no effect on the phosphorylation state of the S869 peptide (97 (± 6.1) %[2] of maximum phosphorylation, $P\sim1$).

4.2.2 Reversible phosphorylation of the GST-STREX fusion protein

To determine whether the STREX insert sequence, in particular the serine-4 putative consensus motif, can function as a phosphorylatable target of PKA, the GST-tagged fusion proteins of the insert were employed (Section 3.2.1.1).

4.2.2.1 PKA-mediated phosphorylation of the GST-STREX fusion protein

GST–fusion proteins were phosphorylated *in vitro* as described in Section 2.8.1. The purified protein of interest was incubated in a magnesium-containing buffer in the

[2] Values quoted as mean ±SEM, n=6.

presence of excess ATP and the constitutively active catalytic subunit of PKA (PKAc) at 30 ^{0}C. Protein phosphorylation was analysed by autoradiography and/or Western blot analysis.

4.2.2.1.1 Autoradiographic analysis of GST-STREX phosphorylation

Phosphorylation reactions using radiolabelled ATP ([γ-^{32}P]-ATP) were separated by electrophoresis on a Tris-Glycine gel and the radiolabelled proteins detected by autoradiography. Figure 4.6 illustrates the results of such an experiment using the GST-STREX fusion proteins.

In the presence, but not in the absence of PKAc, phosphate incorporation was observed from the ~35 kDa GST-STREX and its ~29 kDa proteolytic fragment indicating that the kinase is required for phosphorylation of the fusion proteins, and signifies the catalytic competence of the kinase. Crucially, neither GST-S4A, or GST protein alone were phosphorylated under the experimental conditions demonstrating that the fusion tag, GST, was not the target of phosphorylation, and that an intact Serine-4 residue is required for GST-STREX fusion protein phosphorylation by PKA. PKAc autophosphorylation was visible at ~45 kDa in all lanes where the kinase was included, except with the strongly phosphorylatable positive control peptide, kemptide, providing further evidence for the catalytic competence, activity and specificity of the kinase. The comparative densities of PKAc autophosphorylation between different substrates illustrated that the intensity of the phosphorylation band was related to the extent of

Figure 4.6

Phosphorylation of GST-STREX by PKAc: Autoradiography

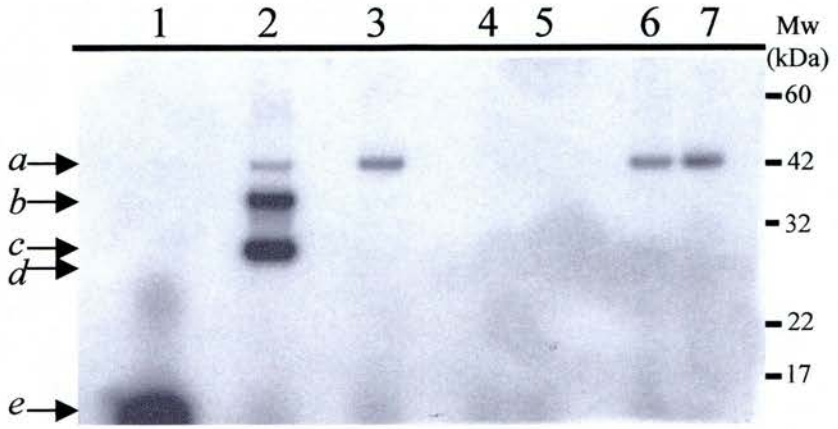

a. ~45 kDa, protein kinase A catalytic subunit (PKAc)
b. ~35 kDa, GST-STREX constructs: GST-STREX:
GST-S4A:

c. ~29 kDa, GST-STREX proteolytic product:
d. ~28 kDa, GST:
e. Kemptide

Figure 4.6: Representative autoradiograph of the *in vitro* PKA-mediated phosphorylation of GST-STREX. 1: Control peptide, kemptide + PKAc; 2: GST-STREX + PKAc; 3: GST-S4A + PKAc; 4: GST-STREX - PKAc; 5: GST-S4A - PKAc; 6: GST + PKAc; 7: PKAc alone. Phosphorylation assays were performed *in vitro* in the presence of 10 μCi [γ-^{32}P]-ATP (10 mins, 30 ^{0}C). Samples separated by electrophoresis were exposed to ^{32}P-sensitive film. Radiolabelled phosphate incorporation was observed with the GST-STREX protein (~35 kDa) and the degradation product (~29 kDa) in the presence of PKAc. Phosphorylation was not observed in the absence of the kinase. The mutant GST-S4A fusion protein (~35 kDa) and GST protein (~28 kDa) were not phosphorylated. The PKAc substrate, kemptide, was phosphorylated, and PKAc autophosphorylation (~45 kDa) was observed. Fusion proteins are represented diagrammatically below the autoradiograph (See Figure 3.5).

phosphorylation of the target substrate. Neither GST nor the GST-S4A fusion protein were phosphorylated within the assays and thus, PKAc autophosphorylation was comparable to that of the kinase assessed in the absence of available and appropriate substrate (P~1). However, in the presence of phosphorylatable GST-STREX the PKAc autophosphorylation signal density was depleted significantly ($P<0.0001$) and was completely undetectable with the model substrate, kemptide.

These data indicate that the 35 kDa GST-STREX fusion protein and the putative 29 kDa proteolytic product were phosphorylated by PKAc specifically *in vitro* at a site likely to be the serine-4 residue.

4.2.2.1.2 Western blot analysis of GST-STREX phosphorylation

To determine whether the serine-4 site of GST-STREX functions as the phosphorylation site of PKA *in vitro*, Western blot analysis was performed with the α-phospho-STREX antibody that is immunoreactive to phosphorylated serine-4 (Section 3.2.3). *In vitro* phosphorylation reactions were conducted with non-radiolabelled ATP. Non-phosphorylation reactions where PKAc was omitted were performed in parallel as controls of both antibody and kinase specificity. Samples were separated by SDS-PAGE and analysed by Western blotting. A representative assay is illustrated in Figure 4.7A.

α-GST analysis

Probing for GST demonstrated the presence of equivalent amounts of the GST-fusion proteins, GST-STREX and GST-S4A, at the appropriate molecular weights, ~35 kDa

Figure 4.7A
PKA phosphorylation of GST-STREX: Western blot analysis

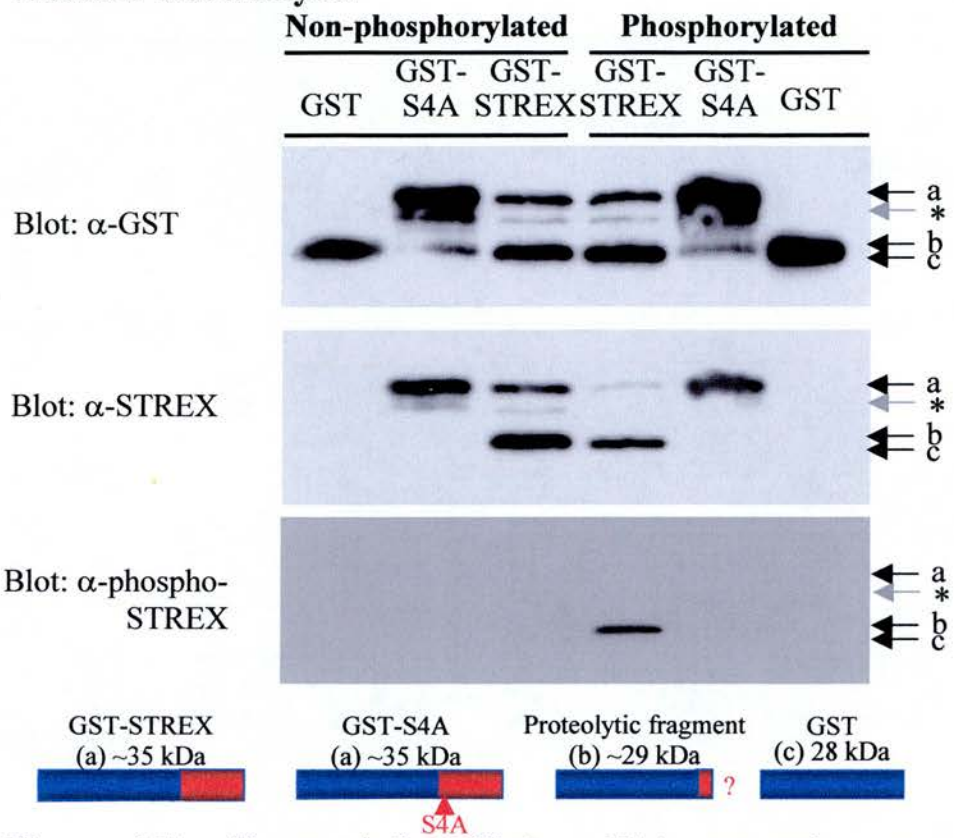

Figure 4.7A: Representative Western blots comparing non-phosphorylated and PKA-phosphorylated GST-fusion proteins. *In vitro* PKAc-phosphorylation assays performed in the absence (non-phosphorylated) or presence (phosphorylated) of PKAc were analysed by Western blotting. The ~35 kDa (**a**) fusion proteins and the 29 kDa (**b**) proteolytic fragments were detected by α-GST and α-STREX, with additional ~32 kDa fragments (*). GST (**c**) was detected by α-GST only. α-phospho-STREX detected the phosphorylated GST-STREX proteins only, suggesting specific, PKA-mediated phosphorylation at serine-4. Fusion proteins are illustrated diagrammatically below the blots (See Figure 3.5). Western blot analysis: goat α-GST 1/1000; sheep α-STREX 1/1000; sheep α-phospho-STREX 1/1000; α-sheep/goat-HRP 1/15000; detection by ECL.

Figure 4.7B
PKA phosphorylation of GST-STREX: Western blot analysis by α-phospho-STREX

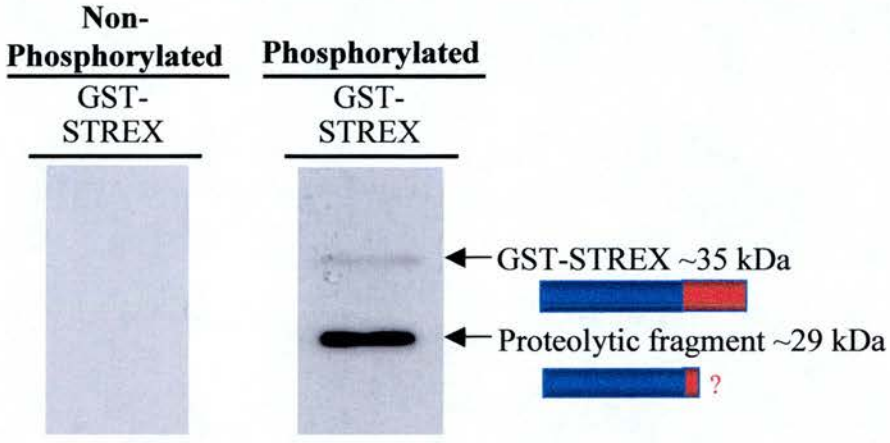

Blot: α-phospho-STREX

Figure 4.7B: Detection of GST-STREX by α-phospho-STREX. Analysis of PKA-phosphorylated GST-STREX by α-phospho-STREX detected the ~35 kDa full-length fusion protein as well as the 29 kDa proteolytic fragment. The non-phosphorylated GST-STREX fusion proteins were not detected by this antibody. This demonstrates that although the ~35 kDa fusion protein was not detected by α-phospho-STREX in the example illustrated in Figure 7A, this may be an artefact of the relatively lower proportion of this protein to the ~29 kDa fragment in that particular experiment (as observed by α-GST analysis, See Figure 7A). Assays and analysis as Figure 7A: sheep α-phospho-STREX 1/1000; α-sheep/goat-HRP 1/15000; detection by ECL.

full-length and the ~29 kDa proteolytic fragment, as described previously (Section 3.2.1.1; Figure 3.5). The purifications employed in this set of experiments resulted in a ~32 kDa protein that was absent from the previous assays and was identified as an additional proteolytic product due to its immunoreactivity to the α-GST and α-STREX antibodies (See below). No difference was observed between phosphorylated and non-phosphorylated samples indicating that phosphorylation and the presence of the kinase does not influence detection by the antibody under these conditions. Additionally, although the total concentration of protein in each reaction was identical, the proportion of full-length protein to degraded fragments differs between the GST-STREX and GST-S4A fusion proteins, with greater degradation of the GST-STREX protein observed.

α-STREX analysis

The α-STREX[3] antibody is immunoreactive to the ~35 kDa full-length GST-STREX and GST-S4A fusion proteins, and the ~29 kDa fragment of the GST-STREX fusion protein. The ~29 kDa GST-S4A fragments were not detected by this antibody, which may be indicative of the relatively lower proportion of this fragment that was detected by α-GST analysis in comparison to the ~35 kDa fusion proteins and the ~29 kDa GST-STREX degradation fragment. As predicted, GST is not detected by this antibody.

The autoradiography (Figure 4.6) demonstrated that the mutant fusion protein was not phosphorylated by PKAc under these experimental conditions, and comparable α-

[3] As described previously (Section 3.2.3), this antibody differs from the α-STREX-1 antibody that was employed formerly as it is targeted to a different epitope of the STREX insert sequence (See Table 2.4 & Figure 4.23).

STREX detection of ~35 kDa non-phosphorylated GST-STREX to ~35 kDa GST-S4A ($P>0.1$) supports the implementation of this antibody as a detector of non-phosphorylated STREX. Additionally, the immunoreactivity of α-STREX to GST-STREX was significantly depleted by phosphorylation of the fusion protein ($P<0.001$) indicating that phosphorylation does inhibit the antibody-antigen association as suggested by the preliminary peptide analyses (Section 3.2.3). The still-present but depleted ~35 kDa phosphorylated GST-STREX α-STREX immunoreactivity may result from a proportion of the fusion protein remaining un-phosphorylated, or from incomplete inhibition of the antibody-epitope interaction.

α-phospho-STREX analysis

Analysis of the phosphorylation state of the serine-4 site of the fusion protein using the α-phospho-STREX antibody demonstrated specific immunoreactivity with the ~29 kDa phosphorylated GST-STREX degradation fragment. In this experiment, the antibody did not detect the ~35 kDa full-length phosphorylated fusion protein which may be an artefact of the relatively lower proportion of this protein to the ~29 kDa fragment as observed by α-GST analysis (See above). The ~35 kDa full-length PKA-phosphorylated GST-STREX was detected by this antibody in other experiments (See Figure 4.7B). No immunoreactivity was detected with the non-phosphorylated GST-STREX proteins, nor with mutant GST-S4A fusion protein or the control, GST.

These data suggest that phosphorylation of the GST-STREX fusion protein by PKA occurs at the serine-4 residue under the experimental conditions applied. Additionally,

the specific immunoreactivity of the α-phospho-STREX antibody to phosphorylated GST-STREX indicates that the antibody can characterise the phospho-serine-4 motif within this fusion protein.

4.2.2.1.3 Time course of PKA-mediated phosphorylation of GST-STREX

Time course assays using radiolabelled ATP were performed to demonstrate that *in vitro* PKA-phosphorylation of the GST-STREX fusion protein was saturatable. Aliquots from the assays were removed at set time points following the start of the reaction initiated by the addition of the kinase. Control reactions of GST-STREX in the absence of PKAc and of PKAc with no substrate were run in parallel. Samples were separated by electrophoresis on Tris-Glycine gels and the radiolabelled proteins were detected by autoradiography. Figure 4.8 illustrates the autoradiograph of an individual assay, and Figure 4.9 demonstrates the resultant time course that was determined by densitometric analysis of eight independent experiments.

The autoradiograph (Figure 4.8) illustrates the *in vitro* phosphorylation of GST-STREX by PKAc with the ~35 kDa full-length protein and ~32 and ~29 kDa fragments incorporating the radiolabel. As described previously (Section 4.2.2.1.1), no phosphorylation of the fusion protein is observed in the absence of PKAc over the experimental period (30 mins) demonstrating that incorporation of the radiolabelled phosphate group requires the catalytically active kinase. The ~45 kDa PKAc autophosphorylation signals have been excluded from the autoradiograph to enable clarification of the fusion protein bands, with the absence of the GST-STREX signals

Figure 4.8

Time course of GST-STREX phosphorylation by PKAc: Autoradiography

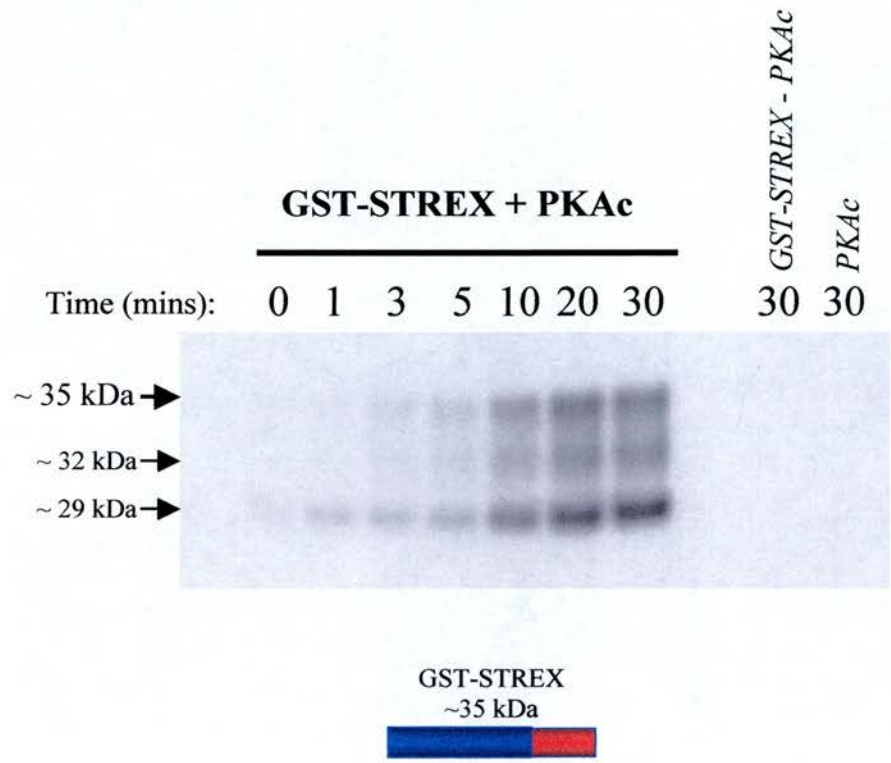

Figure 4.8: Representative autoradiograph of a time course of PKAc-phosphorylation of GST-STREX. Aliquots were removed from a phosphorylation reaction using [γ-^{32}P]-ATP at 1, 3, 5, 10, 20, and 30 minutes following the addition of the kinase to the reaction mixture (0 mins). Phosphorylation of control reactions of GST-STREX without the kinase and of the kinase without the substrate were run in parallel and no phosphorylation was observed. Phosphorylation of full-length GST-STREX protein (~35 kDa) and the ~32 and ~29 kDa proteolytic fragments increased over the experimental period. Densitometric analysis from eight separate time course assays is shown in Figure 4.9.

Figure 4.9
Time course of GST-STREX phosphorylation by PKAc: Densitometric analysis

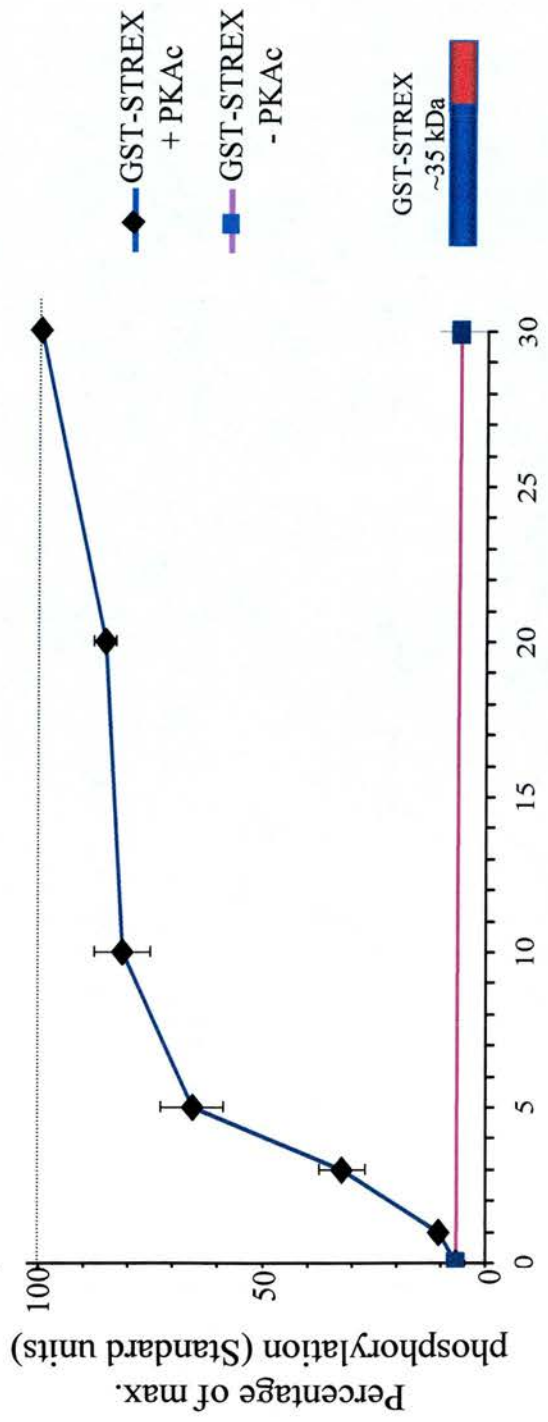

Figure 4.9: Time course of PKAc-phosphorylation of GST-STREX. PKAc-phosphorylation of the ~35 kDa GST-STREX protein from eight independent experiments (As illustrated in Figure 4.8) were analysed by densitometry (ImageJ). Phosphorylation plateaued after 10 minutes and thus the 30 minute time point was taken as maximum phosphorylation (100 %). All other data points were expressed as a percentage of this value (Mean ± SEM). No phosphorylation was observed when PKAc was omitted from the reaction mixture.

from the PKAc-only control highlighting the identification of the GST-STREX signals (As described previously, Section 4.2.2.1.1) and demonstrating that they are not kinase-associated bands.

The phosphorylation signals from the 35 kDa full-length GST-STREX protein were analysed densitometrically (Section 2.10.3) as shown in Figure 4.9. As the density of the GST-STREX phosphorylation signal plateaus between 20-30 minutes following the addition of PKAc, densities at the other time points were normalised to the 30 minute density (Figure 4.9). The curve illustrates an increase in the observed proportion of phosphorylated substrate between ~0 and ~80 % of the maximum phosphorylation over the first ten minutes of analysis. Phosphate incorporation then declines with only a ~20 % increase over the 10-30 minute time points, indicative of saturation of the reaction and demonstrating that a component of the reaction is limiting further phosphorylation. Equivalent assays were performed using non-radioactive ATP and Western blot analysis against the GST fusion tag (Results not shown). These results indicated that, throughout the assay period and conditions, there was no breakdown of the ~35 kDa fusion protein within the limits of detection demonstrating that saturation is not due to substrate degradation.

4.2.2.2 Phosphorylation of the GST-STREX fusion protein by other protein kinases

To investigate the specificity of the GST-STREX fusion protein as a PKA phosphorylation target, *in vitro* phosphorylation assays were performed using two

common protein kinases that are reported to influence BK channel activity; protein kinase C (PKC), and calmodulin kinase II (CaMKII) (See Section 1.4.1).

4.2.2.2.1 PKC phosphorylation of GST-STREX

Phosphorylation reactions employing radiolabelled ATP were performed as described in Section 2.8.1.3 using a lipid-containing buffer to activate the kinase. Assays were separated by electrophoresis on a Tris-Glycine gel and phosphate incorporation detected by autoradiography. Figure 4.10 illustrates the results of such an experiment.

In the presence of PKC, incorporation of the radiolabelled phosphate was observed with the ~35 kDa GST-STREX fusion protein and the ~29 kDa proteolytic product, in addition to the positive control protein, PHAS-I. No signals were observed in the absence of the kinase, nor was PKC-phosphorylation of the mutant, GST-S4A protein or the GST control protein observed, even upon longer exposure periods of the autoradiographs. These data indicate specific catalytic phosphorylation of the GST-STREX fusion protein by PKC, possibly at the serine-4 residue.

4.2.2.2.2 CaMKII phosphorylation of GST-STREX

Phosphorylation reactions employing radiolabelled ATP were performed using a CaMKII activation buffer (Section 2.8.1.4). Control reactions exploited the divalent cation chelator, EDTA, to buffer calcium ions and subsequently inhibit kinase activity. Reactions were separated by electrophoresis on Tris-Glycine gels and phosphate

Figure 4.10

PKC phosphorylation of GST-STREX

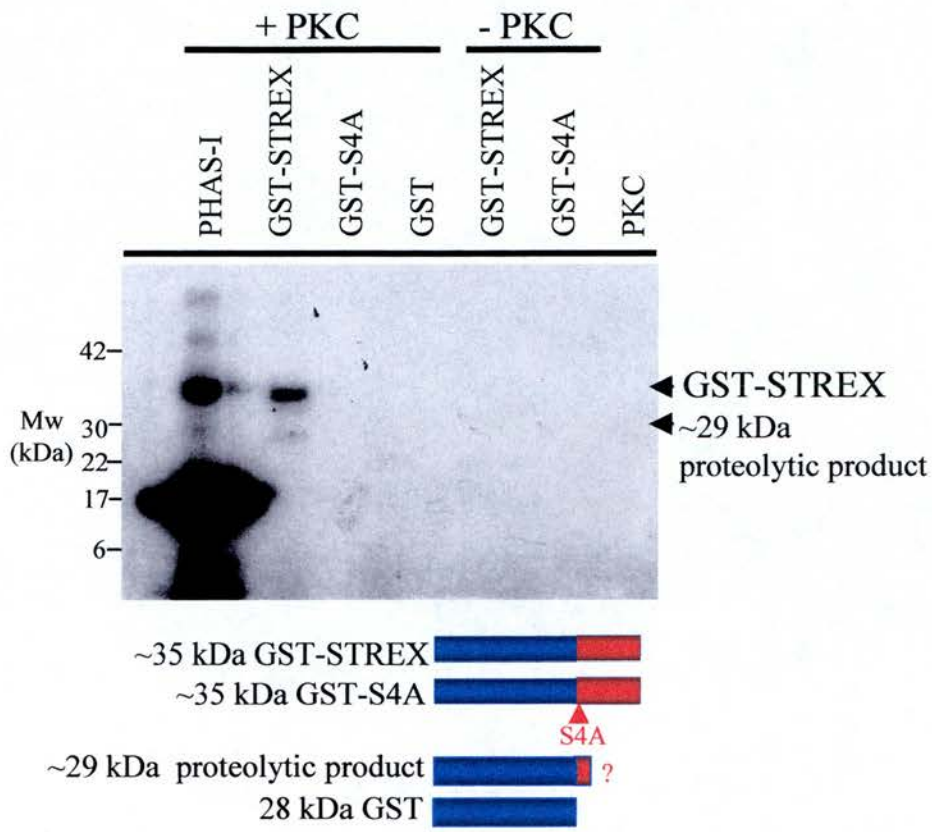

Figure 4.10: Representative autoradiograph of *in vitro* PKC phosphorylation of GST-STREX fusion proteins. Reactions in the presence of 10 μCi γ-^{32}P-ATP were incubated at 37 ^{0}C for 10 mins prior to separation on 4-12 % Tris-Glycine gels and exposure to ^{32}P sensitive film. Phosphate incorporation into the ~35 kDa and ~29 kDa GST-STREX proteins was observed only in the presence of PKC. No phosphorylation was observed with GST-S4A or GST. The positive control PKC-substrate, PHAS-I, was phosphorylated. The fusion proteins are illustrated diagrammatically below the autoradiograph (See Figure 3.5).

Figure 4.11

CaMKII phosphorylation of GST-STREX

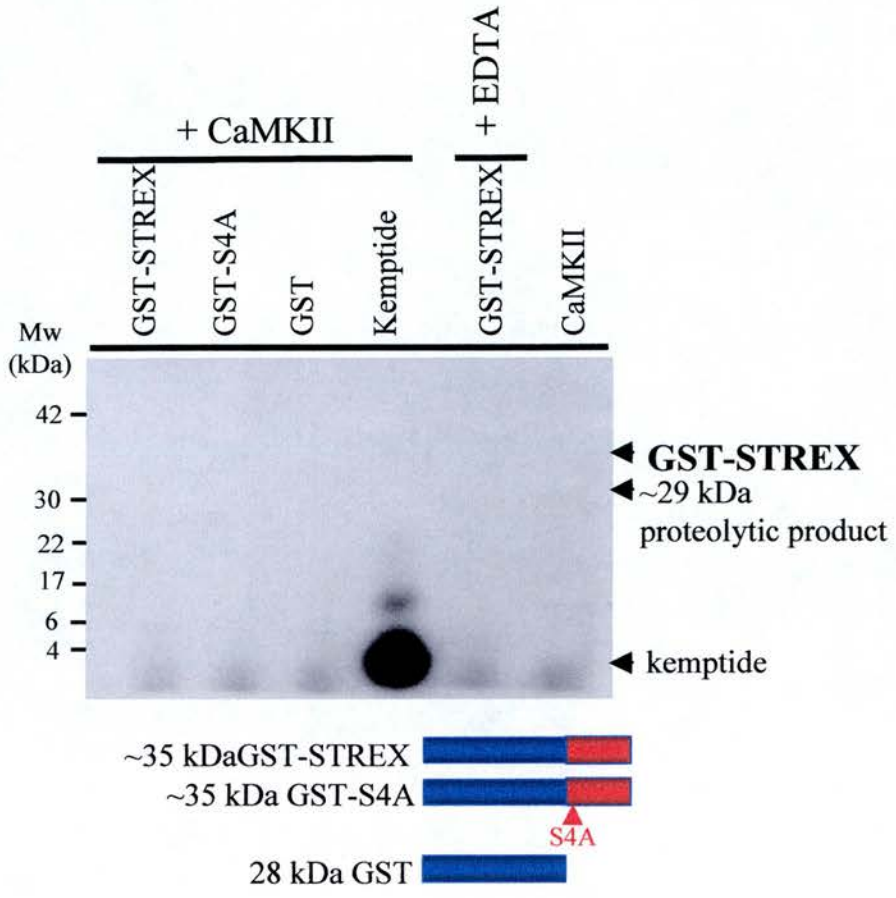

Figure 4.11: Representative autoradiograph of *in vitro* CaMKII-phosphorylation of GST-STREX. CaMKII assays using 10 μCi γ-^{32}P-ATP were incubated at 37 ^{0}C for 10 mins prior to separation on 4-12 % Tris-Glycine gels and exposure to ^{32}P sensitive film. Control reactions with the calcium chelator, EDTA, to inhibit the kinase were performed in parallel. Phosphorylation was only observed using the positive control peptide, kemptide. The assayed fusion proteins are illustrated diagrammatically below the autoradiograph (See Figure 3.5).

incorporation detected by autoradiography. Figure 4.11 illustrates the results of such an experiment.

None of the GST-fusion proteins was phosphorylated by CaMKII. The control peptide, kemptide, is strongly phosphorylated, suggesting that the kinase is catalytically active under the conditions of the experiment and is able to phosphorylate an optimal PKA consensus motif (See Table 1.1). However, the absence of any detectable phosphorylation of the experimental proteins infers that CaMKII cannot phosphorylate GST-STREX *in vitro*.

4.2.2.3 Dephosphorylation of GST-STREX

Dephosphorylation assays employing the serine/threonine protein phosphatases, protein phosphatase 2A (PP2A) and protein phosphatase 1 (PP1), were undertaken using PKAc-phosphorylated GST-STREX as substrate (Section 2.8.1.5.1). The GST-STREX fusion protein was phosphorylated by PKAc using radiolabelled phosphate, as described previously (See above). The kinase inhibitor, H-89, was then added to inhibit further phosphorylation during the dephosphorylation experiment. Aliquots were incubated with a protein phosphatase in the presence or absence of the phosphatase inhibitor, okadaic acid (100 nM). Control reactions were performed in the absence of the protein phosphatases and okadaic acid, and with okadaic acid alone. Figure 4.12 illustrates representative autoradiographs of such assays, with Figure 4.13 demonstrating the results of densitometric analysis (Section 2.10.3) from six independent experiments.

Figure 4.12
Dephosphorylation of GST-STREX: Autoradiography

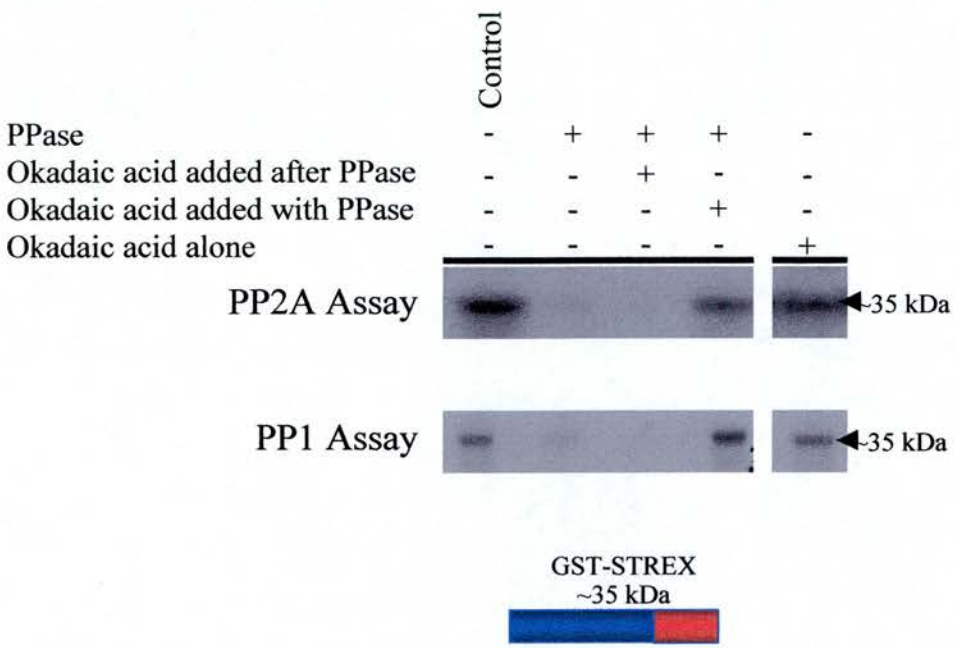

Figure 4.12: Representative autoradiographs of the dephosphorylation of GST-STREX by PP2A and PP1. PKAc-phosphorylated GST-STREX was incubated (30 mins, 37 ^{0}C) with or without protein phosphatase (PPase), either PP2A or PP1, in the presence or absence of okadaic acid. Okadaic acid was added with the PPase or only in the final five minutes of the 30 min incubation. Phosphorylation of ~35 kDa GST-STREX (and the ~29 kDa proteolytic product, not shown) was reduced by PP2A and PP1. Okadaic acid inhibited this reduction, but had no effect when applied alone. Densitometric analysis of the ~35 kDa GST-STREX bands was performed to quantitate the autoradiograph results and is shown in Figure 4.13.

Figure 4.13
Dephosphorylation of GST-STREX: Densitometric analysis

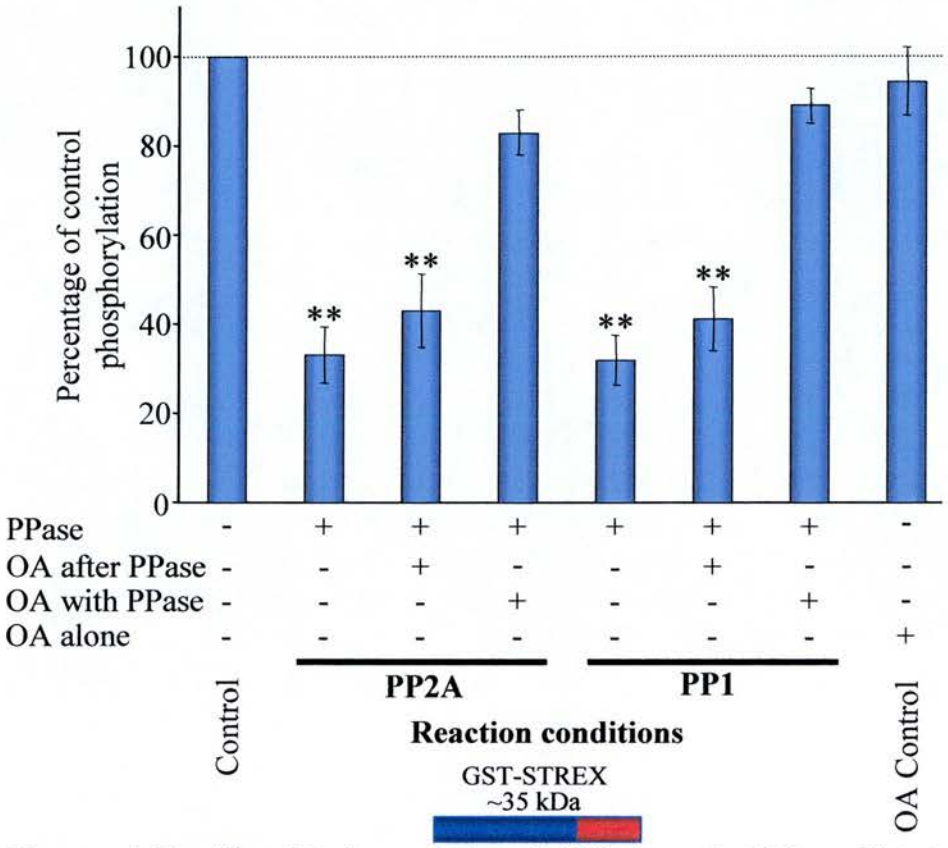

Figure 4.13: Graphical analysis of PP2A and PP1-mediated dephosphorylation of PKAc-phosphorylated GST-STREX. Densitometric analysis of full-length GST-STREX (~35 kDa) phosphorylation from four independent dephosphorylation assays as represented in Figure 4.12. Data was normalised to the PKAc phosphorylation control (100 %; mean ± SEM, n=6, Statistical analysis by T-test comparison to control phosphorylation: ** $P<0.01$). Phosphorylation of ~35 kDa GST-STREX (and the ~29 kDa proteolytic product, not shown) was reduced by PP2A and PP1. Okadaic acid inhibited this reduction but had no effect when applied alone (OA control).

The phosphorylation control was assigned as the maximal phosphorylation (100%) and therefore all experimentally determined values were normalised to the density of this signal. PP2A and PP1 significantly decreased the level of phosphorylation to 33 (± 6.3) and 32 (± 5.7) %[4] of the maximal respectively, suggestive of dephosphorylation of GST-STREX ($P<0.001$). The degree of dephosphorylation is equivalent between the two protein phosphatases ($P\sim1$).

Inclusion of the protein phosphatase inhibitor, okadaic acid (100 nM), inhibits dephosphorylation, with 83 (± 4.9) and 89 (± 3.7) %[4] of maximal phosphorylation observed with PP2A and PP1 respectively ($P>0.01$). Okadaic acid alone has no significant effect upon phosphorylation ($P\sim1$). Furthermore, application of okadaic acid in the final five minutes of the 30 minute dephosphorylation period only did not prevent dephosphorylation of GST-STREX. However, the extent of dephosphorylation was not as pronounced under these conditions as for the respective protein phosphatase alone (43 (± 8.2) %[4] compared to 33 (± 6.3) %[4] for PP2A alone ($P<0.001$), and 41 (± 7.2) %[4] compared to 32 (± 5.7) %[4] for PP1 alone ($P<0.001$)). This suggests that the dephosphorylation reactions have not reached completion at this point in the assay. Therefore, these data demonstrate that protein phosphatases PP2A and PP1 dephosphorylate PKA-phosphorylated GST-STREX *in vitro*.

[4] Values quoted as mean ±SEM, n=6.

4.2.3 Reversible phosphorylation of the ΔN-ΔC fusion proteins

Investigation of the phosphorylation of the C-terminal region, in particular the influence of the STREX insert and the relationship between the serine-869 and STREX serine-4 putative phosphorylation sites, was investigated by the use of the ΔN-ΔC fusion proteins (Section 3.2.1.2).

4.2.3.1 PKA phosphorylation of the ΔN-ΔC fusion proteins

Nickel-sepharose affinity chromatography-purified and α-V5 immunoprecipitated ΔN-ΔC fusion proteins were subjected to *in vitro* phosphorylation and analysed by autoradiography or Western blotting.

4.2.3.1.1 PKA phosphorylation of nickel affinity purified ΔN-ΔC fusion proteins: Autoradiography

In vitro phosphorylation assays were performed in the presence or absence of PKAc using ΔN-STREX-ΔC and ΔN-ZERO-ΔC purified by nickel-sepharose affinity chromatography (As Section 2.8.1). Radiolabelled ATP was used in the assays and proteins were separated by electrophoresis on Tris-Glycine gels prior to autoradiography. Figure 4.14 illustrates the results of such an experiment.

In the presence, but not in the absence of PKAc, ΔN-STREX-ΔC (~70 kDa) and ΔN-ZERO-ΔC (~65 kDa) were phosphorylated. This indicates that the kinase is required for phosphorylation suggesting that the effect is not non-specific interaction of the

Figure 4.14

PKA-mediated phosphorylation of the ΔN-ΔC proteins: Autoradiography of Ni^{2+}-purified fusion proteins

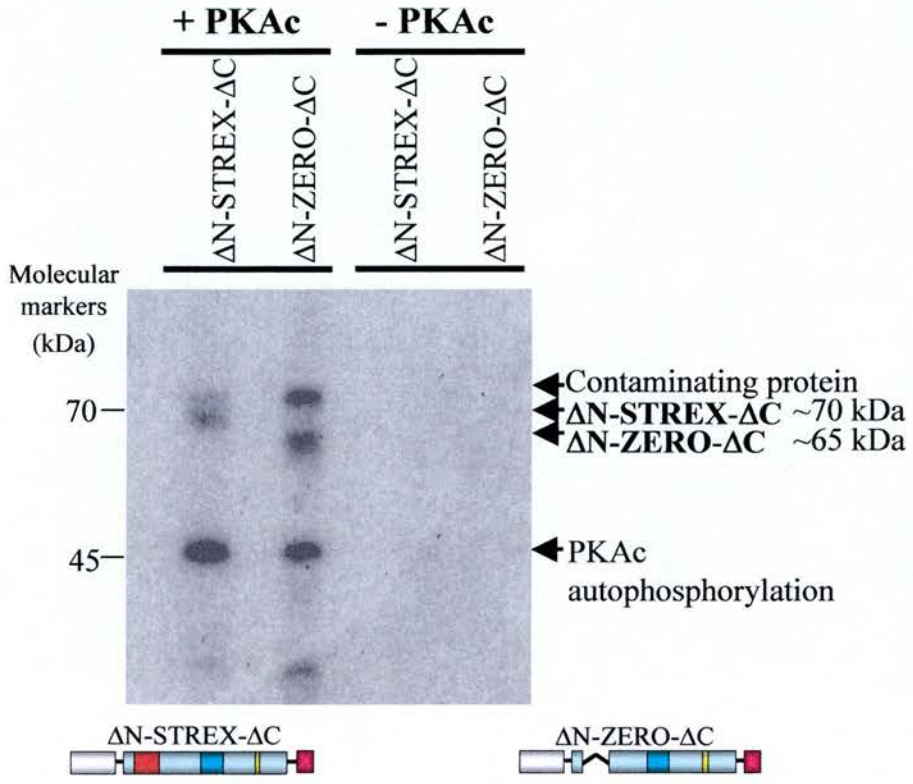

Figure 4.14: Representative autoradiograph of the *in vitro* PKA-mediated phosphorylation of Ni^{2+}-purified ΔN-ΔC fusion proteins. Assays upon ΔN-STREX-ΔC and ΔN-ZERO-ΔC in the presence (+) or absence (-) of PKAc were incubated by *in vitro* phosphorylation in the presence of [γ-^{32}P]-ATP (10 mins, 30 ^{0}C), separated by electrophoresis and analysed by autoradiography. Longer exposure periods did not detect additional signals. In the presence of PKAc, ΔN-STREX-ΔC (~70 kDa) and ΔN-ZERO-ΔC (~65 kDa), and the ~75 kDa contaminating protein are phosphorylated. Phosphorylation was not observed in absence of kinase. PKAc autophosphorylation (~45 kDa) was observed. Fusion proteins represented diagrammatically below autoradiograph (See Figure 3.5).

radiolabel with the proteins, but a specific catalytic event. Thus, this demonstrates that ΔN-STREX-ΔC and ΔN-ZERO-ΔC are phosphorylated by PKAc *in vitro*.

Autophosphorylation of PKAc is observed at 45 kDa, and the ~75 kDa contaminating protein that was observed by Colloidal stain of nickel-affinity purified recombinant proteins (Figure 3.10) is phosphorylated by the kinase also. The proximity of this phosphorylatable protein to ΔN-STREX-ΔC following electrophoresis could cause confusion in signal differentiation. Therefore, immunoprecipitation of the ΔN-ΔC fusion proteins was performed for all further phosphorylation analyses.

4.2.3.1.2 PKA phosphorylation of immunoprecipitated ΔN-ΔC fusion proteins: Autoradiography

Immunoprecipitated ΔN-STREX-ΔC, ΔN-S4A,S868A-ΔC and ΔN-ZERO-ΔC, and control protein, Thioredoxin-V5-H_6, were phosphorylated by PKAc *in vitro* as described in Section 2.8.1. Assays were separated by electrophoresis on Tris-Glycine gels and phosphorylation determined by autoradiography. Such an analysis is illustrated in Figure 4.15.

In the presence of PKAc, ΔN-STREX-ΔC (~70 kDa) and ΔN-ZERO-ΔC (~65 kDa) were phosphorylated indicating, as in Figure 4.14, that ΔN-STREX-ΔC and ΔN-ZERO-ΔC are phosphorylated by PKAc *in vitro*. Omitting the kinase from the assays prevented such phosphorylation (Results not shown) demonstrating the specific catalysis of the reactions. The inability of PKAc to phosphorylate the negative control protein,

Figure 4.15

PKA phosphorylation of the ΔN-ΔC fusion proteins: Autoradiography of immunoprecipitated proteins

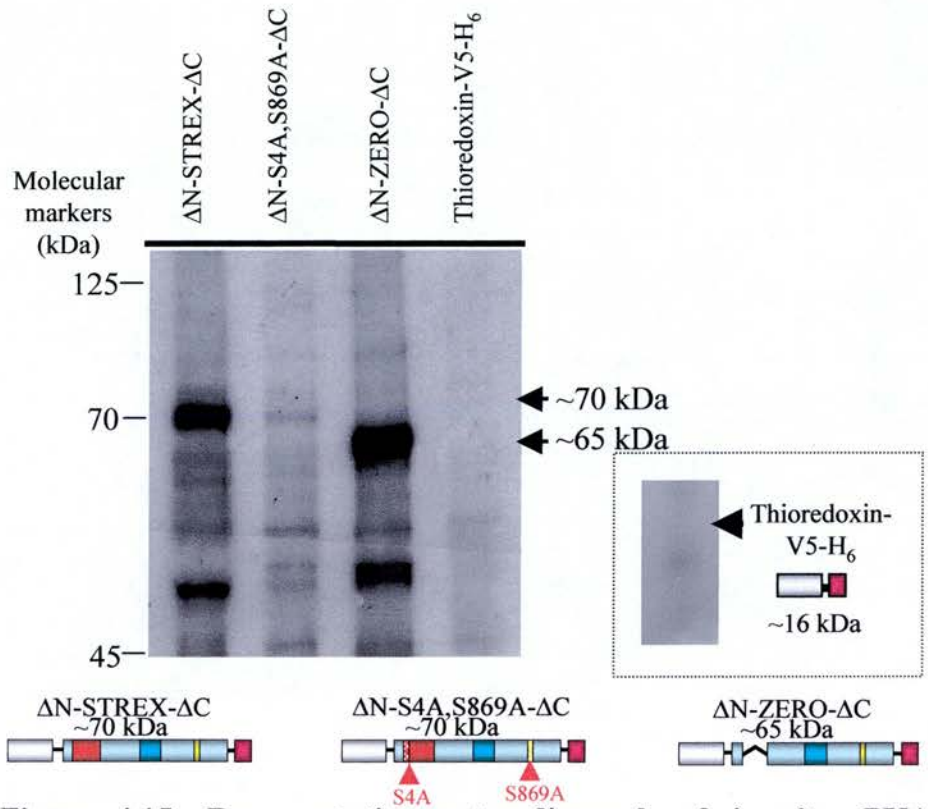

Figure 4.15: Representative autoradiograph of *in vitro* PKA phosphorylation of immunoprecipitated ΔN-ΔC fusion proteins. ΔN-STREX-ΔC, ΔN-S4A,S869A-ΔC, ΔN-ZERO-ΔC and control Thioredoxin-V5-H_6 were incubated by *in vitro* phosphorylation in the presence of PKAc and [γ-^{32}P]-ATP (10 mins, 30 ^{0}C), separated by electrophoresis and analysed by autoradiography. Longer exposure periods did not detect additional signals. ΔN-STREX-ΔC (~70 kDa) and ΔN-ZERO-ΔC (~65 kDa) were phosphorylated by PKAc and no phosphorylation was observed in the absence of the kinase (Results not shown). ΔN-S4A,S869A-ΔC (~70 kDa) and Thioredoxin-V5-H_6 (inset) were not phosphorylated by PKAc. Fusion proteins represented diagrammatically below autoradiographs (See Figure 3.5).

Thioredoxin-V5-H_6, demonstrates that the fusion tags are not phosphorylated *in vitro*, indicating that the tags are not the regions of PKAc phosphorylation in ΔN-STREX-ΔC and ΔN-ZERO-ΔC.

The very weak signal observed at ~70 kDa with the ΔN-S4A,S869A-ΔC fusion protein is of comparable density to protein bands in the negative control, Thioredoxin-V5-H_6, and less dense than those of ΔN-STREX-ΔC and indeed, ΔN-ZERO-ΔC. This suggests that ΔN-S4A,S869A-ΔC is not phosphorylated by PKAc *in vitro* and the ~70 kDa signal is due to non-specific ATP incorporation. This indicates that mutation of the S869 and STREX S4 sites to non-phosphorylatable alanine is sufficient to inhibit PKAc-phosphorylation of the fusion protein. Thus, S869 and STREX S4 are implicated as the *in vitro* phosphorylation targets of PKAc in the ΔN-STREX-ΔC fusion protein, and S869 is implicated as the *in vitro* phosphorylation target of PKAc in ΔN-ZERO-ΔC.

4.2.3.1.3 PKA phosphorylation of immunoprecipitated ΔN-ΔC fusion proteins: Western blot analysis

Determination of the putative *in vitro* PKAc phosphorylation of the S869 and STREX S4 sites of the ΔN-ΔC fusion proteins was performed by Western blot analysis using the phospho-specific antibodies that are immunoreactive to the phosphorylation state of the residues (Section 3.2.3). *In vitro* phosphorylation of the ΔN-ΔC fusion proteins was conducted with non-radiolabelled ATP as described in Section 2.8.1. Control, non-phosphorylation reactions were performed in parallel, omitting PKAc and samples were

separated by SDS-PAGE and analysed by Western blotting. A representative assay is illustrated in Figures 4.16 & 4.17.

The antibody against the V5 fusion tag, α-V5, detected the phosphorylated and non-phosphorylated ΔN-ΔC fusion proteins at the appropriate molecular weights (~65 kDa for ΔN-ZERO-ΔC and ~70 kDa for all the STREX-insert expressing proteins) with approximately equivalent band densities between samples demonstrating equivalent loading of the fusion proteins (Figures 4.16 & 4.17).

S869 site phosphorylation (Figure 4.16)

The intact S869 residues of ΔN-STREX-ΔC and ΔN-ZERO-ΔC are demonstrated by the immunoreactivity of α-S869 for the non-phosphorylated proteins. The alanine substitution of the site within ΔN-S4A,S869A-ΔC and ΔN-STREX,S869A-ΔC reduces, but does not occlude, the association of the antibody with the proteins as the phosphorylated and non-phosphorylated reactions display an immunoreactivity that is notably less than that of the non-phosphorylated ΔN-STREX-ΔC and ΔN-ZERO-ΔC. However, whereas ΔN-S4A,S869A-ΔC and ΔN-STREX,S869A-ΔC are still detected following *in vitro* phosphorylation analysis with PKAc, ΔN-STREX-ΔC and ΔN-ZERO-ΔC lose their immunoreactivity to α-S869. This is counterbalanced by α-phospho-S869 analysis, which detects only the phosphorylated fusion proteins with intact S869 sites: ΔN-STREX-ΔC and ΔN-ZERO-ΔC. These data suggest that PKAc phosphorylates intact S869 residues of ΔN-ΔC fusion proteins *in vitro*.

Figure 4.16
In vitro PKA phosphorylation of ΔN-ΔC fusion proteins: Western blot analysis of S869 site phosphorylation

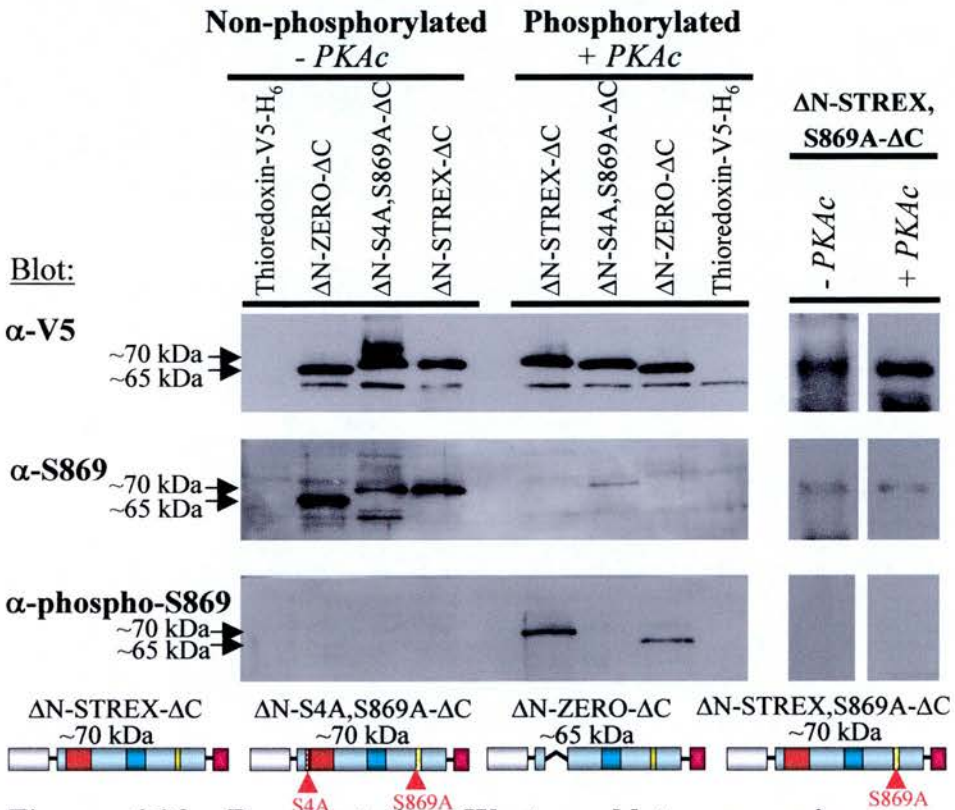

Figure 4.16: Representative Western blots comparing non-phosphorylated and PKA-phosphorylated ΔN-ΔC fusion proteins. *In vitro* PKA phosphorylation of the ΔN-ΔC fusion proteins was performed with (phosphorylated) or without (non-phosphorylated) PKAc. α-V5 detected the proteins at the appropriate molecular weights (as illustrated below blots (See Figure 3.5)). Non-phosphorylated ΔN-STREX-ΔC and ΔN-ZERO-ΔC, and ΔN-S4A,S869A-ΔC and ΔN-STREX,S869A-ΔC with mutated S869 sites, were detected by α-S869. S869 site phosphorylation, indicated by α-phospho-S869, was observed with ΔN-STREX-ΔC and ΔN-ZERO-ΔC only. Control thioredoxin-V5-H_6 (~16 kDa) was detected by α-V5 only (Not shown). Western analysis: mouse α-V5 1/5000; sheep α-S869/α-phospho-S869 1/1000; α-mouse-HRP 1/2000; α-sheep/goat-HRP 1/15000; ECL detection.

Figure 4.17

In vitro PKA phosphorylation of ΔN-ΔC fusion proteins: Western blot analysis of STREX S4 site phosphorylation

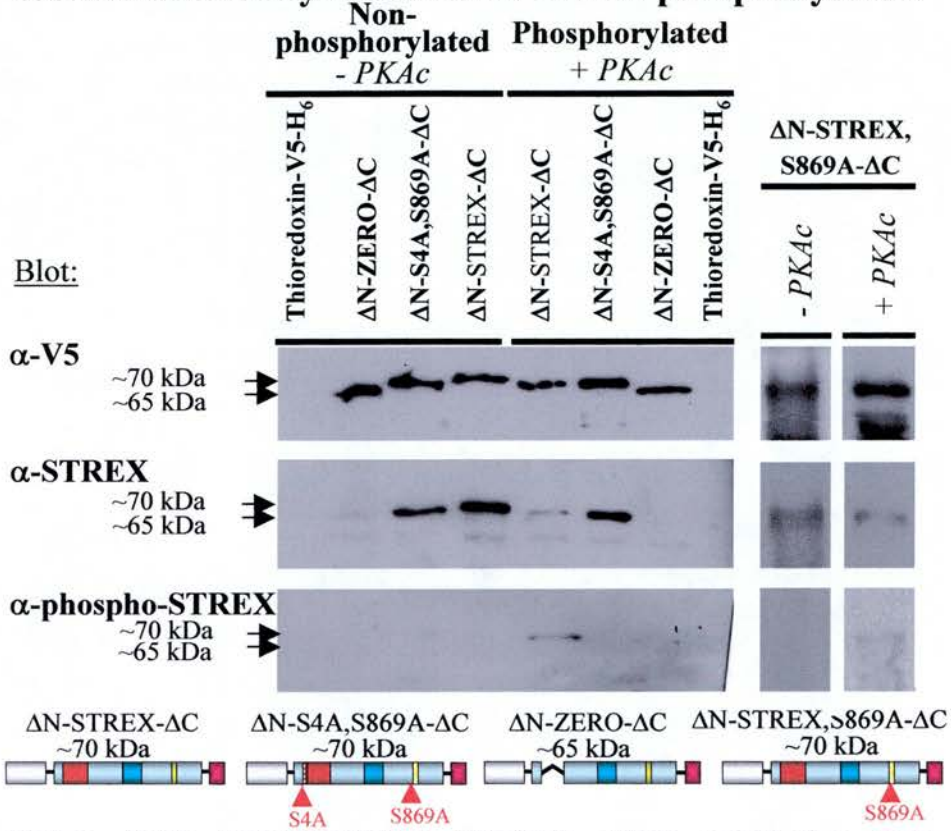

Figure 4.17: Representative Western blots comparing non-phosphorylated and PKA-phosphorylated ΔN-ΔC fusion proteins. *In vitro* PKA phosphorylation was performed with (phosphorylated) or without (non-phosphorylated) PKAc. α-V5 detected the proteins at the appropriate molecular weights (as illustrated below blots (See Figure 3.5)). α-STREX detected fusion proteins expressing the STREX insert only (ΔN-STREX-ΔC, ΔN-S4A,S869A-ΔC & ΔN-STREX,S869A-ΔC). STREX S4 phosphorylation, indicated by α-phospho-STREX, was observed of proteins with intact STREX S4 (ΔN-STREX-ΔC & ΔN-STREX,S869A-ΔC). Control thioredoxin-V5-H_6 (~16 kDa) was detected by α-V5 only (Not shown). Western analysis: mouse α-V5 1/5000; sheep α-STREX/α-phospho-STREX 1/1000; α-mouse-HRP 1/2000; α-sheep/goat-HRP 1/15000; ECL detection.

STREX S4 site phosphorylation (Figure 4.17)

The presence of the STREX insert in ΔN-STREX-ΔC, ΔN-S4A,S869A-ΔC and ΔN-STREX,S869A-ΔC is confirmed by the specific immunoreactivity of the α-STREX antibody to these fusion proteins. ΔN-ZERO-ΔC (Figure 4.17) and Thioredoxin-V5-H_6 (Results not shown) were not detected by this antibody demonstrating the specificity of the antibody to STREX-insert-containing proteins. Further to this, the immunoreactivity of α-STREX to phosphorylated ΔN-STREX-ΔC and ΔN-STREX,S869A-ΔC is reduced in comparison to the non-phosphorylated reactions. Phosphorylated and non-phosphorylated ΔN-S4A,S869A-ΔC, with the STREX S4 residue substituted by alanine, are detected equally.

Phosphorylation of STREX S4 is detected by α-phospho-STREX only with the phosphorylated fusion proteins with intact STREX S4 residues; ΔN-STREX-ΔC and ΔN-STREX,S869A-ΔC. These data suggest that PKAc phosphorylates the STREX S4 residue of STREX insert-containing ΔN-ΔC fusion proteins *in vitro*.

In vitro phosphorylation of the ΔN-ΔC fusion proteins (Figures 4.16 & 4.17)

Thus, Figures 4.16 & 4.17 indicate that the conserved S869 site and the STREX S4 residue are targets of *in vitro* PKAc phosphorylation of the ΔN-ΔC fusion proteins. If both sites are present, as with ΔN-STREX-ΔC, the residues are co-phosphorylated. If one is absent or mutated, the other will continue to be a PKAc–phosphorylation target, as illustrated by the S869 site of ΔN-ZERO-ΔC, and the STREX S4 residue of ΔN-STREX,S869A-ΔC.

Concomitantly, these results demonstrate the successful application of the phospho-specific antibodies; α-phospho-S869 and α-phospho-STREX are immunoreactive to the phosphorylated forms of the sites only and not when the site(s) are mutated or when the kinase is omitted and thus phosphorylation cannot have occurred. α-S869 is immunoreactive to intact, non-phosphorylated S869 sites, although does exhibit a reduced immunoreactivity against the alanine substituted mutant. α-STREX recognizes STREX insert-containing ΔN-ΔC fusion proteins specifically, whether intact or expressing the S4A mutation. The immunoreactivity is reduced by phosphorylation of intact STREX S4 residues and the signal attained with phosphorylated ΔN-STREX-ΔC may result from incomplete PKAc-phosphorylation of the fusion protein population, or by the incomplete specificity of the α-STREX antibody to the dephosphorylation state of the STREX S4 residue.

4.2.3.2 Phosphorylation of the ΔN-ΔC fusion proteins by other protein kinases

To investigate the protein-kinase specificity of the relative phosphorylation of the S869 and STREX S4 putative phosphorylation sites of the ΔN-ΔC fusion proteins, *in vitro* phosphorylation assays were performed using PKC and CaMKII.

4.2.3.2.1 PKC phosphorylation of the ΔN-ΔC fusion proteins

In vitro PKC-phosphorylation assays using non-radiolabelled ATP were performed on immunoprecipitates of the ΔN-ΔC fusion proteins as described in Section 2.8.1.3. Control, non-phosphorylation reactions omitting PKC were performed in parallel and

samples were separated by SDS-PAGE and analysed by Western blotting. A representative assay is illustrated in Figure 4.18.

Detection by the α-V5 antibody determined the presence of the PKC-phosphorylated and the non-phosphorylated ΔN-ΔC fusion proteins at the appropriate molecular weights (As described in Section 4.2.3.1.3). Immunodetection with α-phospho-S869 revealed that the S869 site was not phosphorylated by PKC in any ΔN-ΔC fusion protein. In contrast, although detecting a non-specific protein at ~60 kDa in all immunoprecipitates including that of the control, Thioredoxin-V5-H_6, α-phospho-STREX recognised phosphorylation of STREX S4 in fusion proteins that expressed the intact, non-mutated residue; ΔN-STREX-ΔC and ΔN-STREX,S869A-ΔC. Non-phosphorylated reactions did not display phosphorylation of the site and neither did ΔN-ΔC fusion proteins that do not express the STREX insert (ΔN-ZERO-ΔC) or express an alanine mutation of the STREX S4 residue (ΔN-S4A,S869A-ΔC). This demonstrates that an intact STREX S4 residue is required for *in vitro* PKC phosphorylation of the ΔN-ΔC fusion proteins and indicates that although other regions encompassed by the ΔN-ΔC fusion proteins may function as PKC phosphorylation targets, with respect to the conserved S869 site and STREX S4, PKC does not phosphorylate the S869 residue of the ΔN-ΔC fusion proteins *in vitro*, but does phosphorylate the STREX S4 site.

Figure 4.18
In vitro PKC phosphorylation of ΔN-ΔC fusion proteins

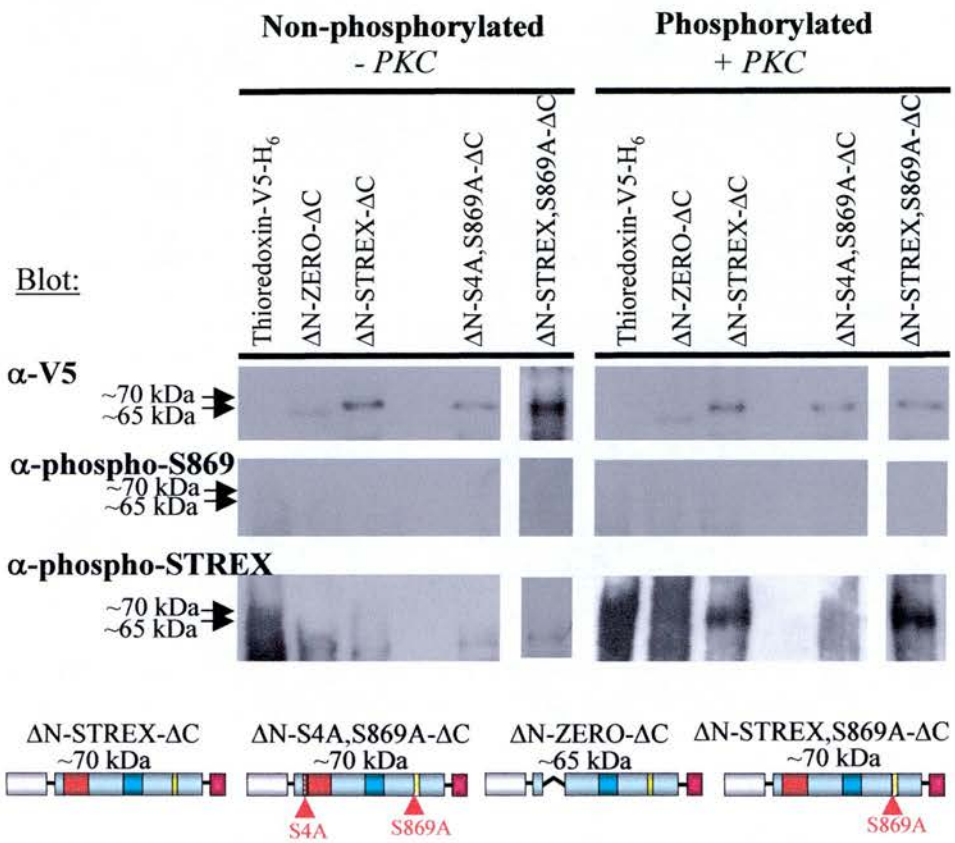

Figure 4.18: Representative Western blots comparing non-phosphorylated and PKC-phosphorylated ΔN-ΔC fusion proteins. *In vitro* PKC phosphorylation was performed with (phosphorylated) or without (non-phosphorylated) PKC. α-V5 detected the proteins at the appropriate molecular weights (as illustrated below blots (See Figure 3.5)). No phosphorylation of the ΔN-ΔC fusion proteins' S869 site is detected by α-phospho-S869. STREX S4 phosphorylation, indicated by α-phospho-STREX, was observed of proteins with intact STREX S4 (ΔN-STREX-ΔC & ΔN-STREX,S869A-ΔC). Control thioredoxin-V5-H_6 (~16 kDa) was detected by α-V5 only (Not shown). Western analysis: mouse α-V5 1/5000; sheep α-phospho-STREX/S869 1/1000; α-mouse-HRP 1/2000; α-sheep/goat-HRP 1/15000; ECL detection.

Figure 4.19

In vitro CaMKII phosphorylation of ΔN-ΔC fusion proteins

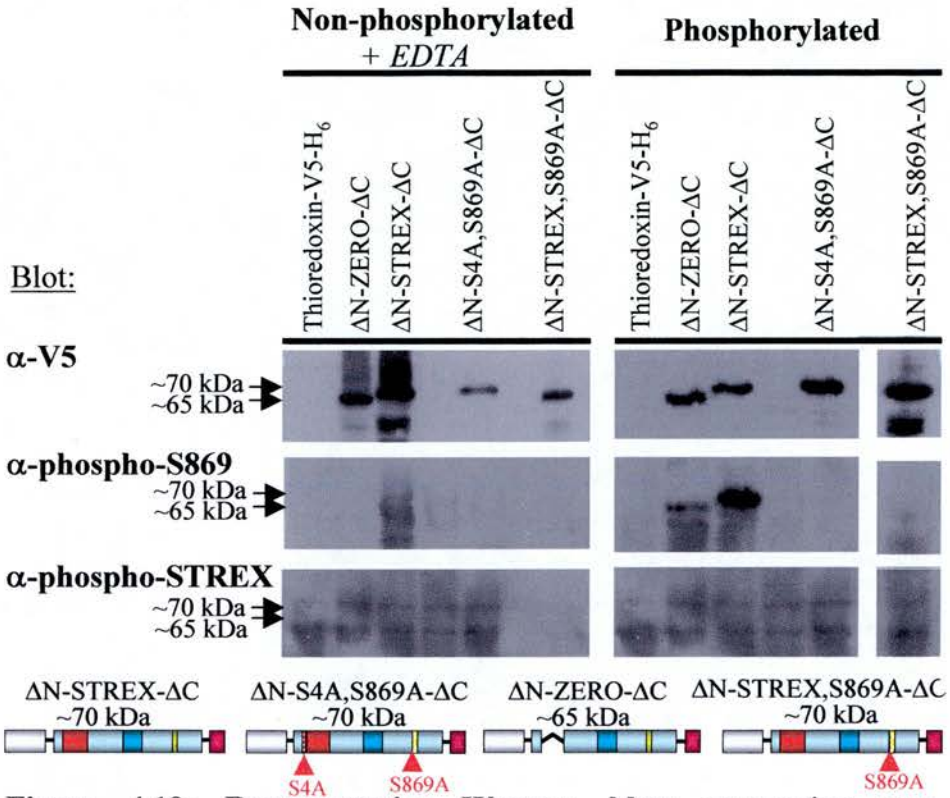

Figure 4.19: Representative Western blots comparing non-phosphorylated and CaMKII-phosphorylated ΔN-ΔC fusion proteins. *In vitro* CaMKII phosphorylation was performed in activation buffer (phosphorylated), or in the presence of the inhibitory divalent cation chelator, EDTA (non-phosphorylated). α-V5 detected the proteins at the appropriate molecular weights (as illustrated below blots (See Figure 3.5)). S869 phosphorylation, indicated by α-phospho-S869, was observed of phosphorylated proteins with intact S869 sites (ΔN-ZERO-ΔC and ΔN-STREX-ΔC). No phosphorylation of the ΔN-ΔC fusion proteins' STREX S4 site is detected by α-phospho-STREX. Control thioredoxin-V5-H_6 (~16 kDa) was detected by α-V5 only (Not shown). Western analysis: mouse α-V5 1/5000; sheep α-phospho-STREX/S869 1/1000; α-mouse-HRP 1/2000; α-sheep/goat-HRP 1/15000; ECL detection.

4.2.3.2.2 CaMKII phosphorylation of the ΔN-ΔC fusion proteins

In vitro phosphorylation reactions employing non-radiolabelled ATP were performed using CaMKII activation buffer (Section 2.8.1.4). Control reactions using EDTA in the buffer were performed in parallel (As described previously, Section 4.2.1.2.2). Reactions were separated by SDS-PAGE and analysed by Western blotting as illustrated in Figure 4.19.

The CaMKII-phosphorylated and the non-phosphorylated ΔN-ΔC fusion proteins were detected at the appropriate molecular weights by α-V5 (Described previously: Section 4.2.3.1.3). Only CaMKII-phosphorylated ΔN-ΔC fusion proteins with intact S869 sites were immunoreactive to α-phospho-S869 (ΔN-ZERO-ΔC and ΔN-STREX-ΔC). EDTA blocked CaMKII *in vitro* phosphorylation of the site in the fusion proteins. The inability of CaMKII to phosphorylate S869 in the alanine-substituted mutants (ΔN-S4A,S869A-ΔC and ΔN-STREX,S869A-ΔC) indicates that such a mutation of the conserved site is sufficient to inhibit *in vitro* phosphorylation of the residue by CaMKII. Thus, although other CaMKII consensus phosphorylation sites may be present in the ΔN-ΔC fusion proteins' sequence, S869 is determined as a definite *in vitro* phosphorylation target.

In contrast, the STREX S4 residue is not an *in vitro* target of CaMKII phosphorylation of the ΔN-ΔC fusion proteins as no phosphorylation is detected by the α-phospho-STREX antibody. In this assay, α-phospho-STREX detected non-specific bands at ~72 and ~62 kDa in all immunoprecipitates; phosphorylated and non-phosphorylated, ΔN-

ΔC fusions and Thioredoxin-V5-H_6. The consistency in the detection of these bands and their non-alignment to the molecular weights of the ΔN-ΔC fusion proteins suggests non-specific immunoreactivity that did not obstruct detection of STREX S4 site phosphorylation.

4.2.4 PKA-phosphorylation of HA-tagged BK channel splice variants

HA-tagged full-length BK channel proteins, expressed in HEK293 cells and immunoprecipitated with the α-HA antibody were used to assess PKA-phosphorylation of the channel in the *in extenso* protein and crucially, *in vivo*.

4.2.4.1 *In vitro* PKA-phosphorylation of immunoprecipitated HA-tagged BK channel variants by exogenous PKAc

Washed PGS pellets with bound α-HA-immunoprecipitated HA-tagged BK channel variants were assayed by *in vitro* phosphorylation as described in Sections 2.8.1.1 and 2.8.1.2. Immunoprecipitations from untransfected HEK293 cells were treated in parallel as controls. Reactions were separated by electrophoresis and analysed by autoradiography when radiolabelled ATP was used in the analysis (Figure 4.20), or by Western blotting when non-radiolabelled ATP was employed (Figure 4.21).

4.2.4.1.1 Autoradiography (Figure 4.20)

Phosphorylation of proteins corresponding to the molecular weight of the HA-tagged BK channels was detected for ZERO-HA and STREX-HA in the presence, but not in the absence of the phosphatase-inhibitor, okadaic acid. Phosphorylation of the mutant, S4A,S869-HA channel was not observed, and a protein of equivalent molecular weight

Figure 4.20

In vitro phosphorylation of HA-tagged, full-length BK channel variants by exogenous PKAc: Autoradiography

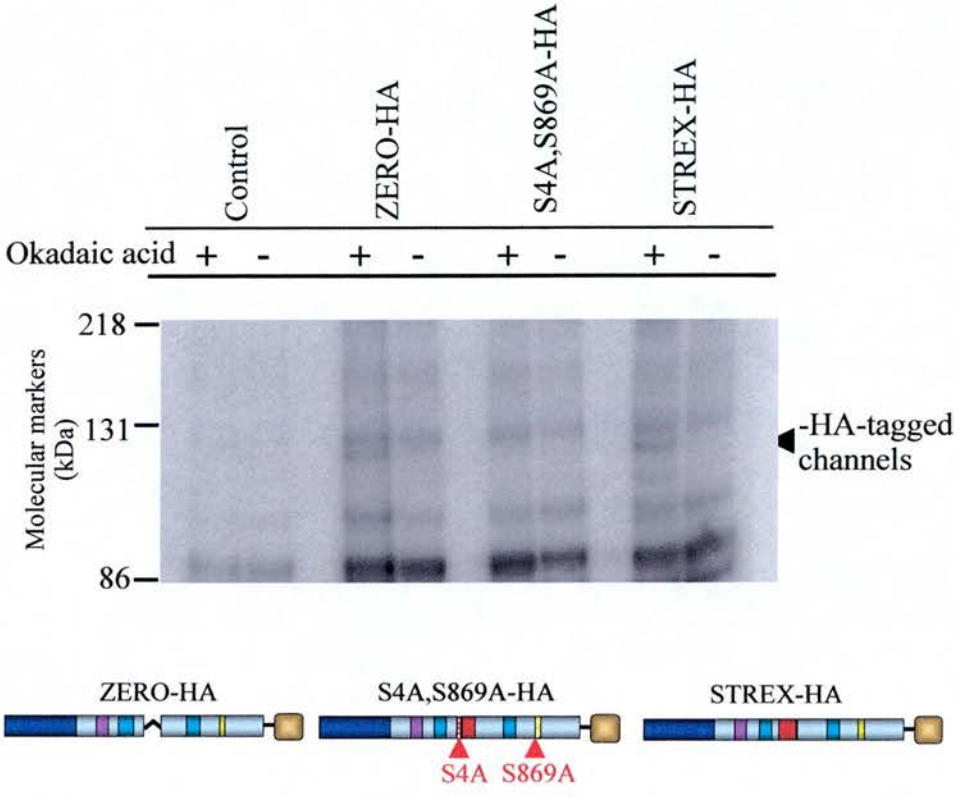

Figure 4.20: Representative autoradiograph of *in vitro* PKA phosphorylation of -HA-tagged BK channel splice variants. Immunoprecipitated (IP) -HA-tagged BK channel splice variants (ZERO, STREX & S4A,S869A; as represented below the autoradiograph (See Figure 3.17)) expressed by HEK293 cells were phosphorylated by *in vitro* phosphorylation in the presence of [γ-^{32}P]-ATP & PKAc (10 mins, 30 ^{0}C) with (+) or without (-) the phosphatase inhibitor, okadaic acid. IP HEK293 cells not expressing BK channels were employed as a control. Assays separated by electrophoresis and exposed to ^{32}P-sensitive film demonstrated phosphorylation of okadaic acid-treated ZERO-HA and STREX-HA. Non-specific protein phosphorylations were detected in all reactions.

Figure 4.21

In vitro phosphorylation of HA-tagged, full-length BK channel variants by exogenous PKAc: Western analysis

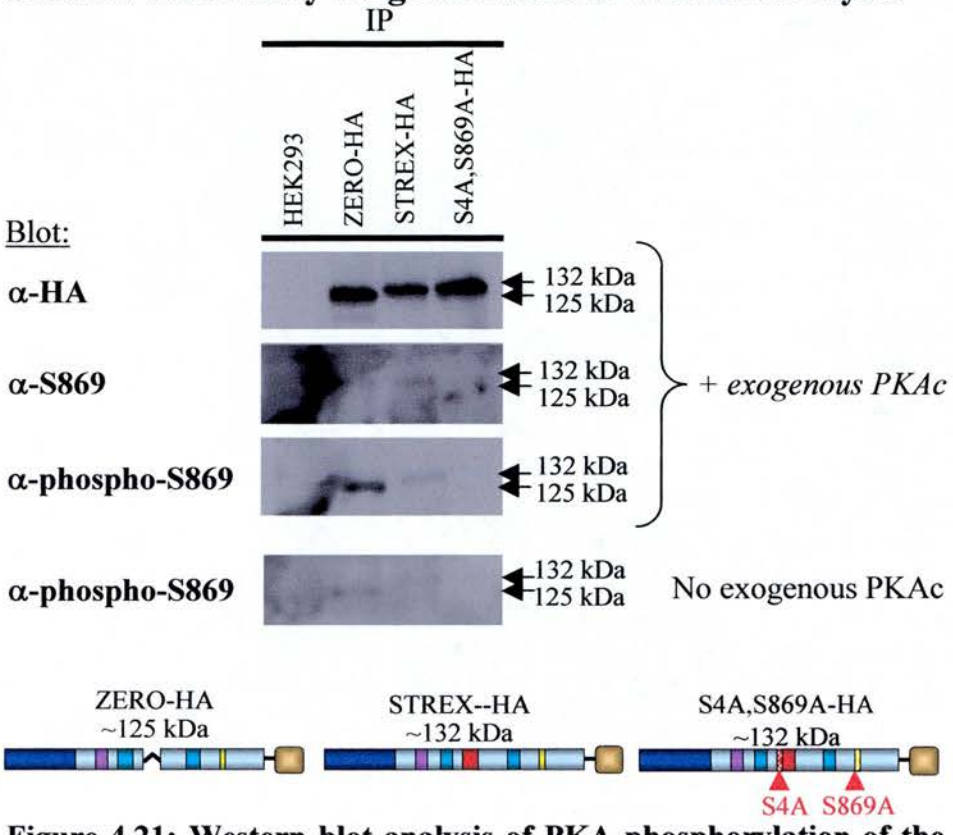

Figure 4.21: Western blot analysis of PKA phosphorylation of the S869 site of -HA-tagged BK channel splice variants. *In vitro* PKA phosphorylation of immunoprecipitated (IP) -HA-tagged BK channel splice variants (ZERO, STREX & S4A,S869A; as represented below the autoradiograph (See Figure 3.17)) was performed with or without exogenous PKAc in the presence of okadaic acid. α-HA detected the proteins at the appropriate molecular weights. Non-phosphorylated ZERO-HA and STREX-HA, and S4A,S869A-HA with a mutated S869 site, were detected by α-S869. S869 site phosphorylation, indicated by α-phospho-S869, was observed with ZERO-HA and STREX-HA only even if no exogenous PKAc was added. Western analysis: rabbit α-HA 1/333; sheep α-S869/α-phospho-S869 1/1000; α-rabbit-HRP 1/5000; α-sheep/goat-HRP 1/15000; ECL detection.

within the HEK293 cell control immunoprecipitations was not detected. Non-BK channel protein phosphorylations that could result from phosphorylation of the immunoprecipitation components, co-immunoprecipitating proteins with affinity for the BK channels and non-specific co-immunoprecipitants were detected in all reactions including the non-transfected HEK293 cell controls.

These data suggest that the ZERO-HA and STREX-HA fusion proteins are putative targets of phosphorylation by exogenous PKAc *in vitro*, but mutation of the conserved S869 and STREX S4 residues in the S4A,S869A-HA channel is sufficient to inhibit this phosphorylation. The necessity of okadaic acid in the reaction mixture to allow this phosphorylation suggests that a protein phosphatase(s) with the ability to dephosphorylate the PKA-phosphorylated residues co-immunoprecipitates and is catalytically active under experimental conditions.

4.2.4.1.2 Western blot analysis (Figure 4.21)

Due to the apparent protein phosphatase activity associated with the immunoprecipitated BK channels (See above; Figure 4.20), okadaic acid was included in all further *in vitro* PKA phosphorylation assays. The phosphorylation state of the BK channel S869 site was assessed by use of the phospho-specific antibodies to the residue (See Section 3.2.3) as illustrated in Figure 4.21.

The phosphorylated HA-tagged BK channel variants, ZERO-HA (~125 kDa), STREX-HA (~132 kDa) and S4A,S869A-HA (~132 kDa), were identified at the appropriate

molecular weights by the immunoreactivity of α-HA to the –HA epitope tag with equivalent band densities indicating equal loading of each channel variant. No HA-tagged proteins were observed in the HEK293 cell immunoprecipitation control. Similarly, the presence of the S869 site in ZERO-HA and STREX-HA was detected by α-S869, although no discernable immunoreactivity was observed with the mutated S4A,S869A-HA.

Phosphorylation of the S869 residue, indicated by the α-phospho-S869 antibody, was observed with the ZERO-HA and STREX-HA channels that express an intact S869 site. However, the antibody did not detect S4A,S869A-HA with the S869A mutation indicating that an intact S869 site is required for phosphorylation by PKAc. However, phosphorylation of the S869 residue of ZERO-HA and STREX-HA is observed when no exogenous kinase is added to the immunoprecipitations. This suggests that the site may be phosphorylated *in vivo* and remain so during immunoprecipitation, or that a serine/threonine PKA-like protein kinase associates by co-immunoprecipitation with the channels and is activated by the *in vitro* phosphorylation assay conditions.

STREX S4 site phosphorylation

Equivalent analysis of STREX S4 site phosphorylation was not possible due to non-specific immunoreactivity of the α-phospho-STREX with the full-length BK channel fusion proteins (Results not shown). The antibody detected the ZERO-HA channel that lacks the STREX insert and thus cannot exhibit STREX S4 phosphorylation. A distinct conformation of the region in the full-length channel protein in comparison with the

recombinant –GST and ΔN-ΔC fusion proteins may inhibit the correct antigen-antibody association and, certainly, α-phospho-STREX is interacting non-specifically with a region(s) of the BK channel protein that is conserved between the ZERO and STREX splice variants.

4.2.4.2 PKA-phosphorylation of immunoprecipitated HA-tagged BK channel variants by endogenous PKAc

As described in Section 2.8.2, determination of the *in vivo* phosphorylation of the conserved S869 site of ZERO-HA and STREX-HA was performed by stimulation of endogenous PKA in the heterologous expression system, HEK293 cells, by 30 μM forskolin (Results not shown) or 1 mM of membrane permeable 8-CPT-cAMP in the presence or absence of 100 nM okadaic acid. Controls were performed in parallel with okadaic acid only and with no reagent addition. Channels were immunoprecipitated using α-HA and phosphorylation of the S869 site assessed by Western blot analysis. A representative assay using 8-CPT-cAMP as the PKA-stimulator is illustrated in Figure 4.22.

Successful immunoprecipitation of the channels was confirmed by the immunoreactivity of α-HA to proteins corresponding to ZERO-HA, ~125 kDa, and STREX-HA, ~132 kDa. Further to this, the intact, conserved S869 site was identified in each splice variant immunoprecipitation by α-S869. Phosphorylation of S869, detected by α-phospho-S869, revealed that the phosphorylated form of the motif was present under all

Figure 4.22

PKA stimulation *in vivo*: Phosphorylation of heterologously expressed -HA-tagged BK channel ZERO and STREX splice variants

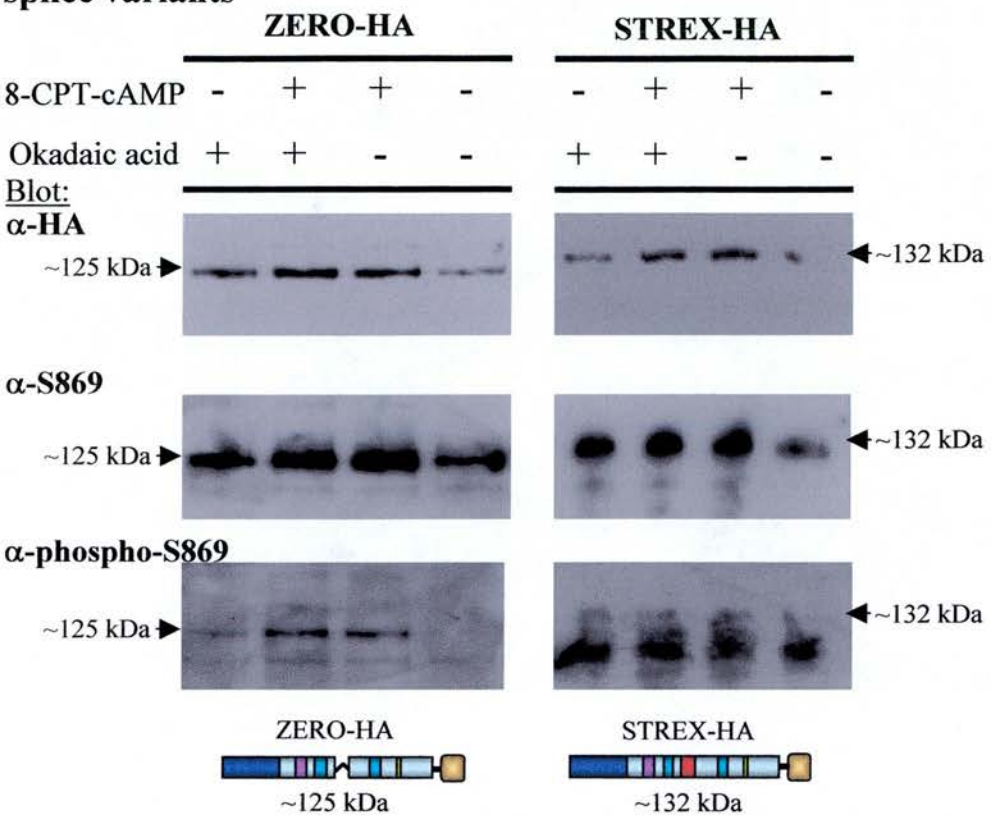

Figure 4.22: Western blot analysis of BK channel splice variants expressed in PKA-stimulated HEK293 cells. Heterologously expressed ZERO-HA or STREX-HA channels were incubated (20 mins, 37 ^{0}C) in the presence or absence of the PKA-stimulator, 1 mM 8-CPT-cAMP, with or without 100 nM okadaic acid (phosphatase inhibitor) prior to immunoprecipitation. The channels were detected by α-HA and α-S869. Following PKA stimulation by 8-CPT-cAMP there was an apparent increase in phosphorylation of the S869 site, demonstrated by α-phospho-S869 antibody analysis. Western analysis: rabbit α-HA 1/333; sheep α-S869/α-phospho-S869 1/1000; α-rabbit-HRP 1/5000; α-sheep/goat-HRP 1/15000; ECL detection.

experimental conditions with both the ZERO and STREX splice variants. However, stimulation of PKA by 8-CPT-cAMP, especially where protein phosphatase activity was inhibited by okadaic acid, produced an increase in the phospho-S869 signal suggesting that PKA phosphorylation of the site occurs following stimulation of the kinase. This implicates the conserved BK channel S869 site of ZERO and STREX splice variants as a target of PKA phosphorylation *in vivo*.

4.3 Discussion

Protein kinase and protein phosphatase regulation of ion channels has been studied and described for numerous ion channels including the ubiquitous BK channels (See Section 1.4.1). The precise molecular mechanism of such regulation varies between direct phosphorylation/dephosphorylation of the ion channel α-subunit protein and activation/inactivation of intermediate, accessory proteins that, in turn, control the required physiological response of the ion channels. Previous electrophysiological analyses of various mutated BK channel variants have proposed that PKA phosphorylates the α-subunit of the channel directly at precise consensus motifs [190, 205, 229]. Through such studies the conserved BK channel S869 residue and, independently, the STREX splice variant S4 residue have been proposed as integral sites in the PKA-mediated regulation of BK channel function through direct phosphorylation by the kinase. The aim of this chapter was to determine whether these residues are, indeed, phosphorylated directly by PKA *in vivo*, and to investigate whether such phosphorylation may underlie PKA-mediated regulation of BK channel splice variants.

The *in vitro* and *in vivo* phosphorylation data presented in this study demonstrate that the two residues are phosphorylated by PKA *in vivo*, and suggest that the residues are co-phosphorylated by the kinase in the STREX splice variant channel.

4.3.1 Phosphorylation of the conserved BK channel S869 residue

The ability of PKA to target and phosphorylate the conserved S869 motif directly and specifically was demonstrated by *in vitro* phosphorylation of the S869 peptides and phospho-specific antibody identification of S869 phosphorylation *in vitro*, with the ΔN-ΔC fusion proteins, and *in vivo*, with the –HA-tagged, heterologously expressed, full-length channels.

In all assays, the substitution of the S869 residue with non-phosphorylatable alanine was sufficient to preclude phosphorylation of the fusion proteins, demonstrating that this serine residue is phosphorylated specifically by PKA. Although, as with any mutagenesis, alanine substitution could induce conformational alterations to the fusion protein as to inhibit phosphorylation of other, distinct sites, the conserved nature of this mutation should minimise such structural disruptions (See Section 4.1.2). Thus, the mutations were used to demonstrate that the S869 residue is phosphorylated directly by PKA both *in vitro* and *in vivo*. Further to this, the reversibility of S869 peptide phosphorylation by PP2A and PP1 demonstrated that the process is reversible and thus may be employed functionally *in vivo*.

Stimulation of endogenous HEK293 cell PKA and the addition of excess exogenous PKAc increased the apparent S869 residue phosphorylation determined by α-phospho-S869 Western blot analysis. Under both assay conditions basal levels of S869 phosphorylation were observed prior to or without the addition/stimulation of the kinase. This indicates that the site functions as a phosphorylation target under basal conditions in HEK293 cells, indicative of native PKA-like protein kinase activity in the heterologous expression system. *In vitro* phosphorylation assays using the S869 peptides and ΔN-ΔC fusion proteins revealed that the site could be phosphorylated by PKA or CaMKII *in vitro*, and thus, indicated that multiple protein kinases may be responsible for basal phosphorylation of S869. However, S869 displays some selectivity as PKC did not phosphorylate the site *in vitro* and thus, is unlikely to phosphorylate S869 *in vivo*. The S869 motif shares limited homology with optimal consensus motifs for PKA, PKC and CaMKII (Scheme 4.2). However, the specificity of the kinases is such that PKC cannot phosphorylate the site *in vitro*. Although complex, future studies could investigate multi-sourced phosphorylation of S869 by inhibition and stimulation of specific protein kinases *in vivo*, and may uncover a phosphorylation target site, used by several, distinct signal transduction pathways collectively and individually.

Scheme 4.2: Alignment of the conserved BK channel S869 motif with protein kinase consensus sequences
(Although several possible consensus sequences are suitable for phosphorylation by the kinases (See Table 1.1), only the consensus sequence with the greatest alignment to the motif is shown). Green residues = alignment. Red residues = non-alignment. Standard one letter amino acid code used.

Motif/Consensus sequence	Residues					Motif = consensus	*In vitro* phosphorylation
S869 motif	**L**	**R**	**Q**	**P**	**S_{869}**	-	-
PKA consensus	-	R	X	X	S	YES	YES
PKC consensus	-	R	X	X	S	YES	NO
CaMKII consensus	X	R	X	X	S	YES	YES

4.3.1.1 Regulatory significance of S869 residue phosphorylation

Such direct and specific PKA-phosphorylation of the conserved S869 residue of the ZERO BK channel splice variant has distinct implications upon the molecular mechanism of splice variant regulation by the kinase. The data accumulated in this chapter proposes that following the *in vivo*, physiological, signal transduced elevation of intracellular cAMP that activates PKA (See Appendix A), target substrates including the conserved S869 residue of BK channels are phosphorylated. This specific catalysis is suggested to stimulate and underlie the cAMP-induced activation of heterologously expressed ZERO BK channel splice variant that has been observed previously [229]. This is proposed due to the lack of additional PKA phosphorylation consensus motifs in the ZERO splice variant and the increased S869 site phosphorylation that follows addition and stimulation of exogenous PKAc. Additionally, the block of cAMP-

mediated stimulation of heterologously expressed ZERO BK channels that has been described in previous mutagenesis studies and phosphorylation investigations of the equivalent motif of *Drosophila* BK channels [190, 202, 205, 229] suggests that this highly conserved PKA consensus motif may be phosphorylated in ZERO splice variant BK channels in other, even non-mammalian, species.

Phosphorylation of the conserved S869 residue in STREX BK channels

The determination of the conservation of the S869 site as a PKA phosphorylation target in STREX channels was observed *in vitro* with the ΔN-ΔC fusion proteins, and *in vivo* with the HA-tagged channels. In the presence of the STREX insert, S869 was phosphorylated consistently by PKA: *in vitro* ΔN-STREX-ΔC (Figure 4.16), *in vivo* STREX-HA (Figure 4.21). However, the distinct responses of the STREX and ZERO BK channel splice variants to PKA regulation; heterologously expressed ZERO channels are activated, STREX channels are inhibited [80, 229], implies that the STREX insert influences the functional effect of the kinase upon the channel through a molecular mechanism that is distinct from/additive to S869 residue phosphorylation.

Heterologous expression of STREX-insert expressing channels with alanine substitution of the S869 residue has demonstrated that such S869A mutation does not impinge upon the inhibitory effect of PKA on STREX BK channel activity [229]. This contrasts the equivalent S869A mutation of the ZERO channel where PKA-mediated stimulation of the splice variant is prevented by the substitution [229]. Thus, although the STREX channel S869 residue is phosphorylated by PKA *in vivo* (Figure 4.21), it appears that its

phosphorylation may not be necessary to the inhibitory effect of PKA upon STREX channels. Thus, the presence of the STREX insert does not appear to conformationally nor competitively inhibit the phosphorylation of the conserved S869 residue and thus, inhibition of S869 site phosphorylation does not underlie the differential responses of the STREX and ZERO BK channel splice variants *in vivo*.

4.3.2 Phosphorylation of the STREX insert S4 residue

The data presented in this thesis suggest that the S4 residue of the STREX insert sequence is a target of PKA phosphorylation *in vitro* and thus, a putative PKA phosphorylation target in the *in extenso* STREX channel *in vivo*. PKA phosphorylation of the site was determined with the STREX insert-expressing GST- and ΔN-ΔC fusion proteins via autoradiography and the use of phospho-specific antibodies to STREX S4 in combination with mutagenesis of the residue. As such, mutation of the residue by substitution with unphosphorylatable alanine inhibited *in vitro* PKA-phosphorylation of the STREX insert sequence of GST-S4A (Figures 4.6 & 4.7) and ΔN-S4A,S869A-ΔC[5] (Figures 4.15 & 4.17).

The 29 kDa GST-STREX proteolytic degradation product

Intriguingly, an artefact of the purification protocol that was initially undesired provided further evidence of the serine-4 site providing the phosphorylation target in GST-STREX. Preliminary characterisation of ~29 kDa proteolytic fragments observed following purification of GST-STREX and GST-S4A (Section 3.2.1.1.3) illustrated that

[5] The phosphorylation of the S869 site, which is mutated in this fusion protein also, is discussed in Section 4.3.1.

these proteins encompassed the GST tag, or at least the epitope to the α-GST antibody, yet running slightly higher than the 28 kDa GST protein, were not contamination from the fusion tag. The lack of α-STREX-1 immunoreactivity, whose epitope is located between residues 27-43 of the insert sequence (Table 2.4 & See Figure 1.6), demonstrated that the fragments did not comprise the STREX insert sequence in its entirety (Figure 3.5). However, the immunoreactivity of α-STREX to the ~29 kDa proteins suggests that they encompass the region at the N-terminal of the STREX insert sequence, at least up to the α-STREX epitope, residue 9, as illustrated in Figure 4.23. Investigation of the STREX insert sequence uncovers several putative protease target sites that may be incised including trypsin and chymotrypsin recognition sites. Thus, proteolytic degradation may have occurred even with the anti-proteolytic measures used; the array of protease inhibitors used in the purification, the choice of *E.coli* strain for expression, and controlled temperatures for protein induction and purification. The differential immunoreactivity of α-STREX and α-STREX-1 to the ~29 kDa fragments implicates a fragmentation point between their epitopes. However, additional proteolytic cleavage targets may be present within the GST-fusion tag sequence, prior to the epitope of the α-GST antibody. Although the absence of proteolytic fragments of the control GST protein does argue against this, as mentioned previously, the creation of a fusion protein can influence the structure of the tag and, therefore, conformational alterations that render protease targets that are inaccessible in GST available within the fusion protein are possible.

The phosphorylation of the ~29 kDa proteolytic fragment was apparent by autoradiography and Western blot analyses (Figures 4.6 & 4.7). As its immunocharacterisation demonstrates that it encompasses the residues at the beginning of the STREX motif near the GST:STREX interface only, these residues are implicated as phosphorylation targets of PKAc. Serine-4 at the start of the STREX insert sequence is, therefore, a prime candidate for PKA phosphorylation, reiterating the autoradiographic mutagenesis results and validating the use of the α-phospho-STREX antibody with this fusion protein.

Assessment of STREX S4 phosphorylation

Indeed, use of the α-phospho-STREX antibody confirmed *in vitro* PKA-phosphorylation of the STREX S4 residue in the ΔN-STREX-ΔC and ΔN-STREX,S869A-ΔC fusion proteins (Figure 4.17) as well as in the ~35 kDa full-length GST-STREX (Figure 4.7B) and its ~29 kDa proteolytic fragment (Figure 4.7A). Although the specificity of the antibody with the full-length channel HA-fusion proteins was not sufficient to enable assessment of the phosphorylation state of the site *in vivo*, the *in vitro* results suggest that the site is likely to function as a PKA phosphorylation target in native, *in vivo* STREX channels. Future investigations may be able to confirm this, but the proposition of STREX S4 site phosphorylation produces a possible mechanism for the distinct inhibition of STREX BK channel activity by PKA.

Figure 4.23
Characterisation of the ~29 kDa proteolytic fragment of the GST-STREX fusion proteins

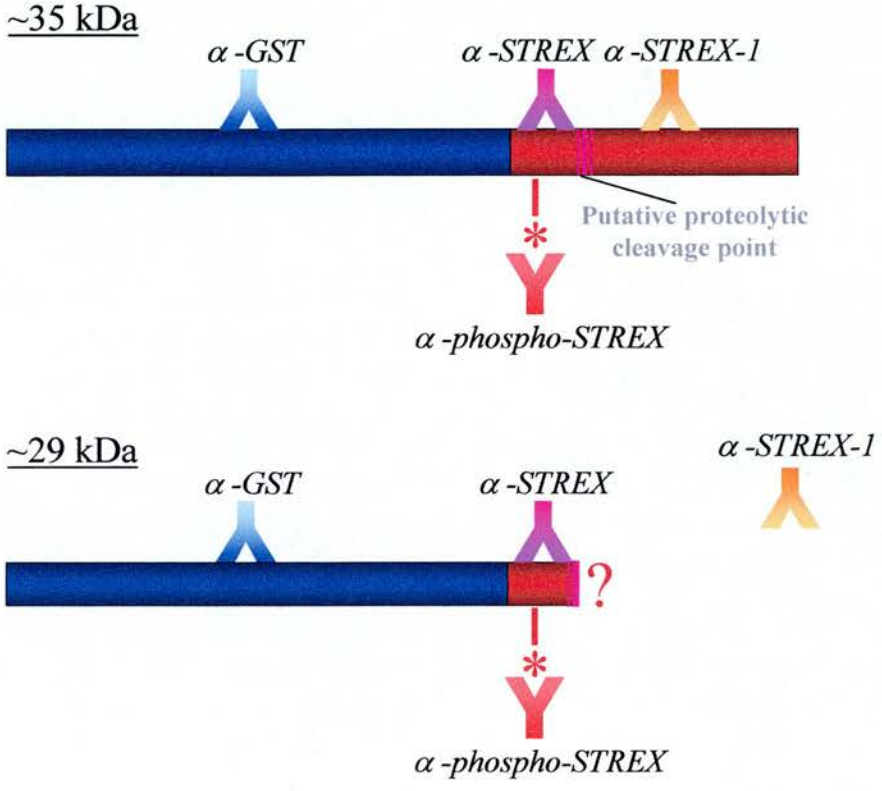

Figure 4.23: Diagrammatic representation of the proposed character of the ~29 kDa proteolytic fragment of the GST-STREX fusion proteins. The α-GST and α-STREX antibodies detect proteins of ~35 and ~29 kDa, whereas α-STREX-1 detects full-length ~35 kDa fusion proteins only. The approximate locations of the respective antibody epitopes are illustrated (Epitopes: α-STREX-1; STREX insert residues 27-43 & α-STREX; 5 residues pre-STREX to STREX insert residue 9: See Table 2.4). The positions suggest that a single proteolytic cleavage occurs at a point following the phosphorylatable STREX S4, producing the ~29 kDa protein. However, the STREX sequence contains several putative proteolytic fracture points as does GST and thus, several proteolytic degradation products are possible.

Specificity of STREX S4 phosphorylation

In vitro phosphorylation assays using the GST-STREX and ΔN-ΔC fusion proteins determined that the STREX S4 site could be phosphorylated by PKA or PKC but not CaMKII *in vitro*. The alignment of the PKC consensus sequence is sufficient to enable the kinase to target and phosphorylate the site successfully, perhaps due to the inclusion of the lysine residue (Scheme 4.3). On the other hand, the specificity of CaMKII is such that the kinase cannot phosphorylate STREX S4. Thus, similarly to the conserved S869 residue, STREX S4 may function as a phosphorylation target following the activation of multiple, distinct serine/threonine protein kinases. The influence of various protein kinases upon STREX BK channel regulation and particularly, STREX S4 site phosphorylation will be an interesting area of future investigation.

Scheme 4.3: Alignment of the STREX insert S4 motif with protein kinase consensus sequences
(Although several possible consensus sequences are suitable for phosphorylation by the kinases (See Table 1.1), only the consensus sequence with the greatest alignment to the motif is shown). Green residues = alignment. Red residues = non-alignment. Standard one letter amino acid code used.

Motif/Consensus sequence	**Residues**						**Motif = consensus**	***In vitro* phosphorylation**
STREX S4 motif	**R**	**R**	**P**	**K**	**M**	**S_4**	-	-
PKA consensus	-	-	-	K	M	S	YES	YES
PKC consensus	-	-	R	K	X	S	YES	YES
CaMKII consensus	-	X	R	X	X	S	NO	NO

Additional PKA consensus motifs created by STREX insertion

Analysis of the protein sequence of the STREX BK channel splice variants uncovers several putative PKA consensus motifs in addition to the conserved S869 and STREX S4 residues that may be *in vivo* phosphorylation targets of the kinase. Mutation of S869 and STREX S4 in the ΔN-S4A,S869A-ΔC and S4A,S869A-HA fusion proteins prevented radiolabelled phosphate incorporation within the limits of detection following *in vitro* phosphorylation and autoradiographic detection (Figures 4.14 & 4.20). Although mutagenesis may have altered the protein structure as to make additional consensus motifs inaccessible to phosphorylation the similar conformation of the substitution makes this unlikely (Discussed Section 4.1.2). Thus, the data suggest that these sites are the only residues in the STREX channel phosphorylated by PKA *in vivo*.

4.3.2.1 Regulatory significance of STREX insert S4 residue phosphorylation

The phosphorylation of the STREX insert S4 residue by PKA is therefore proposed to underlie the inhibitory effect of the kinase upon activity of the STREX BK channel splice variant. By the insertion of this additional phosphorylation consensus motif in STREX splice variants compared to the ZERO channels, the influence of PKA upon channel activity is altered leading to inhibition instead of the stimulatory effect of PKA upon ZERO splice variants.

The results presented in this study suggest that PKA phosphorylation of the STREX insert S4 residue is critical to the differential regulation of the splice variant by the kinase, and that this phosphorylation must functionally dominate that of the conserved

S869 site. The STREX S4 residue is common to all mammalian BK channel STREX splice variants and previous studies on the rat STREX BK channel demonstrated that PKA-inhibition is conserved [251]. Thus, phosphorylation of the STREX S4 site by PKA may be a common regulatory mechanism that is conserved throughout all such mammalian channels and not specific to the murine system. Future investigations of STREX splice variants from other species will be required to confirm this assumption.

4.4 Chapter Summary

This chapter has investigated the phosphorylation of BK channel splice variants by PKA and has characterised the conserved S869 site and the STREX insert S4 residue as targets of PKA *in vitro*. Radiolabelled phosphate incorporation and Western blot analyses demonstrated that the S869 residue is a PKA phosphorylation target *in vitro* and in *vivo*, with its phosphorylation most likely underlying the stimulatory effect of PKA on ZERO BK channels. The residue may act as a phosphorylation motif for CaMKII also, but not for PKC, and its PKA-phosphorylation is conserved in STREX channels. However, the co-phosphorylation and suggested functional dominance of the STREX insert S4 residue is proposed to confer the distinct inhibitory action of PKA on STREX channel activity *in vivo*. Additionally, STREX S4 may be phosphorylated by PKC, but not by CaMKII.

Chapter Five:

The BK Channel Complex

Chapter Five:

The BK Channel Complex

5.1 Introduction

5.1.1 The Ion Channel Complex

5.1.1.1 Accessory proteins

Accessory proteins, distinct from the pore-forming subunits, are critical to the physiological effectiveness of ion channel regulation. These include channel specific subunits, such as the BK channel β-subunit, and multi-targeted enzymes, including protein kinases and protein phosphatases, which influence ion channel regulation by altering channel properties including gating, calcium sensitivity and open probability (See Section 1.5). Stimulation of signal transduction pathways may regulate such accessory proteins in order to induce the appropriate physiological response through the pore-forming subunit. Thus, the accessibility and proximity of accessory proteins to their target ion channel is crucial to the efficiency and effectiveness of ion channel function. Indeed, the regulatory effects of phosphorylation continue to occur following reconstitution of BK channels into artificial lipid bilayers where no exogenous protein kinase or protein phosphatase is applied [193, 204]. This suggests a close association of such regulatory enzymes with the ion channel reiterated by the observation of direct association of the catalytic subunit of protein kinase A (PKAc) with the *Drosophila* BK channel α-subunit [142, 204]. This suggests that a regulatory complex where the BK channel α-subunit functions as a "scaffold" to various regulatory accessory proteins may

exist, facilitating the dynamic regulation of BK channel function [142, 194, 204]. Therefore, this chapter aims to determine whether PKAc associates with the mammalian BK channel α-subunit contributing to a regulatory ion channel complex, and to investigate the nature and character of such an association.

5.1.1.2 Splice variation

The differential regulation of the STREX and ZERO BK channel splice variants by PKA was hypothesised to be due to distinct PKA phosphorylation consensus motifs (Chapter 4), or differences in the association of PKA with the two variants (See Chapter 1). Comprising 58 residues, the STREX insert is of substantial length and encompasses several residues including prolines, cysteines, aromatic and charged amino acids (See Figure 1.6), that impose conformational constraints upon proteins; proline due to its cyclic pyrrolidine side chains, aromatic residues due to their bulk, and cysteines due to their ability to form disulphide bridges. Charged residues may influence local or general charge and thus influence associations of channel regions or other related proteins. Therefore, the presence of the insert may influence the structure and associations of the STREX α-subunit C-terminal region conformationally or electrostatically making it different to that of the ZERO variant. Consequently, binding sites for protein kinases or associated proteins involved in phosphorylation-mediated regulation of the channel may be distinct to each splice variant. The STREX insert itself may occlude a protein-docking site employed in the ZERO variant or produce an additional binding site resulting in the differential regulation of the two splice variants to PKA. Therefore, to

determine whether PKAc association with the BK channel is influenced by STREX insertion, co-immunoprecipitation of PKAc with the STREX and ZERO –HA-tagged proteins was compared. Encompassing the STREX insert sequence in isolation (See Figure 3.1) the GST-STREX fusion protein was used to assess whether the STREX insert itself could function as a PKAc binding site. The longer ΔN-STREX-ΔC and ΔN-ZERO-ΔC fusion proteins of the C-terminal tail region (See Figure 3.1) were employed to determine if the possible association of the kinase with this region is influenced by splicing.

5.1.1.3 Leucine zippers

Leucine zippers are a common motif constituting a repeating sequence where every seventh residue is a leucine or isoleucine [218, 326]. Originally characterised in DNA-regulatory proteins such as transcription factors and proto-oncogene products, the motif is known to enable protein dimerisation inducing the formation of a protein α-helical structure that "clasps" the DNA double helix to exert transcriptional control [214, 218, 327-330]. The efficiency and effectiveness of this interaction is well documented and recently the exploitation of the motif in forming protein-protein interactions between non-DNA binding proteins has been advocated [318]. Indeed, recently several ion channels have been proposed to assemble with regulatory complexes via leucine zipper interactions [331, 332].

Sequence analysis of the BK channel α-subunit identifies two putative leucine zippers; one proximal to the tetramerisation domain at the transmembrane-cytoplasmic C-terminal domain interface, leucine zipper 1, and the second between the S869 phosphorylation site and the putative S10 α-helix, leucine zipper 2, as shown in Figure 3.1. To determine whether these motifs are involved in the association of PKAc with the BK channel protein, the association of the kinase with the ΔN-ΔC fusion proteins that encompass the leucine zipper 2 motif was investigated. The putative influence of leucine zipper 1 was investigated by the study of competing peptides equivalent to the LZ1 sequence upon the association of the kinase with STREX-HA channels. Further to this, the effect of leucine zipper 1 mutation upon channel-PKAc association was investigated via co-immunoprecipitation assays using the mLZ1-HA channel (See Figure 3.13), as well as implementation of the Thio-LZ1 and Thio-mLZ1 fusion proteins that express the motif sequence in isolation (See Figure 3.7). Thus, the characterisation of the association of PKAc with the BK channel protein was studied.

5.1.2 Heteromultimerisation

Although using a distinct conserved RCK domain to assemble multimers (See Section 1.3.2.2.3), BK channels form functional ion channel pores by the tetramerisation of α-subunits in common with other members of the Kv channel superfamily. Rather than forming only homomultimers composed of four identical α-subunits, several examples of members of the Kv channel family forming functional heteromultimeric tetramers within their subfamily have been described ([150-154] Reviewed: [2,3,155]). Subtle

differences between the regulatory and functional properties of heteromultimeric channels and their homomultimeric counterparts increases the functional diversity of an ion channel subfamily and may be invaluable in situations such as the cochlea where slight differences in channel properties may be essential to their physiological role. Previous electrophysiological investigations have described heterologous expression of STREX and ZERO BK channel splice variants [84, 89, 229]. However, in the native system both variants may be co-expressed in the same cell. To examine if heteromultimerisation occurs *in vivo*, preliminary analysis was performed by the heterologous co-expression and assessment of co-immunoprecipitation of STREX and ZERO channels with different epitope tags (Section 5.2.2).

5.1.3 Affinity pull-down techniques

Protein-protein associations, between PKAc and channel proteins and between distinct BK channel α-subunit splice variants, were performed by biochemical affinity pull-down or co-immunoprecipitation assays. These techniques involve the immobilisation of the protein of interest to an insoluble matrix, achieved by the binding of antibodies directed against the protein of interest to protein-G-sepharose as co-immunoprecipitation assays, or binding of GST-STREX to glutathione sepharose for biochemical affinity pull-down assessment of the fusion protein. Thus, following incubation of the protein of interest with a protein solution, unbound proteins can be washed from the matrix whilst those associating with the protein of interest are bridged to the matrix and therefore, can be isolated by extracting the matrix or by altering binding conditions to remove the

associating proteins (See Figure 2.2). The resulting eluate or immunoprecipitation can then be assessed by Western blot analysis to determine the presence, or indeed the absence, of a particular associating protein.

Therefore, the aim of this chapter is to investigate the BK channel complex by affinity pull-down and co-immunoprecipitation techniques to attempt to characterise the association of PKAc with the BK channel α-subunit, and to determine whether BK channels may form heteromultimeric channels of STREX and ZERO splice variants.

5.2 Results

5.2.1 PKAc interaction with BK channels

Investigation of the interaction of the catalytic subunit of protein kinase A with splice variants of the BK channel was performed initially using full-length, HA-tagged channels to determine if interaction occurs *in vivo*, then with the bacterially-expressed fusion proteins to characterise the region and mode of the kinase association with the ion channel.

5.2.1.1 PKAc interaction with HA-tagged BK channels

Stable cell lines of STREX-HA and ZERO-HA splice variants and the mutant S4A-S869A-HA channel (described in Section 3.2.2) were transfected with PKAc or the catalytically inactive PKAc-K72E mutant to ensure an excess of free catalytic subunit

(Section 2.6.2). Controls of untranfected HEK293 cells and the cell line transfected with excess PKAc were performed in parallel, in addition to controls of HEK293-expressed mLZ-HA (Discussed Section 5.2.1.4.2) and the voltage-gated Kv1.4-HA channel, that is structurally analogous to BK channels through the central pore-forming domain (See Section 1.3.2.1). As described in Section 2.6.3, cultures were harvested and the whole cell lysate halved for immunoprecipitation by α-HA or α-PKAc antibodies. Samples of whole cell lysate and immunoprecipitations were analysed by Western blotting probing for HA-tagged channels and free PKAc. A representative assay is illustrated in Figures 5.1, 5.2 & 5.3.

HEK293 cells do not express endogenous HA-tagged protein, but express PKAc in sufficient quantities to enable its detection by immunoblotting. Although co-immunoprecipitation of this endogenous PKAc with the channels occurred (Figure 5.1), levels were near to the limit of detection. This may be due to the high level of channel over-expression in comparison with endogenous PKAc expression and may reflect the proportion of PKAc bound to the channel with respect to PKAc in complex with other proteins and regulatory components. Thus, to increase the overall concentration of free PKAc and thus facilitate detection of channel-kinase co-immunoprecipitation, further analyses were performed with HEK293 cells transfected with excess PKAc. As such, the –HA-tagged channels and PKAc/PKAc-K72E were detected in the whole cell lysates demonstrating successful expression of the proteins (Figures 5.1, 5.2 & 5.3).

Figure 5.1

Co-immunoprecipitation of BK channels with PKAc: Immunoprecipitation by α-HA

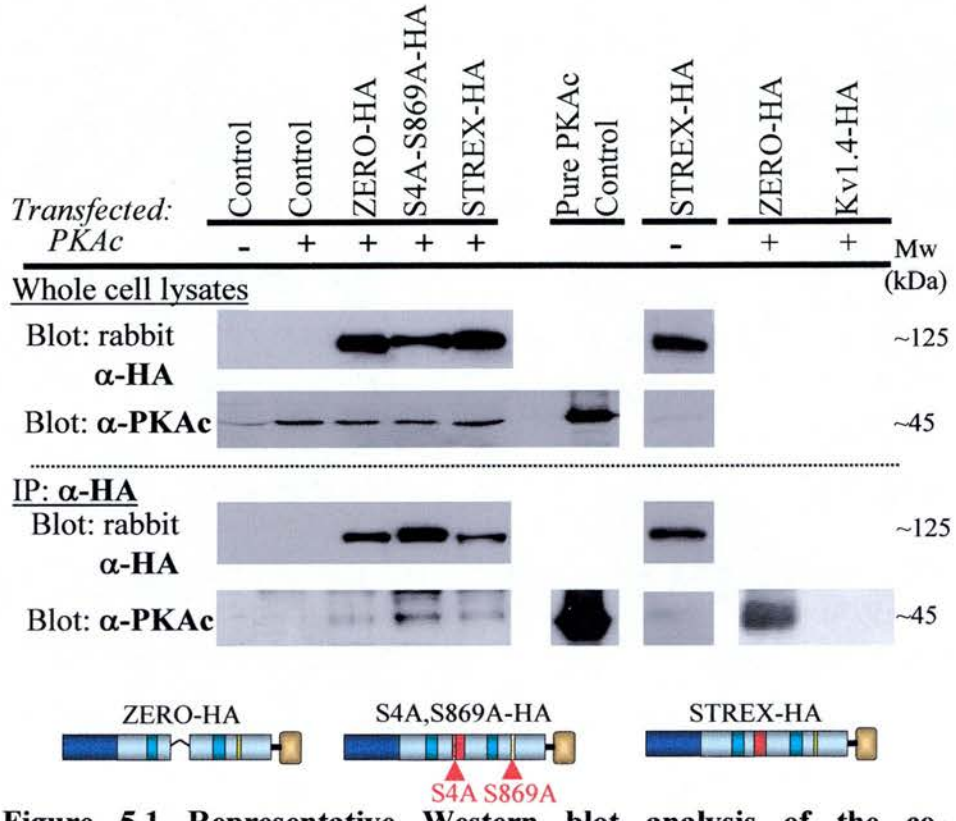

Figure 5.1 Representative Western blot analysis of the co-immunoprecipitation of HA-tagged BK channel splice variants with PKAc. Stable cell lines of ZERO-HA, S4A-S869A-HA, STREX-HA BK channel variants (illustrated below blots, See Figure 3.13) and control Kv1.4-HA channels were transfected with excess free PKAc and immunoprecipitated (IP) by α-HA antibody. HEK293 cell controls were run in parallel. HA-tagged BK channels and PKAc, detected in whole cell lysates, co-immunoprecipitated. PKAc did not co-immunoprecipitate with Kv1.4-HA* and did not pull down non-specifically with α-HA IP of HEK293 cells. Western blot analysis: sheep α-PKAc 1/5000, rabbit α-HA 1/333, α-sheep-HRP 1/2000, α-rabbit-HRP 1/2000, ECL detection.

*Kv1.4-HA data provided by Irwin Levitan and Yi Zhou. Channels were successfully immunoprecipitated and channels & PKAc detected in whole cell lysate (Results not shown).

Figure 5.2
Co-immunoprecipitation of BK channels with PKAc: Immunoprecipitation by α-PKAc

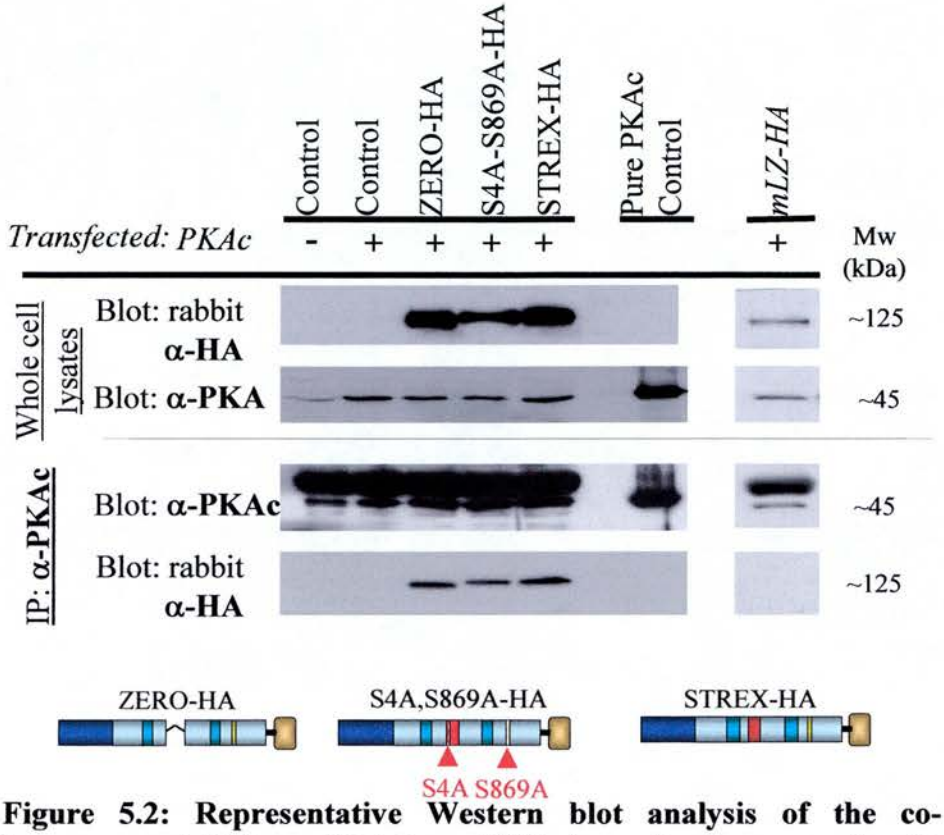

Figure 5.2: Representative Western blot analysis of the co-immunoprecipitation of HA-tagged BK channel splice variants with PKAc. Stable cell lines of ZERO-HA, S4A-S869A-HA, STREX-HA BK channel variants (illustrated below blots, See Figure 3.13) and control mLZ-HA potassium channels (See Figure 5.10) were transfected with excess free PKAc and immunoprecipitated (IP) by α-PKAc antibody. HEK293 cell controls were run in parallel. HA-tagged BK channels and PKAc, detected in whole cell lysates, co-immunoprecipitated. Control mLZ-HA channels did not co-immunoprecipitate with PKAc. Western blot analysis: sheep α-PKAc 1/5000, rabbit α-HA 1/333, α-sheep-HRP 1/2000, α-rabbit-HRP 1/2000, ECL detection.

Figure 5.3

Co-immunoprecipitation of the STREX-HA channel with the catalytically-inactive PKAc mutant, PKAc-K72E

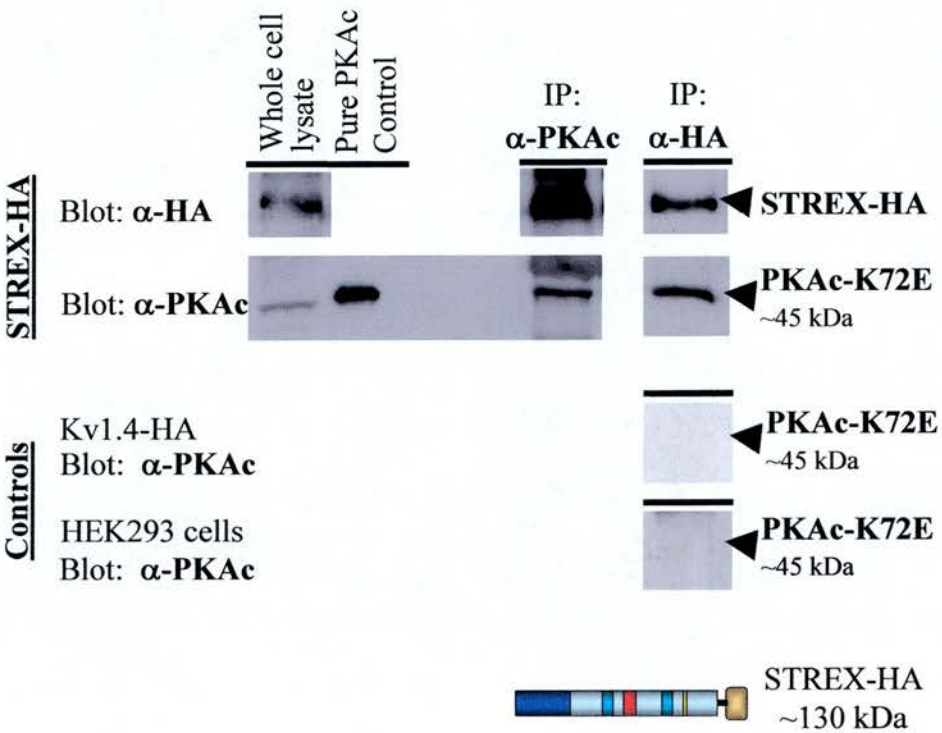

Figure 5.3: Western blot analysis of co-immunoprecipitation assays of STREX-HA with the catalytically inactive PKAc-K72E. Whole cell lysates from STREX-HA stable cell lines (illustrated below blots, See Figure 3.13) and control Kv1.4-HA channels, transfected with excess free, mutant PKAc-K72E were immunoprecipitated (IP) by either α-PKAc or α-HA. HEK293 cell controls were run in parallel. STREX-HA channels and PKAc-K72E, detected in lysates, co-IP together by α-PKAc and α-HA IP. PKAc did not co-IP with Kv1.4-HA and did not pull down with α-HA IP of HEK293 cells. Western blot analysis: sheep α-PKAc 1/5000, rabbit α-HA 1/333, α-sheep-HRP 1/2000, α-rabbit-HRP 1/2000, detection by ECL.

Immunoprecipitation by α-HA pulled down all types of –HA-tagged channel and co-immunoprecipitation of PKAc is observed with the BK channel variants, STREX-HA, ZERO-HA and S4A-S869A-HA (Figure 5.1). Reciprocal co-immunoprecipitation of the –HA-tagged BK channels occurred when the α-PKAc antibody is used to pull down PKAc from the cellular lysate (Figure 5.2), and no difference is detected where PKAc-K72E is transfected in place of PKAc (Figure 5.3). Immunoprecipitation by α-HA did not pull down PKAc in the absence of the BK channels (Figure 5.1), nor was co-immunoprecipitation observed with the control channels, Kv1.4-HA and mLZ-HA (See Section 5.2.1.4.2) (Figures 5.1 & 5.2). This indicates that non-specific associations with the PGS, the antibodies, the HA-tag, or another associating protein do not occur under the immunoprecipitation conditions, and that co-immunoprecipitation is specific and not due to the over-expression of non-HEK293 cell-native potassium channels. Thus, this suggests that the STREX and ZERO BK channels may associate with PKAc *in vivo* and that this association does not depend upon the phosphorylation of the channel protein at sites identified in Chapter 4, as illustrated by the S4A-S869A-HA channel, or the catalytic competence of the kinase, as suggested by the PKAc-K72E mutant.

5.2.1.2 PKAc interaction with the GST-STREX fusion protein

Investigation of association between PKAc and the STREX insert was performed using the GST-STREX fusion protein described in Section 3.2.1.1. GST-STREX was retained bound to glutathione-sepharose matrix and incubated with purified PKAc, HEK293 cell lysate or rat brain lysate in affinity pull-down assays with control, GST protein, assays

Figure 5.4

Affinity pull-down assays of GST-STREX fusion protein: assessment of PKAc association

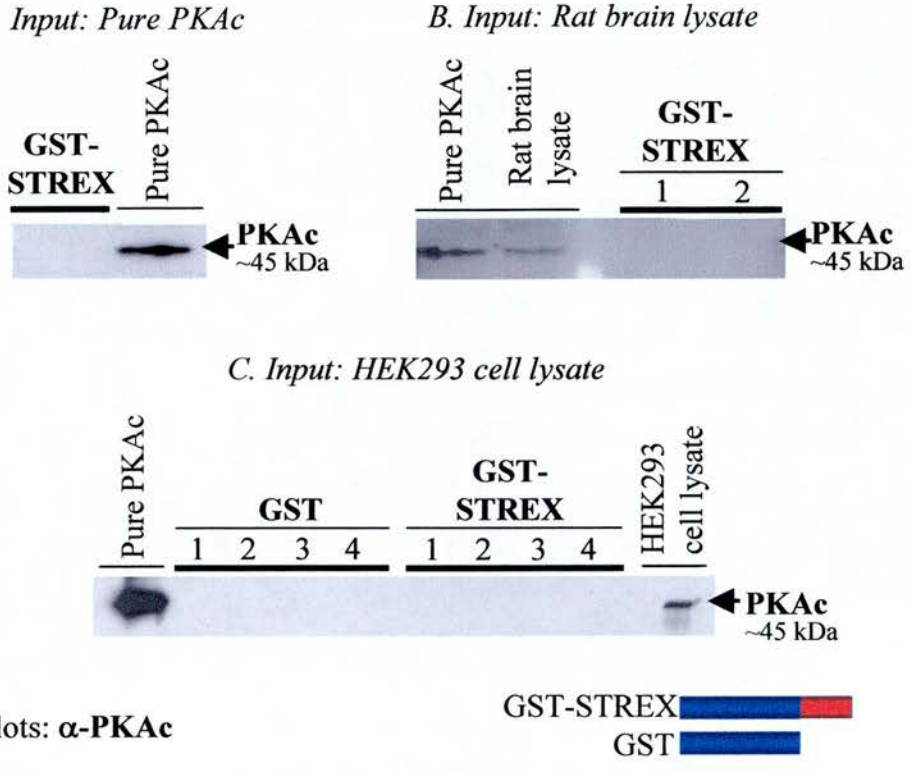

Figure 5.4: GST-STREX affinity pull-down assays with analysis of PKAc association. GST-STREX and control GST protein (illustrated below the blots, see Figure 3.2) bound to glutathione-sepharose matrices were incubated with purified PKAc (**A**), rat brain lysate (**B**), or HEK293 cell lysate (**C**) in affinity pull-down assays. Proteins with affinity for GST-STREX or GST were eluted by high salt buffer and the presence of PKAc analysed by Western blotting. Numbering 1-4 indicates separate elutions. No association of the kinase with the GST-STREX fusion protein was observed. The binding of GST-STREX/GST to the matrix was confirmed by Coomassie staining of matrix samples as illustrated in Figure 3.3. Western blot analysis: sheep α-PKAc 1/5000, α-sheep-HRP 1/2000, detection by ECL.

Figure 5.5

Affinity pull-down assays of GST-STREX fusion protein: assessment of total bound protein

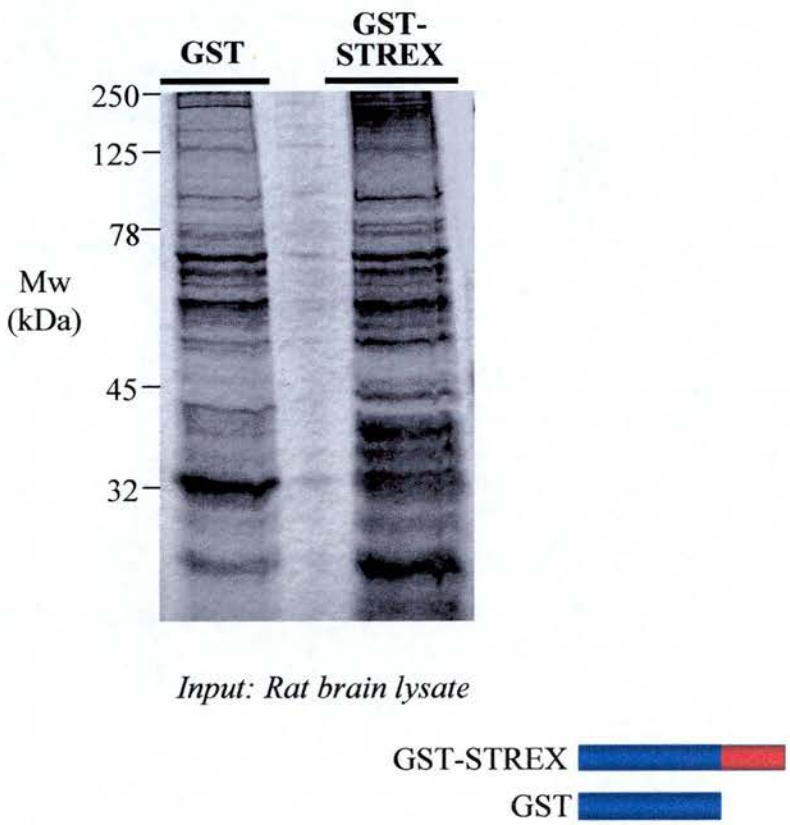

Figure 5.5: Silver stain analysis of affinity pull-down assay of rat brain proteins bound to GST-STREX. GST-STREX and control GST protein (illustrated below the gel, see Figure 3.2) bound to glutathione-sepharose matrices were incubated with rat brain lysate in affinity pull-down assays. Proteins with affinity for GST-STREX or GST were eluted by high salt buffer and analysed by Silver staining. Several proteins associated with GST and GST-STREX. Some proteins appear to have affinity for GST-STREX and not the control GST. These have yet to be identified. The binding of GST-STREX/GST to the matrix was confirmed by Coomassie staining of matrix samples as illustrated in Figure 3.3.

performed in parallel (Section 2.9.2). Proteins bound to the GST-STREX or GST were eluted by a high salt buffer, concentrated, separated by electrophoresis on Tris-Glycine gels and analysed by Silver staining and by Western blotting to investigate the association of PKAc (Sections 2.7.1 and 2.7.2). The analyses of such assays are illustrated in Figure 5.4 with a Silver stain demonstrating the resultant affinity pull-down of proteins from rat brain lysate shown in Figure 5.5.

GST-STREX did not associate with purified PKAc or PKAc from HEK293 cell or rat brain lysates (Figure 5.4). Although the kinase did not associate, other proteins did and were detected by Silver stain analysis (Figure 5.5). Characterisation of these proteins is yet to be performed although their presence indicates that the assay conditions are favourable for protein-protein interactions.

5.2.1.3 PKAc interaction with the ΔN-ΔC fusion proteins

The ΔN-ΔC recombinant fusion proteins encompass a region of the C-terminal domain of the BK channel that spans the splice site two region, the location of the STREX insert, and the putative leucine zipper 2 motif as illustrated in Section 3.2.1.2. To determine if PKAc association with the channel occurs via this region, ΔN-ZERO-ΔC and ΔN-STREX-ΔC fusion proteins immunoprecipitated by the α-V5 antibody were incubated with purified PKAc or rat brain lysate (As Section 2.9.3). Equivalent treatment of control thioredoxin-V5-H_6 was performed in parallel. Immunoprecipitations were separated by electrophoresis and analysed by Colloidal stain

Figure 5.6

Co-immunoprecipitation assays of ΔN-ΔC fusion proteins: assessment of PKAc association

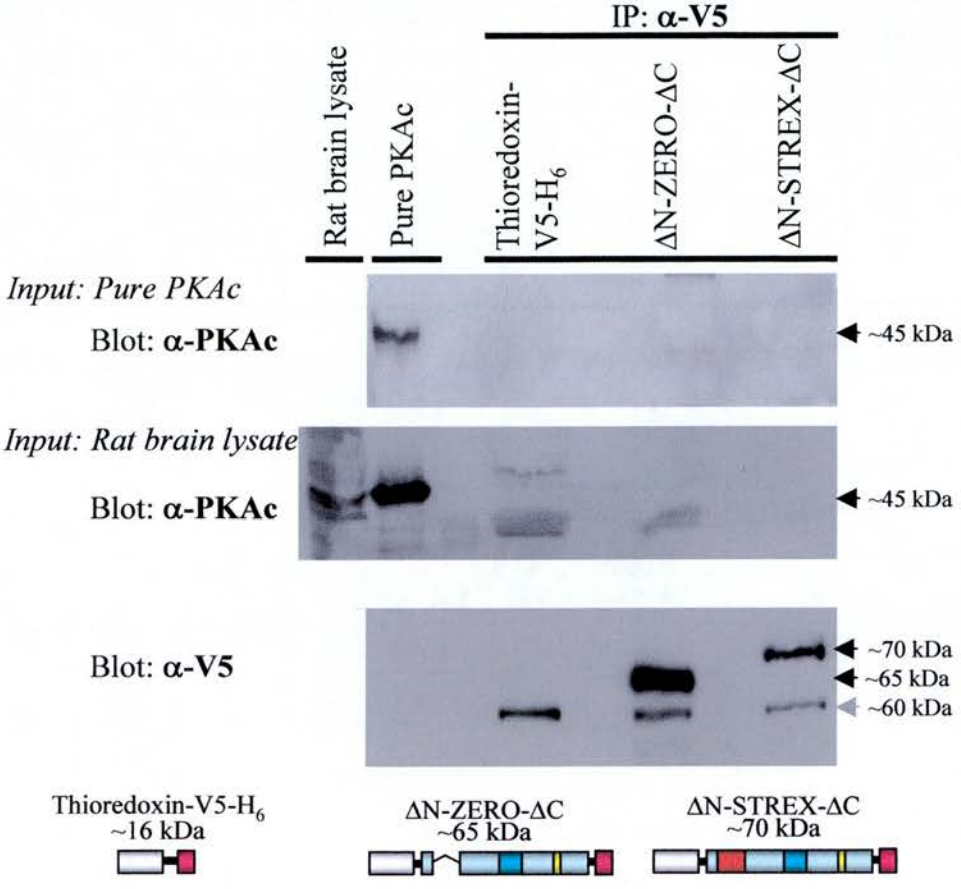

Figure 5.6: ΔN-ΔC fusion protein co-immunoprecipitation assays with analysis of PKAc association. ΔN-ZERO-ΔC, ΔN-STREX-ΔC and control Thioredoxin-V5-H_6 (illustrated below the blots, see Figure 3.7) were immunoprecipitated (IP) by α-V5/protein-G-sepharose and incubated with purified PKAc or rat brain lysate. The co-immunoprecipitation of PKAc was analysed by Western blotting. No association of the kinase with the ΔN-ΔC fusion proteins was observed. ΔN-ZERO-ΔC and ΔN-STREX-ΔC were detected at the appropriate molecular weights (~65 & ~70 kDa respectively). Western blot analysis: sheep α-PKAc 1/5000, mouse α-V5 1/5000, α-sheep-HRP 1/2000, α-mouse-HRP 1/2000 detection by ECL.

Figure 5.7

Co-immunoprecipitation assay of ΔN-STREX-ΔC fusion protein: interaction with rat brain proteins

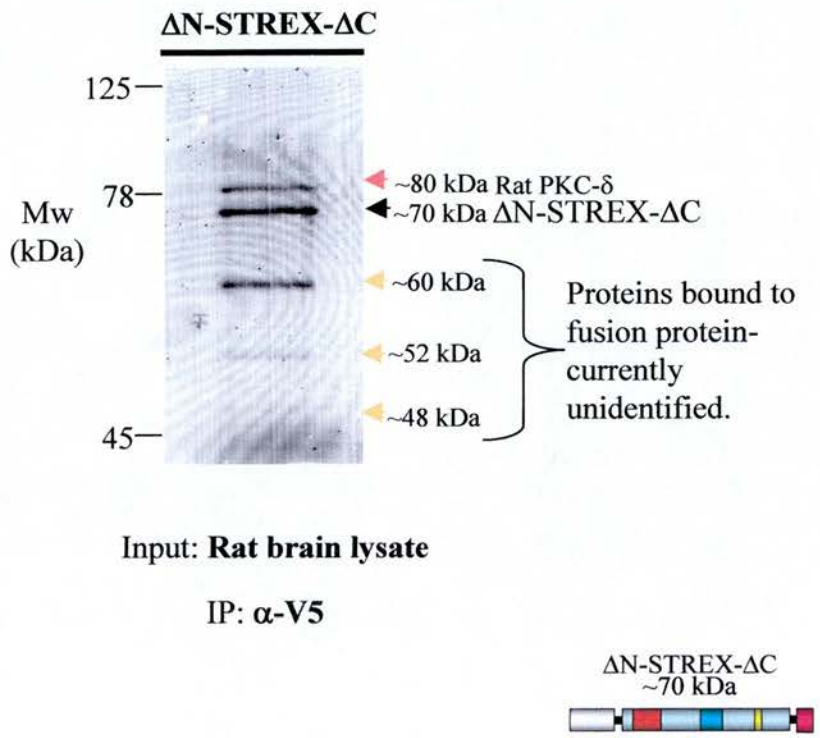

Figure 5.7: Colloidal stain analysis of affinity pull-down assay of rat brain proteins bound to ΔN-STREX-ΔC. Immunoprecipitated by α-V5 antibody, ΔN-STREX-ΔC (illustrated below the gel, see Figure 3.7) was incubated with rat brain lysate. Proteins with affinity for the fusion protein were analysed by Colloidal blue staining. Several proteins were associated with ΔN-STREX-ΔC one of which, at ~80 kDa, was identified as rat PKC-δ, a protein that is known to associate with thioredoxin, the C-terminal tag of the fusion protein [333].

and Western blotting to determine PKAc association (As Sections 2.7.1 & 2.7.2). Such an analysis is illustrated in Figures 5.6 & 5.7.

Figure 5.6 illustrates that ΔN-ZERO-ΔC and ΔN-STREX-ΔC were successfully immunoprecipitated by the α-V5 antibody but PKAc did not bind to the fusion proteins under the assay conditions. Although PKAc did not associate other proteins did as observed following Colloidal blue staining of the total protein eluted (Figure 5.7). Mass spectrometry has identified one of these as PKCδ, a protein known to associate with thioredoxin [333], indicating that the assay conditions are favourable for protein-protein interactions.

5.2.1.4 PKAc interaction with leucine zipper 1

As the ΔN-ΔC affinity pull-down analysis suggested that this region of the C-terminal tail domain was not involved in the association of PKAc with the BK channel protein, other regions of the C-terminal were investigated. This led to the identification and subsequent investigation of the leucine zipper 1 motif by use of competing peptides to the leucine zipper 1 motif, -HA-tagged STREX channels with a mutated leucine zipper 1 sequence, and the Thio-LZ1 fusion proteins that express the region in isolation from the remainder of the channel sequence.

5.2.1.4.1 Competing peptides of the leucine zipper motif

Investigation of the putative role of the BK channel leucine zipper 1 motif in PKAc – BK channel association was initiated by the application of competing peptides generated to mimic the leucine zipper 1 sequence as to inhibit protein-protein interactions that occur via the motif (Table 2.5). The mutant peptide, mLZ1, is ineffectual as a leucine zipper motif as two leucines of the heptad repeat sequence were mutated to alanine (Table 2.5). The influence of the peptides upon the co-immunoprecipitation of PKAc and the STREX-HA channel was investigated by incubation of the peptides throughout immunoprecipitation by the α-HA antibody (Section 2.9.3.1). A representative Western blot analysis of such an assay is illustrated in Figure 5.8.

STREX-HA channel and PKAc were detected in whole cell lysate from PKAc-transfected STREX-HA-expressing HEK293 cells and were successfully co-immunoprecipitated in the absence of competing peptide (Figure 5.8) as observed previously (Figure 5.1). Inclusion of mLZ1 peptide in the immunoprecipitation demonstrated levels of channel pull-down and PKAc co-immunoprecipitation comparable to that in the absence of peptide. Addition of LZ1 peptide to immunoprecipitations maintained equivalent levels of channel pull-down but depleted the apparent quantity of PKAc co-immunoprecipitation suggesting that the intact peptide is inhibitory to the PKAc-BK channel association.

Figure 5.8

Co-immunoprecipitation of PKAc with STREX-HA: inhibition by leucine zipper 1 motif competing peptides

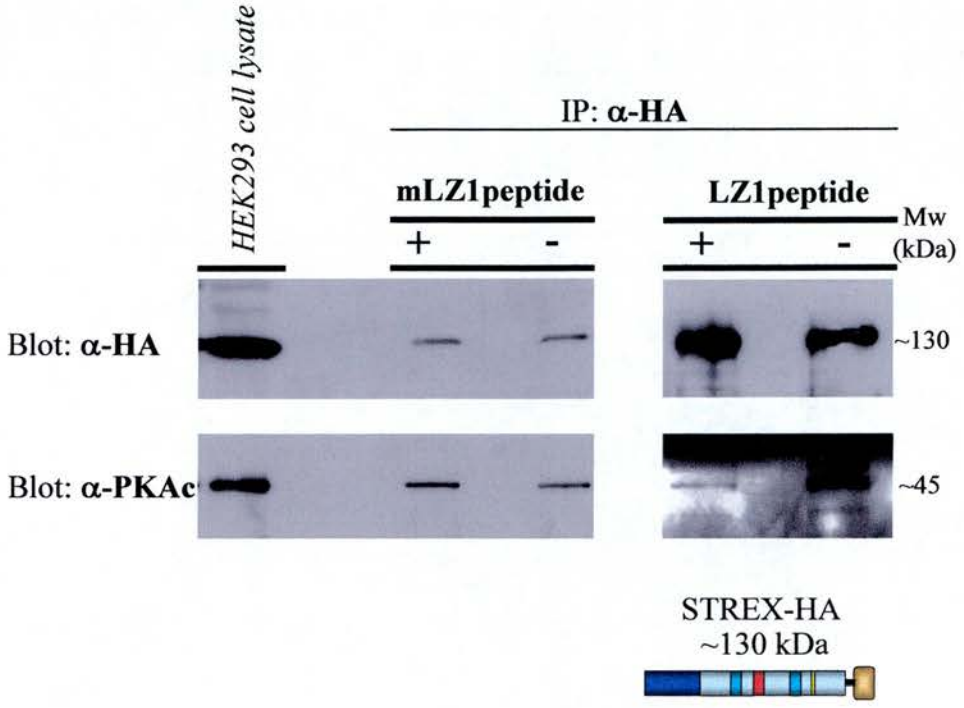

Figure 5.8: Representative Western blot comparison of the co-immunoprecipitation of STREX-HA with PKAc in the presence of of leucine zipper 1 competing peptides. STREX-HA stable cell line (illustrated below blots, See Figure 3.13) transfected with excess free PKAc was immunoprecipitated (IP) by α-HA in the presence (+) or absence (-) of the LZ1 competing peptide or alanine mutant, mLZ1. IPs were separated by electrophoresis and analysed by Western blotting. STREX-HA (~130 kDa) and PKAc (~45 kDa) were detected in HEK293 cell lysate and co-IP observed in the absence of peptide and in the presence of mLZ. Inclusion of competing LZ1 depletes the apparent quantity of PKAc pulled down with STREX-HA. Western blot analysis: sheep α-PKAc 1/5000, rabbit α-HA 1/333, α-sheep-HRP 1/2000, α-rabbit-HRP 1/2000, ECL detection.

The LZ1 peptide mimics the leucine zipper 1 motif but has little homology to other regions of the protein sequence with the exception of the putative LZ2 motif (See Figure 1.3 & Appendix B). To investigate the specificity of the LZ1 peptide for the LZ1 motif, peptides to the LZ2 sequence were applied in equivalent co-immunoprecipitation analyses by Dr Lijun Tian (Results not shown). No inhibition of the PKAc-BK channel association was observed suggesting that the specificity of the peptides to their respective motifs is exclusive and reiterates the inability of the leucine zipper 2-encompassing ΔN-ΔC fusion proteins to associate with PKAc (See Section 5.2.1.3). This demonstrates that LZ2 is not involved in the association of PKAc with the BK channel.

Thus, the inhibitory effect of the inclusion of the LZ1 peptide upon PKAc-STREX-HA channel association, implicates the LZ1 motif in PKAc-channel association.

5.2.1.4.2 mLZ-HA Channels

To investigate whether mutation of the leucine zipper 1 impacted upon the channel association with PKAc, mLZHA channels were employed (See Figure 3.13). The central two leucines of leucine zipper 1 (L503, L510) were mutated to alanine, rendering the motif ineffective as a leucine zipper (See Figure 3.1 & Appendix B). Patch clamp electrophysiology (performed by Dr Lijun Tian, results not shown) demonstrated that the mLZ-HA channels were expressed functionally in HEK293 cells and thus indicated that the channels could be isolated by immunoprecipitation. mLZ-HA stable cell lines

were transfected with excess free PKAc, immunoprecipitated by α-HA or α-PKAc, and the association of PKAc with the channels analysed by Western blotting as described previously (Section 5.2.1.1). As a positive control, STREX-HA/PKAc co-immunoprecipitation assays were performed in parallel and a representative assay is illustrated in Figures 5.9 & 5.10.

Both -HA-tagged channels and free PKAc were detected in the whole cell lysates from stable cell lines of STREX-HA and the mutant channel, mLZ-HA (Figures 5.9 & 5.10). As observed in Figure 5.1, co-immunoprecipitation of STREX-HA with PKAc occurred following immunoprecipitation by α-HA and by α-PKAc. However, immunoprecipitation of the mLZ-HA channel did not result in co-immunoprecipitation of PKAc and equally, immunoprecipitation of PKAc did not pull down the channel. This indicates that mutation of the BK channel leucine zipper 1 motif inhibits PKAc association with the channel implicating the sequence as a possible binding domain for the kinase.

mLZ-HA as a control in Section 5.2.1.1

Crucially, the inability of the mLZ-HA channel to co-immunoprecipitate PKAc enabled its use as a negative control to demonstrate the specificity of BK-channel to PKAc binding that is illustrated in Figure 5.2. As the channel protein is identical except for the mutations of the leucine zipper, the ability of the non-mutated channels to pull down the kinase is validated.

Figure 5.9
Co-immunoprecipitation assays of PKAc with STREX-HA and mLZ-HA channels: Immunoprecipitation by α-HA

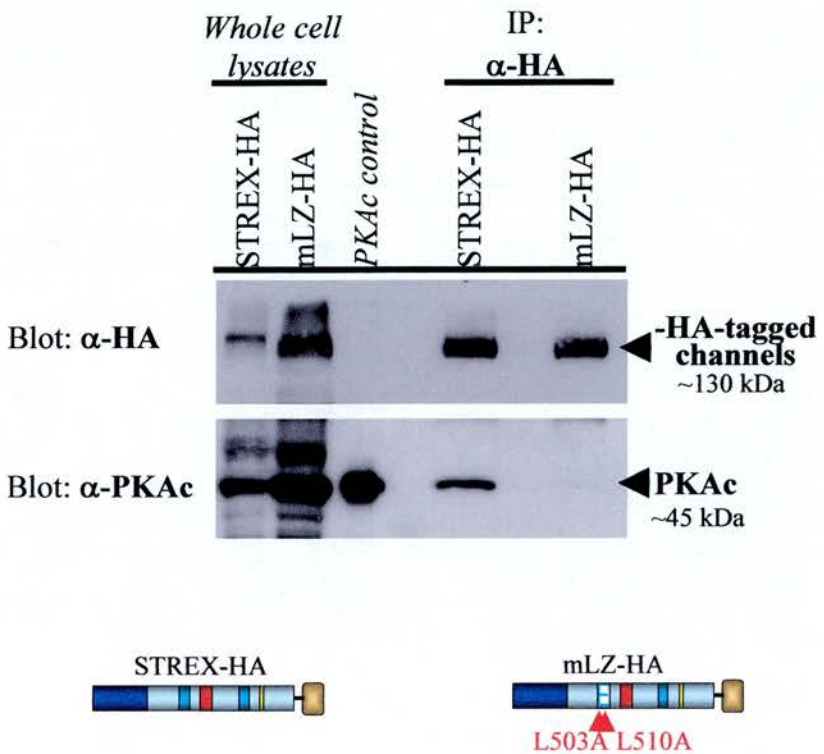

Figure 5.9: Representative Western blots of STREX-HA & mLZ-HA BK channel co-immunoprecipitation with PKAc. HEK293 cell lysates from stable cell lines of STREX-HA & mLZ-HA BK channels (illustrated below blots, See Figure 3.13) transfected with excess free PKAc were immunoprecipitated (IP) by α-HA. IPs were probed for free PKAc & -HA-tagged channels by Western blotting. HA-tagged channels (~130 kDa) and PKAc (~45 kDa) were detected in cell lysates and co-IP of PKAc and STREX-HA was observed following IP. PKAc did not co-IP with mLZ-HA. Western blot analysis: sheep α-PKAc 1/5000, rabbit α-HA 1/333, α-sheep-HRP 1/2000, α-rabbit-HRP 1/2000, detection by ECL.

Figure 5.10
Co-immunoprecipitation assays of PKAc with STREX-HA and mLZ-HA channels: Immunoprecipitation by α-PKAc

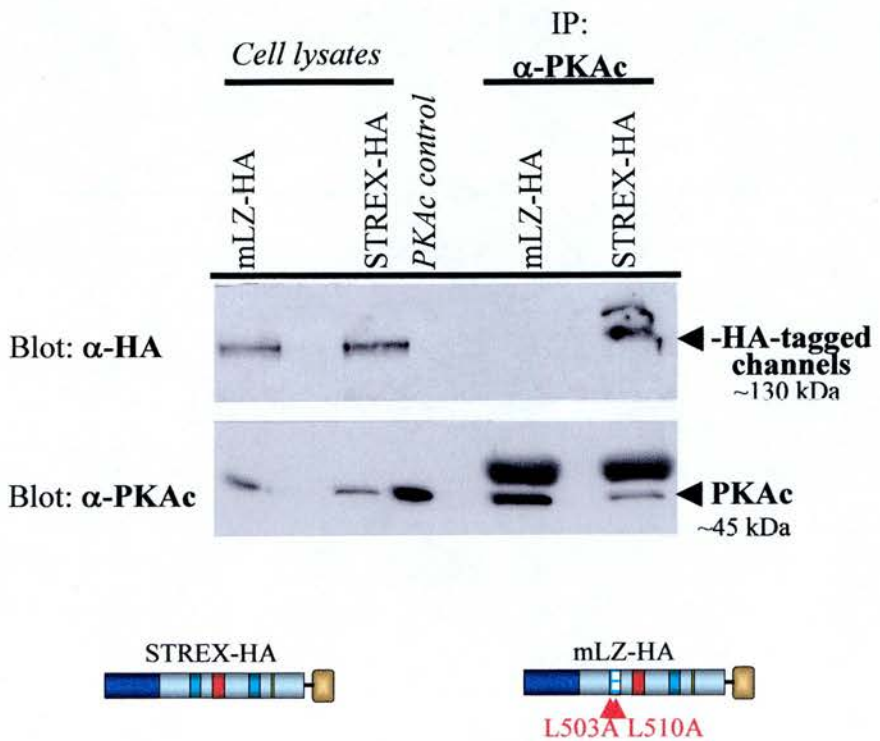

Figure 5.10: Representative Western blots of STREX-HA & mLZ-HA BK channel co-immunoprecipitation with PKAc. HEK293 cell lysates from stable cell lines of STREX-HA & mLZ-HA BK channels (illustrated below blots, See Figure 3.13) transfected with excess free PKAc were immunoprecipitated (IP) by α-PKAc. IPs were probed for free PKAc & -HA-tagged channels by Western blotting. HA-tagged channels (~130 kDa) and PKAc (~45 kDa) were detected in cell lysates and co-IP of PKAc and STREX-HA was observed following IP. mLZ-HA did not co-IP with PKAc. Western blot analysis: sheep α-PKAc 1/5000, rabbit α-HA 1/333, α-sheep-HRP 1/2000, α-rabbit-HRP 1/2000, detection by ECL.

ZERO-mLZ-HA

Equivalent PKAc:channel co-immunoprecipitation assays were performed by Dr Lijun Tian upon a ZERO-HA channel with corresponding mutations of the leucine zipper 1 motif and analogous results were obtained (Appendix C). This indicates that splice variation between the STREX and ZERO variants is unlikely to impact upon the association of PKAc with the channel protein and thereby provides further evidence of the role of the conserved leucine zipper 1 motif.

Phosphorylation of mLZ-HA

The mLZ-HA channel possesses intact S869 and STREX S4 residues equivalent to the STREX-HA channel residues that were suggested to be PKA phosphorylation targets (See Chapter 4). However, mutation of the LZ1 motif confers an inability to co-immunoprecipitate with PKAc (Section 5.2.1) and thus, to investigate whether association of the kinase with the channel is necessary for phosphorylation, mLZ-HA channel immunoprecipitated with α-HA (Section 2.6.3) was exposed to *in vitro* phosphorylation assays with exogenous PKA (Section 2.8.1.1). The assays were assessed by Western blot analysis using phospho-specific antibodies (See Section 3.2.3) as illustrated in Figure 5.11.

Detection of the mLZ-HA channel by the α-phospho-S869 antibody indicates that the S869 site of the mLZ-HA channel was successfully phosphorylated following the addition of exogenous PKAc demonstrating that, with a mutated LZ1 motif, the channel

Figure 5.11
Phosphorylation of mLZ-HA channel by exogenous PKAc

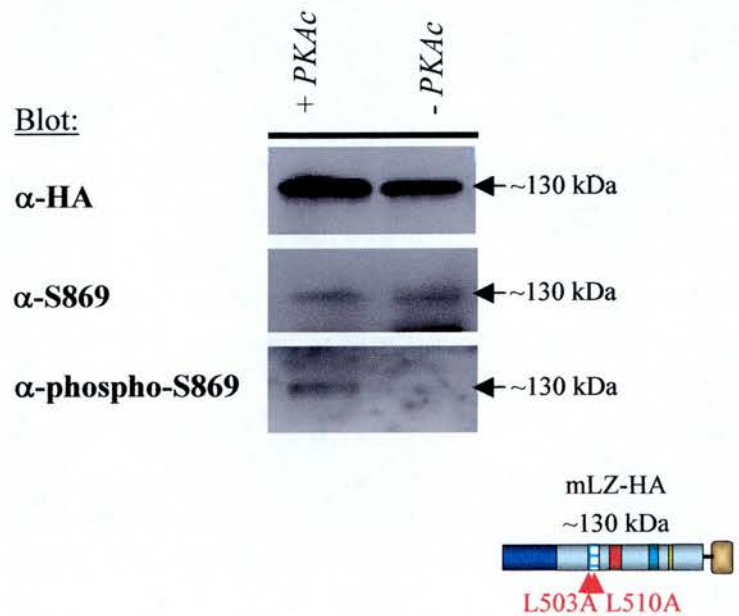

Figure 5.11: *In vitro* phosphorylation of the mLZ-HA channel by exogenous PKAc. mLZ-HA was immunoprecipitated by α-HA and incubated with or without exogenous PKAc as an *in vitro* phosphorylation assay. The mLZ-HA channels are detected by α-HA and α-S869, and phosphorylation of the S869 site is detected by the α-phospho-S869 antibody when exogenous PKAc is included in the assay. The mLZ-HA channel S869 site is not phosphorylated when no exogenous PKAc is added. Western analysis: rabbit α-HA 1/5000; sheep α-S869/α-phospho-S869 1/1000; α-rabbit-HRP 1/2000; α-sheep/goat-HRP 1/15000; ECL detection.

can still be phosphorylated by PKA *in vitro* reiterating the electrophysiologically determined functionality of the mLZ-HA channels. The absence of detectable S869 site phosphorylation without exogenous kinase addition provides corroborating evidence of the lack of kinase co-immunoprecipitation with the channel.

5.2.1.4.3 Thio-LZ1 fusion proteins

Confirmation that the leucine zipper 1 motif is the region of PKAc association with the channel was examined by Thioredoxin-V5-H_6 fusion proteins of the LZ1 region (See Section 3.2.1.2). These fusion proteins were used to assess the binding of PKAc to the leucine zipper 1 motif by exposure of immunoprecipitated LZ fusion proteins to purified PKAc or rat brain lysate (Section 2.9.3) and analysis of the association of PKAc by Western blot analysis (Section 2.7.2) as illustrated in Figure 5.12.

Incubation of the Thio-LZ1 fusion proteins with purified PKAc did not result in co-immunoprecipitation of the kinase. However, PKAc from rat brain lysate associated with the Thio-LZ1 fusion protein although not with the mutant Thio-mLZ1 protein. This suggests that an intact leucine zipper 1 motif is required for the association of PKAc with the sequence, an interaction that requires the presence of auxiliary factors present within the rat brain lysate.

Figure 5.12

Co-immunoprecipitation of the Thio-LZ1 fusion proteins with PKAc

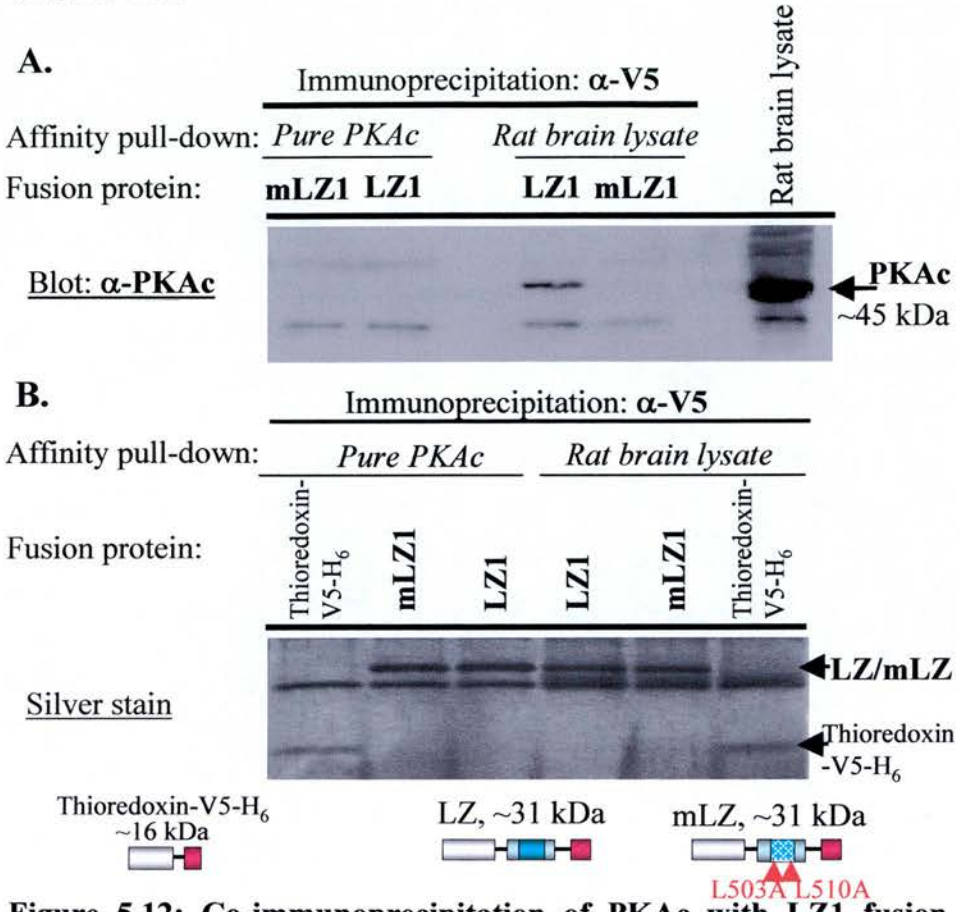

Figure 5.12: Co-immunoprecipitation of PKAc with LZ1 fusion protein. Thio-LZ1 & Thio-mLZ1 fusion proteins (illustrated below the blots, see Figure 3.7) were immunoprecipitated using α-V5 antibody and exposed to pure PKAc or rat brain lysate. Immunoprecipitations were separated by SDS-PAGE and stained by Silver to determine successful & equivalent immunoprecipitation (**B**) or were probed for the presence of PKAc by Western blotting (**A**). PKAc from rat brain lysate co-immunoprecipitated with LZ1, but not the mutant, mLZ1. Pure PKAc did not co-immunoprecipitate with either fusion protein. Western blot analysis: sheep α-PKAc 1/5000, α-sheep-HRP 1/2000, detection by ECL.

5.2.2 Heteromultimerisation

Formation of functional BK channels composed of different individual α-subunit splice variants may contribute to the wide functional and regulatory differentiation attributed to these unique channels. Thus, to determine if splice variants could associate together, HEK293 cells were co-transfected with STREX-V5-H_6 and either STREX-HA or ZERO-HA BK channel splice variants and the cell lysate divided for immunoprecipitation by α-HA or α-V5 (Section 2.9.3). Controls of the channels co-transfected with pcDNA3 vector were performed in parallel. Co-immunoprecipitation was determined via Western blotting as illustrated in Figures 5.13 and 5.14.

The –HA and -V5-H_6 –tagged channels were successfully detected in the appropriate whole cell lysates demonstrating successful transfection of the channels into HEK293 cells (Figures 5.13 & 5.14). Immunoprecipitation by α-HA pulled down the STREX-HA and ZERO-HA channels with co-immunoprecipitation of STREX-V5-H_6 (Figure 5.13). STREX-V5-H_6 was not pulled down in the absence of an –HA-tagged BK channel (Figure 5.13). Reciprocally, immunoprecipitation by α-V5 successfully co-immunoprecipitated STREX-HA and ZERO-HA with STREX-V5-H_6 with no pull down of the –HA-tagged channels in the absence of STREX-V5-H_6 (Figure 5.14). This indicates that non-specific pull-down of channels did not occur following immunoprecipitation with either α-HA or α-V5 and thus demonstrates that STREX-STREX and STREX-ZERO α-subunit associations can occur.

Figure 5.13

Heteromultimerisation of the BK channel: Association of STREX & ZERO-HA with STREX-V5-H_6, Immunoprecipitation by α-HA

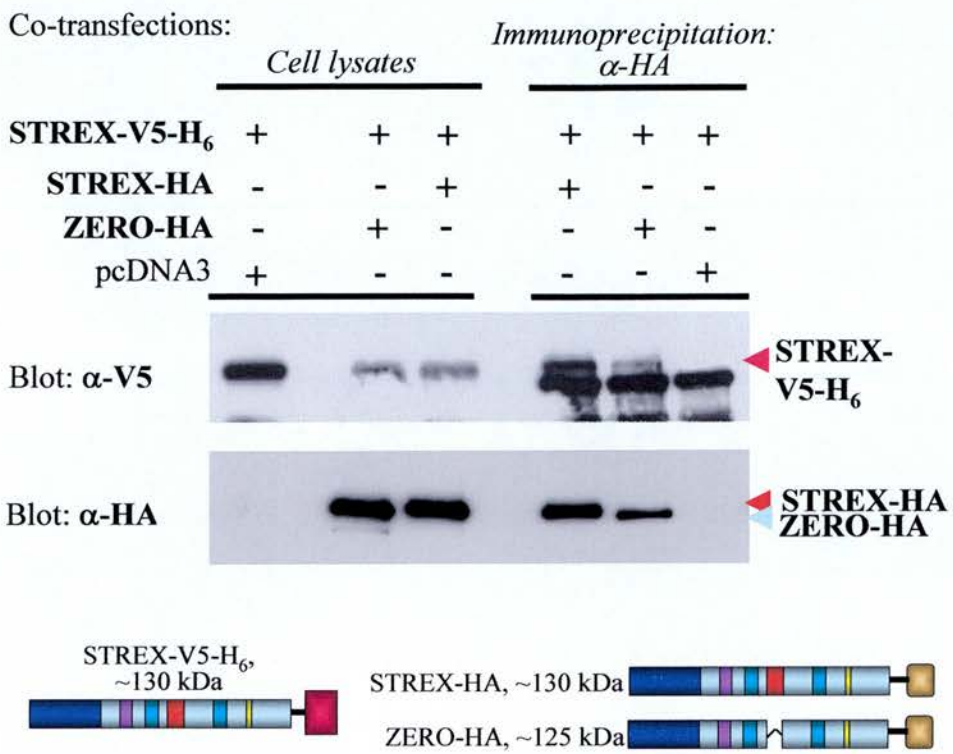

Figure 5.13: Representative co-immunoprecipitation of -HA tagged BK channels with STREX-V5-H_6. STREX-V5-H_6 was co-transfected with STREX-HA, ZERO-HA (Illustrated below the blots, See Figure 3.13) or pcDNA3 and channels immunoprecipitated with mouse α-HA antibody. Immunoprecipitations were separated by electrophoresis and probed for epitope tagged channels by Western blot analysis using rabbit α-HA or α-V5. STREX-V5-H_6 co-immunoprecipitated with STREX-HA and ZERO-HA channels, but did not pull-down in the absence of the HA-tagged channels. α-V5 detected non-specific proteins at ~120 kDa in immunoprecipitations. Western blot analysis: mouse α-V5 1/5000, rabbit α-HA 1/333, α-mouse-HRP 1/2000, α-rabbit-HRP 1/5000, detection by ECL.

Figure 5.14

Heteromultimerisation of the BK channel: Association of STREX & ZERO-HA with STREX-V5-H_6, Immunoprecipitation by α-V5

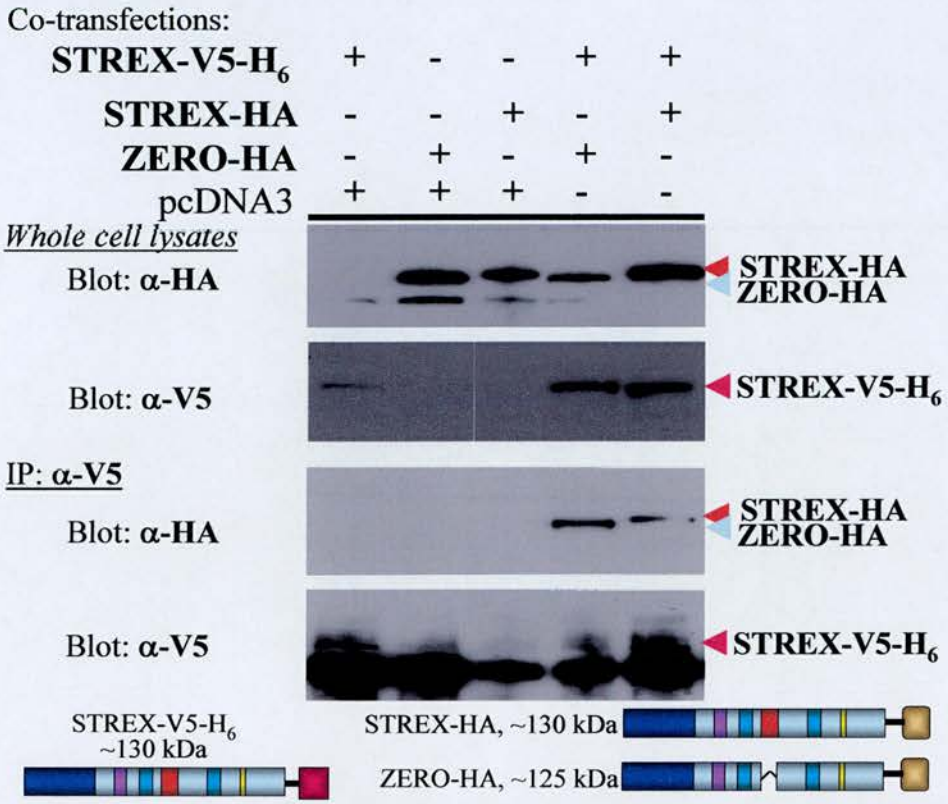

Figure 5.14: Representative co-immunoprecipitation of -HA tagged BK channels with STREX-V5-H_6. -V5-H_6 and -HA epitope-tagged BK channels (Illustrated below the blots, See Figure 3.13) were co-transfected and channels immunoprecipitated with mouse α-V5 antibody. Immunoprecipitations were separated by electrophoresis and probed for epitope-tagged channels by Western blot analysis. STREX-HA and ZERO-HA co-immunoprecipitated with STREX-V5-H_6 channels and did not pull-down in the absence of STREX-V5-H_6. α-V5 detected non-specific proteins at ~120 kDa in immunoprecipitations. Western blot analysis: mouse α-V5 1/5000, rabbit α-HA 1/333, α-mouse-HRP 1/2000, α-rabbit-HRP 1/5000, detection by ECL.

5.3 Discussion

5.3.1 PKAc interaction

Previous studies have described a direct association of the catalytic subunit of PKA, PKAc, with the C-terminal domain of the *Drosophila melanogaster* BK channel [204]. The results described in this study, using the murine BK channel as a model, determine that PKAc and the mammalian BK channel assemble *in vivo*, yet the characteristics of this interaction are distinct from that of the insect channel homologue.

5.3.1.1 Splice variation has no influence upon PKAc-BK channel association

The ability of both the STREX and ZERO BK channel splice variants to co-immunoprecipitate PKAc and reciprocally, the ability of PKAc to co-immunoprecipitate the channels (Figures 5.1 & 5.2), suggests that the splice variation between these BK channel α-subunit proteins does not influence the association of the kinase with the channel. Indeed, *in vitro*, the bacterially-expressed fusion protein, GST-STREX did not associate with PKAc (Figure 5.4) demonstrating that the 58 amino acid long insert cannot, at least in isolation, function as a binding site for the kinase. Further evidence of this determination was indicated by the inability of the ΔN-STREX-ΔC and ΔN-ZERO-ΔC fusion proteins to associate with PKAc (Figure 5.6). The structural influence of the fusion tags, the absence of conformational interactions and constraints induced in the *in extenso*, *in vivo* channel protein, and chemical influences such as pH and ionic environment may generate a conformation of the bacterially-expressed recombinant

STREX insert that is distinct from that in the *in extenso*, *in vivo* channel protein. Similarly, the conformation of associating proteins may be altered as to make binding ineffective and thus, native associations may be inhibited whilst non-native binding could be encouraged. However, binding conditions were equivalent to accepted physiological conditions and were adequately favourable to enable the association of other proteins with the fusion proteins (Figures 5.5 & 5.7). Thus, the STREX insert and splice variation between the STREX and ZERO channels are suggested to not be involved in the association of PKAc with the full-length channel protein implicating a site or sites common to both splice variants as the region responsible for kinase-channel association.

5.3.1.2 Phosphorylation has no influence upon PKAc-BK channel association

The co-immunoprecipitation of PKAc with the S4A-S869A-HA channel paralleled the pull-down observed with the STREX and ZERO variants (Figures 5.1 & 5.2) demonstrating that the serine-869 and STREX serine-4 residues do not have to be intact for the association of PKAc with the BK channel protein. Mutation of these residues to non-phosphorylatable alanine prevented phosphorylation of the –HA-tagged BK channel protein under *in vitro* phosphorylation assays (Figure 4.20). Thus, the ability of S4A-S869A-HA to associate with PKAc suggests that phosphorylation of these residues is not a prerequisite to kinase-channel association and, by inference, implicates a site or sites distinct from these phosphorylation targets as the location of kinase binding.

Further to this, the catalytic competence of the kinase is suggested not to be a factor in the association of PKAc with the BK channel α-subunit. This is implied by the co-immunoprecipitation of the catalytically inert PKAc-K72E with STREX-HA (Figure 5.3). Although HEK293 cells express endogenous PKAc that co-immunoprecipitates with the –HA-tagged BK channels (Figure 5.1), the comparably weaker signal that results without additional co-transfection suggests that, although a proportion of the immunoprecipitated PKAc will originate from this source, the over-expressed PKAc-K72E protein is contributing to this signal. Thus, this suggests that PKAc does not have to catalytically active and hence, does not have to phosphorylate the channel protein to associate with the BK channel α-subunit.

5.3.1.3 The LZ1 motif is responsible for the PKAc-BK channel association

The region identified as the domain responsible for the PKAc-BK channel association in *Drosophila* [204] is equivalent although not identical to residues 806-978 of the murine STREX sequence. This region is encompassed by the ΔN-ΔC fusion proteins, which failed to associate with PKAc under the experimental conditions employed in this study (Figure 5.6). Thus, the differences in the channel sequences must cause a difference in the kinase association, implicating distinct channel-kinase interaction mechanisms employed by the insect and mammalian systems. Therefore, in contrast to the *Drosophila* channel, regions outwith the sequence of the murine ΔN-ΔC fusion proteins are implicated in the BK channel-PKAc association. The inhibition of PKAc co-immunoprecipitation with the STREX-HA channel in the presence of competing

peptides against the LZ1 motif lead to the identification of the motif as a determinant of this interaction (Figure 5.8).

As illustrated in Figure 5.15, the presence of the LZ1 peptide in the α-HA immunoprecipitation of the STREX-HA channel is suggested to inhibit the channel association with PKAc competitively by interacting with the LZ1 motif and/or PKAc or the bridging protein via the dimerisation ability of leucine zipper motifs [214, 218]. The leucine to alanine substitutions of the mLZ1 mutant peptide renders it ineffectual as a leucine zipper, prohibiting dimerisation and thus, preventing the competitive inhibition of PKAc-BK channel association. The slight co-immunoprecipitation that is observed in the presence of the LZ1 peptide may be due to incomplete inhibition. This could result from the LZ1 peptide not encompassing a sufficient length of the leucine zipper 1 motif sequence as to enable some background association, or insufficient peptide concentration to induce complete block. Further studies could investigate this by the application of protein denaturing detergents to inhibit protein-protein interactions, the influence of different lengths of peptide sequence and peptide titration. However, for the purpose of this investigation, the indication of the motif as the PKAc association site was considered sufficient to warrant further study of the region by mutant channel and fusion-protein generation and indeed, this provided corroborate evidence of this role.

The inability of the mLZ-HA channel to co-immunoprecipitate with PKAc (Figures 5.9 & 5.10) demonstrates that the L503 and L510 residues of the murine BK channel LZ1

Figure 5.15
The action of inhibitory peptides upon PKAc association with the BK channel LZ1 sequence

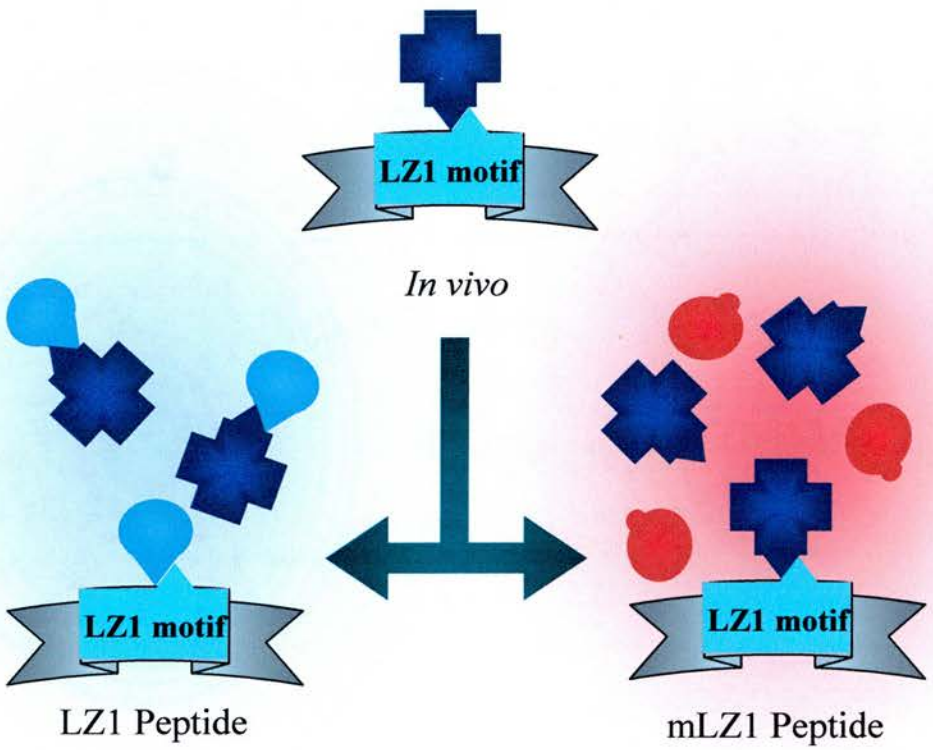

Figure 5.15: Model for the inhibition of PKAc association with the LZ1 motif of the BK channel. PKAc (dark blue) is postulated to associate with the BK channel α-subunit *in vivo* either directly or indirectly via leucine zipper dimerisation involving the channel leucine zipper 1 (LZ1) motif (cyan). The LZ1 peptide (blue circles) parallels the motif sequence and thus, is assumed to inhibit the association by binding the channel LZ1 motif and the PKAc / PKAc-associating protein(s) as to competitively inhibit the interaction. The mutant peptide, mLZ1 (red circles), is altered to make it ineffectual as a leucine zipper (See Section 5.2.1.4.1). Thus, mLZ1 does not interact with the channel LZ1 motif, nor the PKAc / PKAc associating protein(s) and hence, PKAc can associate with the channel protein.

motif are crucial to ability of the channel to associate with the kinase. Although the leucine to alanine substitutions should confer minimal structural disruption to the channel protein, it is possible that the mutations, and indeed the LZ1 peptide, could disrupt the channel conformation as to inhibit the association of the kinase with other regions of the protein. The ability of the mLZ-HA channel to be phosphorylated by exogenous PKAc (Figure 5.11) demonstrates that the channel is still phosphorylatable, and thus the phosphorylation state of the channel is not critical to kinase association and is distinct from the role of the LZ1 motif. The motif could act as a facilitator to the association and not be the target. However, the ability of the Thio-LZ fusion protein to associate with rat brain PKAc indicates that the motif is indeed a critical and sufficient mediator of kinase-channel association (Figure 5.12).

Again, the requirement of an intact LZ1 motif was observed with the leucine to alanine substitutions of the mutant, Thio-mLZ1, preventing kinase association with the recombinant protein (Figure 5.12). Although structural influences of the mutations could affect the association of PKAc with a distinct region(s) of the protein, the short sequence length expressed in the fusion proteins (128 residues; See Table 3.1) implicates the LZ1 motif, or residues proximal to it.

5.3.1.4 The LZ1 motif may enable PKAc-BK channel association through an intermediary, bridging protein(s)

PKAc is highly conserved across species suggesting that the bovine and rat proteins are sufficiently homologous to enable successful substitution (ncbi accession no's: bovine:

P00517; rat: CAA37350). Thus, the affinity of Thio-LZ1 for the rat brain PKAc but not the purified bovine PKAc (Figure 5.12) is not due to characteristic differences of the PKAc proteins, but is indicative of an indirect interaction between the kinase and the fusion protein, involving an intermediary protein or proteins that bridge between the kinase and the leucine zipper (See Figure 6.1). This may facilitate the efficient regulatory phosphorylation of the BK channel residues by PKA by ensuring proximal, and thus effective, positioning of the enzyme. The leucine zipper 1 motif may associate with an adapter protein via leucine zipper dimerisation. This protein may bind directly to PKAc or there may be further intermediary, bridging proteins to facilitate and thus maximise the effective and efficient positioning of the catalytically active kinase to the phosphorylatable residues of the BK channel protein. Such a bridging protein, or proteins, may also be associated with the membrane or cytoskeletal elements to maintain its proximity to the BK channel, and may even be involved in bringing other regulatory proteins into the immediacy of the channel. These may include other protein kinases, protein phosphatases and calcium modulators, and even other ion channels such as calcium channels, described previously as associating with SK channels to enhance the efficiency of ion channel function [334].

The role of AKAPs in directing the anchoring of the regulatory subunit of PKA has been described for several mammalian systems (See Section 1.5.1). However, these proteins are not noted to associate directly with PKAc and their association with PKAr is through hydrophobic and not leucine zipper-mediated interactions [335]. Further studies will be required to investigate whether an AKAP is involved in this association, and whether

PKAr is co-immunoprecipitated by BK channel splice variants. The bridging protein(s) responsible for associating with PKAc and aligning it to the BK channel may not be a typical AKAP and thus, the determination of a novel protein, or group of proteins, that, through the dimerisation of leucine zippers, parallels the action of a typical AKAP but associates with PKAc instead of PKAr is possible. Such an adapter protein is probable, as it would be detrimental to a cell to have uncontrolled, free PKAc capable of phosphorylating proteins non-specifically, regulating cellular pathways inappropriately. Insect cells may exhibit a different mode of PKAc control that results in the direct association of PKAc with the *Drosophila* BK channel protein [204]. Thus, the bridging protein(s) may be specific to mammalian systems. Mass spectrometric analysis of the co-immunoprecipitating bands could identify this protein(s) in future studies. This may uncover an integral anchoring protein(s) that participates in the formation of the BK channel complex to maintain a dynamic, effective and efficient ion channel complex underlying the successful application of BK channels to their numerous physiological roles. The protein(s) may be involved in proximating PKAc with other ion channel and signalling complexes and may function as a linchpin to bring many integral signalling proteins together. Equally, the LZ1 motif of the BK channel may be multi-functional and enable the dynamic association of several, distinct accessory proteins. Future studies of the dimerisation of leucine zipper motifs in non-DNA binding proteins may uncover a more widespread and comprehensive method of protein-protein association than was previously thought.

5.3.2 Heteromultimerisation

The crucial component of the BK channel complex is the BK channel pore itself and the results of Figures 5.13 & 5.14 indicate that channels can assemble as both homo- and heteromultimers *in vivo*. STREX α-subunits can associate with other STREX α-subunits as well as with the ZERO splice variant. However, such multimerisation may result following the cellular lysis of the immunoprecipitation procedure, and functional channels may not be formed between distinct splice variants in the co-transfected HEK293 cells, nor indeed, *in vivo*. Future electrophysiological investigations of co-transfected heterologous systems and native tissues will be required to fully assess this issue. Affirmation of the specificity of such interactions could be confirmed in further studies with BK channel proteins with mutated, ineffective RCK domains and indeed, investigation of chimeras with RCK domains in Kv channels that do not expresses the domain natively will be of interest. However, the conservation of the RCK tetramerisation domain (Figures 1.3 & 1.4) between the STREX and ZERO splice variants implies that the region may be non-specific to splice variation of the BK channel α-subunit enabling such "inter-splice" associations. The conservation of the domain in other BK channel splice variants suggests that many possible permutations of the BK channel tetrameric pore may exist, as illustrated schematically in Figure 5.16. With distinct splice variants displaying unique regulatory and functional characteristics, the ramifications for possible regulatory variation of BK channels are enormous. For example, channels composed of both STREX and ZERO subunits may confer unique properties, or possess a character intermediate between the homomultimeric channels.

Figure 5.16
Heteromultimerisation of tetrameric channels

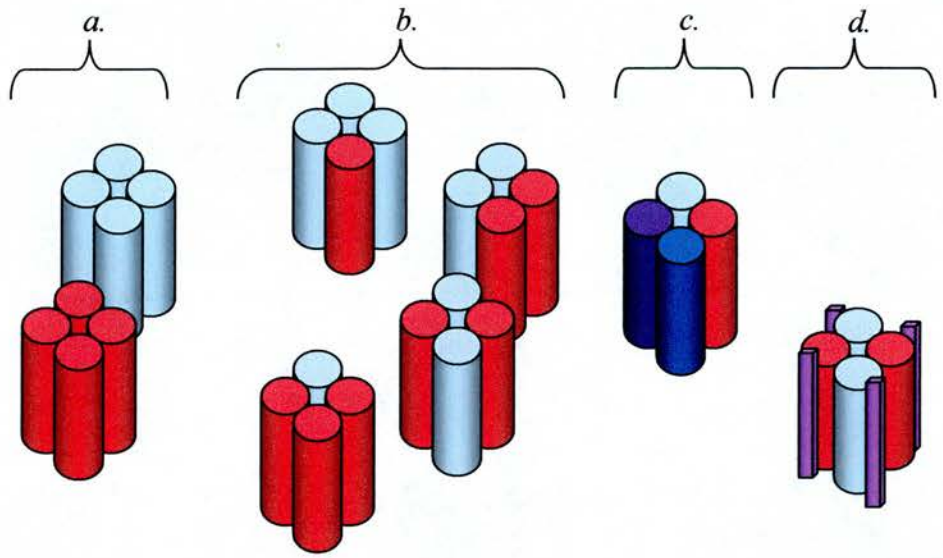

Large cylinders: different colours representing different splice variants of BK channel α-subunits; pale blue could represent ZERO with red representing STREX splice variants.

Purple rectangles: accessory proteins such as β-subunits

Figure 5.16: Heteromultimerisation of tetrameric BK channels may contribute to the wide regulatory & functional variation of the channels. The immunoprecipitation evidence presented in this study suggests that different splice variants of the BK channel α-subunit can associate together. If this occurs *in vivo,* functional channels may result from four identical subunit (*a*) or combinations of different splice variants (*b*). As illustrated above, several combinations could result where two variants are expressed. As several splice variants have been described, channels could result from four individual splice variants (*c*). The presence of accessory proteins such as the β-subunit (*d*) may add to the complexity of regulation.

The ratio of one splice variant to another in a functional tetramer is also likely to impinge upon the precise functional properties of the channel. Cells and tissues that express several unique splice variants may express channels ranging from homomultimers to heteromultimers composed of four different α-subunit isoforms contributing to wide variation in individual channel properties throughout the cell/tissue. Especially in situations such as the cochlea where small differences in BK channel properties are key to the fine-tuning of physiological requirement, splice variant heteromultimerisation in combination with accessory subunit associations may be fundamental. Thus, if different splice variants of the BK channel do form functional channels *in vivo*, this may be a crucial mechanism for achieving the functional and regulatory variation, dexterity and specialisation of these ubiquitous ion channels.

5.4 Chapter Summary

The catalytic subunit of PKAc was shown to associate with the BK channel α-subunit in a manner that was not influenced by splice variation nor the phosphorylation state of the channel protein or catalytic competence of the kinase. This association was dependent upon a conserved leucine zipper 1 motif connecting the cytoplasmic C-terminal domain with the tetramerising RCK domain. The motif is suggested to interact with PKAc via an intermediary protein, or proteins, to facilitate the phosphorylation and subsequent modulation of the BK channel by the kinase and thus contribute to the BK channel complex. At the core of this complex is the BK channel itself, which is suggested to not just to form homotetrameric channels, but also heteromeric channels composed of different interacting α-subunit splice variants.

Chapter Six:

General Discussion & Future Work

Chapter Six:

General Discussion & Future Work

This study aimed to investigate the molecular nature of the regulation and interaction of PKA with BK channel variants with particular emphasis upon the molecular basis of the distinct regulatory responses of the ZERO and STREX BK channel splice variants. Using recombinant fusion proteins of the BK channel α-subunit C-terminal domain in conjunction with heterologously expressed epitope-tagged full-length channels, the investigation of channel phosphorylation and complex assembly was performed *in vitro* and *in vivo*.

In combination, site-directed mutagenesis, biochemical phosphorylation and the use of phospho-specific antibodies revealed PKA phosphorylation of the conserved serine residue, S869, in STREX and ZERO splice variants *in vivo*, a site that is also a potential target for CaMKII but not PKC. Additionally, the STREX insert serine residue, STREX S4, was identified as a PKA-mediated phosphorylation target, possibly functioning as a PKC but not CaMKII phosphorylation target residue. Co-immunoprecipitation strategies determined that the catalytic subunit of PKA co-immunoprecipitated with both the STREX and ZERO BK channel splice variants *in vivo*. Such complex assembly was dependent upon and mediated by a conserved ~130 amino acid region encompassing the α-subunit C-terminal domain leucine zipper motif, LZ1, with association requiring intermediary adapter protein(s) whilst remaining independent upon the phosphorylation state of the channel protein. Thus, these data suggest that the distinct responses of the

STREX and ZERO channels to PKA is likely to result from the differential phosphorylation of specific PKA consensus motifs within the splice variants and not as a result of differential association of the kinase.

Physical interaction of PKAc & BK channels

The determination of the PKAc – murine BK channel α-subunit association through intermediary adapter protein(s) and the conserved BK channel LZ1 region contrasts to the direct binding of PKAc described with the *Drosophila* BK channel [204]. Although *in vivo* phosphorylation of the S869 motif is conserved between insect and mammalian BK channels, it appears that distinct mechanisms of kinase to channel association have developed. The equivalent sequence of the *Drosophila* and, indeed, the *C. elegans* BK channels to the mammalian LZ1 motif region express phenylalanine and lysine residues at the third and fifth ***d*** positions of the heptad motif respectively (Appendix B). Thus, *Drosophila* BK channels may not possess an intact, functional LZ1 that is able to facilitate PKAc-channel interactions. Indeed, the direct association of the kinase with the *Drosophila* BK channel suggests that such a mechanism may not be required in this system. However, further investigations will have to be performed to uncover whether the LZ1 motif is used ubiquitously to enable the PKAc-channel association, including in *Drosophila* BK channels, or whether the mechanism is a specialisation of mammalian or even murine systems.

Phosphorylation of the -HA-tagged channel with a mutated LZ1 motif, mLZ-HA, was still possible with exogenous PKA indicating that association of the kinase with the

channel is not necessary for phosphorylation. However, the effectiveness and efficiency of the phosphorylation remains to be fully assessed and will provide the basis of future electrophysiological studies. It is possible that, *in vivo*, without the excess of PKAc that is applied in these experiments, PKA phosphorylation of murine BK channels with mutated LZ1 motifs cannot be achieved effectively at a level sufficient to enable the required physiological effect of the channels. Thus, the purpose of such an adapter protein-dependent mechanism may be to proximate the kinase to the channel, perhaps even bringing the kinase close to specific consensus motifs, to facilitate the dynamic and effective regulation of the BK channels by PKA-phosphorylation. Such a model is illustrated in Figure 6.1.

Increasingly, evidence of leucine zipper motifs functioning as mediators of protein-protein interactions is mounting and going beyond their long-established role in DNA-binding proteins, being described for other ion channels such as KCNQ1-KCNE1 potassium channels, inositol 1,4,5-triphosphate receptors and ryanodine receptors [318, 331, 332]. Thus, the use of leucine zippers may be found to be a common mechanism of regulating and mediating protein-protein associations with profound implications, especially to the elucidation of the functioning and component identification of dynamic signaling complexes. Mass spectrometric identification of the proteins co-immunoprecipitating with BK channels may help to uncover the nature of proteins that contribute to the BK channel signaling complex and, in time, the complex as a whole may be revealed. Complex characteristics that could be investigated following-on from the findings of this study include; dynamic regulation, positional targeting and

Figure 6.1
Proposed interaction of PKAc with the BK channel

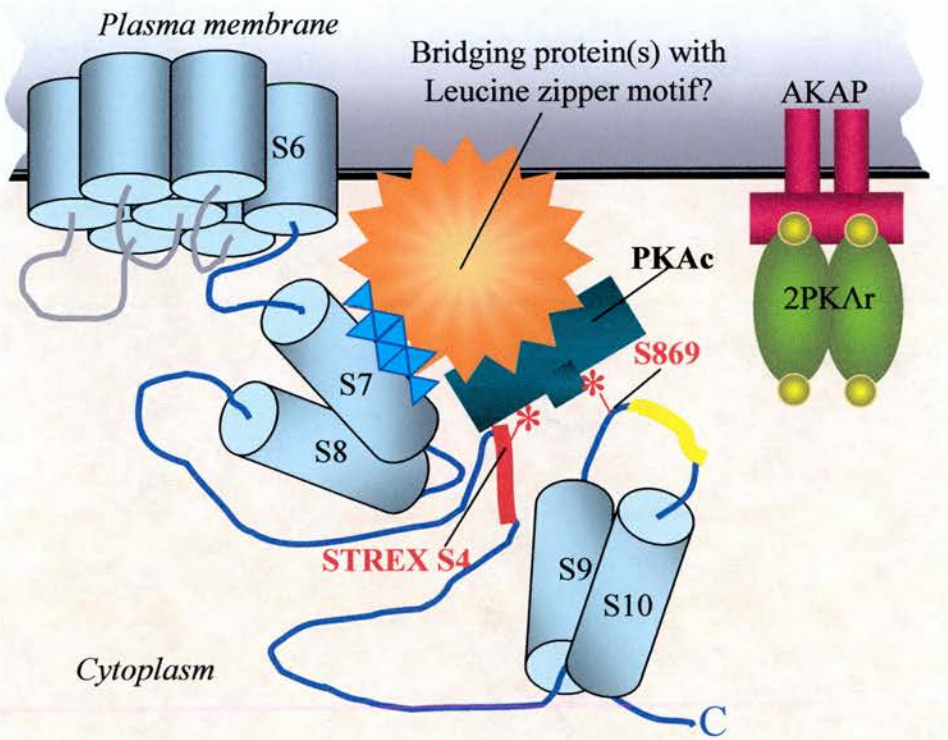

Figure 6.1: Model for the proposed interaction of PKAc with the BK channel α-subunit. The leucine zipper 1 motif of the BK channel α-subunit is integral to the association of the channel with PKAc but does not bind the kinase directly. An associated protein may bind the motif through leucine zipper dimerisation and directly or via other proteins bind PKAc bridging between kinase and channel. This may facilitate PKAc phosphorylation of channel residues namely serine-869 (S869) and STREX serine-4 (S4). The bridging protein(s) may be involved in the associations of other regulatory proteins such as calcium modulators and may even bind an AKAP perhaps facilitating the dynamic PKA-mediated regulation of BK channels via AKAP binding of PKA regulatory subunits (PKAr). For simplicity only the cytoplasmic C-terminal domain of one of the α-subunits forming the tetrameric channel is illustrated. This is represented in blue, is not to scale and the putative α-helices and C-terminal labeled as Figure 1.4.

maintenance of signaling molecules/proteins, whether known proteins such as AKAPs or even other ion channels such as calcium channels are included, and whether such complexes are specific to a particular ion channel/protein kinase/protein phosphatase or are promiscuous in nature.

Differential phosphorylation underlies the distinct regulation of BK channels by PKA

Consistently throughout this study, the S869 residue of ZERO fusion proteins and full-length channels was phosphorylated by PKA *in vitro* and *in vivo*. Together with previous electrophysiological investigation of S869 mutation [190, 202, 205, 229] and by analogy to dual mutation of S869 and STREX S4 residues in STREX-expressing channels, these results indicate that the S869 residue is the only residue that is phosphorylated by PKA in the *in extenso* ZERO channel α-subunit protein *in vivo*. Confirmation of these preliminary analyses could be performed by phosphorylation of ZERO,S869A fusion proteins analogous to the proteins used in this investigation, and by mass spectrometric analysis to determine the phosphorylation target residues in full-length channels. However, the results presented here in combination with the electrophysiological analyses indicate that such phosphorylation of S869 is critical to PKA stimulation of the ZERO splice variant.

Inclusion of the STREX insert within the channel protein does not prevent S869 residue phosphorylation. However, electrophysiological analysis in previous studies has demonstrated that phosphorylation of the site is not critical to the inhibition of the splice variant by PKA; alanine substitution of S869 did not prevent the inhibitory regulation of

the kinase [229]. Further to this, use of the ΔN-ΔC fusion proteins in this investigation indicated that S869 phosphorylation was not prerequisite to phosphorylation of the distinct STREX S4 site. *In vivo* phosphorylation analyses using STREX,S869A channels and, hopefully, antibodies with sufficient specificity to STREX S4 phosphorylation to enable determination of channel phosphorylation will have to be performed in the future to confirm this assumption although, certainly, the current evidence supports this view. Thus, inclusion of the STREX insert is proposed not to inhibit, nor encourage, S869 phosphorylation, whilst the phosphorylation state of the S869 residue is not influential to the regulation of STREX BK channels by PKA (See Figure 6.1). Thus, S869 and STREX S4 residue co-phosphorylation in STREX channels appears to be unimportant to PKA-mediated regulation of the channel. Therefore, STREX S4 residue phosphorylation by PKA is suggested to be dominant to phosphorylation of the S869 site. Why such seemingly inconsequential phosphorylation should still occur remains to be elucidated. It may exert a subtle or a distinct influence upon STREX channel activity that is currently undetermined. The possibility of residual, non-functional phosphorylation appears wasteful and inefficient in such a crucial and dynamic cellular system.

Although PKA-phosphorylation of STREX S4 has been determined *in vitro* through this study, corroborating evidence of *in vivo* phosphorylation remains to be established. Further studies may find an improved method of detection, either through enhanced autoradiographic detection, or by improved, affinity purified antibodies against the phosphorylated STREX S4 residue. Use of a different fusion tag or a distinct expression

system may increase channel expression and subsequent protein levels following isolation, and a method may be determined that removes the complicating non-specific immunodetection that hampered analysis in this study by the α-phospho-STREX antibody. Mass spectrometry, particularly techniques such as MALDI-TOF, may enable the identification and conformation of phosphorylated BK channel residues in further studies. However, the evidence amassed in this investigation through fusion protein phosphorylation analyses suggests that the STREX S4 residue is indeed phosphorylated by PKA *in vivo*, and that it is this unique feature of STREX channels that induces differential regulation of the ZERO and STREX splice variants by the kinase.

Thus, differential phosphorylation is suggested as the molecular mechanism underlying the distinct regulation of STREX and ZERO BK channel splice variants by PKA. However, exactly how the phosphorylation of the splice variants influences channel activity remains to be elucidated. The structural arrangement of the cytoplasmic C-terminal domain of BK channels is currently undetermined, although with improvements in crystallography, the relative topologies of STREX and ZERO variants, and phosphorylated and non-phosphorylated forms may be comparable in the future. Through conjecture, it is possible that the distinct PKA-phosphorylation of STREX and ZERO splice variants could induce different conformational effects upon the α-subunit protein, or upon the association of an accessory protein(s). As the topology of the domain is undetermined, the proximity and relative conformation of the PKA-phosphorylation consensus motifs to other regions of the protein is unknown. PKA phosphorylation of STREX and ZERO channels may exert influence differentially

through a common mechanism, just one inhibitory, one stimulatory, or the mechanisms may be distinct. The gating of the channel may be differentially influenced through phosphorylation-induced conformational constraint upon integral regions such as the P-loop or voltage sensor (See Figure 1.4). This is certainly an area for future investigation.

Physiological implications

Whatever the ensuing mechanism of differential PKA-regulation of the splice variants that results from the distinct phosphorylations, it appears that the STREX and ZERO BK channel splice variants are regulated by PKA via LZ-mediated PKAc association. This means that the signal transduction mechanism and associating accessory proteins, such as the unidentified adapter proteins, are conserved. Thus, to induce a change in the BK channel contribution to the electrical character of the cellular membrane only the BK channel splice variant ratio has to alter. This could be useful *in vivo* especially in the fine-tuning of cellular and tissue responses to particular physiological stimuli and particularly, during negative feedback responses. Such alterations are not immediate due to the requirement of protein transcription and translation and thus, may be of particular influence in longer-term responses. This is likely to contribute to the effective, dynamic responsiveness of BK channels to various physiological stimuli, and may be found with other splice variants too.

Heteromultimerisation

Indeed, such physiological specialisation of BK channels resulting from alterations to

the splice variant expression ratio may be further "fine-tuned" by heteromultimerisation of different splice variant α-subunits into functional, tetrameric channels. The co-immunoprecipitation assays performed in this study suggested that in addition to homomultimers, heteromultimerisation between the STREX and ZERO α-subunit variants could occur *in vivo*. Such interactions may contribute greatly to the regulatory diversity of BK channels and may explain, at least in part, why BK channels are able to be so ubiquitously expressed and integrated into diverse, critical physiological systems requiring a smorgasbord of regulatory and functional diversity. As no alternative splicing within the tetramerisation, RCK domain has been described currently, it is possible that all BK channel splice variants, with all their distinct, displayed characteristics may be able to associate functionally *in vivo* producing BK channels with intermediary, or even unique, wide-ranging features. The benefits of this to BK channel specialisation are immense and may go a way to explaining the evolutionary success of these ubiquitous channels. Further studies upon other splice variants, and electrophysiological analysis of heteromultimeric BK channels will be a fascinating area of future research.

Influence of other protein kinases

Additionally, the molecular influence of other protein kinases upon BK channel splice variants should be addressed in future studies. This investigation has demonstrated that protein kinases, in addition to PKA, can phosphorylate BK channel residues *in vitro*; CaMKII phosphorylated the S869 motif of S869 peptides and ΔN-ΔC fusion proteins,

whilst PKC phosphorylated the STREX S4 residue of GST-STREX and ΔN-ΔC fusion proteins. It will be interesting to see if such phosphorylations occur *in vivo*, and to investigate other putative phosphorylation motifs of other protein kinases. Indeed, with specific antibodies and multiple screenings, the co-immunoprecipitation of several individual protein kinases and phosphatases could be assessed. Although such signalling proteins are stimulated by distinct signal transduction pathways, it is conceivable that they may exert their regulatory influence upon BK channels through common mechanisms and even through phosphorylation of common consensus motifs where applicable. Further analyses, inhibiting other endogenous protein kinases, will have to be performed to confirm and assess their role further.

Final thoughts

How BK channels achieve the amazing regulatory variation that underlies their near-ubiquitous expression, multi-functionality and requirement in diverse, critical physiological processes is a complex and diverse issue of which this study is only preliminary and elementary, a beginning to a more in-depth understanding of these critical ion channels. With future studies, the complete molecular mechanism of the reversible protein phosphorylation of BK channels may be uncovered and may provide an insight into their regulation, diversity, ubiquity and how and why mutations and expressional abnormalities of BK channels may underlie certain disease mechanisms, with significant implications for medical and scientific understanding of ion channel regulation and function.

Appendices

Appendix A

PKA activation mechanism

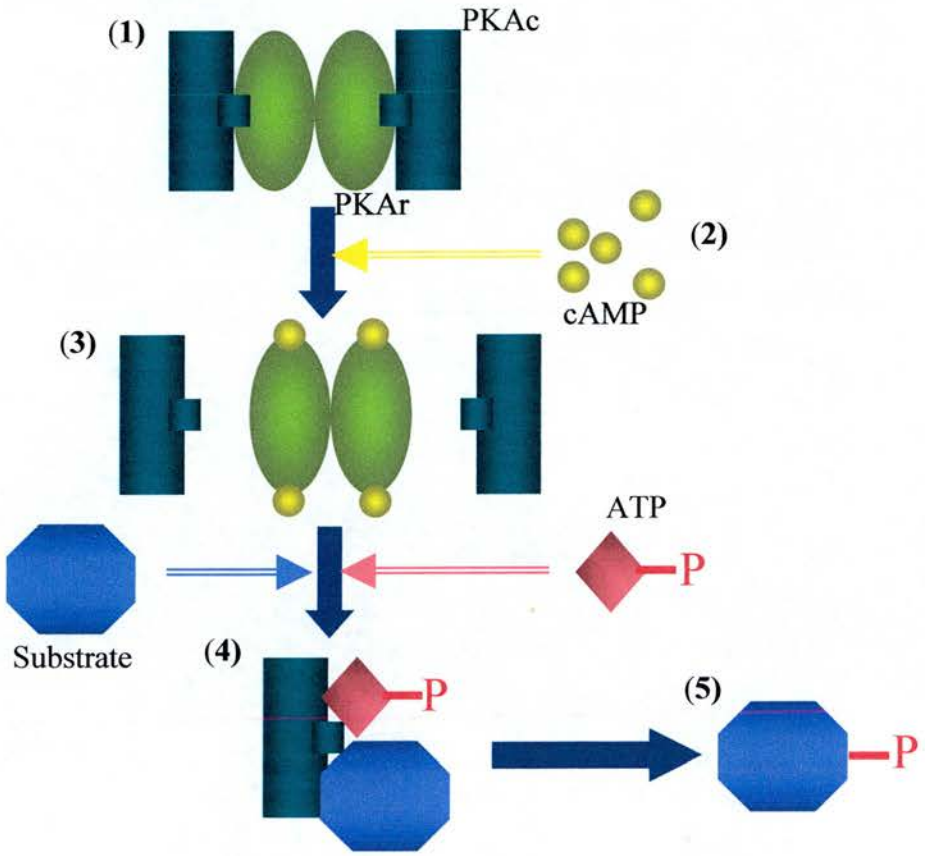

Appendix A: Schematic of the mechanism of PKA activation. **(1)**Unstimulated PKA exists as a a catalytically inactive holoenzyme comprised of two catalytic subunits (PKAc; turquoise rectangles) and two regulatory subunits (PKAr; green ovals). **(2)** With elevation of intracellular cAMP (yellow circles) following adenylate cyclase stimulation, **(3)** cAMP binds PKAr and induces the conformational release of PKAc. **(4)** PKAc is now catalytically active and able to associate with ATP (red square) and substrates (blue octagon) and **(5)** catalyse substrate phosphorylation; the transfer of the terminal phosphate (red P) of ATP to specific serine/threonine residues of the substrate protein.

Appendix B
Comparison of putative BK channel leucine zipper motifs

Appendix B a: The putative leucine zipper 1 (LZ1) and 2 (LZ2) sequences from the murine BK channel. Schematic of channel (not to scale) as Figure 1.4 with numbering as STREX splice variant (See Figure 1.3) illustrating the LZ1 and LZ2 sequences and their positions relative to the STREX S4 and S869 PKA-phosphorylation sites (red asterisks). The standard one letter amino acid code is used.

Appendix B b: Alignment of the region equivalent to the mouse LZ1 motif in the BK channels of other species. Numbering of sequences as http://www.ncbi.gov.uk [341]. Heptad sequence, a-g, is illustrated in the top row with the critical ***d*** residue highlighted. Residues that may function successfully at this point, *i.e.,* leucine (L), isoleucine (I) and phenylalanine (F), valine (V) and asparagine (Q), are also highlighted whereas residue that are unlikely to form a functional leucine zipper ***d*** residue, including aspartate (D), glutamate (E), arginine (R) and lysine (K) are not. For comparison, the LZ2 sequences is illustrated in grey below the alignment and shows that murine LZ2 possesses one less leucine zipper heptad than murine LZ1. This may be an influential factor in the differential abilities of LZ1 and LZ2 to interact with PKAc (See Section 5.2.1.4.1). The leucine residues of LZ1 and LZ2 that were mutated in this study are indicated by blue highlighting. The standard one letter amino acid code is used.

Appendix B

Comparison of putative BK channel leucine zipper motifs

a.

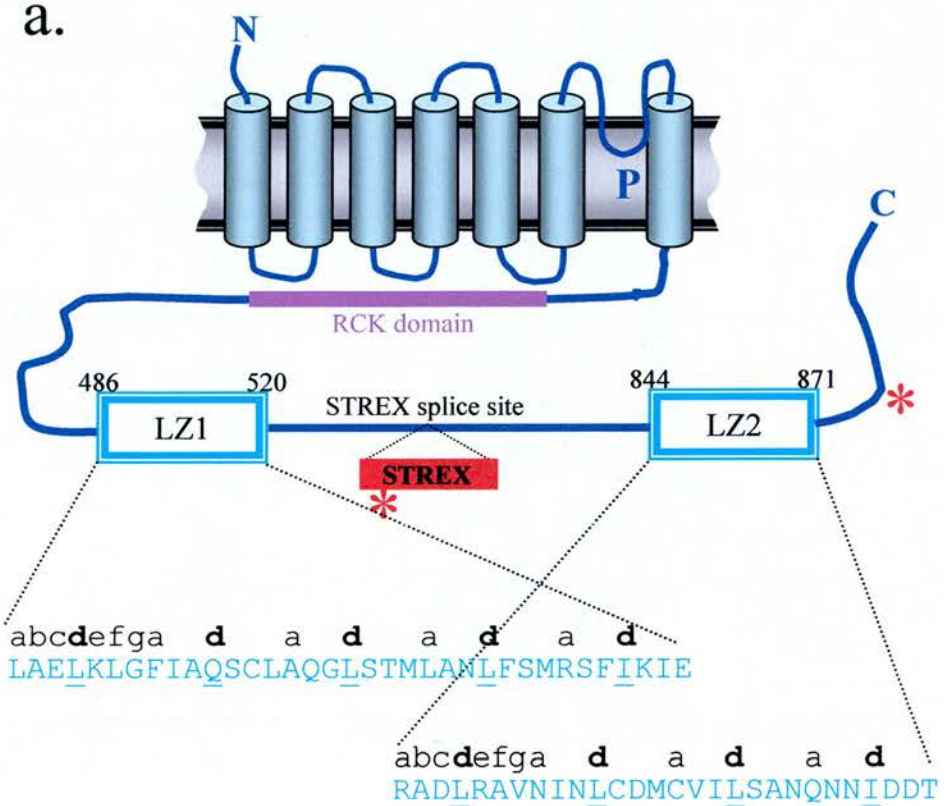

b.

```
                        abcdefga  d   a  d   a  d   a  d
      Mouse    (486)    LAELKLGFIAQSCLAQGLSTMLANLFSMRSFIKIE
      Human    (486)    LAELKLGFIAQSCLAQGLSTMLANLFSMRSFIKIE
        Rat    (539)    LAELKLGFIAQSCLAQGLSTMLANLFSMRSFIKIE
     Bovine    (552)    LAELKLGFIAQSCLAQGLSTMLANLFSMRSFIKIE
        Dog    (486)    LAELRLGFIAQSCLAQGLSTMLANLFSIGSFIKIE
    Chicken    (510)    LAELKLGFIAQSSLAPGLSTMLANLFSMRSFIKIE
    Xenopus    (519)    LAELKLGFIAQSCLAQGLSTMLANLFSMRSFIKIE
Drosophila     (484)    LAELKLGFIAQSCLAPGFSTMMANLFAMRSFKTSP
 C.elegans     (515)    LAELKLGFIAQSCLAPGFSTMMANLFAMRSFKTSQ
    MthK2TM    (231)    PVFISGRLMSRSIDDGYEAMFVQDVLAEESTRRMV

 Mouse LZ2     (844)    RADLRAVNINLCDMCVILSANQNNIDDTSLQDKEC
```

Appendix C

Co-immunoprecipitation assays of PKAc with ZERO-HA and ZERO-mLZ-HA channels: Immunoprecipitation by α-HA

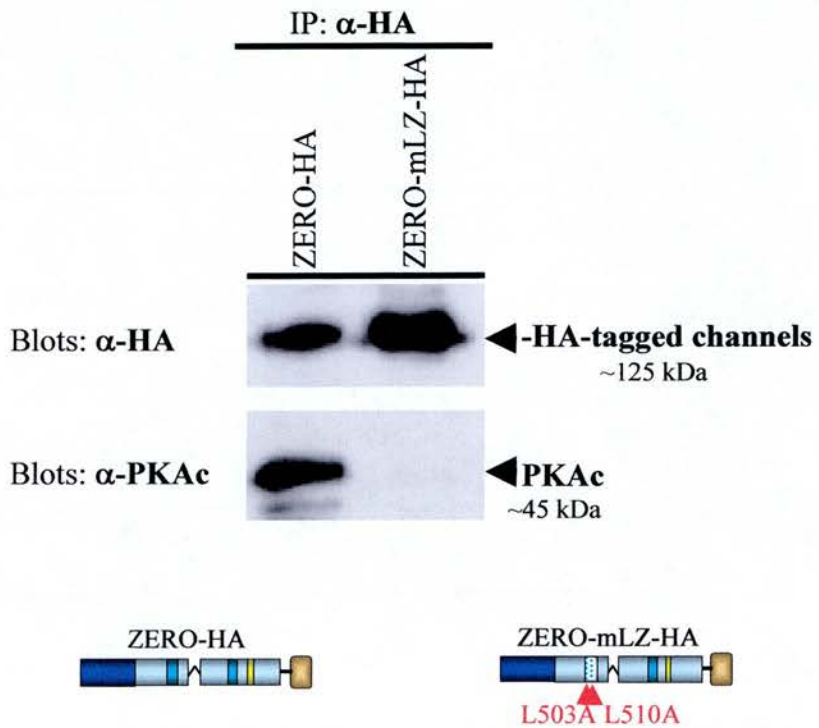

Appendix C: Representative Western blots of ZERO-HA & ZERO-mLZ-HA BK channel co-immunoprecipitation with PKAc. Cell lysates from stable cell lines of ZERO-HA & ZERO-mLZ-HA BK channels (illustrated below blots, See Figure 3.13) transfected with excess free PKAc were immunoprecipitated (IP) by α-HA. IPs were probed for free PKAc & -HA-tagged channels by Western blotting. HA-tagged channels (~125 kDa) and PKAc (~45 kDa) were detected in cell lysates (results not shown) and co-IP of PKAc and ZERO-HA was observed following IP. PKAc did not co-IP with ZERO-mLZ-HA. Western blot analysis: sheep α-PKAc 1/5000, rabbit α-HA 1/333, α-sheep-HRP 1/2000, α-rabbit-HRP 1/2000, detection by ECL.
Results courtesy of Dr Lijun Tian.

Bibliography

1. Hille, B., *Ionic Channels of Excitable Membranes*. 1992, Sunderland, MA: Sinaur.
2. Brown, A., *Functional Basis for Interpreting Amino Acid Sequences of Voltage-Dependent Potassium Channels.* Annual Review Biophysical Biomolecular Structure, 1993. **22**: 173-198.
3. Coetzee, W.A., Amarillo, Y., Chui, J., Chow, A., Lau, D., McCormack, T., Moreno, H., Nadal, M.S., Ozaita, A., Pountney, D., Saganich, M., De Miera, E.V.S. and Ruby, B., *Molecular Diversity of K+ Channels*, in *Molecular and Functional Diversity of Ion Channels and Receptors*. 1999. p. 233-285.
4. Vergara, C., Latorre, R., Marrion, N.V. and Adelman, J.P., *Calcium Activated Potassium Channels.* Current Opinion in Neurobiology, 1998. **8**: 321-329.
5. Toro, L., Wallner, M., Meera, P. and Tanaka, Y., *Maxi-K, A Unique Member of the Voltage Gated K Channel Superfamily.* News Physiological Science, 1998. **13**: 112-117.
6. Weiger, T.M., Hermann, A. and Levitan, I.B., *Modulation of Calcium-Activated Potassium Channels.* Journal of Comparative Physiology a-Neuroethology Sensory Neural and Behavioral Physiology, 2002. **188**: 79-87.
7. Gribkoff, V.K., Starrett, J.E. and Dworetzky, S.I., *Maxi-K Potassium Channels: Form, Function and Modulation of a Class of Endogenous Regulators of Intracellular Calcium.* Neuroscientist, 2001. **7**: 166-177.
8. Schreiber, M., Yuan, A. and Salkoff, L., *Transplantable Sites Confer Calcium Sensitivity to BK Channels.* Nature Neuroscience, 1999. **2**: 416-421.
9. Coronado, R., Rosenberg, R.L. and Miller, C., *Ionic Selectivity, Saturation and Block in a K^+-Selective Channel from Sarcoplasmic Reticulum*, Journal of General Physiology, 1980. **76**: 425-446.
10. Adelman, J.P., Shen, K.Z., Kavanaugh, M.P., Warren, R.A., Wu, Y.N., Lagrutta, A., Bond, C.T. and North, R.A., *Calcium-Activated Potassium Channels Expressed from Cloned Complementary DNAs.* Neuron, 1992. **9**: 209-216.
11. Atkinson, N.S., Robertson, G.A. and Ganetzky, B., *A Component of Calcium-Activated Potassium Channels Encoded by the Drosophila-Slo Locus.* Science, 1991. **253**: 551-555.
12. Butler, A., Tsunoda, S., McCobb, D.P., Wei, A. and Salkoff, L., *mSlo, a Complex Mouse Gene Encoding Maxi Calcium-Activated Potassium Channels.* Science, 1993. **261**: 221-224.
13. TsengCrank, J., Foster, C.D., Krause, J.D., Mertz, R., Godinot, N., DiChiara, T.J. and Reinhart, P.H., *Cloning, Expression and Distribution of Functionally Distinct Ca2+-Activated K+ Channel Isoforms from Human Brain.* Neuron, 1994. **13**: 1315-1330.
14. Dworetzky, S.I., Trojnacki, J.T. and Gribkoff, V.K., *Cloning and Expression of a Human Large-Conductance Calcium-Activated Potassium Channel.* Molecular Brain Research, 1994. **27**: 189-193.
15. Laver, D.R., Fairley, K.A. and Walker, N.A., *Ion Permeation in a K+ Channel in Chara-australis - Direct Evidence for Diffusion Limitation of Ion Flow in a Maxi-K Channel.* Journal of Membrane Biology, 1989. **108**: 153-164.
16. Latorre, R., Oberhauser, A., Labarca, P. and Alvarez, O., *Varieties of Calcium-Activated Potassium Channels.* Annual Review of Physiology, 1989. **51**: 385-399.
17. Behrens, M.I., Vergara, C. and Latorre, R., *Calcium-Activated Potassium Channels of Large Unitary Conductance.* Brazilian Journal of Medical and Biological Research, 1988. **21**: 1101-1117.
18. Jacquin, T. and Grunol, D., *Ca2+ Regulation of a Large Conductance K+ Channel in Cultured Rat Cerebellar Purkinje Neurons.* European Journal of Neuroscience, 1999. **11**: 735-739.

19. Sun, X.P., Schlichter, L.C. and Stanley, E.F., *Single-Channel Properties of BK-Type Calcium-Activated Potassium Channels at a Cholinergic Presynaptic Nerve Terminal.* Journal of Physiology-London, 1999. **518**: 639-651.
20. Dopico, A.M., Widmer, H., Wang, G., Lemos, J.R. and Treistman, S.N., *Rat Supraoptic Magnocellular Neurones Show Distinct Large Conductance, Ca2+-Activated K+ Channel Subtypes in Cell Bodies Versus Nerve Endings.* Journal of Physiology-London, 1999. **519**: 101-114.
21. Sah, P., *Ca2+-Activated K+ Currents in Neurones: Types, Physiological Roles and Modulation.* Trends in Neurosciences, 1996. **19**: 150-154.
22. Sah, P. and Bekkers, J.M., *Apical Dendritic Location of Slow Afterhyperpolarization Current in Hippocampal Pyramidal Neurons: Implications for the Integration of Long-Term Potentiation.* Journal of Neuroscience, 1996. **16**: 4537-4542.
23. Poolos, N.P. and Johnston, D., *Calcium-Activated Potassium Conductances Contribute to Action Potential Repolarization at the Soma but not the Dendrites of Hippocampal CA1 Pyramidal Neurons.* Journal of Neuroscience, 1999. **19**: 5205-5212.
24. Hu, H., Shoa, L.R., Chavoshy, S., Gu, N., Trieb, M., Behrens, R., Laake, P., Pongs, O., Knaus, H.G., Ottersen, O.P. and Storm, J.F., *Presynaptic Ca2+-Activated K+ Channels in Glutamatergic Hippocampal Terminals and Their Role in Spike Repolarization and Regulation of Transmitter Release.* Journal of Neuroscience, 2001. **21**: 9585-9597.
25. Armstrong, C.E. and Roberts, W.M., *Rapidly Inactivating and Non-Inactivating Calcium-Activated Potassium Currents in Frog Saccular Hair Cells.* Journal of Physiology-London, 2001. **536**: 49-65.
26. Navaratnam, D.S., Bell, T.J., Tu, T.D., Cohen, E.L. and Oberholtzer, J.C, *Differential Distribution of Ca2+-Activated K+ Channel Splice Variants Among Hair Cells Along the Tonotopic Axis of the Chick Cochlea.* Neuron, 1997. **19**: 1077-1085.
27. Rosenblatt, K.P., Sun, Z.P., Heller, S. and Hudspeth, A.J., *Distribution of Ca2+-Activated K+ Channel Isoforms Along the Tonotopic Gradient of the Chicken's Cochlea.* Neuron, 1997. **19**: 1061-1075.
28. Wu, Y.C., Art, J.J., Goodman, M.B. and Fettiplace, R., *A Kinetic Description of the Calcium-Activated Potassium Channel and its Application to Electrical Tuning of Hair-Cells.* Progress in Biophysics & Molecular Biology, 1995. **63**: 131-158.
29. Ramanathan, K., Michael, T.H., Jiang, G.J., Hiel, H. and Fuchs, P.A., *A Molecular Mechanism for Electrical Tuning of Cochlear Hair Cells.* Science, 1999. **283**: 215-217.
30. Art, J.J., Wu, Y.C. and Fettiplace, R., *The Calcium-Activated Potassium Channels of Turtle Hair-Cells.* Journal of General Physiology, 1995. **105**: 49-72.
31. Huang, Y., Ko, W.H., Chung, Y.W. and Wong, P.Y.D., *Identification of Calcium-Activated Potassium Channels in Cultured Equine Sweat Gland Epithelial Cells.* Experimental Physiology, 1999. **84**: 881-895.
32. James, A.F. and Okada, Y., *Maxi K+ Channels From the Apical Membranes of Rabbit Oviduct Epithelial-Cells.* Journal of Membrane Biology, 1994. **137**: 109-118.
33. Pardal, R., Ludewig, U., Garcia-Hirschfeld, J. and Lopez-Barneo, J., *Secretory Responses of Intact Glomus Cells in Thin Slices of Rat Carotid Body to Hypoxia and Tetraethylammonium.* Proceedings of the National Academy of Sciences of the United States of America, 2000. **97**: 2361-2366.
34. Lovell, P.V., James, D.G. and McCobb, C.P., *Bovine Versus Rat Adrenal Chromaffin Cells: Big Differences in BK Potassium Channel Properties.* Journal of Neurophysiology, 2000. **83**: 3277-3286.

35. Tabcharani, J.A. and Misler, S., *Ca-2+-Activated K+-Channel in Rat Pancreatic-Islet β-Cells - Permeation, Gating and Blockade by Cations.* Biochimica et Biophysica Acta, 1989. **982**: 62-72.
36. Ahern, G.P., Hsu, S.F. and Jackson, M.B., *Direct Actions of Nitric Oxide on Rat Neurohypophysial K+ Channels.* Journal of Physiology-London, 1999. **520**: 165-176.
37. Stockand, J.D. and Sansom, S.C., *Glomerular Mesangial Cells: Electrophysiology and Regulation of Contraction.* Physiological Reviews, 1998. **78**: 723-744.
38. Schueller, G.H., *Thrill or Chill.* New Scientist, 2000. **166**: 20-24.
39. Faber, E.S.L. and Sah, P., *Physiological Role of Calcium-Activated Potassium Currents in the Rat Lateral Amygdala.* Journal of Neuroscience, 2002. **22**: 1618-1628.
40. Imaizumi, Y., Henmi, S., Uyama, Y., Atsuki, K., Torii, Y., Ohizumi, Y. and Watanabe, M., *Characteristics of Ca2+ Release for Activation of K+ Current and Contractile System in Some Smooth Muscles.* American Journal of Physiology-Cell Physiology, 1996. **40**: C772-C782.
41. Vogalis, F., Vincent, T., Qureshi, I., Schmalz, F., Ward, M.W., Sanders, K.M. and Horowitz, B., *Cloning and Expression of the Large-Conductance Ca2+-Activated K+ Channel from Colonic Smooth Muscle.* American Journal of Physiology-Gastrointestinal and Liver Physiology, 1996. **34**: G629-G639.
42. Imaizumi, Y., Torii, Y., Ohi, Y., Nagano, N., Atsuki, K., Yamamura, H., Muraki, K., Watanabe, M. and Bolton, T.B., *Ca2+ Images and K+ Current During Depolarization in Smooth Muscle Cells of the Guinea-Pig Vas Deferens and Urinary Bladder.* Journal of Physiology-London, 1998. **510**: 705-719.
43. Wu, S.N., Li, H.F. and Lo, Y.C., *Characterization of Tetrandrine-Induced Inhibition of Large-Conductance Calcium-Activated Potassium Channels in a Human Endothelial Cell Line (HUV-EC-C).* Journal of Pharmacology and Experimental Therapeutics, 2000. **292**: 188-195.
44. Adeagbo, A.S.O., *1-Ethyl-2-Benzimidazolinone Stimulates Endothelial K-Ca Channels and Nitric Oxide Formation in Rat Mesenteric Vessels.* European Journal of Pharmacology, 1999. **379**: 151-159.
45. Nelson, M.T., Cheng, H., Rubart, M., Santana, L.F., Bonev, A.D., Knot, H.J. and Lederer, W.J., *Relaxation of Arterial Smooth-Muscle by Calcium Sparks.* Science, 1995. **270**: 633-637.
46. Armstead, W.M., *Hypotension Dilates Pial Arteries by K_{ATP} and K_{Ca} Channel Activation.* Brain Research, 1999. **816**: 158-164.
47. Imai, T., Okamoto, T., Yamamoto, Y., Tanaka, H., Koike, K., Shigenobu, K. and Tanaka, Y., *Effects of Different Types of K+ Channel Modulators on the Spontaneous Myogenic Contraction of Guinea-Pig Urinary Bladder Smooth Muscle.* Acta Physiologica Scandinavica, 2001. **173**: 323-333.
48. Snetkov, V.A., Gurney, A.M., Ward, J.P.T. and Osipenko, O.N., *Inward Rectification of the Large Conductance Potassium Channel in Smooth Muscle Cells from Rabbit Pulmonary Artery.* Experimental Physiology, 1996. **81**: 743-753.
49. Snetkov, V.A. and Ward, J.P.T., *Ion Currents in Smooth Muscle Cells from Human Small Bronchioles: Presence of an Inward Rectifier K+ Current and Three Types of Large Conductance K+ Channel.* Experimental Physiology, 1999. **84**: 835-846.
50. Benkusky, N.A., Fergus, D.J., Zucchero, T.M and England, S.K., *Regulation of the Ca2+-Sensitive Domains of the Maxi-K Channel in the Mouse Myometrium During Gestation.* Journal of Biological Chemistry, 2000. **275**: 27712-27719.
51. Khan, S.A., Higdon, N.R. and Meisheri, K.D., *Coronary Vasorelaxation by Nitroglycerin: Involvement of Plasmalemmal Calcium-Activated K+ Channels and*

Intracellular Ca++ Stores. Journal of Pharmacology and Experimental Therapeutics, 1998. **284**: 838-846.

52. Song, Y.M. and Simard, J.M., *Beta-Adrenoceptor Stimulation Activates Large-Conductance Ca2+-Activated K+ Channels in Smooth-Muscle Cells from Basilar Artery of Guinea-Pig.* Pflugers Archiv-European Journal of Physiology, 1995. **430**: 984-993.
53. Song, M., Zhu, N., Olcese, R., Barila, B., Toro, L. and Stefani, E., *Hormonal Control of Protein Expression and mRNA Levels of the MaxiK Channel Alpha Subunit in Myometrium.* FEBS Letters, 1999. **460**: 427-432.
54. Anwer, K., Oberti, C., Perez, G.J., Perezreyes, N., McDougall, J.K., Monga, M., Sanborn, B.M., Stefani, E. and Toro, L., *Calcium-Activated K+ Channels as Modulators of Human Myometrial Contractile Activity.* American Journal of Physiology, 1993. **265**: C976-C985.
55. Christ, G.J., Day, N.S., Day, M., Santizo, C., Zhao, W., Sclafani, T., Zinman, J., Hsieh, K., Venkateswarlu, K., Valcic, M. and Melman, A., *Bladder Injection of "Naked" hSlo/pcDNA3 Ameliorates Detrusor Hyperactivity in Obstructed Rats in vivo.* American Journal of Physiology-Regulatory Integrative and Comparative Physiology, 2001. **281**: R1699-R1709.
56. Kang, J., Huguenard, J.R. and Prince, D.A., Voltage-Gated Potassium Channels Activated During Action Potentials in Layer v Neocortical Pyramidal Neurons. Journal of Neurophysiology, 2000. **83**: 70-80.
57. Laver, D.R. and Walker, N.A., *Activation by Ca2+ and Block by Divalent Ions of the K+-Channel in the Membrane of Cytoplasmic Drops from Chara-australis.* Journal of Membrane Biology, 1991. **120**: 131-139.
58. Xu, W.H., Liu, Y.G., Wang, S., McDonald, T., Van Eyk, J.E., Sidor, A. and O'Rourke, B., *Cytoprotective Role of Ca2+-Activated K+ Channels in the Cardiac Inner Mitochondrial Membrane.* Science, 2002. **298**: 1029-1033.
59. Siemen, D., Loupatatzis, C., Borecky, J., Gulbins, E. and Lang, F., *Ca2+-Activated K Channel of the BK-Type in the Inner Mitochondrial Membrane of a Human Glioma Cell Line.* Biochemical and Biophysical Research Communications, 1999. **257**: 549-554.
60. Elkins, T., Ganetzky, B. and Wu, C.F., *A Drosophila Mutation that Eliminates a Calcium-Dependent Potassium Current.* Proceedings of the National Academy of Sciences of the United States of America, 1986. **83**: 8415-8419.
61. Atkinson, N.S., Brenner, R., Chang, W.M., Wilbur, J., Larimer, J.L. and Yu, J., *Molecular Separation of Two Behavioral Phenotypes by a Mutation Affecting the Promoters of a Ca-Activated K Channel.* Journal of Neuroscience, 2000. **20**: 2988-2993.
62. Elkins, T. and Ganetzky, B., *The Roles of Potassium Currents in Drosophila Flight Muscles.* Journal of Neuroscience, 1988. **8**: 428-434.
63. Warbington, L., Hillman, T., Adams, C. and Stern, M., *Reduced Transmitter Release Conferred by Mutations in the Slowpoke-Encoded Ca2+-Activated K+ Channel Gene of Drosophila.* Invertebrate Neuroscience, 1996. **2**: 51-60.
64. Jan, L.Y. and Jan, Y.N., *Cloned Potassium Channels from Eukaryotes and Prokaryotes.* Annual Review of Neuroscience, 1997. **20**: 91-123.
65. Kaczorowski, G.J., Knaus, H.G., Leonard, R.J., McManus, O.B. and Garcia, M.L., *High-Conductance Calcium-Activated Potassium Channels; Structure, Pharmacology, and Function.* Journal of Bioenergetics and Biomembranes, 1996. **28**: 255-267.
66. Jiang, G.J., Zidanic, M., Michaels, R.L., Michel, T.H., Griguer, C. and Fuchs, P.A., *cSlo Encodes Calcium-Activated Potassium Channels in the Chick's Cochlea.* Proceedings of the Royal Society of London Series B-Biological Sciences, 1997. **264**: 731-737.

67. Moss, G.W.J., Marshall, J., Morabito, M., Howe, J.R. and Moczydlowski, E., *An Evolutionarily Conserved Binding Site for Serine Proteinase Inhibitors in Large Conductance Calcium-Activated Potassium Channels.* Biochemistry, 1996. **35**: 16024-16035.
68. Pallanck, L. and Ganetzky, B., *Cloning and Characterization of Human and Mouse Homologs of the Drosophila Calcium-Activated Potassium Channel Gene, Slowpoke.* Human Molecular Genetics, 1994. **3**: 1239-1243.
69. Saito, M., Nelson, C., Salkoff, L. and Lingle, C.J., *A Cysteine-Rich Domain Defined by a Novel Exon in a Slo Variant in Rat Adrenal Chromaffin Cells and PC12 Cells.* Journal of Biological Chemistry, 1997. **272**: 11710-11717.
70. Chang, W.M., Bohm, R.A., Strauss, J.C., Kwan, T., Thomas, T., Cowmeadow, R.B. and Atkinson, N.S., *Muscle-Specific Transcriptional Regulation of the Slowpoke Ca2+-Activated K+ Channel Gene.* Journal of Biological Chemistry, 2000. **275**: 3991-3998.
71. Lim, M.C., Shipston, M.J. and Antoni, F.A., *Depolarization Counteracts Glucocorticoid Inhibition of Adenohypophysical Corticotroph Cells.* British Journal of Pharmacology, 1998. **124**: 1735-1743.
72. Schreiber, M., Wei, A.G., Yuan, A., Gaut, J., Saito, M. and Salkoff, L., *Slo3, a Novel pH-Sensitive K+ Channel from Mammalian Spermatocytes.* Journal of Biological Chemistry, 1998. **273**: 3509-3516.
73. Brenner, R. and Atkinson, N., *Developmental- and Eye-Specific Transcriptional Control Elements in an Intronic Region of a Ca2+-Activated K+ Channel Gene.* Developmental Biology, 1996. **177**: 536-543.
74. Brenner, R., Thomas, T.O., Becker, M.N. and Atkinson, N.S., *Tissue-Specific Expression of a Ca2+-Activated K+ Channel is Controlled by Multiple Upstream Regulatory Elements.* Journal of Neuroscience, 1996. **16**: 1827-1835.
75. Brenner, R. and Atkinson, N.S., *Calcium-Activated Potassium Channel Gene Expression in the Midgut of Drosophila.* Comparative Biochemistry and Physiology B-Biochemistry & Molecular Biology, 1997. **118**: 411-420.
76. Sharp, A., *On the Origin of RNA Splicing.* Cell, 1985. **42**: 397-400.
77. Grabowski, P.J. and Black, D.L., *Alternative RNA Splicing in the Nervous System.* Progress in Neurobiology, 2001. **65**: 289-308.
78. Dredge, B.K., Polydorides, A.D. and Darnell, R.B., *The Splice of Life: Alternative Splicing and Neurological Disease.* Nature Reviews Neuroscience, 2001. **2**: 43-50.
79. Akker, S.A., Smith, P.J. and Chew, S.L., *Nuclear Post-Transcriptional Control of Gene Expression.* Journal of Molecular Endocrinology, 2001. **27**: 123-131.
80. Shipston, M.J., Duncan, R.R., Clark, A.G., Antoni, F.A. and Tian, L.J., *Molecular Components of Large Conductance Calcium-Activated Potassium (BK) Channels in Mouse Pituitary Corticotropes.* Molecular Endocrinology, 1999. **13**: 1728-1737.
81. Shipston, M.J., *Alternative Splicing of Potassium Channels: A Dynamic Switch of Cellular Excitability.* Trends in Cell Biology, 2001. **11**: 353-358.
82. Ha, T.S., Jeong, S.Y., Cho, S.W., Jeon, H.K., Roh, G.S., Choi, W.S. and Park, C.S., *Functional Characteristics of Two BK_{Ca} Channel Variants Differentially Expressed in Rat Brain Tissues.* European Journal of Biochemistry, 2000. **267**: 910-918.
83. Liu, X.J., Chang, Y.C., Reinhart, P.H. and Sontheimer, H., *Cloning and Characterization of Glioma BK, a Novel BK Channel Isoform Highly Expressed in Human Glioma Cells.* Journal of Neuroscience, 2002. **22**: 1840-1849.
84. Xie, J.Y. and McCobb, D.P., *Control of Alternative Splicing of Potassium Channels by Stress Hormones.* Science, 1998. **280**: 443-446.

85. Lagrutta, A., Shen, K.Z., North, R.A. and Adelman, J.P., *Functional Differences Among Alternatively Spliced Variants of Slowpoke, a Drosophila Calcium-Activated Potassium Channel.* Journal of Biological Chemistry, 1994. **269**: 20347-20351.
86. Muller, Y.L., Reitstetter, R. and Yool, A.J., *Regulation of Ca2+-Dependent K+ Channel Expression in Rat Cerebellum During Postnatal Development.* Journal of Neuroscience, 1998. **18**: 16-25.
87. Martin-Caraballo, M. and Dryer, S.E., *Activity- and Target-Dependent Regulation of Large-Conductance Ca2+-Activated K+ Channels in Developing Chick Lumbar Motoneurons.* Journal of Neuroscience, 2002. **22**: 73-81.
88. Lovell, P.V. and McCobb, D.P., *Pituitary Control of BK Potassium Channel Function and Intrinsic Firing Properties of Adrenal Chromaffin.* Journal of Neuroscience, 2001. **21**: 3429-3442.
89. Lai, G.J. and McCobb, D.P., *Opposing Actions of Adrenal Androgens and Glucocorticoids on Alternative Splicing of Slo Potassium Channels in Bovine Chromaffin Cells.* Proceedings of the National Academy of Sciences of the United States of America, 2002. **99**: 7722-7727.
90. Prakriya, M., Solaro, C.R. and Lingle, C.J., *[Ca2+](i) Elevations Detected by BK Channels During Ca2+ Influx and Muscarine-Mediated Release of Ca2+ from Intracellular Stores in Rat Chromaffin Cells.* Journal of Neuroscience, 1996. **16**: 4344-4359.
91. Xie, J.Y. and Black, D.L., *A CAMKIV Responsive RNA Element Mediates Depolarization-Induced Alternative Splicing of Ion Channels.* Nature, 2001. **410**: 936-939.
92. Sansom, M.S.P., *Ion Channels: A First View of K Channels in Atomic Glory.* Current Biology, 1998: R450-452.
93. Choe, S., *Potassium Channel Structures.* Nature Reviews Neuroscience, 2002. **3**: 115-121.
94. Doyle, D.A., Cabral, J.M., Pfuetzner, R.A., Kuo, A.L., Gulbis, J.M., Cohen, S.L., Chait, B.T. and MacKinnon, R., *The Structure of the Potassium Channel: Molecular Basis of K+ Conduction and Selectivity.* Science, 1998. **280**: 69-77.
95. Hille, B., *Potassium Channels in Myelinated Nerve: Selective Permeability to Small Cation.* Journal of General Physiology, 1973. **61**: 669-686.
96. Yellen, G., *Permeation in Potassium Channels: Implications for Channel Structure.* Annual Review of Biophysical and Biophysiological Chemistry 1987. **16**: 227-246.
97. Heginbotham, L., Lu, Z., Abramson, T. and MacKinnon, R., *Mutations in the K+ Channel Signature Sequence.* Biophysical Journal, 1994. **66**: 1061-1067.
98. Proks, P., Capener, C.E., Jones, P. and Ashcroft, F.M., *Mutations Within the P-Loop of Kir6.2 Modulate the Intraburst Kinetics of the ATP-Sensitive Potassium Channel.* Journal of General Physiology, 2001. **118**: 341-353.
99. Lopez, G.A., Jan, Y.N. and Jan, L.Y., *Evidence that the S6 Segment of the Shaker Voltage-Gated K+ Channel Comprises Part of the Pore.* Nature, 1994. **367**: 179-182.
100. Heginbotham, L. and MacKinnon, R., *The Aromatic Binding-Site for Tetraethylammonium Ion on Potassium Channels.* Neuron, 1992. **8**: 483-491.
101. Heginbotham, L., Abramson, T. and MacKinnon, R., *A Functional Connection Between the Pores of Distantly Related Ion Channels as Revealed by Mutant K+ Channels.* Science, 1992. **258**: 1152-1155.
102. Kehl, S.J. and Wong, K., *Large-Conductance Calcium-Activated Potassium Channels of Cultured Rat Melanotrophs.* Journal of Membrane Biology, 1996. **150**: 219-230.

103. Lagrutta, A.A., Shen, K.Z., Rivard, A., North, R.A. and Adelman, J.P., *Aromatic Residues Affecting Permeation and Gating in dSlo BK Channels.* Pflugers Archiv-European Journal of Physiology, 1998. **435**: 731-739.
104. Lu, T., Katakam, P.V.G., Vanrollins, M., Weintraub, N.L., Spector, A.A. and Lee, H.C., *Dihydroxyeicosatrienoic Acids are Potent Activators of Ca2+-Activated K+ Channels in Isolated Rat Coronary Arterial Myocytes.* Journal of Physiology-London, 2001. **534**: 651-667.
105. Rudy, B., Kentros, C., Weiser, M., Fruhling, D., Serodio, P., Demiera, E.V.S., Ellisman, M.H., Pollock, J.A. and Baker, H., *Region-Specific Expression of a K+ Channel Gene in Brain.* Proceedings of the National Academy of Sciences of the United States of America, 1992. **89**: 4603-4607.
106. Mullmann, T.J., Spence, K.T., Schroeder, N.E., Fremont, V., Christian, E.P. and Giangiacomo, K.M., *Insights into Alpha-K Toxin Specificity for K+ Channels Revealed Through Mutations in Noxiustoxin.* Biochemistry, 2001. **40**: 10987-10997.
107. Rauer, H., Lanigan, M.D., Pennington, M.W., Aiyar, J., Ghanshani, S., Cahalan, M.D., Norton, R.S. and Chandy, K.G., *Structure-Guided Transformation of Charybdotoxin Yields an Analog that Selectively Targets Ca2+-Activated Over Voltage-Gated K+ Channels.* Journal of Biological Chemistry, 2000. **275**: 1201-1208.
108. Lippiat, J.D., Standen, N.B. and Davies, N.W., *Block of Cloned BK_{Ca} Channels (rSlo) Expressed in HEK 293 Cells by N-Methyl D-Glucamine.* Pflugers Archiv-European Journal of Physiology, 1998. **436**: 810-812.
109. Shi, J.Y. and Cui, J.M., *Intracellular Mg2+ Enhances the Function of BK-Type Ca2+-Activated K+ Channels.* Journal of General Physiology, 2001. **118**: 589-605.
110. Pascual, J.M., Shieh, C.C., Kirsch, G.E. and Brown, A.M., *Multiple Residues Specify External Tetraethylammonium Blockade in Voltage-Gated Potassium Channels.* Biophysical Journal, 1995. **69**: 428-434.
111. Kirsch, G.E., Pascual, J.M. and Shieh, C.C., *Functional-Role of a Conserved Aspartate in the External Mouth of Voltage-Gated Potassium Channels.* Biophysical Journal, 1995. **68**: 1804-1813.
112. Cha, A., Snyder, G.E., Selvin, P.R. and Bezanilla, F., *Atomic Scale Movement of the Voltage-Sensing Region in a Potassium Channel Measured via Spectroscopy.* Nature, 1999. **402**: 809-813.
113. Diaz, L., Meera, P., Amigo, J., Stefani, E., Alvarez, O., Toro, L. and Latorre, R., *Role of the S4 Segment in a Voltage-Dependent Calcium-Sensitive Potassium (hSlo) Channel.* Journal of Biological Chemistry, 1998. **273**: 32430-32436.
114. Liman, E., *Voltage-Sensing Residues in the S4 Region of a Mammalian K Channel.* Nature, 1991. **332**: 837-839.
115. Ohlenschlager, O., Hojo, H., Ramachandran, R., Gorlach, M. and Haris, P.I., *Three-Dimensional Structure of the S4-S5 Segment of the Shaker Potassium Channel.* Biophysical Journal, 2002. **82**: 2995-3002.
116. Giangiacomo, K.M., Garcia, M.L. and McManus, O.B., *Mechanism of Iberiotoxin Block of the Large-Conductance Calcium-Activated Potassium Channel from Bovine Aortic Smooth- Muscle.* Biochemistry, 1992. **31**: 6719-6727.
117. Giangiacomo, K.M., Sugg, E.E., Garciacalvo, M., Leonard, R.J., McManus, O.B., Kaczorowski, G.J. and Garcia, M.L., *Synthetic Charybdotoxin Iberiotoxin Chimeric Peptides Define Toxin Binding-Sites on Calcium-Activated and Voltage-Dependent Potassium Channels.* Biochemistry, 1993. **32**: 2363-2370.

118. Giangiacomo, K.M., Gabriel, J., Fremont, V. and Mullmann, T.J., *Probing the Structure and Function of Potassium Channels with Alpha-K Toxin Blockers.* Perspectives in Drug Discovery and Design, 1999. **16**: 167-186.
119. Molinari, E.J., Sullivan, J.P., Wan, Y.P., Brioni, J.D. and Gopalakrishnan, M., *Characterization and Modulation of [I-125]Iberiotoxin-D19Y/Y36F Binding in the Guinea-Pig Urinary Bladder.* European Journal of Pharmacology, 2000. **388**: 155-161.
120. Mullmann, T.J., Munujos, P., Garcia, M.L. and Giangiacomo, K.M., *Electrostatic Mutations in Iberiotoxin as a Unique Tool for Probing the Electrostatic Structure of the Maxi-K Channel Outer Vestibule.* Biochemistry, 1999. **38**: 2395-2402.
121. Meera, P., Wallner, M., Song, M. and Toro, L., *Large Conductance Voltage- and Calcium-Dependent K+ Channel, a Distinct Member of Voltage-Dependent Ion Channels with Seven N-Terminal Transmembrane Segments (S0-S6), an Extracellular N Terminus, and an Intracellular (S9-S10) C Terminus.* Proceedings of the National Academy of Sciences of the United States of America, 1997. **94**: 14066-14071.
122. Tanaka, Y., Meera, P., Song, M., Knaus, H.G. and Toro, L., *Molecular Constituents of Maxi K-Ca Channels in Human Coronary Smooth Muscle: Predominant Alpha+Beta Subunit Complexes.* Journal of Physiology-London, 1997. **502**: 545-557.
123. Wei, A., Solaro, C., Lingle, C. and Salkoff, L., *Calcium Sensitivity of BK-Type K-Ca Channels Determined by a Separable Domain.* Neuron, 1994. **13**: 671-681.
124. Schreiber, M. and Salkoff, L., *A Novel Calcium-Sensing Domain in the BK Channel.* Biophysical Journal, 1997. **73**: 1355-1363.
125. Zhou, Y., Schopperle, W.M., Murrey, H., Jaramillo, A., Dagan, D., Griffith, L.C. and Levitan, I.B., *A Dynamically Regulated 14-3-3, Slob, and Slowpoke Potassium Channel Complex in Drosophila Presynaptic Nerve Terminals.* Neuron, 1999. **22**: 809-818.
126. Zhang, X., Solaro, C.R. and Lingle, C.J., *Allosteric Regulation of BK Channel Gating by Ca2+ and Mg2+ Through a Nonselective, Low Affinity Divalent Cation Site.* Journal of General Physiology, 2001. **118**: 607-635.
127. Jiang, Y.X., Lee, A., Chen, J.Y., Cadene, M., Chait, B.T. and MacKinnon, R., *Crystal Structure and Mechanism of a Calcium-Gated Potassium Channel.* Nature, 2002. **417**: 515-522.
128. Piskarowski, R. and Aldrich, R.W., *Calcium activation of BKCa Potassium Channels Lacking the Calcium Bowl and RCK Domains.* Nature, 2002. **420**: 499-502.
129. Stefani, E., Ottolia, M., Noceti, F., Olcese, R., Wallner, M., Latorre, R. and Toro, L., *Voltage-Controlled Gating in a Large Conductance Ca2+-Sensitive K(+)Channel (hSlo).* Proceedings of the National Academy of Sciences of the United States of America, 1997. **94**: 5427-5431.
130. Cui, J., Cox, D.H. and Aldrich, R.W., *Intrinsic Voltage Dependence and Ca2+ Regulation of mSlo Large Conductance Ca-Activated K+ Channels.* Journal of General Physiology, 1997. **109**: 647-673.
131. Horrigan, F.T., Cui, J.M. and Aldrich, R.W., *Allosteric Voltage Gating of Potassium Channels i - mSlo Ionic Currents in the Absence of Ca2+.* Journal of General Physiology, 1999. **114**: 277-304.
132. Horrigan, F.T. and Aldrich, R.W., *Allosteric Voltage Gating of Potassium Channels ii - mSlo Channel Gating Charge Movement in the Absence of Ca2+.* Journal of General Physiology, 1999. **114**: 305-336.
133. Cox, D.H., Cui, J. and Aldrich, R.W., *Allosteric Gating of a Large Conductance Ca-Activated K+ Channel.* Journal of General Physiology, 1997. **110**: 257-281.

134. Moss, B.L., Silberberg, S.D., Nimigean, C.M. and Magleby, K.L., *Ca2+-Dependent Gating Mechanisms for dSlo, a Large-Conductance Ca2+-Activated K+ (BK) Channel.* Biophysical Journal, 1999. **76**: 3099-3117.
135. Hong, K.H., Armstrong, C.M. and Miller, C., *Revisiting the Role of Ca2+ in Shaker K+ Channel Gating.* Biophysical Journal, 2001. **80**: 2216-2220.
136. Ahring, P.K., Strobaek, D., Christophersen, P., Olesen, S.P. and Johansen, T.E., *Stable Expression of the Human Large-Conductance Ca2+-Activated K+ Channel Alpha- and Beta-Subunits in HEK293 Cells.* FEBS Letters, 1997. **415**: 67-70.
137. Cox, D.H., Cui, J. and Aldrich, R.W., *Separation of Gating Properties from Permeation and Block in mSlo Large Conductance Ca-Activated K+ Channels.* Journal of General Physiology, 1997. **109**: 633-646.
138. Muller, M., Madan, D. and Levitan, I.B., *State-Dependent Modulation of mSlo, a Cloned Calcium-Dependent Potassium Channel.* Neuropharmacology, 1996. **35**: 877-886.
139. Talukder, G. and Aldrich, R.W., *Complex Voltage-Dependent Behavior of Single Unliganded Calcium-Sensitive Potassium Channels.* Biophysical Journal, 2000. **78**: 761-772.
140. Rothberg, B.S. and Magleby, K.L., *Gating Kinetics of Single Large-Conductance Ca2+-Activated K+ Channels in High Ca2+ Suggest a Two-Tiered Allosteric Gating Mechanism.* Journal of General Physiology, 1999. **114**: 93-124.
141. Magleby, K.L., *Kinetic Gating Mechanisms for BK Channels: When Complexity Leads to Simplicity.* Journal of General Physiology, 2001. **118**: 583-587.
142. Bowlby, M.R. and Levitan, I.B., *Kinetic Variability and Modulation of dSlo, a Cloned Calcium-Dependent Potassium Channel.* Neuropharmacology, 1996. **35**: 867-875.
143. Kreusch, A., Pfaffinger, P.J., Stevens, C.F. and Choe, S., *Crystal Structure of the Tetramerization Domain of the Shaker Potassium Channel.* Nature, 1998. **392**: 945-948.
144. Li, M., Jan, Y.N. and Jan, L.Y., *Specification of Subunit Assembly by the Hydrophilic Amino-Terminal Domain of the Shaker Potassium Channel.* Science, 1992. **257**: 1225-1230.
145. Jiang, Y.X., Pico, A., Cadene, M., Chait, B.T. and MacKinnon, R., *Structure of the RCK Domain from the E. Coli K+ Channel and Demonstration of its Presence in the Human BK Channel.* Neuron, 2001. **29**: 593-601.
146. Quirk, J.C. and Reinhart, P.H., *Identification of a Novel Tetramerization Domain in Large Conductance K-Ca Channels*, Neuron, 2001. **32**: 13-23.
147. Roosild, T.P., Miller, S., Booth, I.R. and Choe, S., *A Mechanism of Regulating Transmembrane Potassium Flux Through a Ligand-Mediated Conformational Switch.* Cell, 2002. **109**: 781-791.
148. Ungar, D., Barth, A., Haase, W., Kaunzinger, A., Lewitzki, E., Ruiz, T., Reilander, H. and Michel, H., *Analysis of a Putative Voltage-Gated Prokaryotic Potassium Channel.* European Journal of Biochemistry, 2001. **268**: 5386-5396.
149. MacKinnon, R., *Determination of the Subunit Stoichiometry of a Voltage-Activated Potassium Channel.* Nature, 1991. **350**: 232-235.
150. Wang, H., Kunkel, D.D., Martin, T.M., Schwartzkroin, P.A. and Tempel, B.L., *Heteromultimeric K+ Channels in Terminal and Juxtaparanodal Regions of Neurons.* Nature, 1993. **365**: 75-79.
151. Isacoff, E.Y., Jan, Y.N. and Jan, L.Y., *Evidence for the Formation of Heteromultimeric Potassium Channels in Xenopus-Oocytes.* Nature, 1990. **345**: 530-534.
152. Ruppersberg, J.P., Schroter, K.H., Sakmann, B., Stocker, M., Sewing, S. and Pongs, O., *Heteromultimeric Channels Formed by Rat-Brain Potassium-Channel Proteins.* Nature, 1990. **345**: 535-537.

153. Christie, M.J., North, R.A., Osborne, P.B., Douglass, J. and Adelman, J.P., *Heteropolymeric Potassium Channels Expressed in Xenopus Oocytes from Cloned Subunits.* Neuron, 1990. **4**: 405-411.
154. Sheng, M., Liao, Y.J., Jan, Y.N. and Jan, L.Y., *Presynaptic A-Current Based on Heteromultimeric K+ Channels Detected in-vivo.* Nature, 1993. **365**: 72-75.
155. Covarrubias, M., Wei, A. and Salkoff, L., *Shaker, Shal, Shab, and Shaw Express Independent K+ Current Systems.* Neuron, 1991. **7**: 763-773.
156. Ding, J.P., Li, Z.W. and Lingle, C.J., *Inactivating BK Channels in Rat Chromaffin Cells May Arise from Heteromultimeric Assembly of Distinct Inactivation-Competent and Noninactivating Subunits.* Biophysical Journal, 1998. **74**: 268-289.
157. Joiner, W.J., Tang, M.D., Wang, L.Y., Dworetzky, S.I., Boissard, C.G., Gan, L., Gribkoff, V.K. and Kaczmarek, L.K., *Formation of Intermediate-Conductance Calcium-Activated Potassium Channels by Interaction of Slack and Slo Subunits.* Nature Neuroscience, 1998. **1**: 462-469.
158. Knaus, H.G., Eberhart, A., Koch, R.O.A., Munujos, P., Schmalhofer, W.A., Warmke, J.W., Kaczorowski, G.J. and Garcia, M.L., *Characterization of Tissue-Expressed Alpha-Subunits of the High-Conductance Ca2+-Activated K+ Channel.* Journal of Biological Chemistry, 1995. **270**: 22434-22439.
159. Wallner, M., Meera, P. and Toro, L., *Determinant for Beta-Subunit Regulation in High-Conductance Voltage-Activated and Ca2+-Sensitive K+ Channels: An Additional Transmembrane Region at the N Terminus.* Proceedings of the National Academy of Sciences of the United States of America, 1996. **93**: 14922-14927.
160. McManus, O.B., Helms, L.M.H., Pallanck, L., Ganetzky, B., Swanson, R. and Leonard, R.J., *Functional-Role of the Beta-Subunit of High-Conductance Calcium-Activated Potassium Channels.* Neuron, 1995. **14**: 645-650.
161. Chang, C.P., Dworetzky, S.I., Wang, J.C. and Goldstein, M.E., *Differential Expression of the Alpha and Beta Subunits of the Large-Conductance Calcium-Activated Potassium Channel: Implication for Channel Diversity.* Molecular Brain Research, 1997. **45**: 33-40.
162. Isom, L.L., Dejongh, K.S. and Catterall, W.A., *Auxiliary Subunits of Voltage-Gated Ion Channels.* Neuron, 1994. **12**: 1183-1194.
163. Wanner, S.G., Koch, R.O., Koschak, A., Trieb, M., Garcia, M.L., Kaczorowski, G.J. and Knaus, H.G., *High-Conductance Calcium-Activated Potassium Channels in Rat Brain: Pharmacology, Distribution, and Subunit Composition.* Biochemistry, 1999. **38**: 5392-5400.
164. Garciacalvo, M., Knaus, H.G., McManus, O.B., Giangiacomo, K.M., Kaczorowski, G.J. and Garcia, M.L., *Purification and Reconstitution of the High-Conductance, Calcium-Activated Potassium Channel from Tracheal Smooth-Muscle.* Journal of Biological Chemistry, 1994. **269**: 676-682.
165. Knaus, H.G., Garciacalvo, M., Kaczorowski, G.J. and Garcia, M.L., *Subunit Composition of the High-Conductance Calcium-Activated Potassium Channel from Smooth-Muscle, a Representative of the mSlo and Slowpoke Family of Potassium Channels.* Journal of Biological Chemistry, 1994. **269**: 3921-3924.
166. Dworetzky, S.I., Boissard, C.G., Lumragan, J.T., McKay, M.C., Postmunson, D.J., Trojnacki, J.T., Chang, C.P. and Gribkoff, V.K., *Phenotypic Alteration of a Human BK (hSlo) Channel by hSlo Beta Subunit Coexpression: Changes in Blocker Sensitivity, Activation/Relaxation and Inactivation Kinetics, and Protein Kinase A Modulation.* Journal of Neuroscience, 1996. **16**: 4543-4550.

167. TsengCrank, J., Godinot, N., Johansen, T.E., Ahring, P.K., Strobaek, D., Mertz, R., Foster, C.D., Olesen, S.P. and Reinhart, P.H., *Cloning, Expression, and Distribution of a Ca2+-Activated K+ Channel Beta-Subunit from Human Brain.* Proceedings of the National Academy of Sciences of the United States of America, 1996. **93**: 9200-9205.
168. Meera, P., Wallner, M., Jiang, Z., Toro, L., *A Calcium Switch for the Functional Coupling Between Alpha (hSlo) and Beta Subunits (K-v,K-Ca Beta) of Maxi K Channels.* FEBS Letters, 1996. **382**: 84-88.
169. Nimigean, C.M. and Magleby, K.L., *The Beta Subunit Increases the Ca2+ Sensitivity of Large Conductance Ca2+-Activated Potassium Channels by Retaining the Gating in the Bursting States.* Journal of General Physiology, 1999. **113**: 425-439.
170. Ramanathan, K., Michael, T.H. and Fuchs, P.A., *Beta Subunits Modulate Alternatively Spliced, Large Conductance, Calcium-Activated Potassium Channels of Avian Hair Cells.* Journal of Neuroscience, 2000. **20**: 1675-1684.
171. Giangiacomo, K.M., Fremont, V., Mullmann, T.J., Hanner, M., Cox, T.H. and Garcia, M.L., *Interaction of Charybdotoxin S10A with Single Maxi-K Channels: Kinetics of Blockade Depend on the Presence of the Beta 1 Subunit.* Biochemistry, 2000. **39**: 6115-6122.
172. Weiger, T.M., Holmqvist, M.H., Levitan, I.B., Clark, F.T., Sprague, S., Huang, W.J., Ge, P., Wang, C.C., Lawson, D., Jurman, M.E., Glucksmann, M.A., Silos-Santiago, I., Distefano, P.S. and Curtis, R., *A Novel Nervous System Beta Subunit that Downregulates Human Large Conductance Calcium-Dependent Potassium Channels.* Journal of Neuroscience, 2000. **20**: 3563-3570.
173. Ramanathan, K. and Fuchs, P.A., *Modelling Hair Cell Tuning by Expression Gradients of Potassium Channel Beta Subunits.* Biophysical Journal, 2002. **82**: 64-75.
174. Garciacalvo, M., Knaus, H.G., Garcia, M.L., Kaczorowski, G.J. and Kempner, E.S., *Functional Unit Size of the Charybdotoxin Receptor in Smooth- Muscle.* Proceedings of the National Academy of Sciences of the United States of America, 1994. **91**: 4718-4722.
175. Brenner, R., Perez, G.J., Bonev, A.D., Eckman, D.M., Kosek, J.C., Wiler, S.W., Patterson, A.J., Nelson, M.T. and Aldrich, R.W., *Vasoregulation by the Beta 1 Subunit of the Calcium-Activated Potassium Channel.* Nature, 2000. **407**: 870-876.
176. Knaus, H.G., Eberhart, A., Kaczorowski, G.J. and Garcia, M.L., *Covalent Attachment of Charybdotoxin to the Beta-Subunit of the High-Conductance Ca2+-Activated K+ Channel - Identification of the Site of Incorporation and Implications for Channel Topology.* Journal of Biological Chemistry, 1994. **269**: 23336-23341.
177. Nimigean, C.M. and Magleby, K.L., *Functional Coupling of the Beta(1) Subunit to the Large Conductance Ca2+-Activated K+ Channel in the Absence of Ca2+-Increased Ca2+ Sensitivity from a Ca2+-Independent Mechanism.* Journal of General Physiology, 2000. **115**: 719-734.
178. Jiang, Z., Wallner, M., Meera, P. and Toro, L., *Human and Rodent MaxiK Channel Beta-Subunit Genes: Cloning and Characterization.* Genomics, 1999. **55**: 57-67.
179. Greenwood, I.A., Miller, L.J., Ohya, S. and Horowitz, B., *The Large Conductance Potassium Channel Beta-Subunit can Interact with and Modulate the Functional Properties of a Calcium-Activated Chloride Channel, CLCA1.* Journal of Biological Chemistry, 2002. **277**: 22119-22122.
180. Xia, X.M., Ding, J.P. and Lingle, C.J., *Molecular Basis for the Inactivation of Ca2+- and Voltage- Dependent BK Channels in Adrenal Chromaffin Cells and Rat Insulinoma Tumor Cells.* Journal of Neuroscience, 1999. **19**: 5255-5264.

181. Bentrop, D., Beyermann, M., Wissmann, R. and Fakler, B., *NMR Structure of the "Ball-and-Chain" Domain of KCNMB2, the Beta(2)-Subunit of Large Conductance Ca2+ and Voltage-Activated Potassium Channels.* Journal of Biological Chemistry, 2001. **276**: 42116-42121.
182. Solaro, C.R., Prakriya, M., Ding, J.P. and Lingle, C.J., *Inactivating and Noninactivating Ca2+- and Voltage-Dependent K+ Current in Rat Adrenal Chromaffin Cells.* Journal of Neuroscience, 1995. **15**: 6110-6123.
183. Hicks, G.A. and Marrion, N.V., *Ca2+-Dependent Inactivation of Large Conductance Ca2+-Activated K+ (BK) Channels in Rat Hippocampal Neurones Produced by Pore Block from an Associated Particle.* Journal of Physiology-London, 1998. **508**: 721-734.
184. Li, Z.W., Ding, J.P., Kalyanaraman, V., Lingle, C.J., *RINm5f Cells Express Inactivating BK Channels Whereas HIT Cells Express Noninactivating BK Channels* Journal of Neurophysiology, 1999. **81**: 611-624.
185. Behrens, R., Nolting, A., Reimann, F., Schwarz, M., Waldschutz, R. and Pongs, O., hKCNMB*3 and* hKCNMB*4, Cloning and Characterization of Two Members of the Large-Conductance Calcium-Activated Potassium Channel Beta Subunit Family.* FEBS Letters, 2000. **474**: 99-106.
186. Jin, P., Weiger, T.M., Wu, Y.Y. and Levitan, I.B., *Phosphorylation-Dependent Functional Coupling of hSlo Calcium-Dependent Potassium Channel and its h Beta 4 Subunit.* Journal of Biological Chemistry, 2002. **277**: 10014-10020.
187. Armstrong, D.L. and Rossie, S., *Ion Channel Regulation.* Advances in Second Messenger and Phosphoprotein Research. Vol. 33. 1999. Academic Press.
188. Levitan, I.B., *Modulation of Ion Channels by Protein Phosphorylation - How the Brain Works*, in *Ion Channel Regulation* (REF: 187). 1999. p. 3-22.
189. Clark, A.G., Hall, S.K. and Shipston, M.J., *ATP Inhibition of a Mouse Brain Large-Conductance K+ (mSlo) Channel Variant by a Mechanism Independent of Protein Phosphorylation.* Journal of Physiology-London, 1999. **516**: 45-53.
190. Esguerra, M., Wang, J., Foster, C.D., Adelman, J.P., North, R.A. and Levitan, I.B., *Cloned Ca2+-Dependent K+ Channel Modulated by a Functionally Associated Protein-Kinase.* Nature, 1994. **369**: 563-565.
191. Klaerke, D.A., Wiener, H., Zeuthen, T. and Jorgensen, P.L., *Regulation of Ca2+-Activated K+ Channel from Rabbit Distal Colon Epithelium by Phosphorylation and Dephosphorylation.* Journal of Membrane Biology, 1996. **151**: 11-18.
192. Hall, S.K. and Armstrong, D.L., *Conditional and Unconditional Inhibition of Calcium-Activated Potassium Channels by Reversible Protein Phosphorylation.* Journal of Biological Chemistry, 2000. **275**: 3749-3754.
193. Reinhart, P.H., Chung, S.K., Martin, B.L., Brautigan, D.L. and Levitan, I.B., *Modulation of Calcium-Activated Potassium Channels from Rat- Brain by Protein Kinase-A and Phosphatase-2A.* Journal of Neuroscience, 1991. **11**: 1627-1635.
194. Tian, L.J., Knaus, H.G. and Shipston, M.J., *Glucocorticoid Regulation of Calcium-Activated Potassium Channels Mediated by Serine/Threonine Protein Phosphatase.* Journal of Biological Chemistry, 1998. **273**: 13531-13536.
195. Zhou, X.B., Arntz, C., Kamm, S., Motejlek, K., Sausbier, U., Wang, G.X., Ruth, P. and Korth, M., *A Molecular Switch for Specific Stimulation of the BKCa Channel by cGMP and cAMP Kinase.* Journal of Biological Chemistry, 2001. **276**: 43239-43245.
196. Hofmann, F., Ammendola, A. and Schlossmann, J., *Rising Behind NO: cGMP-Dependent Protein Kinases.* Journal of Cell Science, 2000. **113**: 1671-1676.

197. White, R.E., Lee, A.B., Shcherbatko, A.D., Lincoln, T.M., Schonbrunn, A. and Armstrong, D.L., *Potassium Channel Stimulation by Natriuretic Peptides Through cGMP-Dependent Dephosphorylation.* Nature, 1993. **361**: 263-266.
198. Zhou, X.B., Schlossmann, J., Hofmann, F., Ruth, P. and Korth, M., *Regulation of Stably Expressed and Native BK Channels from Human Myometrium by cGMP- and cAMP-Dependent Protein Kinase.* Pflugers Archiv-European Journal of Physiology, 1998. **436**: 725-734.
199. Herzig, S. and Neumann, J., *Effects of Serine/Threonine Protein Phosphatases on Ion Channels in Excitable Membranes.* Physiological Reviews, 2000. **80**: 173-210.
200. Gong, L.W., Gao, T.M., Huang, H., Zhou, K.X. and Tong, Z.Q., *ATP Modulation of Large Conductance Ca2+-Activated K+ Channels via a Functionally Associated Protein Kinase A in CA1 Pyramidal Neurons from Rat Hippocampus.* Brain Research, 2002. **951**: 130-134.
201. Denson, D.D., Wang, X.P., Worrell, R.T., Alkhalili, O. and Eaton, D.C, *Cytosolic Phospholipase A(2) is Required for Optimal ATP Activation of BK Channels in GH(3) Cells.* Journal of Biological Chemistry, 2001. **276**: 7136-7142.
202. Zhou, Y., Wang, J., Wen, H., Kucherovsky, O. and Levitan, I.B., *Modulation of Drosophila Slowpoke Calcium-Dependent Potassium Channel Activity by Bound Protein Kinase A Catalytic Subunit.* Journal of Neuroscience, 2002. **22**: 3855-3863.
203. Long, K.J. and Walsh, K.B., *Calcium-Activated Potassium Channel in Growth-Plate Chondrocytes - Regulation by Protein-Kinase-A.* Biochemical and Biophysical Research Communications, 1994. **201**: 776-781.
204. Wang, J. Zhou, Y., Wen, H. and Levitan, I.B., *Simultaneous Binding of Two Protein Kinases to a Calcium Dependent Potassium Channel.* Journal of Neuroscience, 1999. **19**: RC4, 1-7.
205. Nara, M., Dhulipala, P.D.K., Wang, Y.X. and Kotlikoff, M.I., *Reconstitution of Beta-Adrenergic Modulation of Large Conductance, Calcium Activated Potassium (Maxi K) Channels in Xenopus Oocytes.* Journal of Biological Chemistry, 1998. **273**: 14920-14924.
206. Chik, C.L., Li, B., Karpinski, E. and Ho, A.K., *Ceramide Inhibits the Outward Potassium Current in Rat Pinealocytes.* Journal of Neurochemistry, 2001. **79**: 339-348.
207. Shipston, M.J. and Armstrong, D.L., *Activation of Protein Kinase C Inhibits Calcium-Activated Potassium Channels in Rat Pituitary Tumour Cells.* Journal of Physiology-London, 1996. **493**: 665-672.
208. Peers, C. and Carpenter, E., *Inhibition of Ca2+-Dependent K+ Channels in Rat Carotid Body Type I Cells by Protein Kinase C.* Journal of Physiology-London, 1998. **512**: 743-750.
209. Fukao, M., Mason, H.S., Britton, F.C., Kenyon, J.L., Horowitz, B. and Keef, K.D., *Cyclic GMP-Dependent Protein Kinase Activates Cloned BKCa Channels Expressed in Mammalian Cells by Direct Phosphorylation at Serine 1072.* Journal of Biological Chemistry, 1999. **274**: 10927-10935.
210. Han, G.C., Kryman, J.P., McMillin, P.J.P., White, R.E. and Carrier, G.O., *A Novel Transduction Mechanism Mediating Dopamine-Induced Vascular Relaxation; Opening of BKCa Channels by Cyclic AMP-Induced Stimulation of the Cyclic GMP-Dependent Protein Kinase.* Journal of Cardiovascular Pharmacology, 1999. **34**: 619-627.
211. Alioua, A., Tanaka, Y., Wallner, M, Hofmann, F., Ruth, P., Meera, P. and Toro, L., *The Large Conductance, Voltage-Dependent, and Calcium Sensitive K+ Channel, hSlo, is a Target of cGMP-Dependent Protein Kinase Phosphorylation in vivo.* Journal of Biological Chemistry, 1998. **273**: 32950-32956.

212. Stockand, J.D., Silverman, M., Hall, D., Derr, T., Kubacak, B. and Sansom, S.C., *Arachidonic Acid Potentiates the Feedback Response of Mesangial BKCa Channels to Angiotensin II.* American Journal of Physiology-Renal Physiology, 1998. **43**: F658-F664.
213. Ling, S.Z., Woronuk, G., Sy, L., Lev, S. and Braun, A.P., *Enhanced Activity of a Large Conductance, Calcium-Sensitive K+ Channel in the Presence of Src Tyrosine Kinase.* Journal of Biological Chemistry, 2000. **275**: 30683-30689.
214. Alberts, B., Bray, D., Lewis, J., Raff, M., Roberts, K. and Watson, J.D., *Molecular biology of the cell.* 2nd Ed. 1989: Garland Publishing, NY.
215. Stryer. L., *Biochemistry*, 4th Ed. 1995: W.H. Freeman and Co., NY.
216. Flockhart, D.A. and Corbin, J.D., *Regulatory Mechanisms in the Control of Protein-Kinases.* CRC Critical Reviews in Biochemistry, 1982. **12**: 133-186.
217. Taylor, S.S., Buechler, J.A. and Yonemoto, W., *cAMP-Dependent Protein-Kinase - Framework for a Diverse Family of Regulatory Enzymes.* Annual Review of Biochemistry, 1990. **59**: 971-1005.
218. Voet, D. and Voet, J., *Biochemistry.* 2nd Ed. 1995: John Wiley & Son Inc.
219. Montminy, M.R. and Bilezikjian, L.M., *Binding of a Nuclear-Protein to the Cyclic-AMP Response Element of the Somatostatin Gene.* Nature, 1987. **328**: 175-178.
220. Rossie, S., Gordon, D. and Catterall, W.A., *Identification of an Intracellular Domain of the Sodium-Channel having Multiple cAMP-Dependent Phosphorylation Sites.* Journal of Biological Chemistry, 1987. **262**: 17530-17535.
221. Rossie, S. and Catterall, W.A., *Cyclic AMP-Dependent Phosphorylation of Voltage-Sensitive Sodium-Channels in Primary Cultures of Rat-Brain Neurons.* Journal of Biological Chemistry, 1987. **262**: 12735-12744.
222. Rotman, E.I., Murphy, B.J. and Catterall, W.A., *Sites of Selective cAMP-Dependent Phosphorylation of the L-Type Calcium-Channel Alpha-1 Subunit from Intact Rabbit Skeletal- Muscle Myotubes.* Journal of Biological Chemistry, 1995. **270**: 16371-16377.
223. Anderson, A.E., Adams, J.P., Qian, Y., Cook, R.G., Pfaffinger, P.J. and Sweatt, J.D., *Kv4.2 Phosphorylation by Cyclic AMP-Dependent Protein Kinase.* Journal of Biological Chemistry, 2000. **275**: 5337-5346.
224. Dekker, L.V. and Parker, P.J., *Protein-Kinase-C – A Question of Specificity.* Trends in Biochemical Sciences, 1994. **19**: 73-77.
225. Ledoux, J., Chartier, D. and Leblanc, N., *Inhibitors of Calmodulin-Dependent Protein Kinase are Nonspecific Blockers of Voltage-Dependent K+ Channels in Vascular Myocytes.* Journal of Pharmacology and Experimental Therapeutics, 1999. **290**: 1165-1174.
226. Kennelly, P.J. and Krebs, E.G., *Consensus Sequences as Substrate-Specificity Determinants for Protein-Kinases and Protein Phosphatases.* Journal of Biological Chemistry, 1991. **266**: 15555-15558.
227. Kemp, B.E. and Pearson, R.B., *Protein-Kinase Recognition Sequence Motifs.* Trends in Biochemical Sciences, 1990. **15**: 342-346.
228. Prosite: http://ca.Expasy.Org/tools/scanprosite.
229. Tian, L.J., Duncan, R.R., Hammond, M.S.L., Coghill, L.S., Wen, H., Rusinova, R., Clark, A.G., Levitan, I.B. and Shipston, M.J., *Alternative Splicing Switches Potassium Channel Sensitivity to Protein Phosphorylation.* Journal of Biological Chemistry, 2001. **276**: 7717-7720.
230. Schubert, R., Lehmann, G., Serebryakov, V.N., Mewes, H. and Hopp, H.H., *cAMP-Dependent Protein Kinase is in an Active State in Rat Small Arteries Possessing a*

Myogenic Tone. American Journal of Physiology-Heart and Circulatory Physiology, 1999. **46**: H1145-H1155.

231. Zhou, X.B., Ruth, P., Schlossmann, J., Hofmann, F. and Korth, M., *Protein Phosphatase 2A is Essential for the Activation of Ca2+-Activated K+ Currents by cGMP-Dependent Protein Kinase in Tracheal Smooth Muscle and Chinese Hamster Ovary Cells.* Journal of Biological Chemistry, 1996. **271**: 19760-19767.
232. Shipston, M.J., Kelly, J.S. and Antoni, F.A., *Glucocorticoids Block Protein Kinase A Inhibition of Calcium-Activated Potassium Channels.* Journal of Biological Chemistry, 1996. **271**: 9197-9200.
233. Tian, L.J., Hammond, M.S.L., Florance, H., Antoni, F.A. and Shipston, M.J., *Alternative Splicing Determines Sensitivity of Murine Calcium-Activated Potassium Channels to Glucocorticoids.* Journal of Physiology-London, 2001. **537**: 57-68.
234. Valverde, M.A., Rojas, P., Amigo, J., Cosmelli, D., Orio, P., Bahamonde, M.I., Mann, G.E., Vergara, C. and Latorre, R., *Acute Activation of Maxi-K Channels (hSlo) by Estradiol Binding to the Beta Subunit.* Science, 1999. **285**: 1929-1931.
235. Dick, G.M., Rossow, C.F., Smirnov, S., Horowitz, B. and Sanders, K.M., *Tamoxifen Activates Smooth Muscle BK Channels Through the Regulatory Beta 1 Subunit.* Journal of Biological Chemistry, 2001. **276**: 34594-34599.
236. Dick, G.M., Hunter, A.C. and Sanders, K.M., *Ethylbromide Tamoxifen, a Membrane-Impermeant Antiestrogen, Activates Smooth Muscle Calcium-Activated Large-Conductance Potassium Channels from the Extracellular Side.* Molecular Pharmacology, 2002. **61**: 1105-1113.
237. Dopico, A.M., Walsh, J.V. and Singer, J.J., *Natural Bile Acids and Synthetic Analogues Modulate Large Conductance Ca2+-Activated K+ (BKCa) Channel Activity in Smooth Muscle Cells.* Journal of General Physiology, 2002. **119**: 251-273.
238. Rang, H., Dale, M. and Ritter, J., *Pharmacology.* 3rd Ed. 1995: Churchill Livingstone.
239. Bolotina, V.M., Najibi, S., Palacino, J.J., Pagano, P.J. and Cohen, R.A., *Nitric-Oxide Directly Activates Calcium-Dependent Potassium Channels in Vascular Smooth-Muscle.* Nature, 1994. **368**: 850-853.
240. Bang, L., Boesgaard, S., Nielsen-Kudsk, J.E., Vejlstrup, N.G. and Aldershvile, J., *Nitroglycerin-Mediated Vasorelaxation is Modulated by Endothelial Calcium-Activated Potassium Channels.* Cardiovascular Research, 1999. **43**: 772-778.
241. Ye, D., Pospisilik, J.A. and Mathers, D.A., *Nitroblue Tetrazolium Blocks BK Channels in Cerebrovascular Smooth Muscle Cell Membranes.* British Journal of Pharmacology, 2000. **129**: 1035-1041.
242. Ishida, K., Kinoshita, H., Kobayashi, S. and Sakabe, T., *Thiopentone Inhibits Endothelium-Dependent Relaxations of Rat Aortas Regulated by Endothelial Ca2+-Dependent K+ Channels.* European Journal of Pharmacology, 1999. **371**: 179-185.
243. Carter, E.P., Sato, K., Morio, Y. and McMurtry, I.F., *Inhibition of K-Ca Channels Restores Blunted Hypoxic Pulmonary Vasoconstriction in Rats with Cirrhosis.* American Journal of Physiology-Lung Cellular and Molecular Physiology, 2000. **279**: L903-L910.
244. Miura, H., Liu, Y.P. and Gutterman, D.D., *Human Coronary Arteriolar Dilation to Bradykinin Depends on Membrane Hyperpolarization - Contribution of Nitric Oxide and Ca2+-Activated K+ Channels.* Circulation, 1999. **99**: 3132-3138.
245. DiChiara, T.J. and Reinhart, P.H., *Redox Modulation of hSlo Ca2+-Activated K+ Channels.* Journal of Neuroscience, 1997. **17**: 4942-4955.
246. Tang, K.D., Daggett, H., Hanner, M., Garcia, M.L., McManus, O.B., Brot, N., Weissbach, H., Heinemann, S.H. and Hoshi, T., *Oxidative Regulation of Large*

Conductance Calcium-Activated Potassium Channels, Journal of General Physiology, 2001. **117**: 253-273.

247. Slivka, A., Mytilineou, C. and Cohen, G., *Histochemical Evaluation of Glutathione in Brain.* Brain Research, 1987. **409**: 275-284.
248. Slivka, A., Spina, M.B. and Cohen, G., *Reduced and Oxidized Glutathione in Human and Monkey Brain.* Neuroscience Letters, 1987. **74**: 112-118.
249. Sucher, N.J. and Lipton, S.A., *Redox Modulatory Site of the NMDA Receptor-Channel Complex - Regulation by Oxidized Glutathione.* Journal of Neuroscience Research, 1991. **30**: 582-591.
250. Philbert, M.A., Beiswanger, C.M., Waters, D.K., Reuhl, K.R. and Lowndes, H.E., *Cellular and Regional Distribution of Reduced Glutathione in the Nervous-System of the Rat - Histochemical-Localization by Mercury Orange and Ortho-Phthaldialdehyde-Induced Histofluorescence.* Toxicology and Applied Pharmacology, 1991. **107**: 215-227.
251. Erxleben, C., Everhart, A.L., Romeo, C., Florance, H., Bauer, M.B., Alcorta, D.A., Rossie, S., Shipston, M.J. and Armstrong, D.L., *Interacting Effects of N-Terminal Variation and STREX Exon Splicing on Slo Potassium Channel Regulation by Calcium, Phosphorylation, and Oxidation.* Journal of Biological Chemistry, 2002. **277**: 27045-27052.
252. Petkova-Kirova, P., Gagov, H., Krien, U., Duridanova, D., Noack, T. and Schubert, R., *4-Aminopyridine Affects Rat Arterial Smooth Muscle BKCa Currents by Changing Intracellular pH.* British Journal of Pharmacology, 2000. **131**: 1643-1650.
253. Schubert, R., Krien, U. and Gagov, H., *Protons Inhibit the BKCa Channel of Rat Small Artery Smooth Muscle Cells.* Journal of Vascular Research, 2001. **38**: 30-38.
254. Chen, S.J., Wu, C.C. and Yen, M.H., *Role of Nitric Oxide and K+-Channels in Vascular Hyporeactivity Induced by Endotoxin.* Naunyn-Schmiedebergs Archives of Pharmacology, 1999. **359**: 493-499.
255. Mertineit, C., Samlalsingh-Parker, J., Glibetic, M., Ricard, G., Noya, J.D. and Aranda, J.V., *Nitric Oxide, Prostaglandins, and Impaired Cerebral Blood Flow Autoregulation in Group B Streptococcal Neonatal Meningitis.* Canadian Journal of Physiology and Pharmacology, 2000. **78**: 217-227.
256. Yakubovich, N., Eldstrom, J.R. and Mathers, D.A., *Lipopolysaccharide can Activate BK Channels of Arterial Smooth Muscle in the Absence of iNOS Expression.* Biochimica Et Biophysica Acta-Biomembranes, 2001. **1514**: 239-252.
257. Ordway, R.W., Singer, J.J. and Walsh, J.V., *Direct Regulation of Ion Channels by Fatty-Acids.* Trends in Neurosciences, 1991. **14**: 96-100.
258. Holmqvist, M.H., Cao, J., Knoppers, M.H., Jurman, M.E., Distefano, P.S., Rhodes, K.J., Xie, Y. and An, W.F., *Kinetic Modulation of Kv4-Mediated A-Current by Arachidonic Acid is Dependent on Potassium Channel Interacting Proteins.* Journal of Neuroscience, 2001. **21**: 4154-4161.
259. Denson, D.D., Wang, X.P., Worrell, R.T. and Eaton, D.C., *Effects of Fatty Acids on BK Channels in GH(3) Cells.* American Journal of Physiology-Cell Physiology, 2000. **279**: C1211-C1219.
260. Giangiacomo, K.M., Garciacalvo, M., Knaus, H.G., Mullmann, T.J., Garcia, M.L. and McManus, O., *Functional Reconstitution of the Large-Conductance, Calcium- Activated Potassium Channel Purified from Bovine Aortic Smooth- Muscle.* Biochemistry, 1995. **34**: 15849-15862.
261. Moczydlowski, E., Alvarez, O., Vergara, C. and Latorre, R., *Effect of Phospholipid Surface-Charge on the Conductance and Gating of a Ca-2+-Activated K+ Channel in Planar Lipid Bilayers.* Journal of Membrane Biology, 1985. **83**: 273-282.

262. Gruss, M., Henrich, M., Konig, P., Hempelmann, G., Vogel, W. and Scholz, A., *Ethanol Reduces Excitability in a Subgroup of Primary Sensory Neurons by Activation of BKCa Channels.* European Journal of Neuroscience, 2001. **14**: 1246-1256.
263. Walters, F.S., Covarrubias, M. and Ellingson, J.S., *Potent Inhibition of the Aortic Smooth Muscle Maxi-K Channel by Clinical Doses of Ethanol.* American Journal of Physiology-Cell Physiology, 2000. **279**: C1107-C1115.
264. Peoples, R.W., Li, C.Y. and Weight, F.F., *Lipid vs Protein Theories of Alcohol Action in the Nervous System.* Annual Review of Pharmacology and Toxicology, 1996. **36**: 185-201.
265. Gribkoff, V.K., Lumragan, J.T., Boissard, C.G., Postmunson, D.J., Meanwell, N.A., Starrett, J.E., Kozlowski, E.S., Romine, J.L., Trojnacki, J.T., McKay, M.C., Zhong, J. and Dworetzky, S.I., *Effects of Channel Modulators on Cloned Large-Conductance Calcium-Activated Potassium Channels.* Molecular Pharmacology, 1996. **50**: 206-217.
266. Olesen, S.P., Munch, E., Watjen, F. and Drejer, J., *NS-004 - An Activator of Ca2+-Dependent K+ Channels in Cerebellar Granule Cells.* Neuroreport, 1994. **5**: 1001-1004.
267. Olesen, S.P., Munch, E., Moldt, P. and Drejer, J., *Selective Activation of Ca2+-Dependent K+ Channels by Novel Benzimidazolone.* European Journal of Pharmacology, 1994. **251**: 53-59.
268. Sellers, A.J. and Ashford, M.L.J., *Activation of BKCa Channels in Acutely Dissociated Neurons from the Rat Ventromedial Hypothalamus by NS-1619.* British Journal of Pharmacology, 1994. **113**: 659-661.
269. Yamamura, H., Ohi, Y., Muraki, K., Watanabe, M. and Imaizumi, Y., *BK Channel Activation by NS-1619 is Partially Mediated by Intracellular Ca2+ Release in Smooth Muscle Cells of Porcine Coronary Artery.* British Journal of Pharmacology, 2001. **132**: 828-834.
270. Kirkup, A.J., Edwards, G., Green, M.E., Miller, M., Walker, S.D. and Weston, A.H., *Modulation of Membrane Currents and Mechanical Activity by Niflumic Acid in Rat Vascular Smooth Muscle.* European Journal of Pharmacology, 1996. **317**: 165-174.
271. Gelband, C.H. and McCullough, J.R., *Modulation of Rabbit Aortic Ca2+-Activated K+ Channels by Pinacidil, Cromakalim, and Glibenclamide.* American Journal of Physiology, 1993. **264**: C1119-C1127.
272. Hollywood, M.A., Cotton, K.D., McHale, N.G. and Thornbury, K.D., *Enhancement of Ca2+-Dependent Outward Current in Sheep Bladder Myocytes by Evans Blue Dye.* Pflugers Archiv-European Journal of Physiology, 1998. **435**: 631-636.
273. Wu, S.N., Jan, C.R., Li, H.F. and Chen, S.A., *Stimulation of Large-Conductance Ca2+-Activated K+ Channels by Evans Blue in Cultured Endothelial Cells of Human Umbilical Veins.* Biochemical and Biophysical Research Communications, 1999. **254**: 666-674.
274. Hu, S.L., Fink, C.A., Kim, H.S. and Lappe, R.W., *Novel and Potent BK Channel Openers: CGS 7181 and its Analogs.* Drug Development Research, 1997. **41**: 10-21.
275. Knaus, H.G., McManus, O.B., Lee, S.H., Schmalhofer, W.A., Garciacalvo, M., Helms, L.M.H., Sanchez, M., Giangiacomo, K., Reuben, J.P., Smith, A.B., Kaczorowski, G.J. and Garcia, M.L., *Tremorgenic Indole Alkaloids Potently Inhibit Smooth-Muscle High-Conductance Calcium-Activated Potassium Channels.* Biochemistry, 1994. **33**: 5819-5828.
276. Kaczorowski, G.J. and Garcia, M.L., *Pharmacology of Voltage-Gated and Calcium-Activated Potassium Channels.* Current Opinion in Chemical Biology, 1999. **3**: 448-458.

277. Harper, A.A., Catacuzzeno, L., Trequattrini, C., Petris, A. and Franciolini, F., *Verapamil Block of Large-Conductance Ca-Activated K Channels in Rat Aortic Myocytes.* Journal of Membrane Biology, 2001. **179**: 103-111.
278. Gray, P., Scott, J. and Catterall, W., *Regulation of Ion Channels by cAMP-Dependent Protein Kinase and A Kinase Anchoring Proteins.* Current Opinion in Neurobiology, 1998. **8**: 330-334.
279. Morohashi, Y., Hatano, N., Ohya, S., Takikawa, R., Watabiki, T., Takasugi, N., Imaizumi, Y., Tomita, T. and Iwatsubo, T., *Molecular Cloning and Characterization of CALP/KChIP4, a Novel EF-Hand Protein Interacting with Presenilin 2 and Voltage-Gated Potassium Channel Subunit Kv4.* Journal of Biological Chemistry, 2002. **277**: 14965-14975.
280. Mason, H.S., Latten, M.J., Godoy, L.D., Horowitz, B. and Kenyon, J.L., *Modulation of Kv1.5 Currents by Protein Kinase A, Tyrosine Kinase, and Protein Tyrosine Phosphatase Requires an Intact Cytoskeleton.* Molecular Pharmacology, 2002. **61**: 285-293.
281. Witcher, D.R., Dewaard, M., Kahl, S.D. and Campbell, K.P., *Purification and Reconstitution of N-Type Calcium-Channel Complex from Rabbit Brain*, in *Heterotrimeric G-protein Effectors*. Methods in Enzymology, 1994. **238**: 335-348.
282. Grant, S.G.N. and O'Dell, T.J., *Multiprotein Complex Signaling and the Plasticity Problem.* Current Opinion in Neurobiology, 2001. **11**: 363-368.
283. Husi, H., Ward, M.A., Choudhary, J.S., Blackstock, W.P. and Grant, S.G.N., *Proteomic Analysis of NMDA Receptor-Adhesion Protein Signalling Complexes.* Nature Neuroscience, 2000. **3**: 661-669.
284. Reinhart, P.H. and Levitan, I.B., *Kinase and Phosphatase-Activities Intimately Associated with a Reconstituted Calcium-Dependent Potassium Channel.* Journal of Neuroscience, 1995. **15**: 4572-4579.
285. Swope, S.L. and Huganir, R.L., *Binding of the Nicotinic Acetylcholine-Receptor to SH2 Domains of fyn and fyk Protein-Tyrosine Kinases.* Journal of Biological Chemistry, 1994. **269**: 29817-29824.
286. Holmes, T.C., Fadool, D.A., Ren, R.B. and Levitan, I.B., *Association of Src Tyrosine Kinase with a Human Potassium Channel Mediated by SH3 Domain.* Science, 1996. **274**: 2089-2091.
287. Yu, X.M., Askalan, R., Keil, G.J. and Salter, M.W., *NMDA Channel Regulation by Channel-Associated Protein Tyrosine Kinase Src.* Science, 1997. **275**: 674-678.
288. Rosenmund, C., Carr, D.W., Bergeson, S.E., Nilaver, G., Scott, J.D. and Westbrook, G.L., *Anchoring of Protein-Kinase-A is Required for Modulation of AMPA/Kainate Receptors on Hippocampal-Neurons.* Nature, 1994. **368**: 853-856.
289. Davare, M.A., Dong, F., Rubin, C.S. and Hell, J.W., *The A-Kinase Anchor Protein MAP2b and cAMP-Dependent Protein Kinase are Associated with Class C L-Type Calcium Channels in Neurons.* Journal of Biological Chemistry, 1999. **274**: 30280-30287.
290. Wang, Z.W. and Kotlikoff, M.I., *Activation of K-Ca Channels in Airway Smooth Muscle Cells by Endogenous Protein Kinase A.* American Journal of Physiology-Lung Cellular and Molecular Physiology, 1996. **15**: L100-L105.
291. Schopperle, W.M., Holmqvist, M.H., Zhou, Y., Wang, J., Wang, Z., Griffith, L.C., Keselman, I., Kusinitz, F., Dagan, D. and Levitan, I.B., *Slob, a Novel Protein that Interacts with the Slowpoke Calcium-Dependent Potassium Channel.* Neuron, 1998. **20**: 565-573.

292. Xia, X.M., Hirschberg, B., Smolik, S., Forte, M. and Adelman, J.P., *dSlo Interacting Protein 1, A Novel Protein that Interacts with Large-Conductance Calcium-Activated Potassium Channels.* Journal of Neuroscience, 1998. **18**: 2360-2369.
293. Sambrook, J., Fritsch, E.F. and Maniatis, T., *Molecular Cloning: A Laboratory Manual.* 2nd Ed., 1989. Cold Spring Harbor Laboratory Press, NY, USA.
294. Stratagene Manual #230240.
295. http://www.kazusa.or.jp/codon/
296. Hanahan, D., In: *Cloning, Volume 1.* Glover, D., Ed, 1985. IRL Press Ltd., London.
297. Promega Protocols & Applications Guide, 3rd Ed, 1996. Promega.
298. Bradford, M., *A Rapid and Sensitive Method for the Quantitation of Microgram Quantities of Protein Utilizing the Principle of Protein Dye-Binding.* Analytical Biochemistry, 1976. **72**: 248-254.
299. Birnboim, H.C. and Doly, J., *A Rapid Alkaline Extraction Procedure for Screening Recombinant Plasmid DNA.* Nucleic Acid Research, 1979. **7**: 1513.
300. Promega Technical Bulletin #TB507.
301. Invitrogen Instruction Manual #000919-D.
302. Stratagene Instruction Manual #200518.
303. Amersham Pharmacia GST-Gene Fusion System Manual.
304. QIAGEN: The QIAexpressionist Handbook, 2001.
305. Invitrogen Instruction Manual #073001-F.
306. Freshney, R.I., *Culture of Animal Cells: A Manual of Basic Technique.* 1988, 2nd Ed., Alan R.Liss, Inc., New York.
307. Fanger, C.M., Ghanshani, S., Logsdon, N.J., Rauer, H., Kalman, K., Zhou, J.M., Beckingham, K., Chandy, K.G., Cahalan, M.D. and Aiyar, J., *Calmodulin Mediates Calcium-Dependent Activation of the Intermediate Conductance K-Ca Channel, IKCa1.* Journal of Biological Chemistry, 1999. **274**: 2746-2754.
308. Roche General Laboratory Manual 1999.
309. Wray, W., Boulikas, T., Wray, V.P. and Hancock, R., *Silver Staining of Proteins in Polyacrylamide Gels.* Analytical Biochemistry, 1981. **118**: 197-203.
310. Towbin, H., Staehelin, T. and Gordon, J., *Electrophoretic Transfer of Protein From Polyacrylamide Gels to Nitrocellulose Sheets: Procedures and Some Applications.* Proceedings of the National Academy of Science, USA, 1979. **76**: 4350-4354.
311. Aspbury, R.A., Fisher, M.J., Rees, H.H. and Clegg, R.A., *N-myristoylation of the catalytic subunit of cAMP-depecdent protein kinase in the free living nematode Caenorhabditis elegans.* Biochemical and Biophysical Research Communications, 1997. **238**: 523-527.
312. Stratagene Technical Bulletin #279/528
313. Agostoni, E., Gobessi, S., Petrini, E., Monte, M. and Schneider, C., *Cloning and Characterization of the C. elegans gas1 Homolog: PHAS-I.* Biochimica et Biophysica Acta, 2002. **1574**: 1-9.
314. Murphy, B. J., Rossie, S., Dejongh, K.S. and Catterall, W.A., *Identification of the Sites of Selective Phosphorylation and Dephosphorylation of the Rat Brain Na^+ Channel Alpha Subunit by cAMP-Dependent Protein Kinase and Phosphoprotein Phosphatases,* Journal of Biological Chemistry, 1993. **268**: 27355-27362.
315. Mammen, A.L., Kamboi, S. and Huganir, R.L., *Protein Phosphorylation of Ligand-Gated Ion Channels,* In: *Methods In Enzymology, Vol. 294 Ion Channels Part C.* Conn, P.M. Ed., 1999. Academic Press: p. 353-370.

316. Shipston, M.J., Antoni, F.A. and Kelly, J.S, *Glucocorticoids Prevent cAMP-Mediated Inhibition of Potassium Currents in a Clonal Pituitary Corticotroph Cell Line, AtT20 D16/16.* Journal of Physiology – London, 1995. **489**: 174-175.
317. http://www.ncbi.gov.uk
318. Marx, S.O., Kurokawa, J., Reiken, S., Motoike, H., D'Armiento, J., Marks, A.R. and Kass, R.S., *Requirement of Macromolecular Signalling Complex for Beta-Adrenergic Receptor Modulation of the KCNQ1-KCNE1 Potassium Channel.* Science, 2002. **295**: 496-499.
319. Meyer, E., Fromherz, P., *Ca2+ Activation of hSlo K+ Channel is Suppressed by N-Terminal GFP Tag.* European Journal of Neuroscience, 1999. **11**: 1105-1108.
320. Wilson, I.A., Niman, H.L., Houghten, R.A., Cherenson, A.R., Connelly, M.L. and Lerner, R.A., *The Structure of an Antigenic Determinant in a Protein.* Cell, 1984. **37**: 767-778.
321. Southern, J.A., Young, D.F., Heaney, F., Baumgartner, W.K. and Randall, R.E., *Identification of an Epitope on the P-Proteins and V-Proteins of Simian-Virus 5 That Distinguishes Between 2 Isolates with Different Biological Characteristics.* Journal of General Virology, 1991. **72**: 1551-1557.
322. Lindner, P., Bauer, K., Kremmer, E., Krebber, C., Honegger, A., Klinger B., Mocikat, R. and Pluckthun, A., *Specific Detection of His-Tagged Proteins With Recombinant Anti-His Tag scFv-Phosphatase or scFv-Phage Fusions.* Biotechniques, 1997. **22**: 140
323. Levitan, E.S., *Tagging Potassium Ion Channels with Green Fluorescent Protein to Study Mobility and Interactions with Other Proteins.* In: *Methods In Enzymology, Vol. 294 Ion Channels Part C,* Conn, P.M. Ed., 1999. Academic Press: p. 47-58.
324. Living Colors User Manual #PT2040-1/Version #PR1Y691, BD Biosciences.
325. Blumental, E.M. and Kaczmarek, L.K., *Modulation by cAMP of Slowly Activating Potassium Channel Expressed in Xenopus Oocytes.* Journal of Neuroscience, 1992. **12**: 290-296.
326. Lackie, J.M. and Dow, J.A.T. (Ed.), *The Dictionary of Cell Biology.* 2nd Ed. 1995: Academic Press.
327. McKnight, S.L., *Molecular Zippers in Gene Regulation.* Scientific American, 1991. **264**: 54.
328. Lamb, P. and McKnight, S.L., *Diversity and Specificity in Transcriptional Regulation – The Benefits of Heterotypic Dimerization.* Trends in Biochemical Science, 1991. **16**: 417-422.
329. O'Shea, E.K., Klemm, J.D., Kim, P.S. and Alber, T., *X-ray Structure of the GCN4 Leucine Zipper, a Two Stranded, Parallel Coiled Coil.* Science, 1991. **254**: 539-544.
330. Landshultz, W.H., Johnson, P.F. and McKnight, S.L., *The Leucine Zipper – a Hypothetical Structure Common to a New Class of DNA Binding Proteins*, 1988. Nature, **240**: 1759-1764.
331. deSousa, N., Reiken, S., Ondrias, K., Yang, Y.M., Matkovich, S. and Marks, A.R., *Protein Kinase A and Two Phosphatases are Components of the Inositol 1,4,5-Triphosphate Receptor Macromolecular Signalling Complex.* Journal of Biological Chemistry, 2002. **277**: 39397-39400.
332. Marks, A.R., Marx, S.O. and Reiken, S., *Regulation of Ryanodine Receptors via Macromolecular Complexes: A Novel Role for Leucine/Isoleucine Zippers.* Trends in Cardiovascular Medicine, 2002. **12**: 166-170.
333. Watson, J.A., Rumsby, M.G. and Wolowacz, R.G., *Phage Display Identifies Thioredoxin and Superoxide Dismutase as Novel Protein Kinase C Interacting Proteins:*

Thioredoxin Inhibits PKC-Mediated Phosphorylation of Histone. Biophysical Journal, 1999. **343**: 301-305.

334. Wolfart, J. and Roeper, J., *Selective Coupling of T-Type Calcium Channels to SK Potassium Channels Prevents Intrinsic Bursting in Dopaminergic Midbrain Neurons.* Journal of Neuroscience, 2002. **22**: 3404-3413.
335. Dell'Acqua, M.L. and Scott, J.D., *Protein Kinase A Anchoring.* Journal of Biological Chemistry, 1997. **272**: 12881-12884.

Publications

Tian, L.J., Duncan, R.R., Hammond, M.S.L., Coghill, L.S., Wen, H., Rusinova, R., Clark, A.G., Levitan, I.B. and Shipston, M.J., *Alternative Splicing Switches Potassium Channel Sensitivity to Protein Phosphorylation.* Journal of Biological Chemistry, 2001. **276**: 7717-7720.

Coghill, L.S., Florance, H., Antoni, F.A. and Shipston, M.J., *Protein Kinase A Regulation of BK Channel Splice Variants*. Pflugers Archiv European Journal of Physiology, 2002. **443**(Supplement):Abs.

Protein Kinase A Regulation of BK Channel Splice Variants

Coghill, L.S., Florance, H., Antoni, F.A. and Shipston, M.J.

Large conductance calcium- and voltage- activated potassium (BK) channels are important determinants of endocrine, vascular and neuronal cell excitability. Despite being the product of only one gene (*KCNMA1*), native BK channels display diverse functional properties. Such diversity results from alternative splicing of the nuclear pre-mRNA, and is exemplified by the different response of two major BK channel splice variants to protein kinase A (PKA). Channels expressing a unique 59 residue, cysteine-rich insert (STREX) located within the channel's intracellular C-terminal domain are inhibited by PKA, whereas channels lacking this insert (ZERO) are activated. The aim of this study was to investigate the interaction of PKA with STREX BK channels.

Hemagglutinin (HA)-tagged STREX BK channel splice variant was co-expressed with PKA catalytic subunit (PKAc) in HEK293 cells, and immunoprecipitated (IP) with anti-HA or anti-PKAc antibodies. Final IPs were analysed by SDS-PAGE, blotted, and probed for HA or PKAc. IP with anti-HA resulted in co-IP of PKAc and, reciprocally, IP with anti-PKAc resulted in co-IP of HA-tagged STREX channels suggesting that PKAc and the STREX channel exist as a complex. To investigate whether the STREX insert is a possible PKAc binding site, the 59 residue STREX insert was expressed as a GST-fusion protein (GST-STREX) in *E.coli* and purified by glutathione sepharose (GS4B) chromatography. PKAc did not directly interact with GST-STREX in an *in vitro* pull-down assay. To investigate whether PKAc can interact with GST-STREX as part of a larger complex pull-down assays were performed using rat brain lysate or HEK293 cells as sources of endogenous PKAc. However, although PKAc was not found to associate with the GST-STREX fusion protein, PKAc phosphorylated GST-STREX in an *in vitro* phosphorylation assay. *In vitro* phosphorylation of GST-STREX was completely abolished on mutation of a single serine residue (S4A) within a putative PKA-consensus site within STREX.

These data suggest that PKAc associates with the STREX channel as observed by IP. However, although the STREX insert is a target for phosphorylation by PKAc, affinity pull-down assays indicate that the STREX insert is not required for interaction of PKAc with the channel.

This work was supported by grants from the BBSRC to MJS. LSC is supported by a Crichton Scholarship from the University of Edinburgh Medical School.

Membrane Biology Group, Section of Biomedical Sciences, University of Edinburgh, Hugh Robson Building, George Square, Edinburgh, Scotland, EH8 9XD.

Tian, L.J., Coghill, L.S., MacDonald, S.H.-F., Armstrong, D.L. and Shipston, M.J., *Leucine Zipper Domain Targets PKA to Mammalian BK Channels*. Journal of Biological Chemistry, 2003. **278**: 8669-8677.